THE METABOLISM OF PYRUVATE IN THE LIGHT IN PLANTS WITH CRASSULACEAN ACID METABOLISM

A Thesis Submitted for the Degree of
Doctor of Philosophy
in the Australian National University

by

JOSEPH ANDREW MAXTED HOLTUM

AUGUST 1979

DECLARATION

The work presented in this thesis is my own. Specific contributions and co-operative work with others are referred to in the acknowledgements and in the text where relevant.

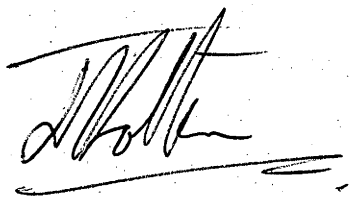

J.A.M. HOLTUM

Department of Environmental Biology
Research School of Biological Sciences
The Australian National University
Canberra A.C.T.

ABSTRACT

This thesis is concerned with the pathways for conversion of pyruvate and phosphoenolpyruvate (PEP) to carbohydrate in the light in CAM plants. These 3-carbon substrates are produced by the decarboxylation of malic acid which accumulates in the dark in these plants. It is shown that these 3-carbon compounds are principally converted to carbohydrate by a reversal of glycolysis (gluconeogenesis) and that oxidative metabolism to CO_2, and refixation in photosynthesis is probably of minor significance.

Two approaches were used. In the first, $^{14}CO_2$ or ^{14}C labelled pyruvate was fed to leaf slices during deacidification. The leaf slices in solution were shown to deacidify in the same way as intact tissues in air, and to display the same rates and products of $^{14}CO_2$ fixation as intact tissues. CAM plants in which deacidification involves NADP malic enzyme convert 2-^{14}C and 3-^{14}C pyruvate to carbohydrate much more readily than C_3 plants or than *Stapelia*, a CAM plant in which deacidification involves phosphoenol-pyruvate carboxykinase (PEPCK). A comparison of the products of 2-^{14}C- and 3-^{14}C-pyruvate metabolism in *Kalanchoe* and *Stapelia* suggests that pyruvate is converted to carbohydrate via gluconeogenesis in *Kalanchoe*, whilst in *Stapelia* pyruvate is mainly metabolised within the mitochondria. The differences in pyruvate metabolism between the malic enzyme CAM plants and PEPCK CAM plants are consistent with the observation that malic enzyme CAM plants, which produce pyruvate during deacidification, possess pyruvate, Pi dikinase which converts pyruvate to PEP, whereas the others do not. In the absence of this enzyme pyruvate cannot enter the gluconeogenic reaction sequence as PEP and is metabolised to organic acids rather than carbohydrates. In both *Kalanchoe* and *Aloe*, ^{14}C-succinate is metabolised in mitochondria but is not cycled or oxidised via the TCA cycle to any significant extent.

These studies with leaf slices were extended by the isolation of intact, physiologically active mesophyll cells from *Kalanchoe* and *Stapelia*. Pyruvate stimulated $^{14}CO_2$ fixation by up to 50% in *Kalanchoe* cells but had no effect on fixation by *Stapelia* cells. The difference is also consistent with presence of pyruvate, Pi dikinase in *Kalanchoe* but not in *Stapelia*, and confirms that pyruvate is converted to PEP in *Kalanchoe in vivo*. Although PEP stimulated $^{14}CO_2$ fixation in the light, 3-PGA did not. Both PEP and 3-PGA stimulated dark $^{14}CO_2$ fixation implying that the glycolytic reaction 3-PGA $\longrightarrow$ PEP may not function in the light.

The second approach involved a survey of the activities of the enzymes involved in acidification, deacidification, pyruvate metabolism and glycolysis in the above plants. Glycolytic enzymes were assayed in the gluconeogenic direction wherever possible. The activity of these enzymes was adequate to account for the measured rates of deacidification, CO_2 fixation, and conversion of pyruvate or PEP to carbohydrate *in vivo*. The presence of pyruvate, Pi dikinase in a range of malic enzyme CAM plants and its absence in a range of PEPCK CAM plants was confirmed.

The activities of a number of photosynthetic and glycolytic enzymes were measured during the induction of CAM in *M. crystallinum* in an attempt to assess their relative importance to the expression of CAM. The activity of PEP carboxylase, NADP malic enzyme and pyruvate, Pi dikinase increased from low levels to levels adequate to account for the observed rates of acidification and deacidification as CAM was induced. With the notable exceptions of RuP_2 carboxylase and FDPase, the activity of several other enzymes also increased during the induction period. The importance of these changes is unresolved because their original activities were already much greater than the maximum rates of acidification and deacidification attained after the induction of

CAM. Interestingly, phosphoglyceromutase activity increased 10 fold when assayed in the gluconeogenic direction but only 3 fold when assayed in the glycolytic direction. This observation may be important with respect to the response of isolated cells to 3-PGA in the light, described above. NADP MDH had a surprisingly low pH optimum before induction of CAM but developed activity at pH 8.0 during the induction period.

These results are consistent with the operation of gluconeogenesis in the light during deacidification in CAM plants. Schemes are presented outlining the possible pathways of carbon flow during deacidification in both malic enzyme and PEPCK CAM plants. These are discussed in relation to our present understanding of enzyme localisation, the transport of metabolites, energy requirements and charge balance. The implications of these schemes for the regulation of glucan and sucrose synthesis in the light, and the degradation in the dark in CAM plants, are discussed.

ABBREVIATIONS

ADP	Adenosine diphosphate
AMP	Adenosine monophosphate
ATP	Adenosine triphosphate
Bicine	N,N-bis(2Ohydroxyethyl)glycine
BSA	Bovine serum albumin
CAM	Crassulacean acid metabolism
CHO	Carbohydrate
DCMU	3-(3,4-dichlorophenyl)-1,1-dimethylurea
DHAP	Dihydroxy-acetone phosphate
DNPH	Dinitrophenyl hydrazine
1,3-DPGA	1,3-diphosphoglyceric acid
2,3-DPGA	2,3 diphosphoglyceric acid
DTT	Dithiothreitol
EDTA	Ethylenediamine tetraacetate
EMP	Embden-Meyerhof pathway
EtOH	Ethanol
FCCP	Carbonyl cyanide, p-trifluoro-methoxy phenyl hydrazone
FDPase	Fructose diphosphatase
F-6-P	Fructose-6-phosphate
F-1,6-P_2	Fructose-1,6-diphosphate
f.wt	fresh weight
G-1-P	Glucose-1-phosphate
G-3-P	Glyceraldehyde-3-phosphate
G-6-P	Glucose-6-phosphate
HEPES	(N-2-hydroxyethylpiperazine-N-2-ethanesulfonic acid)
Keq	Equilibrium constant
Km	Michaelis constant

Ki	Inhibition constant
LDH	Lactate dehydrogenase
MDH	Malate dehydrogenase
MES	(2[N-morpholino]ethane sulfonic acid)
MPA	Mercaptopicolinic acid
NAD	Nicotinamide adenine dinucleotide
NADH	Reduced nicotinamide adenine dinucleotide
NADP	Nicotinamide adenine dinucleotide phosphate
NADPH	Reduced nicotinamide adenine dinucleotide phosphate
OAA	Oxalacetate
PCR	Photosynthetic carbon reduction cycle
PEP	Phosphoenolpyruvate
PEPCK	Phosphoenolpyruvate carboxykinase
PFK	Phosphofructokinase
2-PGA	2-phosphoglyceric acid
3-PGA	3-phosphoglyceric acid
Pi	Orthophosphate
PPi	Pyrophosphate
PPO	2,5-diphenyloxazole
PVP	Polyvinylpyrrolidone
Q_{10}	Temperature quotient
RNA	Ribonucleic acid
R-5-P	Ribose-5-phosphate
Ru-5-P	Ribulose-5-phosphate
RuP_2	Ribulose bisphosphate
TCA	Tricarboxylic acid
TES	(N-tris[hydroxymethyl]methyl-2-aminoethane sulfonic aci

ACKNOWLEDGEMENTS

This thesis is directly or indirectly the result of contributions, not necessarily academic, by many people with whom I came in contact in Canberra.

Lyn Cambridge, Prue Kell, Liz Marchant, Dixie Nott, Sally Thompson and Erika Winter came to my aid at various times, when two hands were not enough. Jean Hardy washed mountains of glassware often without thanks.

Dr Klaus Winter grew the *Mesembryanthemum* plants used in these experiments, and the enzyme studies presented in Chapter 4.3 were done jointly with him.

Vic Southwell and his staff maintained the growth cabinets and the gentlemen from the workshop forgave me for kicking the spectrophotometer.

Dr Roger Summons instructed me in the use of the gas chromatograph/ mass spectrometer when he had other, more important, things to do.

Dr Murray Badger, Dr Dave Day, Madeleine Jones, Dixie Nott, Steve Powles and Dr Chin Wong came to my aid in a number of capacities, particularly as recipients and contributors of ideas, proof readers and, not in anyway least, as friends. I am especially endebted to Dr Klaus Winter who not only taught me about CAM plants that live outside constant environment chambers, but was always willing to discuss what were frequently untenable ideas and who was an active and conscientious critic.

Both Dr Dave Day and Dr Klaus Winter allowed me to quote their unpublished data.

Peter Cochrane, Anne Gallagher, Madeleine Jones, Dixie Nott, Anne Warrener, Erika Winter and Dr Chin Wong helped with many of the illustrations. Jill Hardy deciphered my writing, defied my grammar and endured my inconsistencies to type this thesis with skill.

I would like to express my gratitude to my supervisors, Dr Hal Hatch and Professor Barry Osmond, who always made their valuable time available for me to waste, and who were a source of ideas and critical comments. In particular I would like to thank Barry Osmond who initially suggested the project, and who acted as both a supervisor and, at times, a confessor, and whom, I suspect, had more confidence in me than, I must admit, I did.

TABLE OF CONTENTS

TABLE OF CONTENTS (continued)

TABLE OF CONTENTS (continued)

TABLE OF CONTENTS (continued)

1 CAM: A REVIEW OF THE LITERATURE

1.1 Introduction

Crassulacean acid metabolism (CAM) is a term used to describe a set of physiological and biochemical properties of photosynthetic tissues of numerous leaf, stem and root succulent plants. The possession of CAM infers the ability of the tissue to fix CO_2 in the dark, resulting in the synthesis, and subsequent accumulation, of free malic acid in the vacuole. The acid is decarboxylated in the following light period and the CO_2 is refixed by the PCR (or Calvin) cycle. Both the CO_2 and the 3-carbon skeleton produced during decarboxylation are converted to storage carbohydrates. This biochemical rhythm is reflected in a reciprocal day/night acid carbohydrate fluctuation and is integrated with stomatal opening during the night, and stomatal closure at least during the first few hours of the light period. Although the phenomena of CAM is defined in biochemical and physiological terms, the basic rhythm is modulated by a variety of developmental and environmental factors. These factors include day/night temperatures, water stress, day length, light intensity, leaf age and prehistory, and the state of development of the plant. These factors regulate and determine both the daily cycles and the overall total expression of CAM.

The early investigations of CAM, which were mainly concerned with the biochemistry and physiology of dark metabolism have been reviewed by Evans (1932), Bennett-Clark (1933), Burris (1953), Bruinsma (1958), Wolf (1960), Ranson and Thomas (1960) and Walker (1962). CAM has since been the subject of a number of either general reviews, or reviews which have, in the majority, reflected the relatively recent trend towards ecophysiological studies (Ting, 1971; Ting *et al.*, 1972; Ting and Szarek, 1975; Marcelle, 197

Kluge, 1976a, 1976b; Ting, 1976, Winter and Lüttge, 1976; Queiroz, 1977; Osmond, 1978; Dittrich, 1979; Queiroz, 1979; Kluge and Ting, 1979; Osmond and Holtum, in prep.).

The review by Osmond (1978) and the monograph by Kluge and Ting (1979) are probably the most informative general reviews, whilst Kluge (1976b) summarises the major schools of thought concerning the day/night regulation of CAM. For discussions of the environmental and developmental factors affecting CAM, the reader can refer to reviews by Osmond (1978), Queiroz (1977, 1979) and Kluge and Ting (1979). The latter authors have also discussed the taxonomic and geographic distribution of CAM plants, and species check lists have been produced by Black and Williams (1976) and Szarek and Ting (1977). The former list however contains some misinterpretations and some non-CAM succulents are listed as CAM plants.

As the ecophysiological aspects of CAM have been both recently and adequately reviewed, the following literature review will be limited to a discussion of biochemistry and physiology of CAM and of those factors which regulate the daily rhythm of CAM.

1.2 The Biochemistry and Physiology of CAM

At least four phases of CO_2 assimilation can be distinguished during the day/night rhythm of well-watered CAM plants (Figure 1.1)(Osmond, 1975). Even though three of these phases represent non steady state conditions and the overall magnitude of their expression is determined by developmental and environmental factors, the biochemical events which take place during each phase are sufficiently distinct that they can be discussed separately. It is logical to consider these in a sequence

Figure 1.1 Day/night fluctuations of CO_2 uptake, stomatal resistance and malic acid content in a well-watered CAM plant, showing the 4 phases of CO_2 assimilation described in the text (after Osmond, 1978).

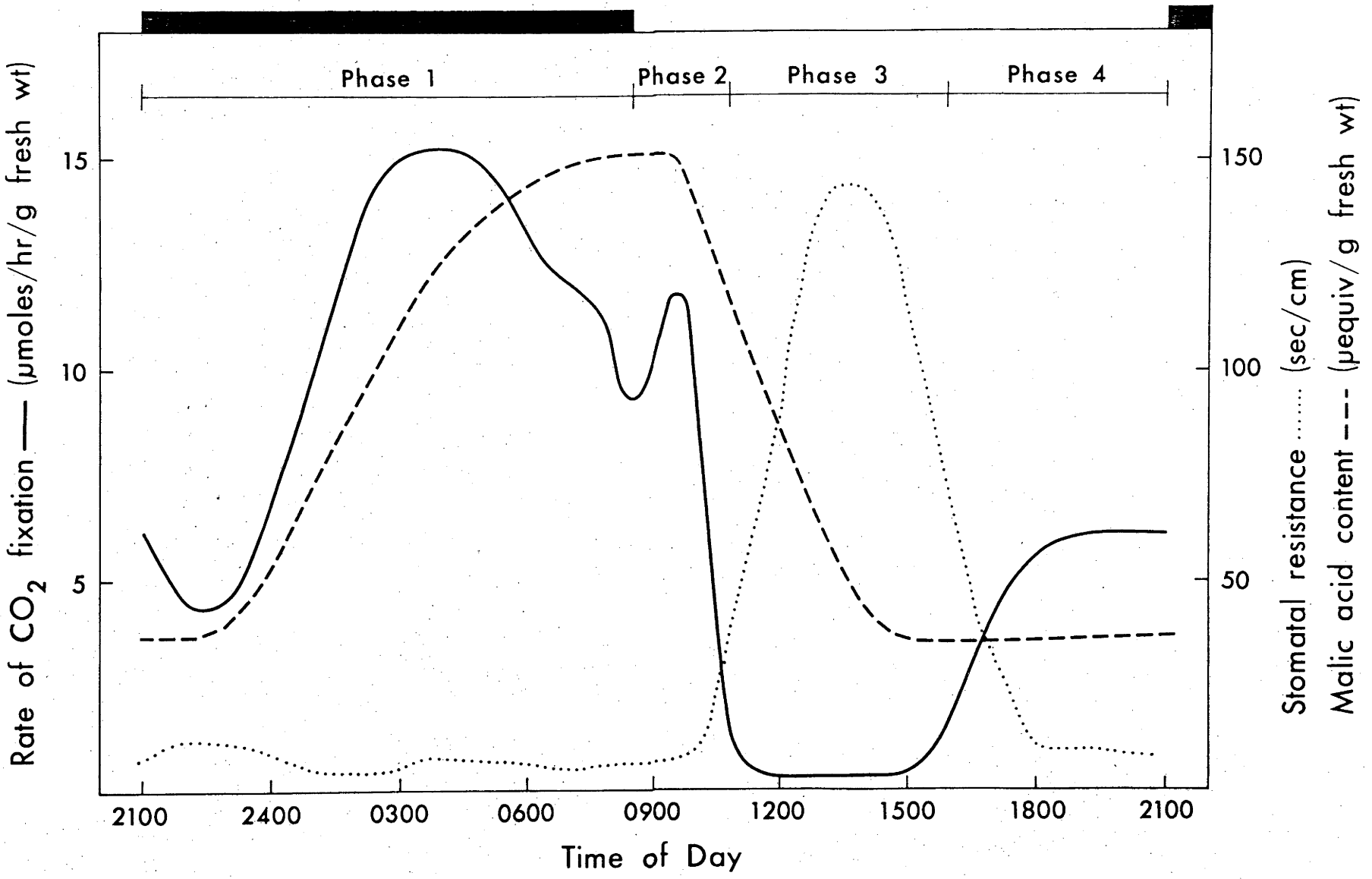
Phase 1
Phase 2
Phase 3
Phase 4
15
10
5
150
100
50
2100
2400
0300
0600
0900
1200
1500
1800
2100
Time of Day
Rate of CO_2 fixation —— (μmoles/hr/g fresh wt)
Stomatal resistance ..... (sec/cm)
Malic acid content - - - (μequiv/g fresh wt)

starting with the unique dark CO_2 fixation processes which lead to malate synthesis as outlined below. However, the experimental work described in this thesis relates principally to processes in phases 3 and 4 and is primarily concerned with pyruvate metabolism in the light.

1.2.1 The dark processes

1.2.1.1 *CO_2 fixation and malic acid synthesis (Phase 1)*

A major distinguishing feature of CAM plants is their ability to fix CO_2 in the dark and to accumulate the malic acid so synthesised. Tissue malate may fluctuate by as much as 200 μEq g^{-1} f.wt during a single diurnal period (eg. Kluge, 1968b). Although it is now well established that malate is produced via the action of PEP carboxylase and NAD MDH according to equation 1 (cf. Wolf, 1960; Ranson and Thomas, 1960; Walker, 1962; Sutton, 1974; Kluge and Ting, 1979)

$$\text{PEP} + CO_2 \xrightarrow[\text{PEP carboxylase}]{Mg^{2+}} \text{OAA} + \text{Pi} \xrightarrow[\text{NAD MDH}]{\text{NADH} \rightarrow \text{NAD}} \text{MALATE} \qquad (1)$$

there has been a prolonged controversy as to whether a double carboxylation involving an earlier carboxylation by RuP_2 carboxylase, occurs (Figure 1.2).

The double carboxylation hypothesis, originally suggested as a possible option by Beevers and Gibbs (1954) and Gibbs and Beevers (1955), was developed by Bradbeer *et al.* (1958) to explain why the ratio of label between carbons 4 and 1 of dark labelled malate was always about 2:1 (Varner and Burrell, 1950; Stiller, 1959). One would predict that $^{14}CO_2$ solely incorporated by PEP carboxylase should result in malate labelled only in the carbon-4 position. This 2:1 ratio has been frequently observed (eg. Jolcine, 1959; Bradbeer, 1963; Avadhani *et al.*, 1971). Recent investigation

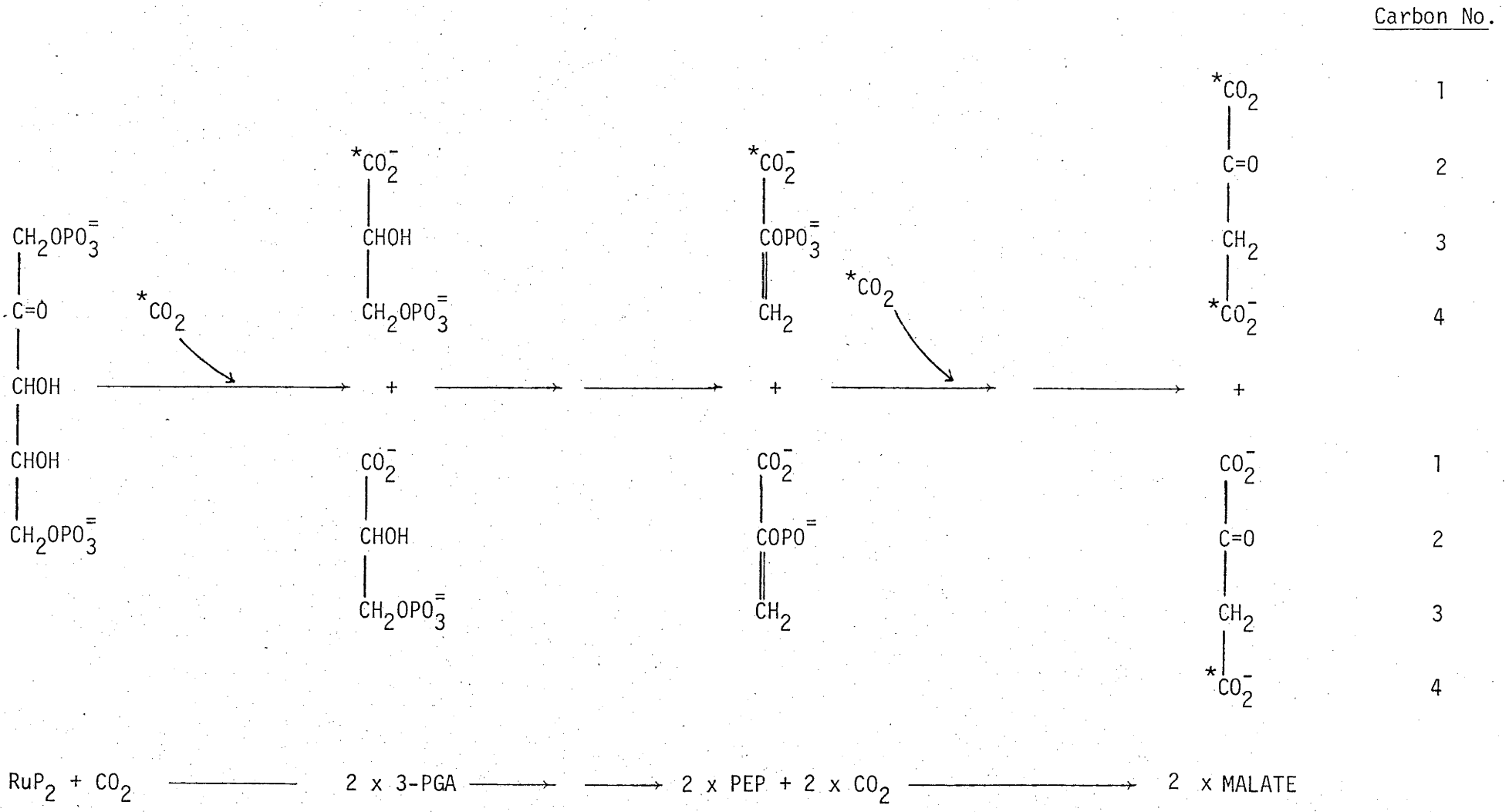

Figure 1.2 The principal reactions of the double carboxylation hypothesis proposed by Bradbeer *et al* (1958) to explain the 2:1 distribution of ^{14}C between carbons 4 and 1 in dark synthesised malate.

have unequivocally shown that although the 2:1 ratio is not an artefact, it is not the result of a double carboxylation. Short term $^{14}CO_2$ feeding experiments, in which ^{14}C-malate was degraded using malic enzyme, demonstrated that after 1 minute labelling > 90% of the label was in the C-4 position although randomisation did occur after longer exposure time (Sutton and Osmond, 1972; Bradbeer *et al.*, 1975).

Cockburn and McAulay (1975a, 1975b) showed, using mass spectrometry, that although malate was labelled in a 2:1 ratio after 12 hours $^{13}CO_2$ fixation, no malate molecules contained ^{13}C in both 1 and 4 carbons. They concluded that a single carboxylation occurred and this was followed by randomisation of the label. The same conclusion was reached by Kluge *et al.* (1974, 1975) who demonstrated that exogenously applied PEP, although it stimulated carboxylation, did not alter the ratio.

The low $\delta^{13}C$ values, high CO_2 affinity and the insensitivity of dark CO_2 assimilation to O_2 concentrations above 2% also support the sole participation of PEP carboxylase in dark CO_2 fixation, rather than a mechanism involving RuP_2 carboxylase (Nalborcyzk *et al.*, 1975; Osmond and Björkman, 1975).

The randomisation of the 1 and 4 carbons of malate by fumarase activity in the mitochondria, a possibility earlier discounted by Bradbeer *et al.* (1958), was supported by Dittrich (1976) who showed that in *K. fedtschenkoi* cell aggregates (1) no 3-PGA was labelled during dark $^{14}CO_2$ fixation, (2) Ru-5-P and R-5-P did not stimulate dark $^{14}CO_2$ fixation, (3) randomisation was independent of $^{14}CO_2$ fixation, (4) 4-^{14}C-aspartate also gave rise to 2:1 labelled malate, and (5) the cells were capable of converting malate to fumarate. The fairly rapid randomisation of label suggests that a large

proportion of malate enters the mitochondria before being stored in the vacuole. Recent studies have shown that isolated *K. daigremontiana* and *Sedum praealtum* mitochondria are highly permeable to malate (Arron *et al.*, 1979; Day, unpublished; Spalding *et al.*, unpublished). The permeability of CAM mitochondria to malate probably also explains the small amount of label present in TCA cycle acids, serine and glycine often observed in dark $^{14}CO_2$ labelling experiments (cf. Saltman *et al.*, 1957; Ting and Dugger, 1968).

1.2.1.2 *Provision of substrates for carboxylation*

During the 1940's and 50's, investigators from several laboratories demonstrated that the carbon loss from starch was adequate to account for the increase of carbon in malic acid (Pucher *et al.*, 1949; Vickery, 1953, 1957). Soluble sugar pools were shown to undergo little or no change and so were not considered as a source, although the possibility that they may be involved in the flow of carbon from starch to malate was not excluded.

Sutton (1974, 1975a) however, observed that the carbon loss from starch, defined as perchloric acid-soluble polysaccharides which can be precipitated in iodine, in *K. daigremontiana* and *B. tubiflorum* accounted for only between 34% and 93% of the carbon required for the observed malic acid synthesis. He then demonstrated that the carbon shortfall is most probably supplied by perchloric acid soluble polysaccharides which do not co-precipitate with starch in the presence of iodine, and which appear to possess some of the characteristics of dextrins. The term glucan will henceforth be used to describe the combined fractions.

The precise mechanism of glucan catabolism is uncertain. Initially, *K. daigremontiana* and *B. tubiflorum* were observed to possess an active phosphorylase whereas amylase was inactive and glucokinase activities were very low (Sutton, 1974, 1975b,c). This enzyme distribution was interpreted as further circumstantial proof that a major fraction of glucan consisted of α-D-(1→4) linked glucose chains such as make up dextrins. However, in subsequent studies Vieweg and de Fekete (1977) and Dittrich (unpublished) demonstrated the presence of active α- and β-amylases in *K. daigremontiana*. Consequently the relative contributions of phosphorylase and amylase to glucan breakdown remains unresolved.

Sutton (1974, 1975b) was also able to demonstrate that the soluble sugar pools were not in the mainstream of carbon flow from glucan to malate. Furthermore, the low G-6-P dehydrogenase capacity in *K. daigremontiana* and *B. tubiflorum* compared to the higher glucose-phosphate isomerase and phosphofructokinase capacities indicated, in contrast to the findings of Beevers and Gibbs (1954) and Stiller (1959) who used ^{14}C glucose tracing techniques, that the pentose phosphate pathway is not involved to any great extent in dark malate synthesis.

Further support for the views of Sutton has been provided by Deleens and Garnier-Dardart (1977) who studied the $\delta^{13}C$ values of various fractions isolated from *K. daigremontiana* and observed that the $\delta^{13}C$ values of dark synthesised malate were not consistent with being derived from a sugar precursor, but were consistent with a glucan origin. Sutton (1974, 1975a,b) showed that the capacities of the various glycolytic enzymes in *K. daigremontiana* and *B. tubiflorum* are sufficient to convert glucan to PEP at the rates required for maximum acidification (about 0.5 μmoles mg chl^{-1} min^{-1}) and concluded that PEP was produced in the dark by glycolysis.

1.2.1.3 *Compartmentation*

CAM chloroplasts commonly possess large numbers of starch grains (Kluge and Ting, 1979) and it is reasonable to assume that, in common with C_3 and C_4 plants, starch and the other polysaccharides which constitute the glucan fraction are synthesised in the chloroplasts.

Recent evidence on the compartmentation of enzymes in *Sedum praealtum*, *K. daigremontiana* and *Ananas comosus* indicates that, similar to C_4 plants, at least 90% of the PEP carboxylase is cytoplasmic (Spalding *et al.*, 1979; Dittrich, unpublished). In *Sedum praealtum* PGA-mutase and enolase also appear restricted to the cytoplasm and NAD MDH, as in *Kalanchoe*, was observed in both the cytoplasmic and mitochondrial fractions (Spalding *et al.*, 1979). However, in contrast to NAD malic enzyme type C_4 plants, only 10-15% of the aspartate aminotransferase activity in *K. daigremontiana* is located in the mitochondria (D. Day, unpublished).

The view has long been held, without any experimental basis, that the malic acid synthesised and accumulated during dark CO_2 fixation is stored in the vacuole. CAM cells are characterised by the possession of large vacuoles which occupy over 90% of their total cell volume and which can presumably adequately store the large volumes of acid accumulated nightly (cf. Kluge and Ting, 1979). Calculations based on leaf volumes and dark acid accumulation suggest that if the malic acid was stored in the cytoplasm the concentration would be 7-8 M as compared with 0.25 M if it was stored in the vacuole (Stiller, 1959). Such high cytoplasmic concentrations would undoubtedly lower the pH and damage most cytoplasmic metabolism. Furthermore, ^{14}C feeding experiments indicate that less than 30% of the malic acid in the dark is in equilibrium with the mitochondria in *Bryophyllum* (MacLennan *et al.*, 1963). Kluge and Heininger (1973) demonstrated three malate

containing compartments in malate efflux studies with *K. daigremontiana* leaf slices. Malate was rapidly released from the first two compartments which the authors interpreted as representing the free space in the cell walls and cytoplasm respectively, but was only slowly released from the third compartment which was interpreted as being the vacuole. Although this study can be criticised on methodological grounds (Osmond, 1978) it indicates the presence of a large, malate containing compartment which is almost certainly the vacuole.

Intact vacuoles have been obtained from enzymatically isolated *K. daigremontiana* protoplasts by lysing the protoplasts with DEAE dextran (Buser and Matile, 1977). The vacuoles contained more than 84% of the malic acid present in the protoplasts. The vacuoles also contained 60-80% of the potassium ions, 86-90% of the calcium ions and about 50% of the total amino acids. Although acid RNase and phosphatase were present, the vacuoles contained virtually no protein and no NADP malic enzyme or RNA. A subsequent investigation of vacuoles from *Sedum telephium* (Kenyon *et al.*, 1978) demonstrated that vacuoles isolated in the light period contained about 0.02-0.04 nmole malic acid vacuole^{-1} whereas vacuoles isolated at the end of the dark period contained 0.5-0.75 nmoles malic acid vacuole^{-1}. The isocitric acid levels remained constant at 0.12 nmoles vacuole^{-1} throughout a 24 hour cycle. Moreover, vacuoles isolated from tissue fed $^{14}CO_2$ in the dark contained 46% of the label and 5% was in insolubles as compared with 4% in the vacuoles and 92% in insolubles in light fed tissue.

Figure 1.3 represents a scheme which incorporates present concepts of the compartmentation and biochemistry involved in dark CO_2 fixation

Figure 1.3 Schematic representation of the principal processes, and their possible compartmentation, involved in carbohydrate metabolism from glucan to malic acid synthesis in CAM plant in the dark.

Solid lines (——) represent the most likely processes, broken lines (---) represent processes of uncertain significance and open arrows (⇨) or (⇢) denote transport across a membrane. The arrows do not imply the irreversibility of reactions.

The enzymes involved in the various reactions are (1) phosphorylase (2) amylase (3) hexokinase (4) phosphoglucomutase (5) hexosephosphate isomerase (6) phosphofructokinase (7) aldolase (8) triosephosphate isomerase (9) G-3-P dehydrogenase (10) phosphoglycerokinase (11) phosphoglyceromutase (12) enolase (13) PEP carboxylase (14) carbonic anhydrase (15) malate dehydrogenase and (16) fumarase.

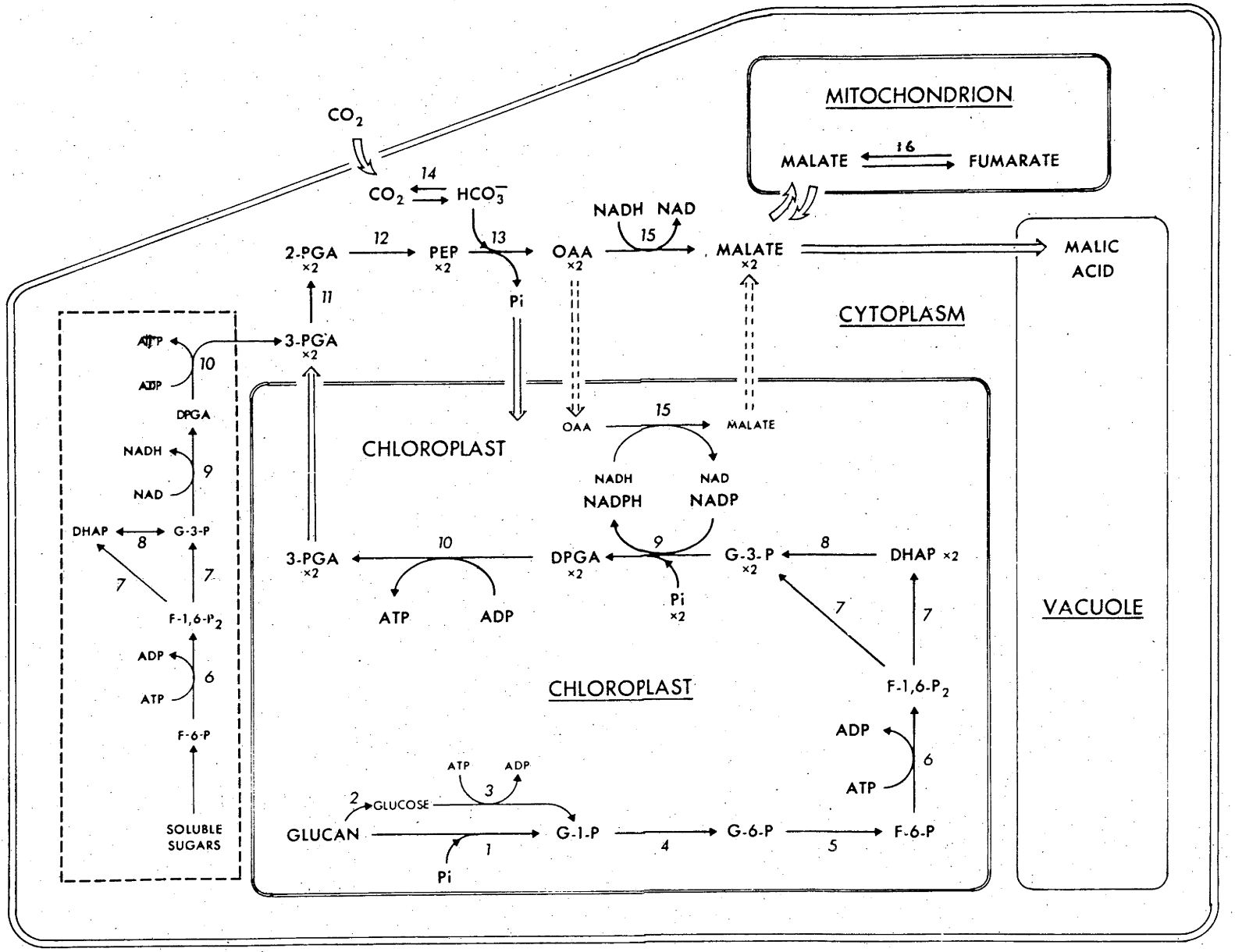
MITOCHONDRION
MALATE
16
FUMARATE
CO_2
14
CO_2
HCO_3^-
NADH NAD
15
2-PGA ×2
12
PEP ×2
13
OAA ×2
MALATE ×2
MALIC ACID
11
Pi
CYTOPLASM
3-PGA ×2
ATP
ADP
10
DPGA
NADH
NAD
9
DHAP
8
G-3-P
7
7
F-1,6-P_2
ADP
ATP
6
F-6-P
SOLUBLE SUGARS
CHLOROPLAST
OAA
15
MALATE
NADH
NADPH
NAD
NADP
3-PGA ×2
10
DPGA ×2
9
G-3-P ×2
8
DHAP ×2
ATP
ADP
Pi ×2
7
7
CHLOROPLAST
F-1,6-P_2
ADP
ATP
6
ATP
ADP
3
2
GLUCOSE
GLUCAN
1
Pi
G-1-P
4
G-6-P
5
F-6-P
VACUOLE

and acid accumulation. The regulation of some of these processes will be considered in the following section.

1.2.1.4 *Regulation*

In this study I shall only discuss the short-term regulation of the dark processes, that is those factors which regulate the dark processes on a daily basis.

It is often noticed both in field and laboratory studies that the light intensity of the previous day determines the rate and total amount of acidification in the following dark period. Both dark CO_2 assimilation and acid synthesis are more rapid after bright days than after dull days. Osmond (1978) considers that the explanation is simply that high light intensities stimulate the rate of deacidification, and thus the tissues are able to both deacidify all the malate formed during the previous night, and to fix CO_2 for longer periods in the late afternoon. Such conditions result in a larger carbohydrate pool being available for dark malate synthesis. For example, the tissue malate content of field grown *Opuntia* is usually much higher at the end of a cloudy day than at the end of a sunny day.

If the malate produced during dark carboxylation remained in the cytoplasm it would reach inhibitory concentrations within 10 minutes (Kluge and Osmond, 1972). It follows that the rate of malate uptake into the vacuoles, and consequently any factors which regulate such uptake, will regulate the cytoplasmic malate concentration and thus will regulate dark CO_2 fixation. As the postulated mechanisms of malate influx and efflux the vacuole will be discussed in Section 1.2.2, it will

suffice to state here that malate influx appears to be an active process and that the extent of dark CO_2 fixation appears to depend on the capacity of the vacuole to store malic acid. As the capacity of vacuoles to store malic acid becomes exhausted towards the end of the dark period the cytoplasmic malate concentration increases, due either to a reduced ability of the influx mechanism to pump malate against an ever increasing concentration gradient or to increased passive diffusion from the vacuoles. This causes PEP carboxylation to slow and eventually cease altogether (see Figure 1.1). Thus the increasing malate concentration at the site of PEP carboxylase may, at least in part, account for the gradually decreasing rate of net malate synthesis.

Phosphorylase and phosphofructokinase may be important in the regulation of the flow of carbon from glucan to PEP (Sutton, 1974, 1975b,c). Phosphorylase from *K. daigremontiana* is inhibited 60% by 1 mM Pi, 20% by 2 mM PEP and 40% by 4 mM glucose. However, speculations on the importance of the regulatory properties of phosphorylase must remain tentative as the relative contributions of phosphorylase and amylase to glucan breakdown are unknown (Sutton, 1974; Vieweg and de Fekete, 1977; Dittrich, unpublished). Phosphofructokinase, which is known to be an important glycolytic regulatory enzyme in animal tissues, has all the characteristics of a regulatory enzyme. It possesses allosteric regulatory properties, catalyses a physiologically irreversible reaction, and is present with an activity just sufficient to accommodate starch degradation. The enzyme from different plant tissues exhibits either positive or negative co-operativity towards the substrate F-6-P, inhibition by ATP when $[ATP]>[Mg^{2+}]$ and is regulated allosterically by a number of metabolites including glycollate-2-phosphate, PEP, 2-PGA, 3-PGA, citrate, and Pi;

Pi also relieves PEP inhibition (Kelly and Latzko, 1977a,b). Chloroplastic and cytoplasmic forms have been shown to be present in spinach (Kelly and Latzko, 1975). The enzyme from *K. daigremontiana* is inhibited 40% by 4 mM malate and 70% by 1 mM PEP (with or without Pi), although the enzyme is 100 fold less sensitive to PEP at low F6P concentrations, than the enzyme from the C_4 plant *Atriplex spongiosa* (Sutton, 1974, 1975c). It is unlikely however that either PEP or malate influences either phosphorylase or PFK *in vivo* since, as shown in Figure 1.3, both are most likely to be chloroplastic whilst PEP and malate are most likely to be formed in the cytoplasm. If however, either malate enters the chloroplast during acidification or OAA is converted to malate in chloroplasts, and if the chloroplasts of some CAM plants are capable of PEP exchange via a phosphate translocator (see Chapter 5), these metabolites may interact with PFK during glucan mobilisation. The PFK in the cytoplasm, which makes up about 70% of the spinach enzyme, is presumably readily modified by these effectors.

Glucose-6-phosphate concentration increases during the early part of the dark period in both *K. daigremontiana* and *K. blossfeldiana* (Cockburn and McAuley, 1977; Pierre and Queiroz, 1979) and it has been suggested that this increased G-6-P concentration may activate PEP carboxylase (Cockburn and McAuley, 1977). The suggestion depends upon whether G-6-P and PEP carboxylase are in the same compartment. Increases in chloroplastic G-6-P concentration will not affect the cytoplasmic PEP carboxylase since chloroplasts are not readily permeable to hexose phosphates (Walker, 1976). G-6-P is particularly efficient at relieving malate inhibition of CAM PEP carboxylase by lowering the Km PEP (Ting and Osmond, 1973; Nott, personal communication). This may be a more logical role again assuming it is in the same compartment.

PEP carboyxlase is also subject to feedback inhibition by malate and activation by Pi (Kluge and Osmond, 1972). Recent evidence (Greenway *et al.*, 1978; Winter, unpublished) has shown that PEP carboxylase from CAM *Mesembryanthemum crystallinum* and *Aloe arborescens*, when assayed in the first 2-3 minutes following extraction, may exist in either a relatively malate insensitive state with a high PEP affinity or in a malate sensitive state with a lower PEP affinity. It is possible that such changes in characteristics may involve changes in the form of the enzyme. Jones *et al.* (1978) purified PEP carboxylase from *K. fedtschenkoi* and found no evidence of isoenzymes or sub-unit heterogeneity. They speculated that any regulation of, or by, PEP carboxylase would most probably involve reversible conformation changes.

It has been argued that two separate glycolytic pathways operate in CAM cells during the dark (Deleens and Garnier-Dardart, 1977). The proposal is that carbon for acidification is provided by the mobilisation of glucan and carbon for respiration is supplied from the soluble sugar pools. Bradbeer and Ranson (1963) fed U-^{14}C labelled glucose to *K. crenata* leaf fragments in the dark and concluded that the glucose was metabolised via the TCA cycle. However, after 5 minutes exposure all the detectable label was in alanine and malate, and after 1 hour exposure 72% of the label wasin malate. It is possible that a proportion of the label in malate may have been due to the refixation of respired $^{14}CO_2$ but the conclusion is equivocal. Although the size of the soluble sugar pools in *K. daigremontiana* does not change during the light, the sugars which were previously labelled by 2 hours $^{14}CO_2$ fixation in the light lose ^{14}C during the dark and a similar increase in the radioactivity of the citrate and isocitrate fractions is observed (Sutton, 1974, 1975a). Deleens and Garnier-Dardart (1977) interpreted this observation as evidence that soluble sugars are metabolised

solely by the TCA cycle. This does not follow, since the pool sizes of the sugar and acid fractions may be different and a substantial part of the isocitric and possibly also the citric acid pool is located in the vacuole, not in the mitochondria (Kenyon *et al.*, 1978). Furthermore, it is well know that there is a substantial transfer of label between malate and the TCA cycle acids. The reciprocal change in radioactivity of the two fractions may be nothing more than coincidence.

Another argument for the participation of two glycolytic pathways in the dark involves the observation that at high night temperatures both glucan degradation and malic acid synthesis cease but respiration continues at an increased rate (Sutton, 1974; Kaplan *et al.*, 1976). The implication is that the carbon source for TCA cycle activity must be the soluble sugars. It is possible that the increased rate of respiration provides energy for the initiation or increase of malate decarboxylation which would in turn provide PEP or pyruvate for respiration, whilst simultaneously stopping any net malate synthesis.

It is hard to envisage how two glycolytic streams could be spatially separated within the cell, particularly since the PGA mutase, enolase, PEP carboxylase and, presumably, also the pyruvate kinase are all cytoplasmic enzymes. Whereas in C_4 plants the carboxylating and decarboxylating enzymes are spatially separated, in CAM plants they are in the same cell and in the cases of PEP carboxylase, NADP malic enzyme and PEPCK, the same compartment. Presumably for net acid accumulation to occur either decarboxylation has to be suppressed, the rate of carboxylation must be greater than that of decarboxylation, or possibly the malate is rapidly removed to another compartment. The activities in the dark of the

decarboxylases involved in CAM are not known, although it is assumed that they will mainly be regulated by the availability of NAD, NADP and ATP rather than by the availability of substrates. However, as deacidification does occur under conditions of continuous darkness, presumably these co-factors can be provided by dark respiration. Dark deacidification can be initiated in *K. daigremontiana* illuminated with far red light in the presence of oxygen (Nalborcyzk *et al.*, 1975). The deacidification depends on the continued presence of far red light. This interesting effect has yet to be explained or confirmed but presumably the O_2 requirement implies the involvement of respiration. It is not known whether malate efflux from the vacuoles is stimulated or whether deacidification *per se* by NADP and/or NAD malic enzyme is involved. NADP malic enzyme from C_4 plants appears to be inactive in the dark, although this may be due to a restricted supply of NADP (Osmond, 1974).

Brandon (1967) observed that NADP malic enzyme and PEP carboxylase from *B. tubiflorum* have different thermal stabilities. He concluded that the common observation that dark acidification is favoured by cooler night temperatures indicates that the short term regulation of dark acid synthesis is determined by the relative activities of the carboxylating and decarboxylating enzymes. The effect of temperature on the amplitude of CAM is probably due to other reasons since acid fluctuations are often observed in plants growing under constant temperature conditions (Kluge, 1976). For example, acidification in field grown *Opuntia inermis* which kept their stomata open throughout the night, was insensitive to temperatures between 5 and 25°C (Osmond, 1978).

Osmond (1978) argues that if both carboxylation and decarboxylation rates are higher at increased temperatures then one would expect a

commensurate increase in glucan degradation. However, glucan mobilisation appears to decrease with increasing temperature (Kluge, 1969b; Sutton, 1974). An increase in temperature is often accompanied by a decrease in net CO_2 assimilation, or sometimes even an efflux, which is most probably due to an increase in dark respiration which increases between 14°C and 24°C with a Q_{10} of about 2.4 (Brunnhöfer *et al.*, 1968; Neales, 1973; Allaway *et al.*, 1975; Kaplan *et al.*, 1976).

Queiroz and co-workers have argued that the regulation of both the light and dark processes of C_3 and CAM *K. blossfeldiana* var. Tom Thumb and possibly other CAM plants as well, is under endogenous circadian control (see Queiroz, 1979, for a recent review). The current concept appears to be that the daily CAM rhythm is dependent ("entrained") upon the combined effects of a dawn signal and a dusk signal driving two different "clock-controlled" oscillators. This can be observed on a metabolic level as rhythmical, diurnal fluctuations in various glycolytic metabolite levels and in the crude activities of PEPC, NADP malic enzyme, aspartate aminotransferase and various glycolytic enzymes (Pierre and Queiroz, 1979; Queiroz, 1979). The relevance of these rhythmical, diurnal variations to the diurnal regulation of CAM is conjectural since the minimum daily activities of all the enzymes studied, with the exception of PFK and NADP malic enzyme which are present in low activities, are between 12 and 150 times the maximum rates of dark acidification (data from Pierre and Queiroz (1979), assuming a fresh weight/dry weight ratio of 10, chlorophyll content of 0.4 mg chl^{-1} g^{-1} f.wt, and a maximum acidification rate of 30 µmoles mg chl^{-1} hr^{-1}). A major criticism of the report of Pierre and Queiroz (1979) is that although the enzyme rhythms were shown for *K. blossfeldiana* during the development of CAM under short day conditions,

no data was presented on the rhythms in control plants kept under long day conditions for a similar period of time. Such information is important so that the reader can assess the effects of any developmental changes. It also remains to be shown whether the rhythms observed in *K. blossfeldiana* var. Tom Thumb are observed in other CAM plants.

1.2.2 Vacuolar influx and efflux

The accumulation of malic acid in the vacuoles requires the transport of malate from the cytoplasm against a steadily increasing concentration gradient, and implies the possession of an active pumping mechanism. The accumulation of malic acid is unusual in view of the amount of acid which is accumulated (up to 200 $\mu eq\ g^{-1}$ fr. wt.), the speed at which the acid is accumulated, and because hydrogen malate ($malate^{-1}$) rather than the more common anionic malate ($malate^{-2}$), is accumulated (Osmond, 1978). Lüttge and Ball (1979, in press) have proposed that, in *K. daigremontiana*, hydrogen malate is formed inside the vacuole and the actual pump involves the active transport of protons coupled with a passive co-transport of $malate^{2-}$. The energy requirements of the system are unknown.

The efflux of malic acid from the vacuoles, rather than requiring a reversal of the influx mechanism, appears to be passive, i.e. the influx pump appears to be either deactivated or possibly less active in relation to the efflux forces (Lüttge and Ball, 1974a, 1977). In leaf slices, malate efflux can be initiated by changing cell turgor, but not by changing cell water potential. The efflux is dependent on the turgor at any one time and is not triggered by transient changes in cell turgor (Lüttge *et al.*, 1977). This model of vacuolar control requires a, as yet unproven, sudden pressure dependent alteration of the tonoplast

permeability at a critical turgor pressure. The turgor effect has been demonstrated *in vitro* by Lüttge *et al.* (1975) who induced a diurnal rhythm of acid accumulation and loss in leaf slices from *K. daigremontiana* by varying the osmotic pressure of the suspension medium. Subsequent observations with intact *Kalanchoe* tissue indicated that although the malic acid rhythm contributed to a rhythm of water potential, the turgor remained practically unchanged during the diurnal cycle (Lüttge and Ball, 1977). Day/night acid fluctuations have also been observed in the field in water stressed CAM plants which kept their stomates shut throughout the day and night and which presumably remain at a constant low turgor (Szarek *et al.*, 1973).

Vacuolar influx and efflux is probably not under the singular control of turgor. Light/dark transients often trigger changes in tissue malate levels although it is unclear whether this is a direct light effect since there is usually a lag phase and such transients often induce changes in stomatal aperture. Moreover acid fluctuations have been observed during periods of continuous light (eg. Kluge, 1969c), and when stomates are continuously open or closed. Such observations are hard to interpret since periods of malate accumulation and loss (which are the only presently measureable parameters) may not be strictly related to changes in the tonoplast permeability, but are also functions of the availability of substrate and the relative activities of PEP carboxylase and the decarboxylating enzymes. The levels of adenylate and pyridine nucleotides, Pi and of other metabolites may be important in such regulation.

1.2.3 The light processes

1.2.3.1 *The initial burst of CO_2 assimilation (Phase 2)*

Many CAM plants, under both field and laboratory conditions, exhibit a burst of CO_2 fixation immediately after the onset of illumination which is independent of further stomatal opening (Phase 2, Figure 1.1). Carbon 4 labelled malate is the principal product of $^{14}CO_2$ fixation during this period and, although the bulk of the label stays in malate, there appears to be a slow transfer of label into sugars. This is probably due to either malate decarboxylation and subsequent $^{14}CO_2$ refixation by RuP_2 carboxylase or by fixation directly by RuP_2 carboxylase (Osmond and Allaway, 1974) (Figure 1.4).

Except under certain environmental conditions, the tissue malate content appears to stay more or less constant during this period. Marcelle (1975) observed an increase in O_2 and CO_2 evolution in *K. daigremontiana* tissue exposed to CO_2 free air which demonstrated that some dark fixed malate is decarboxylated during this period. In contrast to plants exposed to long nights (16 hr), plants exposed to short nights (8 hr) show a lag before decarboxylation occurs (Marcelle, 1975). During this lag which lasts about 2 hours, the tissue malate content continued to increase due to the continual transfer of malate into the vacuoles. This indicates that malate leakage from vacuoles which are not near their storage capacity, is minimal. It also suggests that PEP is still being supplied from storage carbohydrates i.e. both the regulation of glucan degradation and vacuolar malate efflux are not directly controlled by light *per se*.

The period and magnitude of the CO_2 fixation burst, which commonly lasts between 30 minutes and 2 hours, is subject to regulation by a variety of environmental factors. However, in general, the effects can be explained

Figure 1.4 Diagramatic representation of the path of carbon during the initial light fixation burst (Phase 1) in a malic enzyme CAM plant (modified from Osmond, 1976).

The thickness of the lines represents the possible activity of the alternative pathways. Broken lines represent uncertain processes. CO_2 enclosed in a box represents endogenously produced CO_2, 3-PGA similarly enclosed represents 3-PGA produced in the PCR cycle and malate, also boxed, represents malate stored in the vacuole.

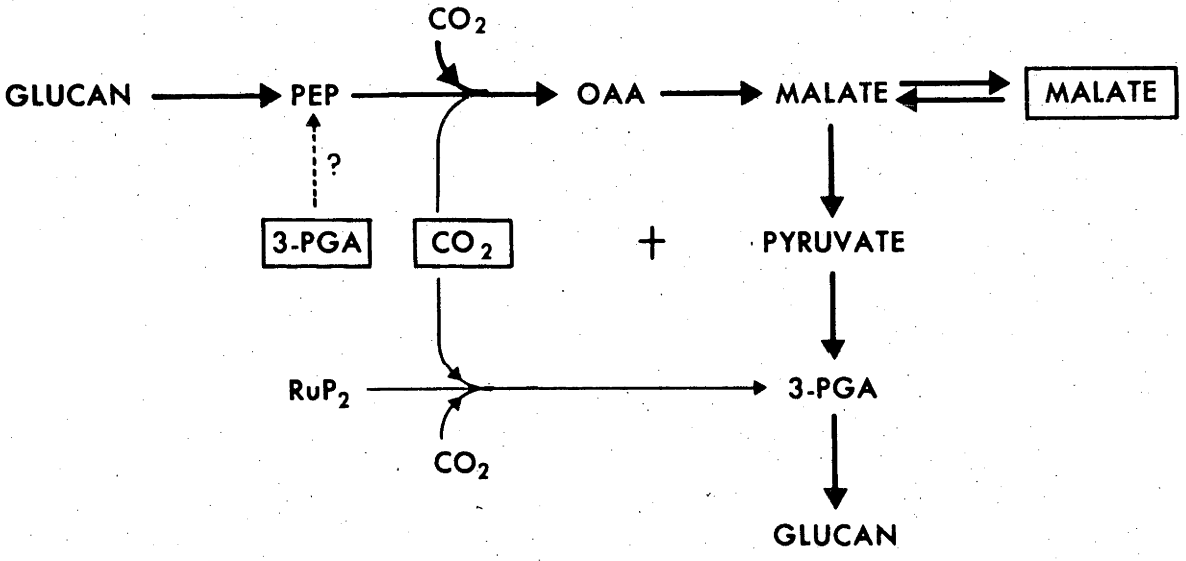
CO2
GLUCAN
PEP
OAA
MALATE
MALATE
?
3-PGA
CO2
+
PYRUVATE
RuP2
3-PGA
CO2
GLUCAN

in terms of tissue malate levels and stomatal opening and closure. The illumination burst is both greater in magnitude and period under conditions in which dark malate accumulation has been inhibited by, for example, extremely low night temperatures (Kluge, 1968b), withholding CO_2 during the dark (Kluge, 1968b) or, as already mentioned, by shortening the dark period (Marcelle, 1975). These factors possibly stimulate the illumination burst because they result in low vacuolar malate contents during the light period and consequently, as long as the substrate PEP is being produced, the tissue will pump light synthesised malate into the vacuole. The effect of turgor on malate accumulation and its possible role in regulating vacuolar influx, efflux and stomatal opening and closure was discussed in Section 1.2.2.

The illumination burst, if not totally suppressed, is smaller in magnitude and period when the previous night temperatures are high (Kluge, 1968b), under long night conditions (Marcelle, 1975), in water stressed tissue (Kluge *et al.*, 1973) and under low light conditions (Kluge *et al.*, 1973; Nobel, 1976). Under long night conditions the vacuoles are probably filled to capacity and the cytoplasmic malate content will be high and thus PEP carboxylase will most likely be inhibited. Under water stress conditions the stomates tend to either close rapidly upon illumination or remain closed throughout a 24 hour cycle. High night temperatures are known to inhibit glucan degradation and prevent any malate accumulation (Kluge, 1968b; Sutton, 1974) and it is possible under these conditions PEP is limiting although one might expect CO_2 fixation by RuP_2 carboxylase. It is possible tha if the stomates have been open during the previous night then the high temperatures could stimulate transpiration, and the resulting drop in leaf water potential may induce stomatal closure.

As Kluge and Ting (1979) have observed, the mechanisms which control the burst of CO_2 uptake will not be fully understood until it is known what controls both the efflux of malate from the vacuole and stomatal opening and closure, and why neither takes place until 30-60 minutes after the onset of illumination. A similar and probably related effect is also consistently observed by Winter (unpublished). PEP carboxylase from CAM *Mesembryanthemum crystallinum* and *Aloe arborescens* switches from a malate insensitive to a malate sensitive form at the same time that efflux and deacidification begins. The switch is independent of illumination as it is also observed under continuous dark conditions when dark deacidification occurs.

1.2.3.2 *Deacidification (Phase 3)*

The dark synthesised and accumulated malic acid is decarboxylated the period following the initial light CO_2 fixation burst (Phase 3 in Figure 1.1, Figure 1.5). During this deacidification period the stomates are closed, there is a minimal fixation of external CO_2, (cf. Kluge *et al.*, 1973; Allaway *et al.*, 1974; Osmond and Allaway, 1974; Sutton, 1974; Neales, 1975) and, concomitant with the decrease in acid level there is an approximately equal increase in the amount of carbon in storage carbohydrates or glucan (Sutton, 1974).

CAM plants contain one or more of 3 malate or OAA decarboxylating enzymes similar in function to those reported in C_4 plants (Dittrich *et al.*, 1973; Hatch *et al.*, 1975; Dittrich, 1976). The distribution of these enzymes between different species, particularly phosphoenolpyruvate carboxykinase (PEPCK), appears to be determined along taxonomic lines. PEPCK is found in the Asclepiadaceae, Bromeliaceae, Euphorbiaceae, Vitaceae and Portulacaceae, but is absent from the Agavaceae, Aizoaceae,

Asteraceae, Cactaceae, Crassulaceae and the Orchidaceae. In the Liliaceae, *Aloe arborescens* and *Apiera spiralis* possess PEPCK but the enzyme is absent from two *Sanseveria* species (*S. hahnii* and *S. trifasciata*). The distribution of the other two decarboxylating enzymes, NADP and NAD malic enzymes, although also separated along taxonomic lines is not so distinct since all CAM plants (or at least the 31 surveyed for both enzymes by Dittrich (1976), and the 25 assayed solely for NADP malic enzyme (Dittrich *et al.*, 1973) appear to possess some activity of both enzymes. However, all those species which do not possess PEPCK have high NADP malic enzyme capacities which are adequate to account for the maximum observed rates of deacidification.

The NADP malic enzyme capacities of PEPCK CAM plants are generally barely sufficient to account for the maximum deacidification rates, except in the Euphorbiaceae which have high activities, but even in these plants the activities are only about 15% of the observed PEPCK activities. NAD malic enzyme activities are well below those required for deacidification, except in the Crassulaceae, and in the Orchidaceae. On average, not counting the Crassulaceae and Orchidaceae, the NAD malic enzyme activities are about 40-50% of the NADP malic enzyme activities in both PEPCK and in non-PEPCK CAM plants.

Strong circumstantial evidence exists which shows that the above-mentioned decarboxylases are involved in deacidification in the light although the relative contributions of different decarboxylases, when more than one decarboxylating enzyme is present in a single tissue, are unknown. The evidence includes (1) radioactivity from dark ^{14}C labelled malate is released as $^{14}CO_2$ from stripped leaves in the light (Kluge, 1968a); (2) a massive

rise in internal CO_2 concentration, which is greater than can be expected from respiratory CO_2, occurs during deacidification (Cockburn *et al.*, 1979; Spalding *et al.*, unpublished); (3) Milburn *et al.*, (1968) observed that in *Bryophyllum* pyruvate levels increased during deacidification; and (4) mitochondria isolated from *K. daigremontiana* and *S. praealtum* contain NAD malic enzyme, and are capable of decarboxylating malate at physiological rates (Day, unpublished; Spalding *et al.*, unpublished).

The transfer of label from malate to carbohydrate has been verified in experiments which have shown that almost all the ^{14}C from dark labelled malate appears in carbohydrates during the following light period (Kunitake and Saltman, 1958; Ting and Dugger, 1968; Sutton, 1974). There may, however, be some loss of CO_2 under high daytime temperature conditions particularly if the light intensity is high (Kluge *et al.*, 1973; Lange *et al.*, 1975).

It is most likely that the CO_2 produced during deacidification is converted to glucan via the PCR cycle since the products of $^{14}CO_2$ fixation during this period are characteristic of fixation by RuP_2 carboxylase (Kluge, 1969; Avadhani *et al.*, 1971). PEP carboxylase is probably inhibited by the high cytoplasmic malate content which is most likely present during deacidification (Kluge and Osmond, 1972; Lüttge and Ball, 1974a 1977). It appears that both the CO_2 and the 3-carbon skeleton products during deacidification are converted to glucan rather than to soluble sugars (Kluge *et al.*, 1973; Sutton, 1974). The path by which the 3-carbon produces of decarboxylation, pyruvate and PEP, are converted to glucan is the principal concern of this thesis and is discussed in more detail below.

Figure 1.5 Diagrammatic representation of the path of carbon during deacidification (Phase 3) in CAM plants in the light (modified from Osmond, 1976). Symbols same as in Figure 1.4.

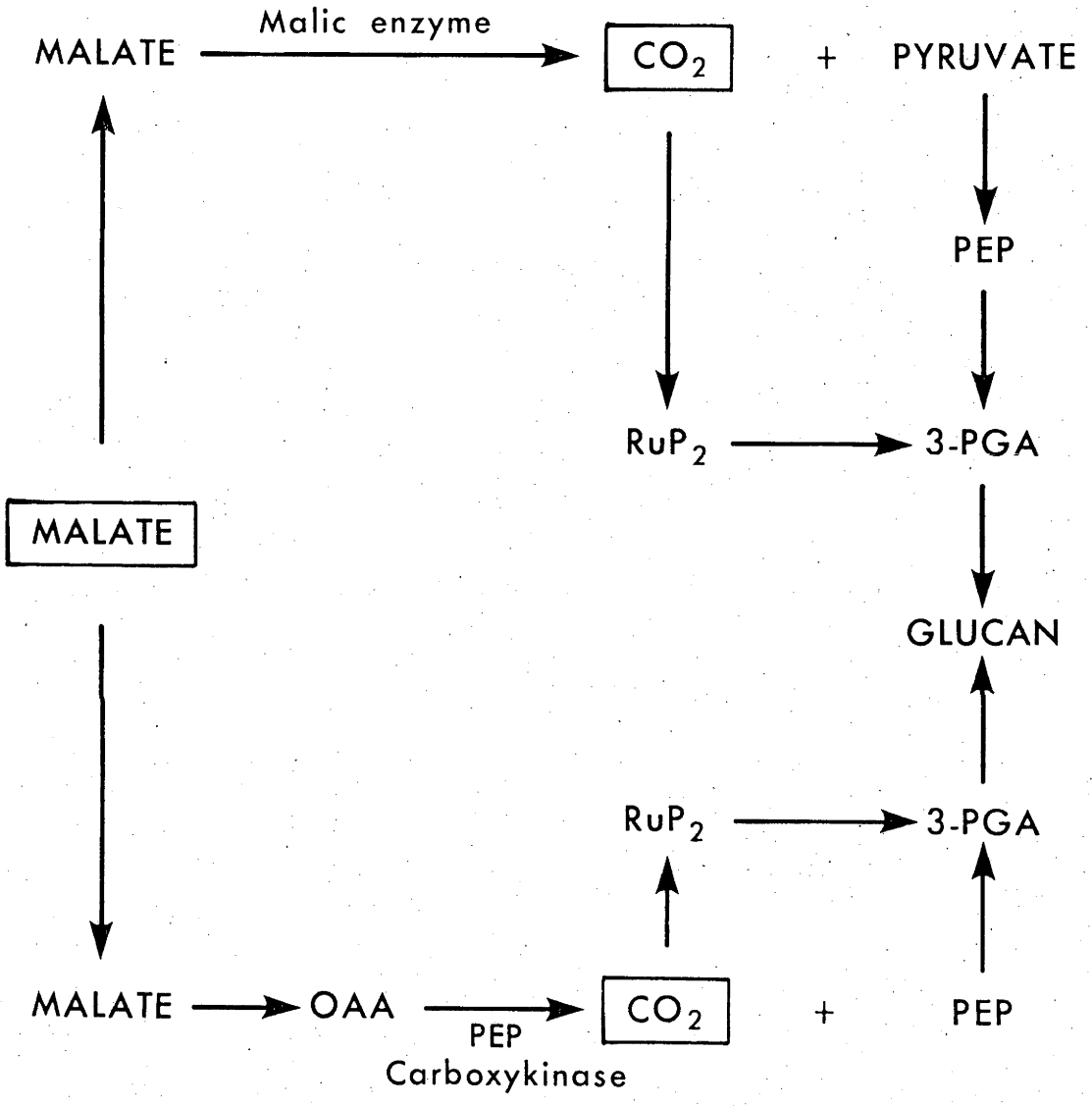
MALATE
Malic enzyme
CO_2
+
PYRUVATE
PEP
RuP_2
3-PGA
GLUCAN
MALATE
MALATE
OAA
PEP
Carboxykinase
CO_2
+
PEP
RuP_2
3-PGA

1.2.3.3 *Post-deacidification light fixation (Phase 4)*

Steady state CO_2 fixation in the light during the post-deacidification period is often observed in CAM plants (Phase 4, Figure 1.1). Osmond and Allaway (1974) demonstrated that in *K. daigremontiana* the initial products (15 second exposure) of $^{14}CO_2$ assimilation during this period were 3-PGA and other phosphorylated compounds. In longer term feeding experiments label accumulates in malate (Kluge, 1969c; Kluge *et al.*, 1973), particularly under low light intensities (Kluge, 1971b), however only between 35% and 55% of ^{14}C malate is in the carbon 4 position which indicates that a considerable proportion of the substrate PEP was previously labelled (Osmond and Allaway, 1974). These observations suggest that a greater part of $^{14}CO_2$ is fixed by RuP_2 carboxylase and a proportion of this carbon is released from the chloroplast into the cytoplasm as ^{14}C-triose phosphate which can then be converted to PEP via a glycolytic sequence. Thus in this instance, PEP supply, unlike in the dark, is not provided by degradation of glucan but is dependent upon the rate of $^{14}CO_2$ fixation by the PCR cycle. As both Osmond (1978) and Kluge and Ting (1979) have pointed out, this proposed scheme of events (Figure 1.6) is similar to the double carboxylation scheme proposed by Bradbeer *et al.*, (1958) for dark fixation of CO_2 (see Figure 1.2).

The involvement of RuP_2 carboxylase/oxygenase is also supported by the observations that, during this period, CO_2 fixation is O_2 sensitive (Osmond and Björkman, 1975). The CO_2 compensation point is 50 ppm in air (Allaway *et al.*, 1974), and when CO_2 is provided to *K. daigremontiana* plants only in the light the $\delta^{13}C$ values of -25.9‰ are characteristic of the fixation of CO_2 by RuP_2 carboxylase (Nalborcyzk *et al.*, 1975).

Figure 1.6 Diagrammatic representation of the path of carbon during late light CO_2 fixation in malic enzyme CAM plants. (Modified from Osmond, 1976). Symbols as in Figure 1.4.

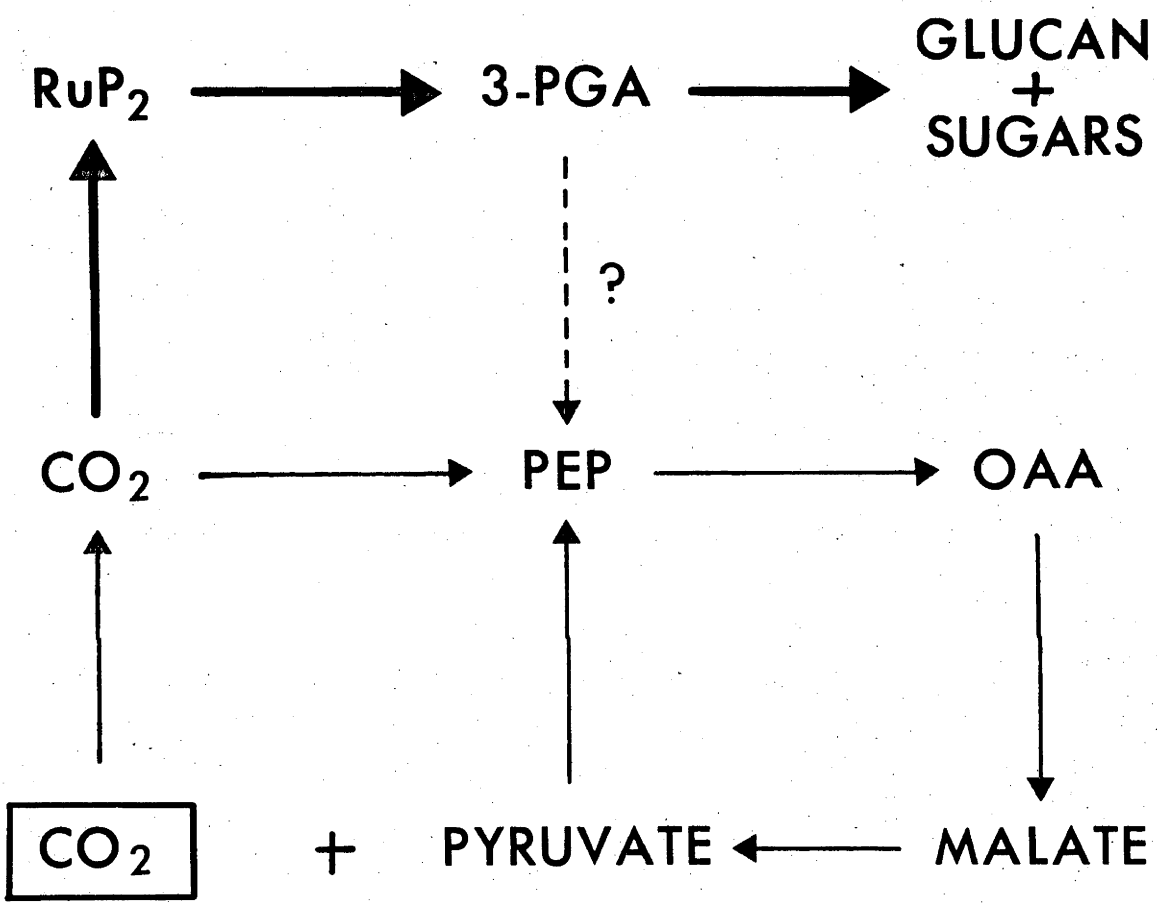
RuP2
3-PGA
GLUCAN
+
SUGARS
?
CO2
PEP
OAA
CO2
+
PYRUVATE
MALATE

As with the pre-deacidification burst of CO_2 uptake, both the period and magnitude of steady-state post-deacidification CO_2 fixation is regulated by a number of environmental factors which, in general, keep the stomates closed during this period. CO_2 fixation is suppressed in water stressed tissue (Kluge *et al.*, 1973; Lange *et al.*, 1975; Osmond, 1979), and under conditions which suppress deacidification such as low light intensity (Kluge, 1971b; Kluge *et al.*, 1973).

1.2.3.4 *Photorespiration*

CAM tissues possess all the necessary enzymatic and compartmental requirements for photorespiration. They possess chloroplasts, mitochondria and peroxisomes in close contact (Kapil *et al.*, 1975). Moreover RuP_2 carboxylase from *K. daigremontiana* also exhibits oxygenase activity (Badger *et al.*, 1975). Isolated peroxisomes from spinach and from CAM species, *Crassula lycopodiodes*, *Bryophyllum calycinum* and *Sedum rubiotinctum*, contain glycollate oxidase, catalase, hydroxypyruvate reductase, glycine aminotransferase, serine-glyoxylate aminotransferase and aspartate aminotransferase (Herbert *et al.*, 1978). Serine-glyoxylate and, in particular, glycine aminotransferase activities were much lower in the CAM tissue than in spinach. Adequate catalase, glyoxylate oxidase, and hydroxypyruvate reductase capacities have also been observed in *K. daigremontiana*, *Aloe arborescens*, and in *Sedum praealtum* (Denius and Homann, 1972; Osmond, 1976; Spalding *et al.*, 1979). Arron *et al.* (1979) reported low rates of glycine oxidation in mitochondria from *Sedum praealtum* which they attributed to either a low inherent rate or to enzyme deactivation during isolation. K.C. Woo (unpublished) observed an intact glycine decarboxylation system in mitochondria isolated from *K. daigremontiana*.

The observation, described in the previous section, that during post-deacidification light CO_2 fixation (Phase 4), CO_2 fixation is inhibited by O_2 concentrations above 2% is indicative of RuP_2 carboxylase/oxygenase activity and photorespiration. However, high CO_2 concentrations do not completely reverse the O_2 inhibition (Björkman and Osmond, 1974). The same workers (Osmond and Björkman, 1975) observed that the post-illumination burst in *K. daigremontiana* was present even at low O_2 concentrations. Crews *et al.* (1975, 1976) observed two post-illumination CO_2 bursts. The first, which is present during deacidification (Phase 3), is insensitive to O_2 and CO_2 and appears to be due to decarboxylation of malate, but the second, which is present during Phase 4, is suppressed by low O_2 and high CO_2.

Although the O_2 levels in deacidifying tissues are higher than ambient (up to 26%), the CO_2 concentrations are up to about 12 times higher than ambient (up to .4%) and probably cancel out any effect of O_2 inhibition on RuP_2 carboxylase activity during deacidification (Osmond, 1976; Cockburn *et al.*, 1979; Spalding *et al.*, unpublished).

Both Osmond (1978) and Kluge and Ting (1979) have concluded that CAM plants actively photorespire during the afternoon light CO_2 fixation period but probably do not during deacidification.

1.2.3.5 *Compartmentation*

There is no intercellular separation of the carboxylating and decarboxylating enzymes in CAM plants. *In situ* immunofluorescent labelling of RuP_2 carboxylase/oxygenase with anti-RuP_2 carboxylase/oxygenase demonstrated that RuP_2 carboxylase/oxygenase was present in all chloroplasts

in *K. daigremontiana* leaves (Hattersley *et al.*, 1977). Moreover, isolated mesophyll cells from *Sedum telephium, S. praealtum, Opuntia polycantha, O. monocantha, K. daigremontiana* and *Stapelia gigantea* are able to fix CO_2 via PEP carboxylase or by RuP_2 carboxylase, exhibit CO_2 dependent O_2 evolution, synthesise malate and convert $^{14}CO_2$ to starch (Rouhani *et al.*, 1973; Spalding and Edwards, 1978; Gerwick *et al.*, 1979; see also Chapter 3).

Some of the early reports on the localisation of enzymes based on mitochondrial or chloroplastic isolation are now considered unreliable mainly on methodological grounds. Often isolation was performed using non-aqueous separation (eg. Garnier-Dardart,1965; Mukerji and Ting, 1968a) a technique which has been shown to be prone to cytoplasmic contamination (Bird *et al.*,1973). Brandon (1967) used an aqueous technique to isolate mitochondria from *B. tubiflorum* and reported the presence of PGA-mutase, enolase and possibly some RuP_2 carboxylase/oxygenase in these organelles. These three enzymes have since been shown to be non-mitochondrial in a number of C_3, C_4 and CAM tissues.

The location of various photosynthetic, glycolytic and respiratory enzymes have recently been re-investigated using more reliable separation techniques which are now available. Spalding *et al.*, (1979) have shown that NADP malic enzyme from *S. praealtum* is solely restricted to the cytoplasm, which is contrary to early reports for CAM plants (Brandon, 1967; Garnier-Dardart,1965; Mukerji and Ting 1968a; Khan *et al.*, 1970). Although Khan *et al.* (1970) did find the majority of NADP malic enzyme from the cactus *Nopalea dejecta* in the cytoplasm and Mukerji and Ting (1968a,b) observed chloroplastic, cytoplasmic and mitochondrial isoenzymes in *Opuntia phylloclades*.

NADP malic enzyme and PEPCK are also restricted totally to the cytoplasm in *K. daigremontiana* and *Ananas comosus* respectively (Dittrich, unpublished). Hitherto no differences in enzyme locations have been reported for similar enzymes from CAM and C_4 plants. The cytosolic location of CAM NADP malic enzyme has been considered to represent a major and unpredicted difference. With hindsight, however, the cytosolic location of the CAM enzyme is not so unexpected since it has previously been recognised that plant NADP malic enzymes can be categorised into the more general "C_3 + CAM" type, which has similar properties to malic enzymes from non-photosynthetic tissues and vertebrates (Garnier-Dardart, 1965; Brandon and von Boekel-Mol, 1973; Pupillo and Bossi, 1979), and a "C_4 type", which has a higher affinity for malate (Nishikido and Wada, 1974). The enzyme from corn root tips, which appears to be of the "C_3 + CAM" type is restricted to the soluble fraction (Danner and Ting, 1967), although animal tissues contain both soluble and mitochondrial forms (Li *et al.*, 1975). Pupillo and Bossi (1979) have demonstrated the presence of both forms, but predominantly the "C_3 + CAM" form, in etiolated maize tissue. With greening the tissue synthesised the "C_4 type" and after 6 days light treatment this was the predominant form. It was suggested that the C_3 form from etiolated leaves was in the cytoplasm.

The NAD malic enzyme from CAM plants is a mitochondrial enzyme (Dittrich, 1976; Arron *et al.*, 1979; Day unpublished; Spalding *et al.*, unpublished) as is the C_4 enzyme (Hatch and Kagawa, 1974a,b). Khan *et al.* (1970) has shown that mitochondria from the cactus *Nopalea dejectus* contain a regular complement of TCA cycle and respiratory chain enzymes, whilst as previously stated, K.C. Woo (unpublished) has observed a glycine decarboxylating system, similar to that found in C_3 plants, in mitochondria

isolated from *K. daigremontiana*. In *S. praealtum* pyruvate, Pi dikinase is restricted to chloroplasts as it is in C_4 plants (Spalding *et al.*, 1979; Hatch *et al.*, 1975).

Herbert *et al.* (1979) have demonstrated the presence of 2 distinct forms of each of the following enzymes from *B. calycinum:* glucosephosphate isomerase, phosphoglucomutase, G-6-P and 6-phosphoglucono dehydrogenase. Although the compartmentation of these enzymes has not been studied, the data is strongly suggestive of cytoplasmic and chloroplastic forms, since all 4 enzymes isolated from spinach in the same study had a chloroplastic and a non-chloroplastic form.

1.2.3.6 *Regulation and transport*

It is commonly accepted that PEP carboxylase is active during Phases 1 and 2 but is inactive during deacidification. It is also known that PEP carboxylase is inhibited by malate (cf. Kluge and Osmond, 1972), however it is becoming increasingly obvious that PEP carboxylase is subject to other forms of regulation about which there is both disagreement and ignorance.

Queiroz and co-workers argue that feedback control of malate cannot, by itself, explain the day/night rhythm of CAM and proposed that, in *K. blossfeldiana,* PEP carboxylase and NADP malic enzyme act as the two separate "clock-controlled" oscillators which are "entrained" by the combined effects of dusk and dawn signals. (see recent review by Queiroz (1979)).

The most commonly accepted concept of PEP carboxylase regulation in the light is actually a flexible composite of several previously proposed schemes.

Basically, it recognises the individual metabolic events which occur during each light phase. During Phase 2 PEP carboxylase is generally not inhibited but the activity of the enzyme is dependent upon the vacuolar malate content. During Phase 3, PEP carboxylase is inhibited by malate released from the vacuoles the control of which is possibly related to cell turgor (see Section 1.2.2). During Phase 4 PEP carboxylase is not inhibited *per se* but its activity is limited by the availability of substrate and malate accumulation is dependent upon the activity of the various decarboxylases.

The observation by Winter and co-workers (Greenway *et al.*, 1978; Winter and Greenway, 1978) previously mentioned in relation to the regulation of PEP carboxylase in the dark, may be particularly relevent to the regulation of PEP carboxylase in the light. PEP carboxylase from CAM *M. crystallinum* and *Aloe arborescens* at the onset of deacidification (which usually is associated with vacuolar efflux), both in the light and in continuous darkness, undergoes a change from a malate insensitive form to a malate sensitive form (Winter, unpublished).

NADP malic enzyme, although important as a decarboxylase, does not appear to perform an important regulatory role. This also seems to be true of PEPCK and possibly also of NAD malic enzyme. NADP malic enzymes from CAM plants are, as already mentioned, similar in many respects to the C_3 enzymes and are characterised by having a pH optimum around 7, and a K_m malate of 0.3-1.0 mM (Walker, 1960; Brandon, 1967; Garnier-Dardart and Queiroz, 1974; Brandon and van Boekel-Mol, 1973; Pupillo and Bossi, 1979).

Although NADP malic enzyme from *K. daigremontiana* appears to be subject to complex regulatory control (Garnier-Dardart and Queiroz, 1974) much of the regulation involves variations in the Mg^{2+} concentrations which are most probably of little physiological significance to a cytoplasmic enzyme. The enzyme is also characterised by malate co-operativity at low malate and NADP concentrations. Two possibly important features of the enzyme are its insensitivity to high malate concentrations, and its rather broad pH optimum which is particularly evident at high malate concentrations (Kluge and Osmond, 1972; Garnier-Dardart and Queiroz, 1974; Holtum and Winter, unpublished). Such characteristics could enable the enzyme to operate, during Phase 3, in a cytoplasmic milieu that may well have a low pH and a high malate content due to the efflux of malic acid from the vacuole.

Brandon and van Boekel-Mol (1973) have reported that the NADP malic enzyme from *B. tubiflorum* increases in activity up to 55°C, and this activity is stimulated by high malate levels. The implication is that the decarboxylase is particularly active during the warm, daylight hours.

The generally low tissue pyruvate concentrations (Milburn *et al.*, 1968; Cockburn and McAuley, 1977) coupled with both the efficient $NADPH_2$ oxidising system on the external walls of CAM mitochondria (Arron *et al.*, 1979; Day, unpublished) and the malate co-operativity at low malate and NADP concentrations, should ensure that the enzyme rarely, if ever, operates in a reverse direction. The same reasoning suggest that the enzyme could be active in the dark (see discussion in Section 1.2.1.4).

The PEPCK from *Ananus comosus* (pineapple), a CAM plant, appears to be similar to that extracted from *Panicum maximum*, a C_4 plant (Ray and

Black, 1976a;Daley *et al.*, 1976). They have similar pH optima of 6.8-7.0 and the K_m ATP and K_m OAA are similar in the decarboxylating direction. Both enzymes appear to be capable of decarboxylation using ADP but it is possible that this activity is due to contamination by adenylate kinase. The suggestion that ADP catalyses the converion of OAA $\longrightarrow$ pyruvate + CO_2 as has been observed in yeast, pig liver and avian liver (Chang *et al.*, 1966; Connata and DeFlombaum, 1974; Noce and Utter, 1975), has been tested and discounted by Hatch and Mau (1978). The CAM enzyme has lower affinities for ADP, HCO_3^- and PEP (K_m's of 0.13 mM, 34 mM and 5 mM respectively) compared with the C_4 enzyme (0.05 mM, 11 mM, 0.38 mM respectively) in the carboxylating direction. The CAM enzyme is also sensitive to temperatures below 15°C at which point there is a large increase in the energy of activation (from $\simeq$ 12-13 to $\simeq$ 80 kcal.mol^{-1}).

The cytoplasmic location of PEPCK in CAM plants (Dittrich, unpublished) may be problematical since it is thought that the cytoplasmic pH is low, due to the high malate concentration during deacidification. Although the enzyme has a narrow pH optimum (Daley *et al.*, 1976), PEPCK activities are always much higher than required by deacidification (Dittrich *et al.*, 1973) and even at pH 6.0 it is mostly likely the activity would be sufficient.

Mitochondria isolated from NAD malic enzyme containing CAM plants are capable of high rates of Pi-dependent malate decarboxylation. These rates can be further stimulated by ADP, NAD, OAA, aspartate and oxoglutarate, or uncouplers of oxidative phosphorylation such as FCCP (Day, unpublished, Spalding *et al.*, unpublished). It has yet to be shown, however, that the mitochondria contribute to deacidification *in vivo*. This question is particularly relevent in the light of recent reports

(Cockburn *et al.*, 1979; Spalding *et al.*, unpublished) that the internal CO_2 concentration during deacidification in CAM plants may be as high as 0.4%. In contrast to NADP malic enzyme which appears to be relatively insensitive to CO_2 concentration (Hatch, pers. comm.; Walker, 1960) decarboxylation by both NAD malic enzyme and isolated mitochondria from *Atriplex spongiosa*, a NAD malic enzyme C_4 plant, is strongly inhibited by HCO_3^- (Hatch *et al.*, 1974; Chapman and Hatch, 1977). This inhibition appears to be competitive with malate. The enzyme from *Panicum miliaceum*, also a C_4 plant, is relatively insensitive to HCO_3^- and in the presence of 5 mM malate and 20 mM HCO_3^- is only inhibited by 7% compared with 95% for the *A. spongiosa* enzyme. The enzyme from the CAM plant *S. praealtum*, like that from *P. miliaceum*, is relatively insensitive to HCO_3^- inhibition (Spalding *et al.*, unpublished). This insensitivity is most pronounced at high malate concentrations and may reflect the sigmoidal response to increased malate concentration which has been observed in both *Sedum* and *Kalanchoe* (Dittrich, 1976; Day, unpublished; Spalding *et al.*, unpublished).

However, despite these *in vitro* observations, a simple, albeit rough, calculation suggeststhat the observed internal CO_2 concentration in deacidifying CAM tissue will not significantly affect the activity of NAD malic enzyme. If we assume that, at 25°C, 330 ppm CO_2 is equivalent to 9.9 µM CO_2 (Ku and Edwards, 1977) and deacidifying CAM tissue contains about 4,000 µl CO_2/l (4,000 ppm CO_2), then the CO_2 concentration of the intercellular spaces will be about 0.13 mM. The inhibitory effect of this low CO_2 concentration, which represents the maximum observed concentration in a number of tissues (and is equivalent to about 0.93 mM $NaHCO_3^-$ in an aqueous medium at 25°C, pH 7.2), will be minimal and will presumably be offset by the high tissue malate contents which are present during this period.

For example, the data of Spalding *et al.*, predicts that 0.13 mM CO_2 in the presence of 2.5 mM or 0.5 mM malate (in an aqueous medium of pH 7.2) will inhibit NAD malic enzyme from *S. praealtum* by only 10% and 15% respectively. It is possible, however, that the mitochondrial malate concentration may be very different to the cytoplasmic concentration.

Spalding *et al.* (unpublished) demonstrated that after 5 minutes U-^{14}C-malate incorporation by decarboxylating mitochondria (pH of the medium was 7.2) from *S. praealtum* nearly all the non-malate label was observed in pyruvate and $^{14}CO_2$. As partate was the next most heavily labelled compound.

In mitochondria isolated from *K. daigremontiana* the relative carbon fluxes through NAD malic enzyme and NAD malate dehydrogenase are affected by the pH of the external medium (Day, unpublished). At a pH below 7.2-7.4 pyruvate is the principal product but above pH 7.4 there is a rapid shift towards OAA production. This pH sensitivity is not reflected in the pH response of the isolated enzyme and may indicate an *in vivo* mechanism of mitochondrial regulation. If, during deacidification the cytoplasmic pH is reduced by malate efflux from the vacuole, then pyruvate production via NAD malic enzyme would be stimulated. However, once the vacuolar malate has been decarboxylated, the cytoplasmic pH may increase and normal TCA cycle activity will be favoured.

Nothing is known of the transport capabilities of CAM chloroplasts as intact, photosynthetically active chloroplasts have yet to be isolated from a CAM plant. Levi and Gibbs (1975) isolated chloroplasts from *K. daigremontiana* with CO_2 fixation rates of only 0.95 μmoles CO_2 mg chl^{-1} hour^{-1}, and Nishida and Sanada (1977) isolated *K. daigremontiana* chloroplasts,

after a 14 day dark period to reduce the starch content, and obtained a maximal rate of only 3.2 μmoles CO_2 mg chl^{-1} $hour^{-1}$.

1.3 The Metabolism of Pyruvate and PEP during Deacidification

1.3.1 Unresolved questions

As mentioned in the preceding sections, it has been established that all 4 carbons of dark synthesised malate are converted to glucan during Phase 3 in the following light period (Pucher *et al.*, 1947; Kunitake and Saltman, 1958; Ting and Dugger, 1968; Sutton, 1974). The first step of this conversion appears to involve the decarboxylation of malate to produce CO_2 and a 3-carbon compound either pyruvate or PEP, depending upon the particular decarboxylating enzyme involved. The CO_2 is refixed by RuP_2 carboxylase and converted to glucan via the PCR cycle. However the route by which the 3-carbon compounds PEP and pyruvate are converted to glucan is uncertain.

The distribution of ^{14}C in glucose, derived from starch formed in the light from dark ^{14}C labelled malate, suggests that the transfer of ^{14}C most likely involves both a decarboxylation step and a reversal of glycolysis, rather than either the direct reduction of malic acid to glucan or an oxidation of malic acid to CO_2 followed by refixation and conversion to glucan via the PCR cycle (Varner and Burrell, 1950). This conclusion was supported by Haidri (1955a,b) who attempted to trace the fate of 2-^{14}C-pyruvate and 2-^{14}C-malate in the light in *B. calycinum* and *Nicotiana* leaves (Table 1.1). The leaves were labelled in the dark, illuminated for 3 hours, and the distribution of ^{14}C in glucose isolated from starch was measured.

Table 1.1 Distribution of ^{14}C in glucose isolated from starch in *B. calycinum* mesophyll tissue fed 2-^{14}C-pyruvate in the light. (Data of Haidri, 1955a)

	Position of ^{14}C in glucose	% distribution of ^{14}C in *B. calycinum*
Carbons	3-4	28-33
	2-5	43-46
	1-6	25-28

The occurrence of the highest ^{14}C concentration in carbons 2 and 5 suggests that a major part of the 2-^{14}C acids were converted to starch via a reversal of the glycolytic pathway. That the next highest concentration of ^{14}C is in carbons 3 and 4 suggests either that some of the acid was oxidised and the CO_2 was refixed or, alternatively, some randomisation occurred. These interpretations are however, equivocal for although assimilation of $^{14}CO_2$ by the PCR cycle should produce glucose with the highest ^{14}C concentration in carbons 3 and 4 one would also expect the remaining label to be equally distributed between carbons 1,2,5 and 6 (Bassham, 1965). If the carbon 1 and 6 figures are subtracted from the carbon 2 and 5 figures, acid metabolism via a reverse glycolytic (or gluconeogenic) pathway begins to appear small. Neal and Beevers (1960) showed that in castor-bean endosperm slices, which are known to convert fats via pyruvate to sugars by gluconeogenesis, only 9% of the ^{14}C incorporated into glucose after 4 hours 3-^{14}C-pyruvate incorporation in the dark was in carbons 3 and 4.

The data of Haidri (1955a,b) is also puzzling insomuch as that there is virtually no variation in the labelling patterns of both 2-^{14}C-malate and 2-^{14}C-pyruvate between *B. calycinum*, a CAM plant, and both *Nicotiana* sp. and *Avena* sp., two C_3 plants. This is particularly so since *B. calycinum* probably possesses pyruvate, Pi dikinase (Kluge and Osmond, 1971; Chapter 4.1), an enzyme that converts pyruvate $\longrightarrow$ PEP, and which is absent from C_3 plants. There is no indication however, whether the *Bryophyllum* plants were actively deacidifying, and converting malate $\longrightarrow$ glucan, during the experiments. Moreover, it is possible that since a dark/light transition was involved,a large proportion of the experimental light period was spent undergoing Phase 2 metabolism which may involve the conversion of pyruvate to PEP to malate, followed by randomisation of the label in malate prior to decarboxylation.

Moyse and co-workers (Moyse *et al.*, 1958; Champigny *et al.*, 1958) suggested that, during deacidification, malate may be completely oxidised to CO_2 prior to starch formation. They suggested that the *in vivo* equilibrium of the reaction PGA $\rightleftharpoons$ PEP is towards PEP formation and thus the gluconeogenic formation of sugars was unlikely. These conclusions were supported by Champigny (1960, unseen, cited by Kluge and Ting, 1979).

Although CAM plants possess conventional TCA cycles in the dark (Bradbeer, 1963; Bradbeer and Ranson, 1963; Kaplan *et al.*, 1976), Milburn *et al.* (1968) and Denius and Homann (1972), using intact *B. calycinum* leaves and leaf slices from *Aloe arborescens* respectively, showed that the maximal rates of O_2 uptake in the light were between 10 and 2.5 times less than those required for the complete oxidation of malate. Although O_2 evolution increased with increasing tissue acidity in *Aloe* leaf slices

(Denius and Homann, 1972), the reverse was observed in *Opuntia* stem tissue (Szarek and Ting, 1974). In both tissues increasing temperature increased O_2 consumption in the light. Unfortunately, simultaneous deacidification and O_2 exchange rates were not measured in either study and, moreover, in the *Opuntia* study a proportion of the tissue was non-chlorophyllous pith tissue. Recent studies (Cockburn *et al.*, 1979; Spalding *et al.*, unpublished) have established that during deacidification, the tissue O_2 concentration may be as high as 40% which indicates that the net oxygen uptake at higher acid levels observed by Szarek and Ting (1974) may be an artefact.

It is evident that opinion is divided as to the pathways by which PEP and pyruvate are converted to glucan in the light. Although malate is obviously not directly converted to glucan, CAM plants may have the ability to convert pyruvate or PEP to carbohydrate via a gluconeogenic sequence. The early data of Varner and Burrell (1950) and Haidri (1955a) however, are based on long term feeding experiments in which the flow of carbon through intermediates was not studied. These data need to be confirmed and expanded. CAM plants also appear to have the capacity to oxidise at least a proportion of the carbon via the TCA cycle, this capacity needs to be investigated with relation to any gluconeogenic capacity.

1.3.2 Aim of thesis and working hypothesis

In the following dissertation I shall attempt to test the hypothesis that CAM plants convert the bulk of the pyruvate and PEP formed during deacidification directly to glucan via a mechanism akin to gluconeogenesis.

This hypothesis, presented in the schemes in Figure 1.7, suggests that in malic enzyme plants, the flow of carbon from pyruvate to carbohydrate

Figure 1.7 Possible pathways of pyruvate and PEP metabolism in malic enzyme and PEPCK CAM plants during deacidification (Phase 3) in the light.

The thickness of the lines represents the proposed relative activities of alternative processes. Broken lines represent processes of uncertain significance.

A. MALIC ENZYME CAM PLANTS

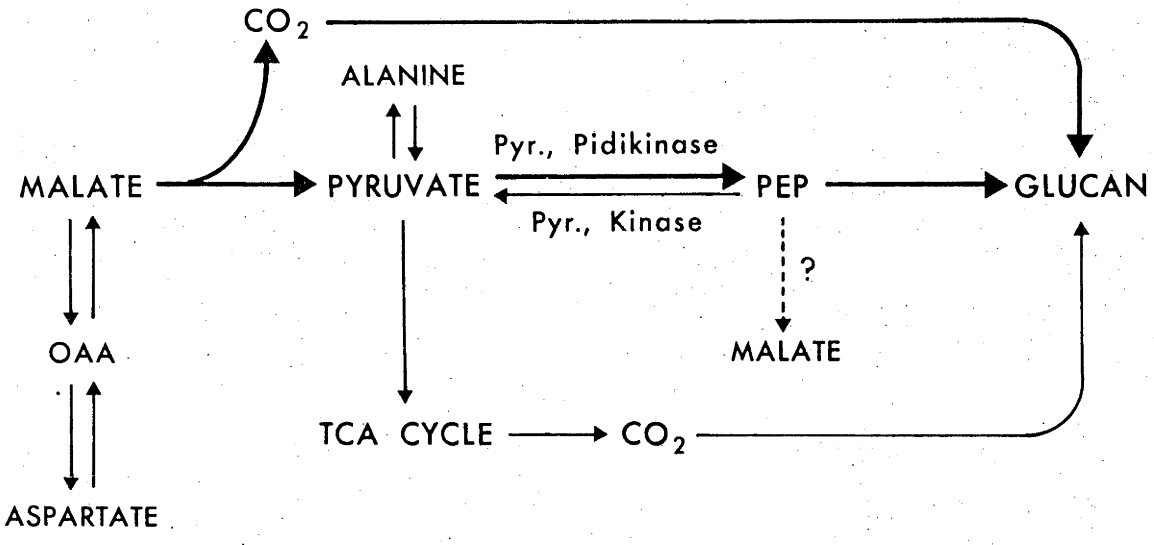

B. PEPCK CAM PLANTS

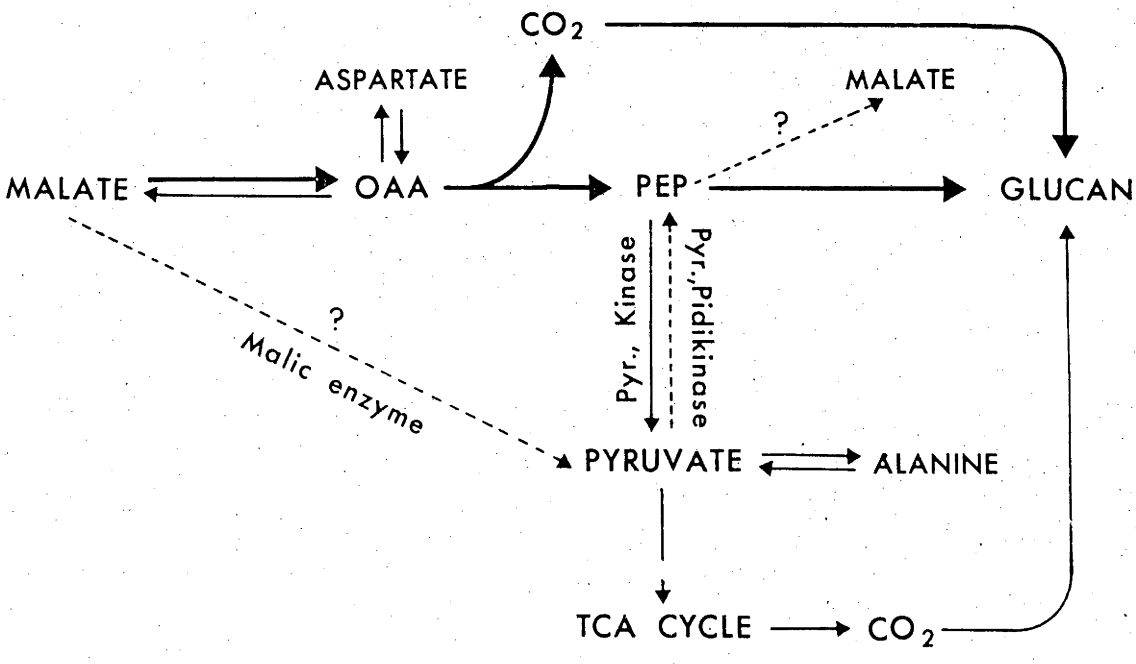

will depend on the relative activities of pyruvate kinase, which is present in low activities in *K. daigremontiana* (Sutton, 1974, 1975b), and pyruvate, Pi dikinase, which is present in 5-6 fold higher activities in *K. daigremontiana* (Kluge and Osmond, 1971; Sugiyama and Laetsch, 1975). The schemes also predict that PEP carboxylase must either be inactivated or compartmented away from the site of PEP formation to prevent a futile cycle, and that the glycolytic enzymes are capable of converting PEP ⟶ glucan.

In PEPCK plants the carbon flow will depend upon the relative activities of PEP carboxylase, pyruvate kinase and enolase all of which are cytoplasmic and use PEP as a substrate. If pyruvate, Pi dikinase is present in these plants it may well reverse any pyruvate kinase activity.

The metabolism of pyruvate and PEP in the light will be investigated in deacidifying tissue slices from malic enzyme and PEPCK CAM plants. Initially, it will be shown that the tissue slices behave, in terms of their malate content, deacidification capacities, and $^{14}CO_2$ assimilation capacities and products, similarly to intact tissues. The tissue slice system will then be used to examine the short term labelled products formed from the metabolism of variously labelled ^{14}C-pyruvate during deacidification in the light. Figure 1.7 predicts that, if gluconeogenesis occurs in CAM plants possessing malic enzyme, ^{14}C-pyruvate will be rapidly converted to glucan via phosphorylated compounds. TCA cycle acids will be the initial products of incorporation of ^{14}C-pyruvate by the mitochondria. The rate of mitochondrial $^{14}CO_2$ evolution, and thus refixation by RuP_2 carboxylase, will depend upon the position of the label in the pyruvate. In PEPCK plants, the conversion of exogenously labelled pyruvate to PEP will

depend on the presence of pyruvate, Pi dikinase which has not yet been observed in any of these species.

The metabolism of ^{14}C-pyruvate in C_3 and CAM *M. crystallinum* will also be studied. Just as one might expect differences in the capacity to metabolise pyruvate, and possibly also differences in the pathways or pyruvate metabolism, between malic enzyme species which produce pyruvate during deacidification and PEPCK plants which produce PEP, one might possibly expect similar differences in the metabolism of pyruvate by C_3 and CAM *M. crystallinum* plants.

A survey will be presented of the capacities of various enzymes involved in carboxylation, decarboxylation, and pyruvate and PEP metabolism as well as the capacities of the various glycolytic enzymes to operate in a gluconeogenic direction in several malic enzyme plants, PEPCK plants, and in C_3 and CAM *Mesembryanthemum*. The survey will be used to demonstrate the capacities of the various experimental tissues to convert pyruvate and PEP to glucan.

CHAPTER 2 THE METABOLISM OF PYRUVATE, MALATE AND CO_2 DURING DEACIDIFICATION

2.1 Deacidification in Intact Tissues and in Leaf Slices

2.1.1 Introduction

If one is to use leaf slice data to explain events which occur in intact tissue it is necessary to show that, under the experimental conditions used, the leaf slices behave in a similar manner to intact tissue. Recent studies, using acidified leaf slices of *Bryophyllum tubiflorum, Kalanchoe daigremontiana* and *K. blossfeldiana* have shown that malate efflux increases exponentially with increasing washing time (Kluge and Heininger, 1973), decreases with increasing osmotic pressure of the external medium (Lüttge and Ball, 1974a, 1977; Lüttge *et al.* 1975, 1977), but is insensitive to light (Lüttge and Ball, 1974a; Lüttge *et al.*, 1975), independent of the pH of the external medium between pH 4 and pH 8, and is insensitive to FCCP an uncoupler of oxidative and photophosphorylation (Lüttge and Ball, 1977). In contrast, deacidification is light stimulated and dependent upon the tissue malate content, but is independent of change in the osmotic pressure of the medium.

In this section the rates of deacidification in the light, which should be stoichiometrically related to pyruvate production in malic enzyme CAM plants, are examined in leaf slices and in intact tissue from several CAM and C_3 plants. The effect of varying both pH and osmotic pressure of the external medium on deacidification and malate efflux in acidified *K. daigremontiana* leaf slices is also briefly investigated.

2.1.2 Materials and methods

2.1.2.1 *Experimental material*

Aloe arborescens (Figure 2.1A), *Bryophyllum tubiflorum* (Figure 2.1B), and *Kalanchoe daigremontiana* (Figure 2.1C) were grown from plantlets, and *Stapelia*

Figure 2.1 A. *Aloe arborescens*

B. *Bryophyllum tubiflorum*

C. *Kalanchoe daigremontiana*

D. *Stapelia gigantea*

E. *Hoya carnosa*


A


B


C

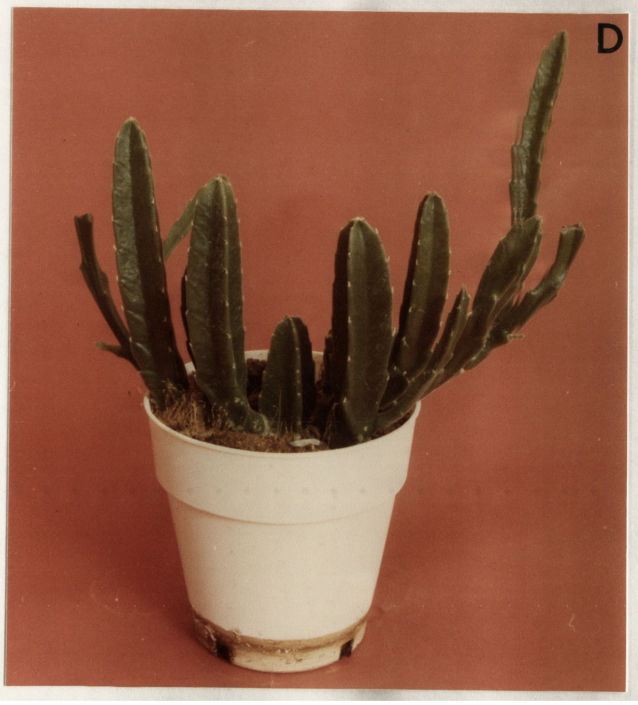
D


E

gigantea (Figure 2.1D) and *Hoya carnosa* (Figure 2.1E) were grown from stem cuttings, under natural light and daylength in a glasshouse.

The plants were placed in a growth cabinet (10 hour day, 400 μeinstein m^{-2} s^{-1}, 23°C, 60% relative humidity/14 hour night, 17°C, 75% relative humidity) at least 10 days before experiments were to be performed, and were watered daily and given nutrient solution (½ strength Hoaglands) three times a week.

Mesembryanthemum was grown from seed in a greenhouse. The seedlings were watered daily. After about 3 weeks seedlings, which were selected for their healthy appearance and uniformity of size, were transferred to a growth cabinet (12 hour day, 400 μeinstein m^{-2} s^{-1}, 25°C, ≃ 60% relative humidity/12 hour night, 15°C, ≃ 75% relative humidity) and were grown in water culture. The culture medium contained 3 mM KNO_3, 2 mM $Ca(NO_3)_2$, 0.5 mM $NH_4H_2PO_4$, 0.5 mM $(NH_4)_2HPO_4$, 0.5 mM $MgSO_4$, 12.5 μM H_3BO_4, 1 μM $MnSO_4$, 1 μM $ZnSO_4$, 0.25 μM $CuSO_4$, 0.25 μM H_2MoO_4, 10 μM FeH_2-EDTA and 100 mM NaCl (modified after Johnson, 1957). Each pot was aerated and contained 5 plants in 6 litres of nutrient medium which was changed every 7 days. When the plants were about 7 weeks old the NaCl concentration was increased in some pots in daily steps of 50 mM to a final concentration of 400 mM. Tissue was not used for experiments until at least 7 days after the plants had been in 400 mM NaCl.

Plants grown in 100 mM NaCl exhibit characteristics of C_3 photosynthesis whilst plants grown in 400 mM NaCl fix substantial amounts of carbon in the dark and exhibit the large day/night malic acid fluctuations characteristic of CAM plants (Winter and Lüttge, 1976b). Consequently for

convenience, 100 mM NaCl grown *Mesembryanthemum* will be called C_3 *Mesembryanthemum* and 400 mM NaCl grown plants will be called CAM *Mesembryanthemum*.

Spinach was grown hydroponically in full strength Hoaglands solution under natural light and daylength in a greenhouse.

2.1.2.2 *Preparation of leaf slices*

The age of the experimental tissue varied between species due to differences in growth rate, growth media and in growth habit. As a consequence the tissue used in these studies was standardised for each species as follows:

Aloe arborescens - The third to sixth phyllodes were used. The basal 1 cm and the thorns were discarded. Each leaf was then cut laterally and the adhering water tissue was gently scraped away using a scalpel.

Bryophyllum pinnatum - The third and fourth fully expanded leaf pairs were used. The midribs and leaf margins were discarded.

Bryophyllum tubiflorum - The fourth to tenth whorls were used.

Hoya carnosa - Fully expanded green leaves from anywhere along the vine, except the basal leaves, were used. The midribs and leaf margins were discarded.

Kalanchoe daigremontiana - The third and fourth fully expanded leaf pairs were used. The midribs, leaf margins and lower epidermis were removed.

Mesembryanthemum crystallinum - The third and fourth expanded foliar leaves were used from both C_3 and CAM *Mesembryanthemum* (cf. Winter, 1973a). The midribs were discarded.

Spinacea oleracea (spinach) - The second fully expanded leaf pair was used. The midribs were discarded.

Stapelia gigantea - The tissue between about 1 cm below the tip and 1-2 cm above the base of actively growing stems was used. The central pith was carefully removed using a scalpel.

Transverse slices of the above tissues (approximately 0.5-1 mm thick and 1-1.5 cm long) were placed, as they were sliced, in a petri dish containing 50 mM HEPES-NaOH pH 7.5, 0.1 mM $CaSO_4$ and 0.3M Mannitol (0.6 M mannitol in the cases of spinach and CAM *Mesembryanthemum* (Winter, 1973a). The slices were then dried on paper towelling and placed in preweighed 15 ml glass vials (0.6-1 g tissue per vial). The vials were quickly reweighed and 3.0 ml of a suspension medium was added before sealing with Nescofilm. The medium consisted of either 25 mM HEPES-NaOH pH 7.5 or 25 mM MES-NaOH pH 6.0, 0.1 mM $CaSO_4$ and varying concentrations of mannitol (precise contents are given in the appropriate figures).

2.1.2.3 *Malate estimation*

After appropriate illumination the tissue was quickly washed with H_2O and then extracted for 10 minutes in boiling 20% EtOH. The supernatant was decanted and the tissue was re-extracted in boiling H_2O for a further 10 minutes. The supernatants were then pooled. If, in leaf slice experiments, the malate content of the suspension medium was to be measured the H_2O washings were added to the suspension medium which was then boiled for 5 minutes, cooled and stored frozen until required for the assay.

Titratable acidity was determined by titrating the pooled supernatants against 50 mM KOH to an endpoint of pH 7.3. Acidity was expressed as μequivalents g^{-1} fresh weight (2 μequivalents ≡ 1 μmole malate).

Malate was determined enzymatically using the method of Hohorst (1963).

2.1.2.4 *Chlorophyll estimation*

Intact tissues or leaf slices (1 g) were ground with a known volume of 100% acetone in a glass homogeniser. The extract was transferred to a centrifuge tube and spun for 5 minutes at maximum speed (about 4,000 rpm) in a MSE benchtop centrifuge. The supernatant was decanted, and made up to 80% acetone with H_2O.

The absorbance spectrum was measured using a Varian series 634 dual beam spectrophotometer, and chlorophyll content was calculated using the following formula (Arnon, 1949):

$$\frac{(20.2 \times OD_{645} + 8.0 \times OD_{663}) \times V}{1000 \times W} = \text{chlorophyll content (mg chl g fwt}^{-1})$$

where V = total volume of extract in ml and W = weight of tissue in grams.

2.1.3 Results and discussion

Day/night fluctuation of titratable acidity, a characteristic of CAM tissue, was observed in intact tissue from all plants used in these studies with the exception of C_3 *Mesembryanthemum* and spinach (Figure 2.2A and B). Net malate consumption in the light by leaf slices of acidified *A. arborescens, B. tubiflorum, K. daigremontiana, S. gigantea* and CAM *Mesembryanthemum* tissue is shown in Figures 2.3A and B and 2.4. The malate content of the C_3 *Mesembryanthemum* and spinach slices was low throughout every experiment and in fact tended to increase slightly with exposure to light (Figure 2.4). The decrease in tissue malate content observed in the CAM tissue was due to the *in vivo* consumption of malate and not due to efflux of malate into the bathing medium (Figures 2.3A and B).

Figure 2.2 A. Diurnal variation in titratable acidity in intact leaves of three NADP ME CAM plants: *Bryophyllum pinnatum* ■——■ *Bryophyllum tubiflorum* ● —— ● , and *Kalanchoe daigremontiana* o —— o.

B. Diurnal variation in titratable acidity in intact leaves of three PEPCK CAM plants: *Aloe arborescens* ■——■ , *Hoya carnosa* ● —— ●, and *Stapelia gigantea* o —— o. The *Aloe* and *Stapelia* data have been corrected for the presence of water tissue.

All points are the means of duplicate samples.

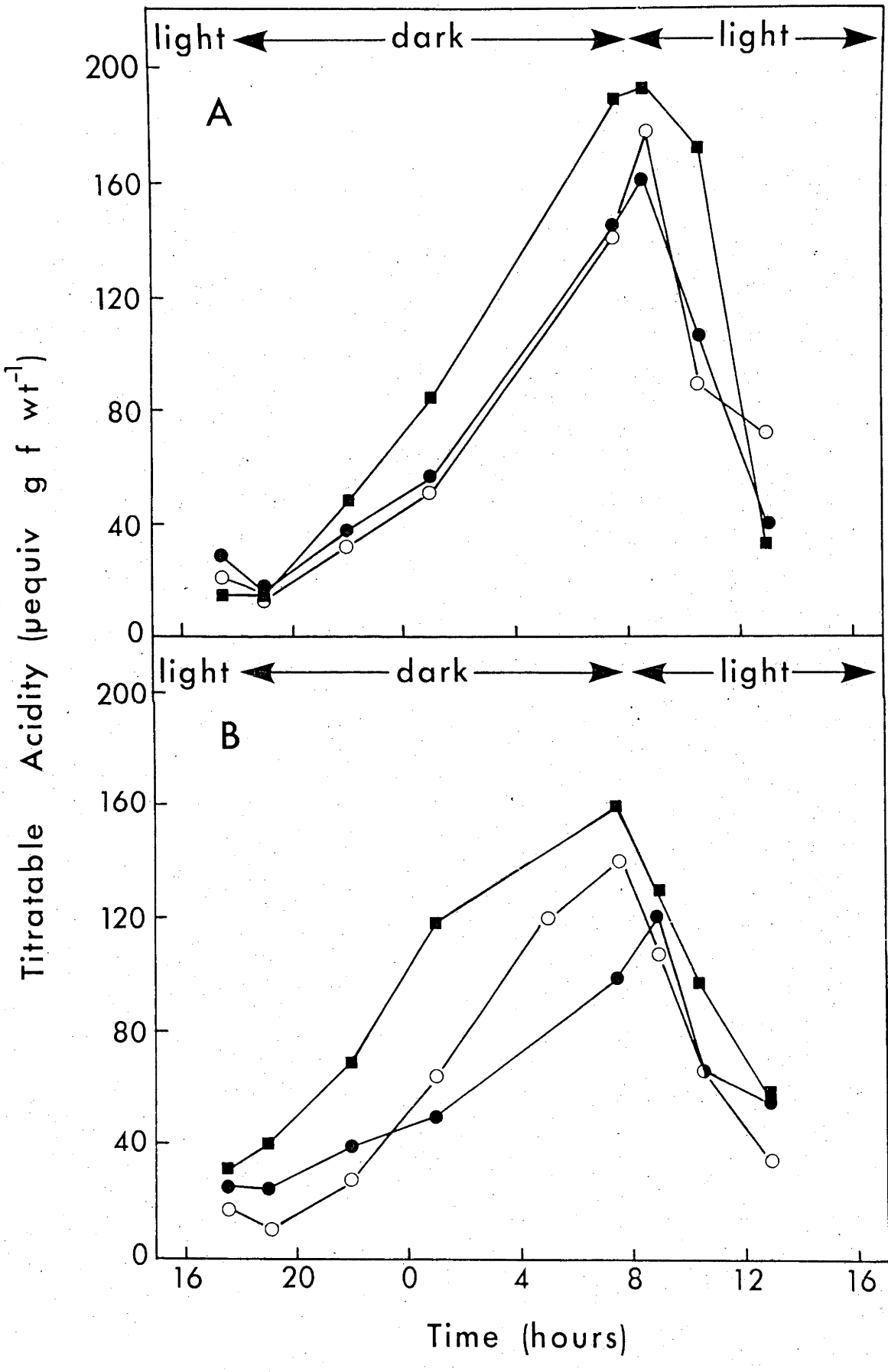
light
dark
light
A
B
200
160
120
80
40
0
16
20
0
4
8
12
16
Titratable Acidity (μequiv g f wt^{-1})
Time (hours)

Figure 2.3 A. Change of malate content in acidified *Kalanchoe daigremontiana* leaf slices, and in the bathing medium (broken lines), under different osmotic and pH conditions.

0 M mannitol, pH 4.0 ◔ —— ◔
0 M mannitol, pH 6.2 ● —— ●
0 M mannitol, pH 7.5 o —— o
0 M mannitol, pH 6.0 ▲ —— ▲
0.1 M mannitol, pH 6.0 □ —— □
0.3 M mannitol, pH 6.0 ■ —— ■

B. Change of malate content in acidified leaf slices, and in the bathing medium (broken line), from the three species of CAM plant.

Aloe arborescens 0 M mannitol, pH 6.0 ● —— ●
Aloe arborescens 0 M mannitol, pH 6.0 o —— o
Aloe arborescens 0 M mannitol, pH 6.0 ■ —— ■
Aloe arborescens 0 M mannitol, pH 6.0 □ —— □
Aloe arborescens 0 M mannitol, pH 6.2 ◔ —— ◔
Stapelia gigantea 0 M mannitol, pH 6.0 ▲ —— ▲
Bryophyllum tubiflorum 0 M mannitol, pH 6.0 △ —— △

The position H on the mantissa denotes malate content of intact tissue at time of harvest.

All data points the mean of either duplicate or triplicate samples.

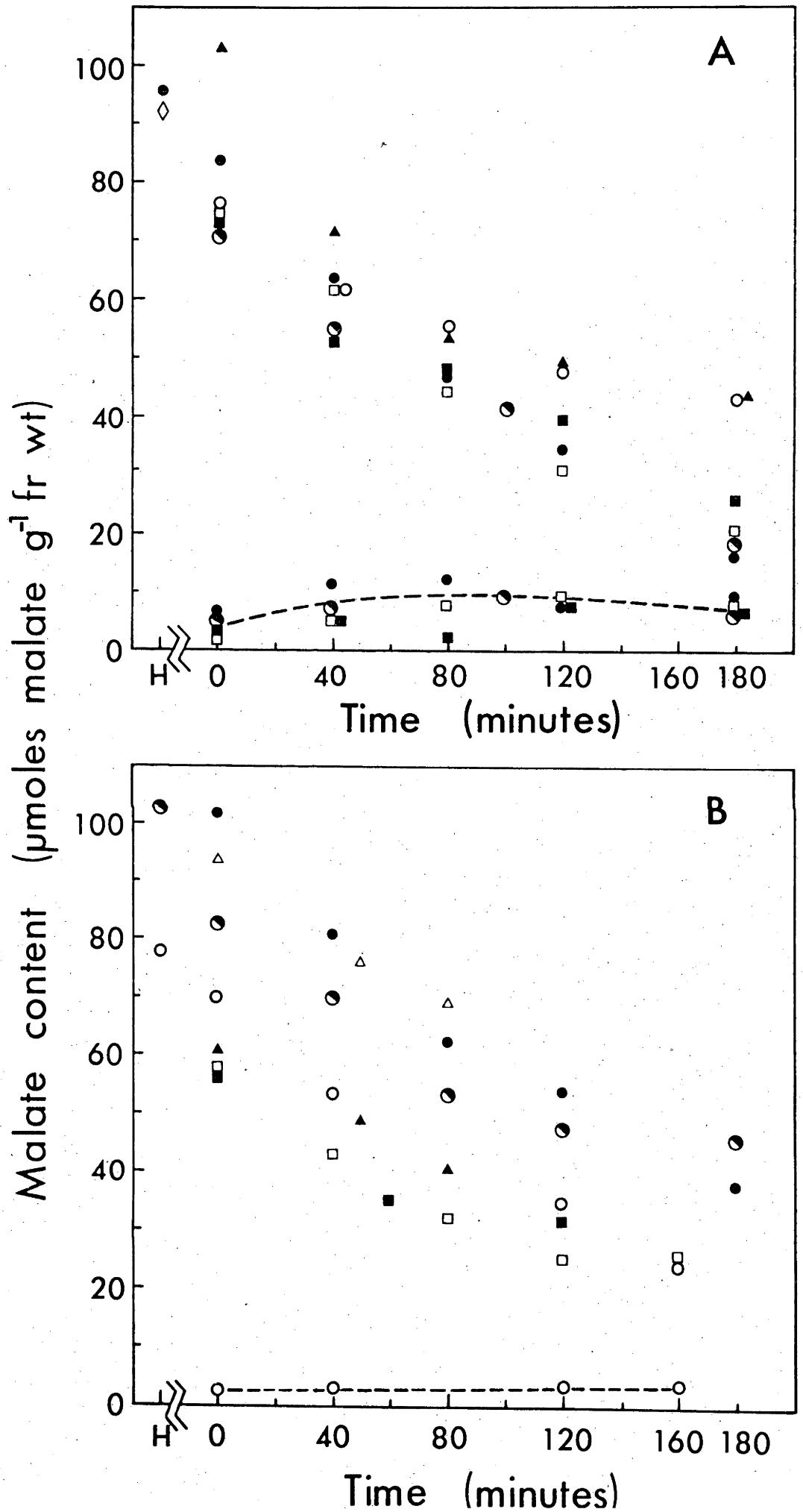
A
B
Malate content (μmoles malate g⁻¹ fr wt)
100
80
60
40
20
0
H
0
40
80
120
160
180
Time (minutes)

Figure 2.4 Change of malate content in leaf slices of 100 mM NaCl grown or C_3 (■——■), and 400 mM NaCl grown or CAM (● —— ●) *M. crystallinum*, and in leaf slices of spinach (▲——▲).

All data point are the means of duplicate samples. The position H on the mantissa denotes the malate content of intact tissue at the time of harvesting.

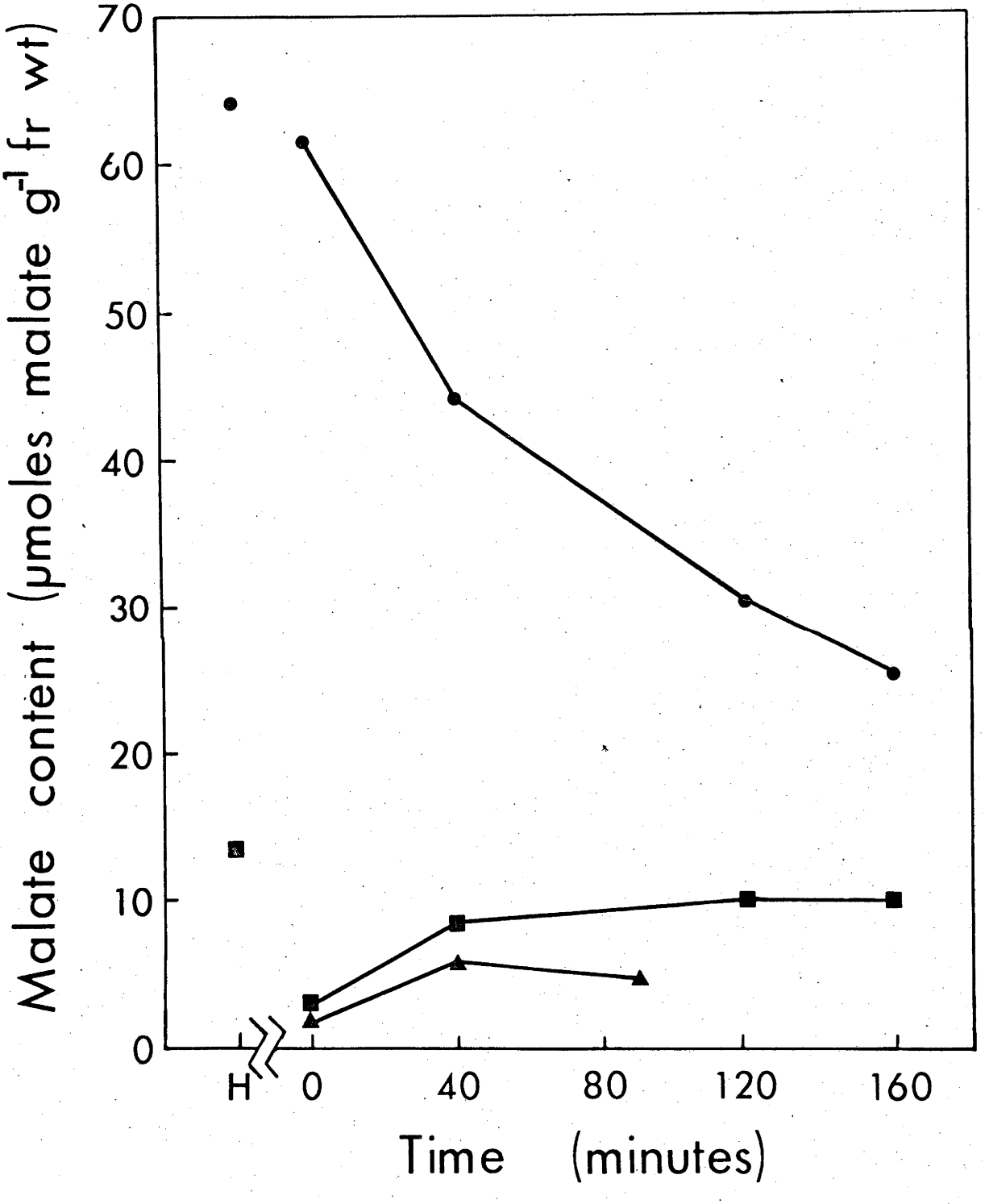
Malate content (μmoles malate g-1 fr wt)
70
60
50
40
30
20
10
0
H
0
40
80
120
160
Time (minutes)

In leaf slices from *Kalanchoe*, malate consumption and efflux are not affected by changing the pH of the external medium from pH 7.5 to pH 4.0, nor are they affected by increasing the osmotic pressure of the medium from 0 to ≃ -7.5 bar by increasing the mannitol concentration from 0 to 0.3 M (Figure 2.3A). The low rates of malate efflux and the lack of any effect of increasing the osmotic pressure of the external medium on malate efflux observed in these experiments do not necessarily contradict the observations of Lüttge and his co-workers (Lüttge and Ball, 1974a, 1977a) as, in their studies, malate efflux across the plasmalemma may have been artificially stimulated by washing the slices in a large external aqueous phase. In the present studies the volume of the bathing medium was purposely kept very small because I wished to feed ^{14}C intermediates of the maximum possible specific activity in later experiments.

In a subsequent study, Lüttge, Ball and Greenway (1977) measured malate efflux from leaf slices in media containing 0 and -5 bar mannitol, a slowly permeating osmoticum which affects both water and turgor potential, or -5 bar ethylene glycol a rapidly permeating osmoticum which changes water potential but only transiently effects turgor potential. Malate efflux which occurred at 0 bar was halted by mannitol at -5 bar but not by ethylene glycol. The authors concluded that malate efflux depended on turgor potential only, not water potential. Moreover, efflux was a function of the turgor at any one time i.e. transient fluctuations in turgor potential cannot act as a trigger for longer term changes in malate efflux.

The initial tissue malate content varied between experiments presumably due to a variety of factors such as natural variations between plants or even leaves on the same plant, differences in prehistory, age, leaf

shading, the exact time of harvesting, and the time taken between harvesting the tissue and beginning each experiment. In *Aloe* and, in particular, *Stapelia*, the initial tissue weights varied depending upon the amount of water tissue still adhering to the slices. Nevertheless, as shown in Table 2.1, the average maximum rates of decarboxylation by leaf slices were similar to, or more often higher than, those observed in intact tissue. These higher rates are most likely due to the higher light intensity used in the *in vitro* experiments. In the leaf slices from CAM tissue the maximum rates of decarboxylation are the rates observed over the first 40 to 60 minutes of each experiment. In both intact tissues and leaf slices, the rates of decarboxylation constantly decreased with decreasing internal malate content and increasing time of exposure to light. This agrees with the observations of Denius and Homann (1972) that photosynthetic O_2 production by *Aloe* leaf slices is linearly related to tissue malate content.

The preceding data suggests that malate decarboxylation is not affected by the mannitol concentrations or pH's of the external media used in this study. It does not necessarily follow, however, that the consumption of the products of malate decarboxylation, that is, CO_2 and the relevant 3 carbon compound (s), are not affected. For example Jones (1973) observed 15% inhibition of $^{14}CO_2$ fixation by 0.3 M mannitol in leaf slices of cotton, and variation in the products of $^{14}CO_2$ fixation have been reported in spinach leaf slices in media of different pH (Böcher and Kluge, 1977) and in *K. daigremontiana* leaf slices in media of varying osmotic pressure (Kluge and Heininger, 1973).

Table 2.1 Average maximum rates of change in malate content[a], in the light, in leaf slices of six CAM and non-CAM species.

Species		No. of Expts.	Initial malate content		Maximum rate of change		
			Harvest[b] (μmoles g^{-1} fr wt)	Expt. start[c]	Intact tissue (μmoles g^{-1} fr wt hr^{-1})	Slices	Slices (μmoles mg chl^{-1} hr^{-1})
S. oleracea		1	-[d]	3.7	-	+0.5	+0.4
M. crystallinum	C_3	1	14	3.0	-	+7.5	+22
	CAM	1	64	61	-	-14	-26
A. arborescens		8	78-120	52-102	-26	-25	-111
B. tubiflorum		1	-	94	-19	-22	-45
K. daigremontiana		9	92-120	69-103	-15	-22	-44
S. gigantea		3	103[e]	43-90	-20	-25	-100

a Malate assayed using the method of Hohorst (1963)

b Intact tissue

c Leaf slices

d -, not determined

e Single determination only

2.1.4 Conclusions

Malate decarboxylation occurs in acidified isolated leaf slices at rates similar to or higher than those observed in intact tissue. The higher rates are probably due to the high light intensity used in the leaf slice experiments. In contrast to many reports in the literature no significant malate efflux was observed from leaf slices suspended in media of low osmotic pressure. This is most likely due to the high tissue to volume ratio used in my experiments.

During periods of maximum deacidification, assuming a stoichiometric production of pyruvate or PEP from malate, *Kalanchoe daigremontiana* and *Bryophyllum tubiflorum* produce about 45 μmoles pyruvate mg chl^{-1} hr^{-1}, *Aloe arborescens* and *Stapelia gigantea* produce about 100-110 μmoles of PEP (and possibly pyruvate) mg chl^{-1} hr^{-1}, and CAM *Mesembryanthemum* produces about 26 μmoles pyruvate mg chl^{-1} hr^{-1}. These rates are certainly minimum estimates as one would expect that under natural conditions of high sunlight and high day temperatures deacidification rates would be increased.

Although conventional malate decarboxylation occurs in leaf slices this does not necessarily imply that the pyruvate and CO_2 consumption mechanisms are functioning similarly. This will be one of the problems investigated in the next section.

2.2 Metabolism of $^{14}CO_2$ During Deacidification

2.2.1 Introduction

The rates and pathways of CO_2 production and consumption in the light in CAM tissue are functions of the tissue prehistory, tissue malate content, PEP concentration, stomatal resistance, light intensity, and the relative activities of the two carboxylases and the decarboxylases which reside in each cell. It is nevertheless possible, as described in Section 1.2, to recognise 3 distinct CO_2 fixation phases in the light. In this section, $^{14}CO_2$ fixation during the deacidification phase (Phase 3) will be examined in acidified *Kalanchoe* and *Stapelia* leaf slices. Some data on dark fixation by deacidified leaf slices will also be presented for comparative purposes. To the best of my knowledge this is the first time that $^{14}CO_2$ fixation in the light has been reported in PEPCK CAM plants.

A study of the products of $^{14}CO_2$ fixation during deacidification in leaf slices may

1. Indicate, by comparison with the products of $^{14}CO_2$ fixation in deacidifying intact tissue, whether the CO_2 consuming pathways in leaf slices are functioning similarly to intact tissue.

2. Indicate whether NADP malic enzyme and PEPCK CAM tissues have similar CO_2 fixing pathways during deacidification.

3. Show whether the rates of CO_2 fixation are adequate to fix the CO_2 produced during deacidification.

4. Indicate, by the distribution of label among ^{14}C labelled products, the relative *in vivo* activity of PEP carboxylase during deacidification. If any malate is formed one should be able to estimate the extent of any mixing of the cytoplasmic and vacuolar malate pools, and

5. Establish whether there is any substantial diversion of photosynthetic intermediates, via glycolysis or otherwise, through the TCA cycle. If this occurs one might be able to estimate the extent of any such transfer of carbon between the mitochondria and the cytoplasm.

2.2.2 Materials and methods

2.2.2.1 *$^{14}CO_2$ labelling and extraction*

Plants were grown and leaf slices prepared as described in Sections 2.1.2.1 and 2. The leaf slices were suspended in 3.0 ml of a medium containing 25 mM HEPES-NaOH pH 7.5, 0.1 mM $CaSO_4$ and 0.25 M mannitol. The sealed vials containing the slices were preincubated for 10 minutes at room temperature in a shaker (about 100 strokes per minute). The vials were illuminated with a quantum flux density of 1,200 μeinstein m^{-2} s^{-1} at vial top height by a Philips 1000 W HPLR high pressure mercury fluorescent lamp shining through 5 cm of water. Dark labelling experiments were performed in a dark room. Light, which was necessary for experimental manipulations, was provided by a torch fitted with a green filter. Tissue in control flasks was killed by boiling for 2-3 minutes prior to preincubation.

After preincubation 30 μmoles $NaH^{14}CO_3$ (usually about 1.4 x 10^6 dpm $\mu mole^{-1}$) in 0.1 ml was injected into each vial to give a final $NaH^{14}CO_3$ concentration of 10 mM. The tissue was removed from the vials after appropriate intervals, and plunged into 20 ml of boiling 80% EtOH. About 10 to 15 seconds elapsed between removal of the slices from the vials and killing the tissues. During this time the tissue was exposed to low laboratory light conditions. When the volume had halved, the extraction medium was made up to 20 ml with H_2O and boiled again for 5 minutes before being ground in a 15 ml Ten-Broeck glass homogeniser and filtered under

vacuum through glass microfibre filter paper (Whatman GF/C, 5.5 cm). The residue was washed with hot H_2O and then with EtOH before drying and counting. The filtrate was dried in a rotary evaporator at 33°C and resuspended in 10% isopropanol.

In experiments in which the labelled products were identified by paper or by thin layer chromatography, the filtrate was extracted with chloroform prior to rotary evaporation as described in Section 2.3.2.4. A flow chart illustrating the extraction procedure is given in Figure 2.5.

2.2.2.2 *Ion exchange chromatography*

The resuspended extract was passed through a cation column (7 cm x 0.5 cm diam, Dowex 50W 200-400 mesh, hydrogen form) and an anion column (5 cm x 0.5 cm diam, Biorad AG1 x 8 200-400 mesh, formate form) prepared as follows:

Cation column. The resin was thoroughly washed two to four times with 10-20 bed volumes of H_2O and stored in 2N HCl at 4°C until required. The resin was then brought to room temperature, pippetted into columns and washed with about 5 volumes of H_2O and 5 volumes of 2N HCl. The columns were then washed with H_2O until the eluant pH > 5.5.

Anion column. The methods of washing, storing, pouring and charging the anion columns were identical to those used for the cation columns except that 1N formic acid was used instead of 2N HCl.

The anion columns were attached to the bottom of the cation columns with tubing and the air space between the columns was filled with H_2O. The tissue extract was passed through the connected columns followed by

Figure 2.5 A flow chart illustrating the time taken to harvest the leaves, cut the leaf slices and to label and kill the tissue. The chart also illustrates some of the following steps involved in extracting the labelled metabolites.

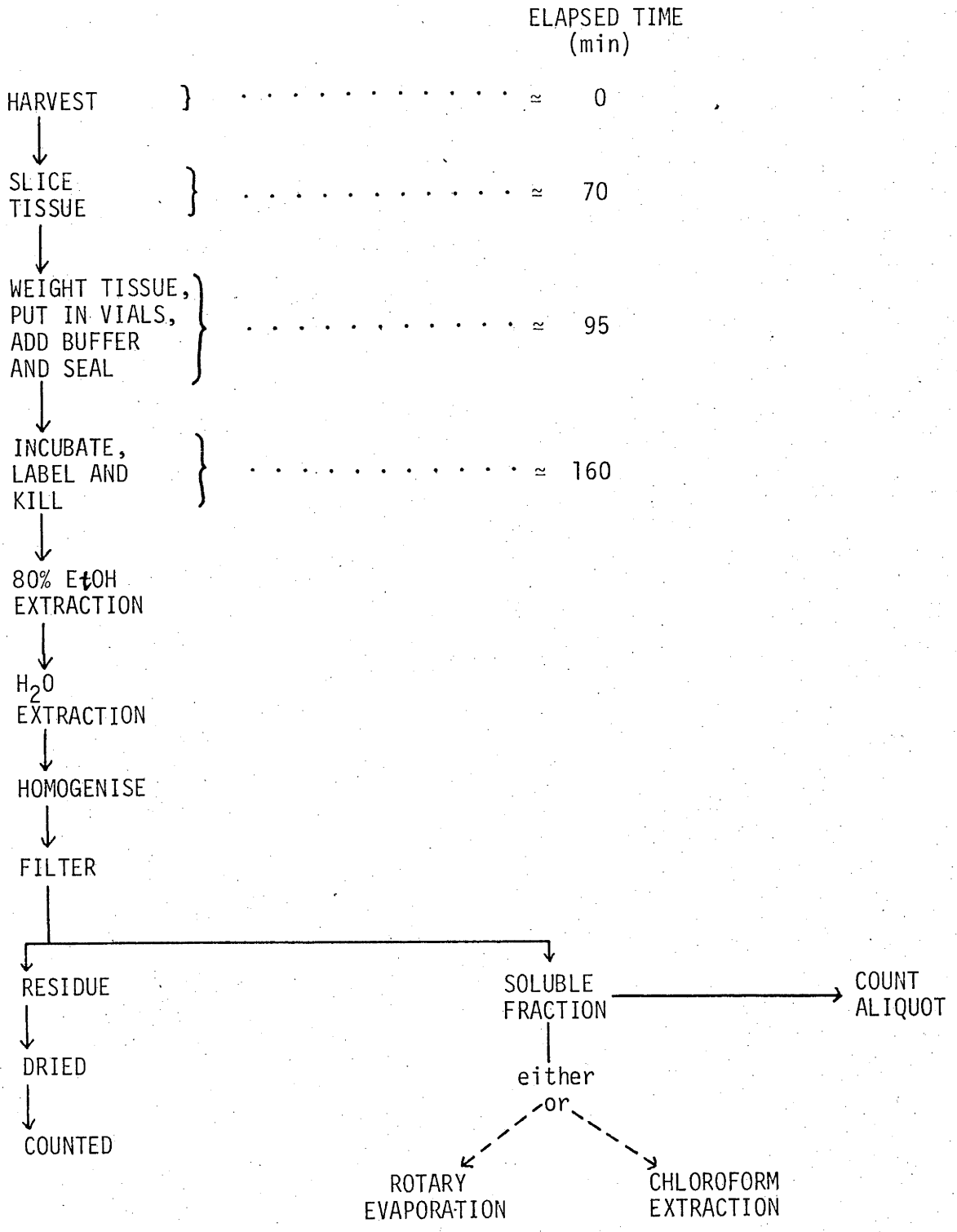

7 ml H_2O. The cation columns were then disconnected and the anion columns were washed with a further 3 ml H_2O. The eluant contained sugars and other uncharged compounds. Amino acids and other basic compounds were eluted from the cation columns with 10 ml of 10% (v/v) NH_4OH. Organic acids and phosphorylated compounds were eluted from the anion columns with 10 ml 6N formic acid and 10 ml 2N HCl respectively. Whenever chromatographic separation of phosphorylated compounds was required the phosphorylated compounds were eluted with 10 ml of 15 N formic acid since HCl salts, formed during subsequent rotary evaporation, caused tailing of chromatograms. ^{14}C was measured in samples from the initial and the eluted fractions, and occasionally the resins were also checked for any non-eluted radioactivity.

2.2.2.3 *Paper and thin layer chromatography*

When necessary the ion exchange fractions were rotary evaporated, resuspended in 200 µl 10% (v/v) isoproponal and separated and identified using one or more of the following chromatographic techniques:

Amino acids. (A) Two dimensional ascending paper chromatography with 1 MM or 3 MM Whatman paper (10 cm x 10 cm). The papers were run for 3 hours in the first dimension in EtOH/NH_4OH/H_2O (4:1:1) and for about 3 hours in the second dimension in diethyl ether/formic acid/H_2O (7:2:1) (Osmond, 1974). (B) One dimensional descending paper chromatography using Whatman 1MM or 3 MM paper (46 cm x 57 cm) in acetone/triethylamine/H_2O (16:3:1) for 7-8 hours (Wright and Stadtman, 1956). (C) One dimensional thin layer chromatography. Merck prelayered HPTLC F_{254} silica 60 plates were run twice for about 6 hours in a n-propanol/NH_4OH (7:3).

Organic acids and phosphorylated compounds. (A) See solvent system A above. (B) One dimensional descending paper chromatography using Whatman 1 MM or 3 MM paper (46 cm x 57 cm) (Walker, 1957). Tertiary amyl alcohol, formic acid and water (3:1:3) were mixed in a separating column and allowed to stand for 4-5 hours. The lower phase was decanted and placed in the bottom of the chromatography tank. The chromatograms were equilibrated for an hour in the tank before being run overnight in the upper phase. (C) One dimensional thin layer chromatography. Thin layer plates (10 cm x 10 cm) were spread with a 0.3 mm layer of cellulose (15 g Machery and Nagel MN300 cellulose homogenised in 90 ml H_2O. Approximately 20 ml per plate) and dried for 2-3 days at room temperature. The plates were run twice for 6-8 hours in the same direction in a solvent mixture containing 33% (v/v) NH_4OH/n-propanol/isopropanol/n-butanol/iso-butyric acid/H_2O (4:14:3:3:100:38) and EDTA (0.3 g l^{-1} solvent) (Feige *et al.*, 1969).

Sugars. (A) See solvent (a) for amino acids. (B) One dimension descending paper chromatography using Whatman 1 MM or 3 MM paper (46 cm x 57 cm) twice for 20 hours in butanol/pyridine/H_2O (10:3:3) (Hough and Jones, 1962).

2.2.2.4 *Colourimetric detection*

The following sprays were used to identify non-radioactive chromatogram spots.

Amino acids. A ninhydrin spray was prepared containing 28 ml acetic acid and 1 g ninhydrin made up to 400 ml with acetone. The chromatograms were lightly sprayed and dried for 10 minutes in a fume hood. They were then placed in an oven and heated at 70°C until the spots had developed their full colour. Amino acids showed up as purple, blue, yellow or brown spots on a white background.

Organic acids. A commercially prepared bromocresol green spray (Merck) was used. Organic acids appeared as blue or yellow spots against a green background.

Phosphorylated compounds. A modified Hanes-Isherwood Reagent (Aronoff, 1961) was used. The spray consisted of 1 g ammonium molybdate dissolved in 8 ml H_2O containing 3 ml concentrated HCl. 3 ml of 70% perchloric acid was then added and the solution was made up to 100 ml with acetone. The chromatograms were lightly sprayed, dried at 70°C for 5 minutes, and developed for ½ hour under ultraviolet light. Organic phosphates showed up as dark blue spots on a light blue background. This spray affected the chromatograms by making the paper very fragile.

Sugars. Two sprays were used. In the first spray 20 ml of 10% (w/v) ammonium molybdate was added to 3 ml of concentrated HCl. The solution was shaken and 5 g of NH_4Cl was added. The chromatogram was sprayed lightly and heated for 20 minutes at 70°C in the dark. Sugars showed up as blue spots, phosphates as yellow spots and phosphorylated reducing compounds were green. In the second spray 1 g p-anisidine and 3 g trichloroacetic acid was dissolved in 70% EtOH. The chromatograms were sprayed and heated at 70°C for 5-10 minutes. Sugars appeared as brown or yellow spots on a white background (Aronoff, 1961).

2.2.2.5 *Autoradiography*

The chromatograms were marked on the corners with radioactive ink (Indian ink with added $Na^{36}Cl$) and laid face down on sheets of either Kodirex or Ilford Rapid R Type S 25 FW x-ray film. Each chromatogram was separated by a cardboard spacer and each block of chromatograms was covered by a wooden board and stored in a deep freeze for 2-3 weeks. The films were then developed, the ink marks on the chromatograms were

aligned with the corresponding marks on the film, and the positions of the labelled compounds were marked on the chromatograms. The spots were then removed and either counted in non-aqueous fluor or eluted and rechromatographed in another solvent system.

Spots on chromatograms that contained large amounts of ^{14}C were identified using a strip counter (Berthold; Dünnschicht-Scanner II).

2.2.2.6 *^{14}C determinations*

Two scintillation fluors were used, one for aqueous samples (5 g PPO l^{-1} toluene/triton x 100 (2:1)) and one for non-aqueous samples (5 g PPO l^{-1} toluene). When aqueous samples were counted 1 ml of sample was added to 9 ml fluor.

Amino acid fractions, which contained 10% (v/v) NH_4OH, and chloroform samples caused strong quenching. This was overcome by drying the samples on filter paper and counting the filter paper in the non-aqueous fluor.

Samples were counted after 15 minutes dark storage in a scintillation counter (Nuclear Chicago Delta 300). Quench curves were constructed for each sample type and fluor and all ^{14}C measurements were corrected for machine counting efficiency and sample quenching.

2.2.3 Results and discussion

The incorporation of $^{14}CO_2$ in the light by deacidifying *K. daigremontiana* and *S. gigantea* leaf slices was linear (Figure 2.6). The rates, of about 80 µmoles CO_2 fixed mg chl^{-1} hr^{-1} in *Kalanchoe*

Figure 2.6 A. $^{14}CO_2$ fixation by acidified *Kalanchoe* leaf slices in the light o —— o, and deacidified *Kalanchoe* leaf slices in the dark • —— •.

B. $^{14}CO_2$ fixation by acidified *Stapelia* leaf slices in the light o —— o, and deacidified *Stapelia* leaf slices in the dark • —— •.

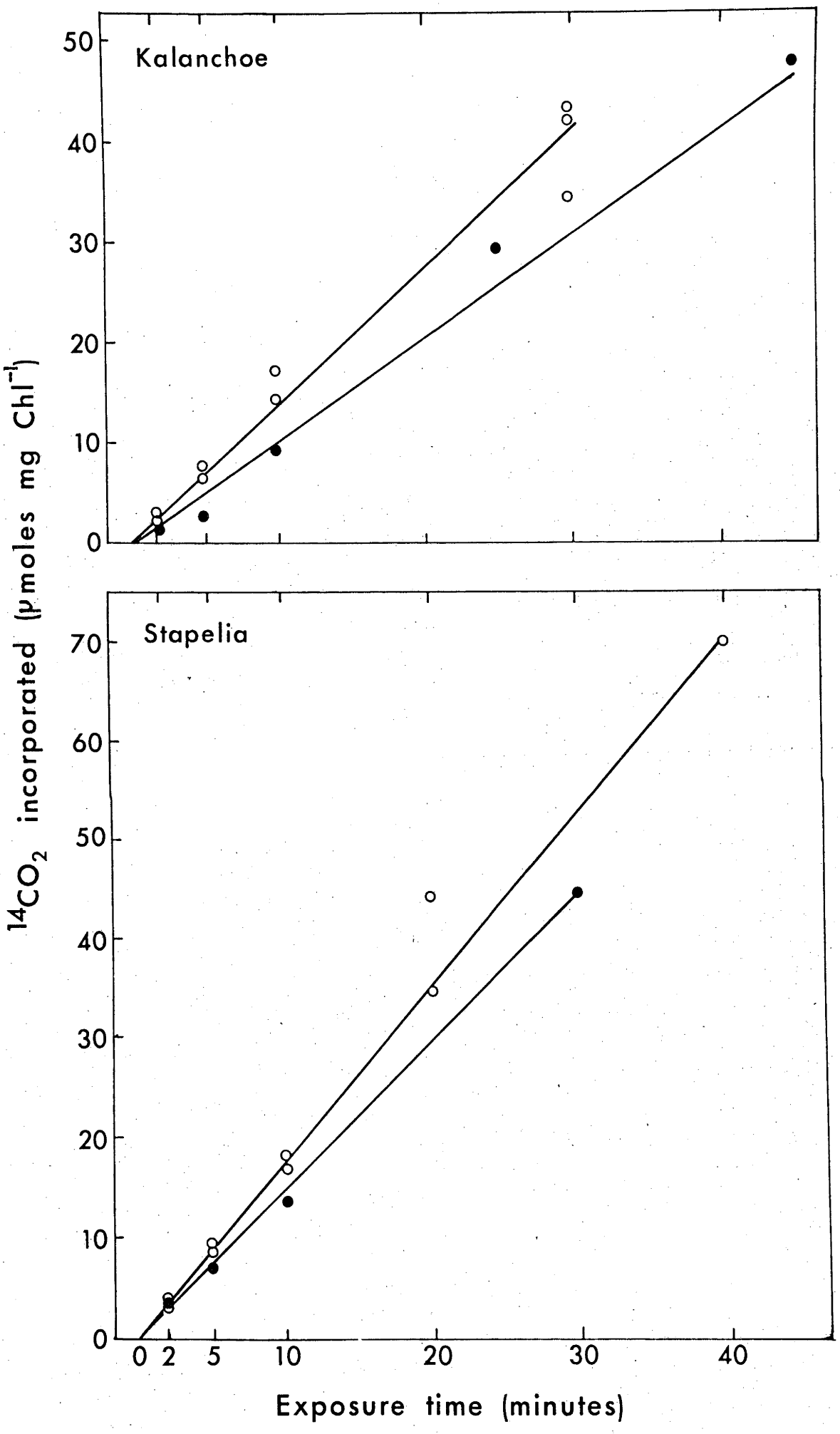
Kalanchoe
Stapelia
$^{14}CO_2$ incorporated (μmoles mg Chl^{-1})
Exposure time (minutes)
0
10
20
30
40
50
60
70
0 2 5 10 20 30 40

and about 110 μmoles mg chl^{-1} hr^{-1} in *Stapelia*, are more than adequate to account for the refixation of all the CO_2 produced during the periods of maximum deacidification in leaf slices from both species (viz ≃ 45 μmoles mg chl^{-1} hr^{-1} for *Kalanchoe* and ≃ 100 μmoles mg chl^{-1} hr^{-1} for *Stapelia*). These rates are minimum estimates since the specific activity of the $^{14}CO_2$ will most likely be reduced due to dilution of the labelled CO_2 by unlabelled CO_2 produced during deacidification. The rates of dark $^{14}CO_2$ fixation by deacidified tissue were only slightly lower than the light rates (Figure 2.6).

Although *Stapelia* exhibits higher rates of light and dark $^{14}CO_2$ fixation on a chlorophyll basis the distribution of ^{14}C in labelled products was similar for each treatment in both species (Figures 2.7 and 2.8). The principal labelled products in both species after 2 minutes $^{14}CO_2$ exposure in the light were phosphorylated compounds and carbohydrates. The organic acid and amino acid fractions contained only 24% and 7% respectively of the total label in *Kalanchoe* and 17% and 4% respectively of the label in *Stapelia*. In contrast, when $^{14}CO_2$ was fed to deacidified *Kalanchoe* and *Stapelia* leaf slices in the dark the organic acid fractions contained 66% and 82% respectively of the total label and 32% and 17% respectively was in amino acids (Figure 2.9).

The percentage of the total light assimilated label in the carbohydrate fraction increased with exposure time so that, after 40 minutes, 85% - 90% of the total label in both species was in the carbohydrate fraction, 5% - 10% was in phosphorylated compounds, 3% - 5% was in organic acids and only about 1% was in amino acids. The amount of ^{14}C in the organic acids appeared to be close to saturation after 40 minutes.

Figure 2.7 A. Distribution of ^{14}C in products of light $^{14}CO_2$ fixation by deacidifying *Kalanchoe* leaf slices. ● —— ● sugars plus starch (carbohydrate), o —— o phosphorylated compounds, ▲——▲ organic acids, ■——■ amino acids.

B. Distribution of ^{14}C in products of light CO_2 fixation by deacidifying *Stapelia* leaf slices. ● —— ● sugars plus starch (carbohydrate), o —— o phosphorylated compounds, ▲——▲organic acids, ■——■amino acids.

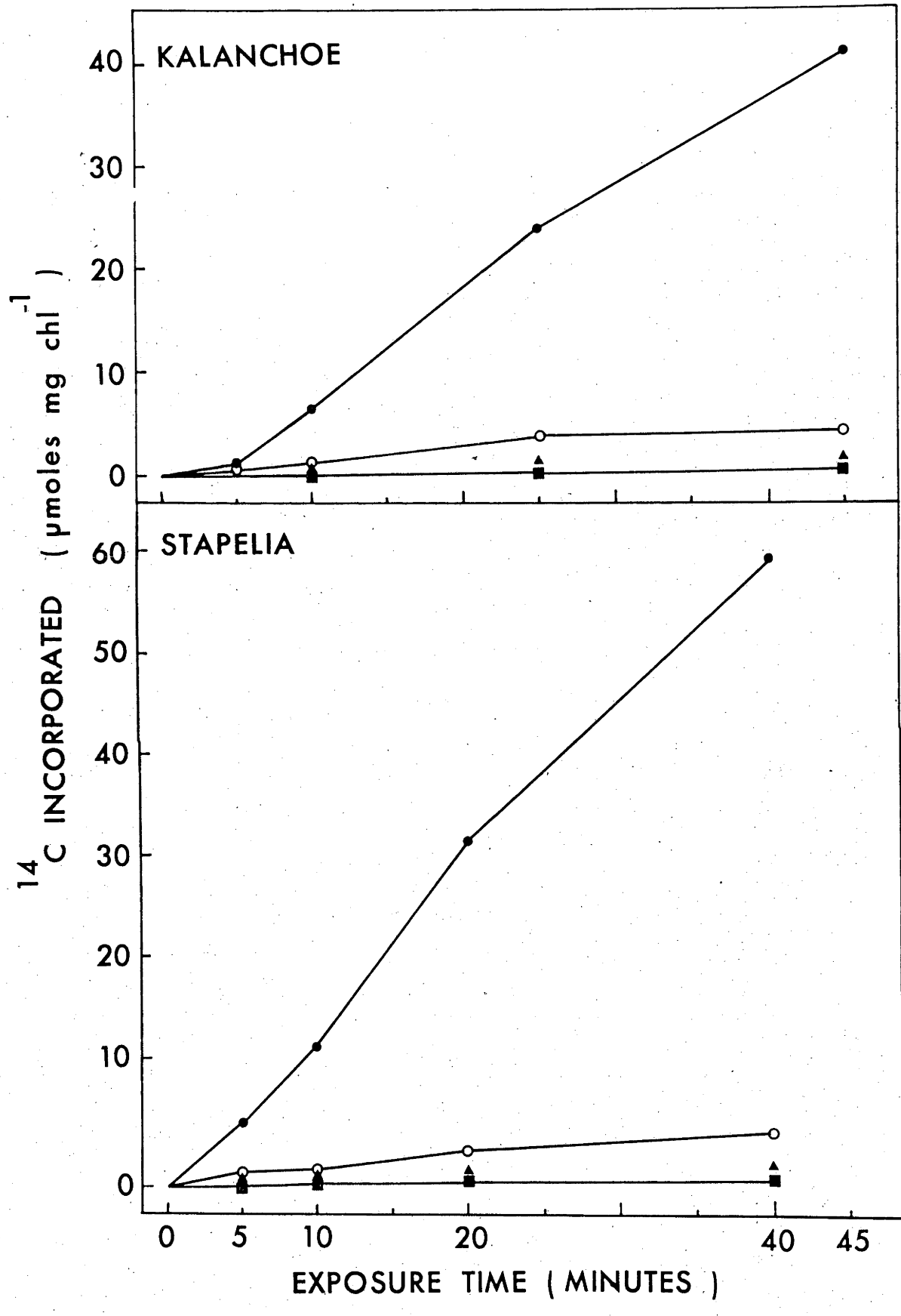
KALANCHOE
STAPELIA
40
30
20
10
0
60
50
40
30
20
10
0
0
5
10
20
40
45
^{14}C INCORPORATED (μmoles mg chl^{-1})
EXPOSURE TIME (MINUTES)

Figure 2.8 A. Percentage distribution of ^{14}C in products of $^{14}CO_2$ assimilation in the light by deacidifying *Kalanchoe* leaf slices. ● —— ● sugars and starch (carbohydrates), o —— o phosphorylated compounds, ▲ —— ▲ organic acids, ■ —— ■ amino acids.

B. Percentage distribution of ^{14}C in products of $^{14}CO_2$ assimilation in the light by deacidifying *Stapelia* leaf slices. ● —— ● sugars and starch (carbohydrate), o —— o phosphorylated compounds, ▲ —— ▲ organic acids, ■ —— ■ amino acids.

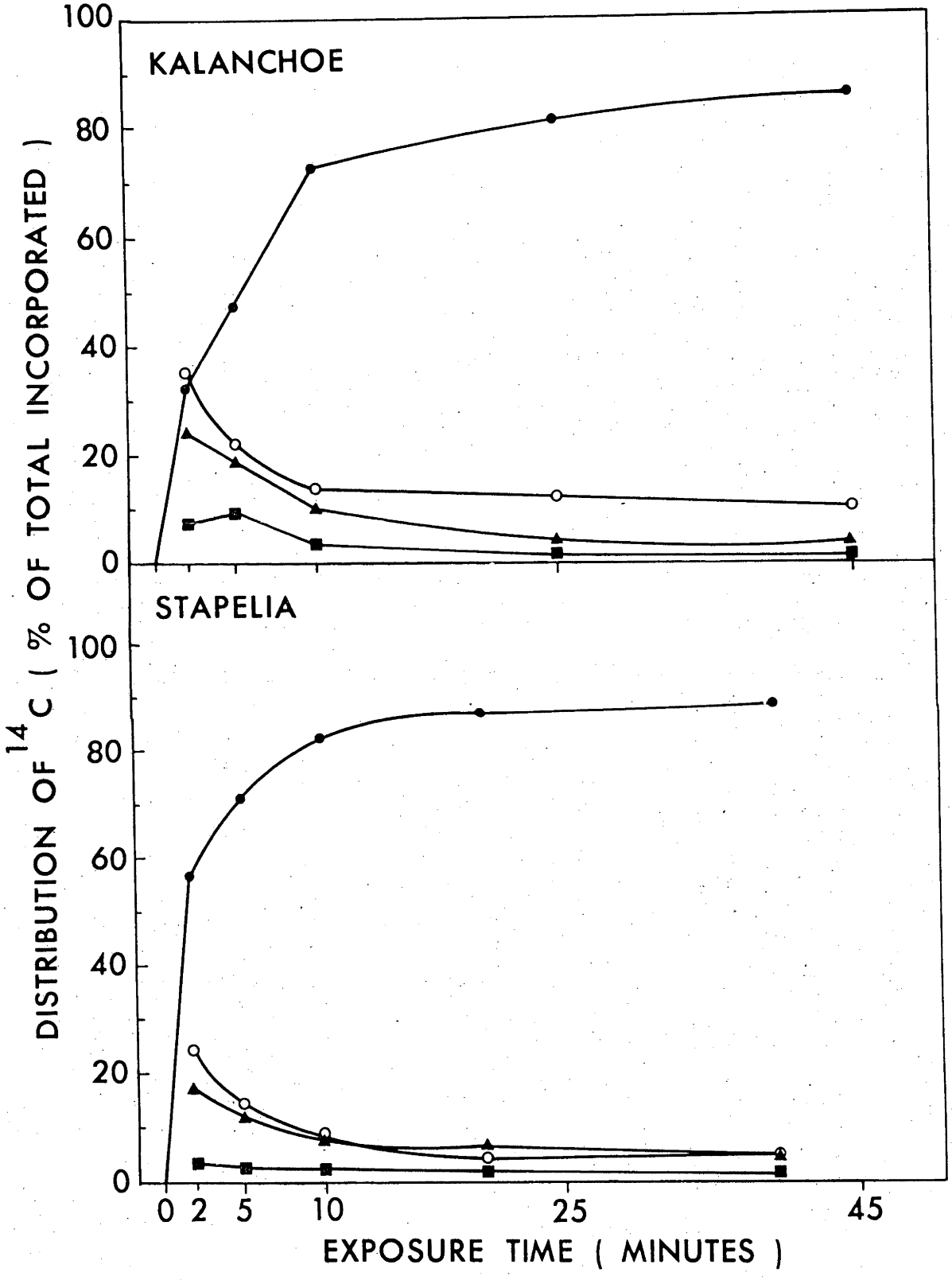
KALANCHOE
STAPELIA
DISTRIBUTION OF ^{14}C (% OF TOTAL INCORPORATED)
EXPOSURE TIME (MINUTES)
0
20
40
60
80
100
0 2 5 10 25 45

Figure 2.9 A. Percentage distribution of ^{14}C in products of dark $^{14}CO_2$ incorporation by deacidified *Kalanchoe* leaf slices ● —— ● sugars and starch (carbohydrate), ▲ —— ▲ organic acids, ■——■ amino acids.

B. Percentage of ^{14}C in products of dark $^{14}CO_2$ incorporation by deacidified *Stapelia* leaf slices ● —— ● sugars and starch (carbohydrate), ▲ —— ▲ organic acids, ■——■ amino acids.

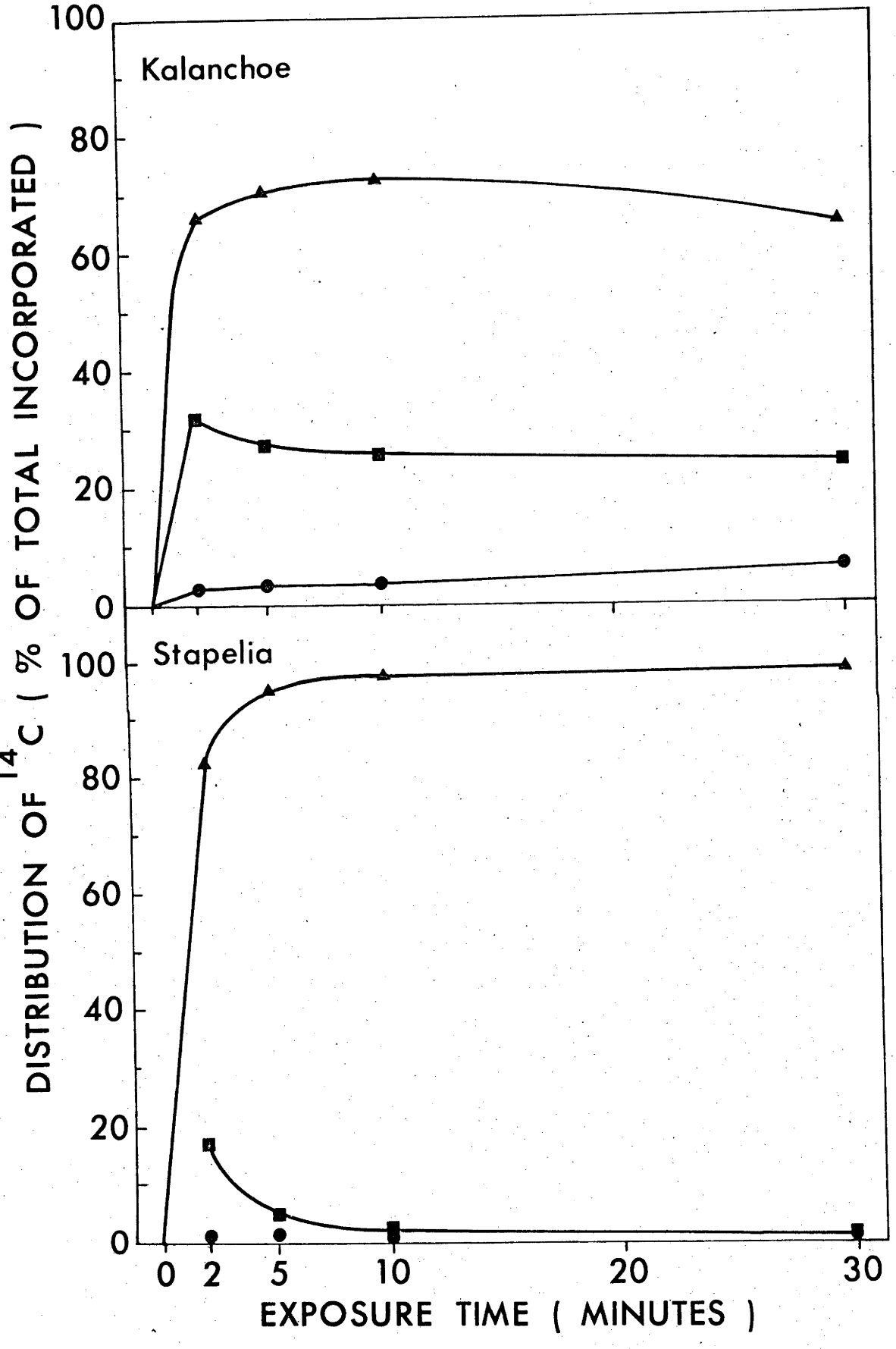
Kalanchoe
Stapelia
100
80
60
40
20
0
0
2
5
10
20
30
DISTRIBUTION OF ^{14}C (% OF TOTAL INCORPORATED)
EXPOSURE TIME (MINUTES)

However, a closer examination of the label in individual organic acids in *Kalanchoe* (Figure 2.10) shows that although the amount of ^{14}C in malate had saturated, the amount of label in citrate and isocitrate was slowly increasing, and the amount of label in fumarate and succinate was increasing rapidly. Only about 1% of the ^{14}C in the acid fraction of dark labelled *Kalanchoe* was in fumarate and succinate after 40 minutes compared with about 45% (equivalent to 1.3% of the total carbon fixed) in light exposed tissue.

In *Kalanchoe* slices, alanine was the major light labelled amino acid after 5 minutes exposure, and whereas the amount of label in aspartate/glutamate saturated after about 5 minutes and the amount in glycine and serine only slowly increased, the amount in alanine continued to increase linearly for at least 45 minutes (Figure 2.11). Aspartate/glutamate were the major dark labelled amino acids in deacidified *Kalanchoe* slices and after 5 minutes exposure contained almost 400 nmoles ^{14}C mg chl^{-1} which was about 88% of the label in the amino acids fraction. The remaining 50 nmoles mg chl^{-1} was in alanine. The amount of label in aspartate/glutamate steadily declined however and after 30 minutes exposure contained only 250 nmoles ^{14}C mg chl^{-1}. In contrast the label in alanine steadily increased until after 30 minutes alanine contained about 140 nmoles ^{14}C mg chl^{-1}. No label was detected in glycine and serine in the dark.

In both species the distribution of label in the light amongst the various metabolites is very similar to that reported by Kluge (1969c) for detached deacidifying phyllodes of *B. tubiflorum*, and by Osmond and Allaway (1974) in pulse chase experiments with the C_3 plant *Atriplex*

Figure 2.10 Distribution of ^{14}C in various organic acids during $^{14}CO_2$ assimilation in the light fixation by deacidifying *Kalanchoe* leaf slices. ● —— ● malate, o —— o citrate, plus isocitrate, ▲ —— ▲ fumarate and succinate.

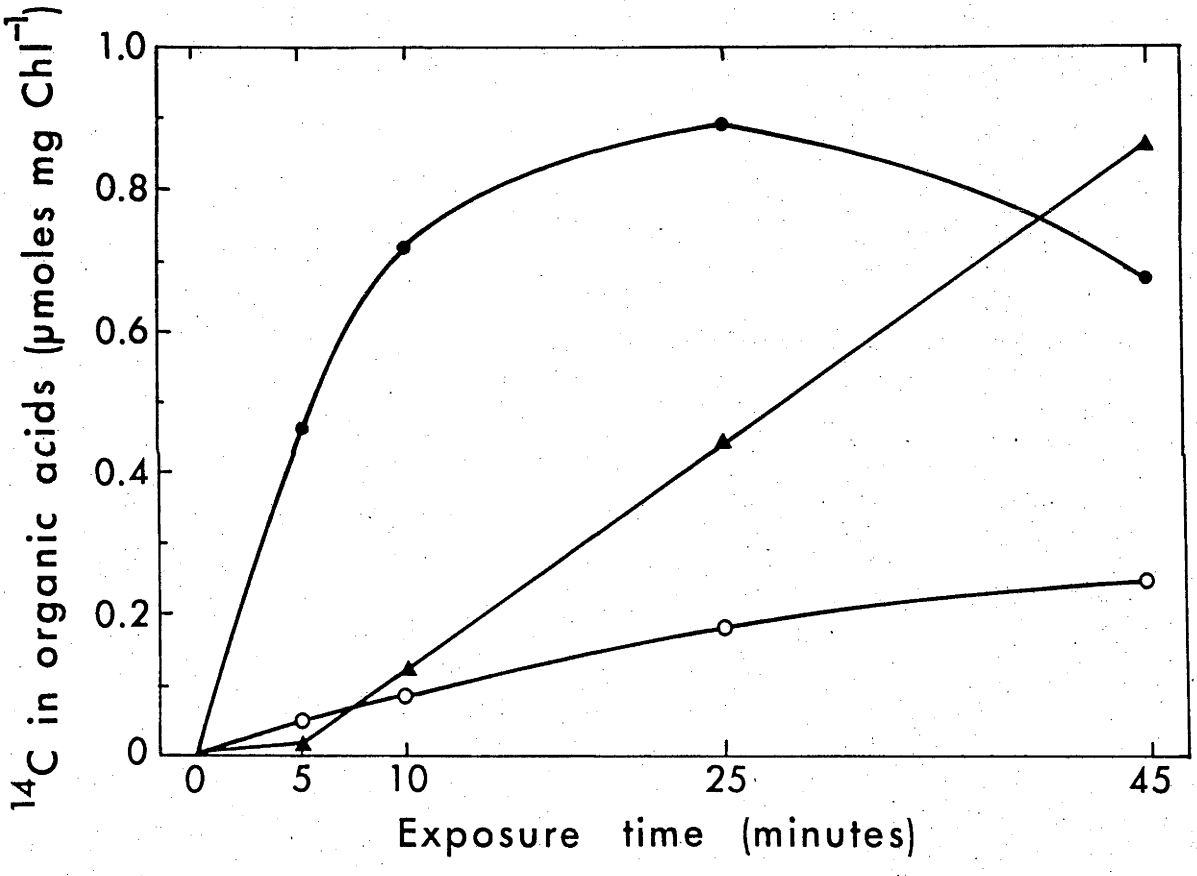
^{14}C in organic acids (μmoles mg Chl^{-1})
1.0
0.8
0.6
0.4
0.2
0
0
5
10
25
45
Exposure time (minutes)

Figure 2.11 Distribution of ^{14}C in various amino acids during $^{14}CO_2$ assimilation in the light by deacidifying *Kalanchoe* leaf slices (open symbols) and during dark by deacidified *Kalanchoe* leaf slices (closed symbols). o —— o, ● —— ● aspartate plus glutamate, □—— □ , ■—— ■ alanine, Δ —— Δ, ▲ —— ▲ glycine plus serine.

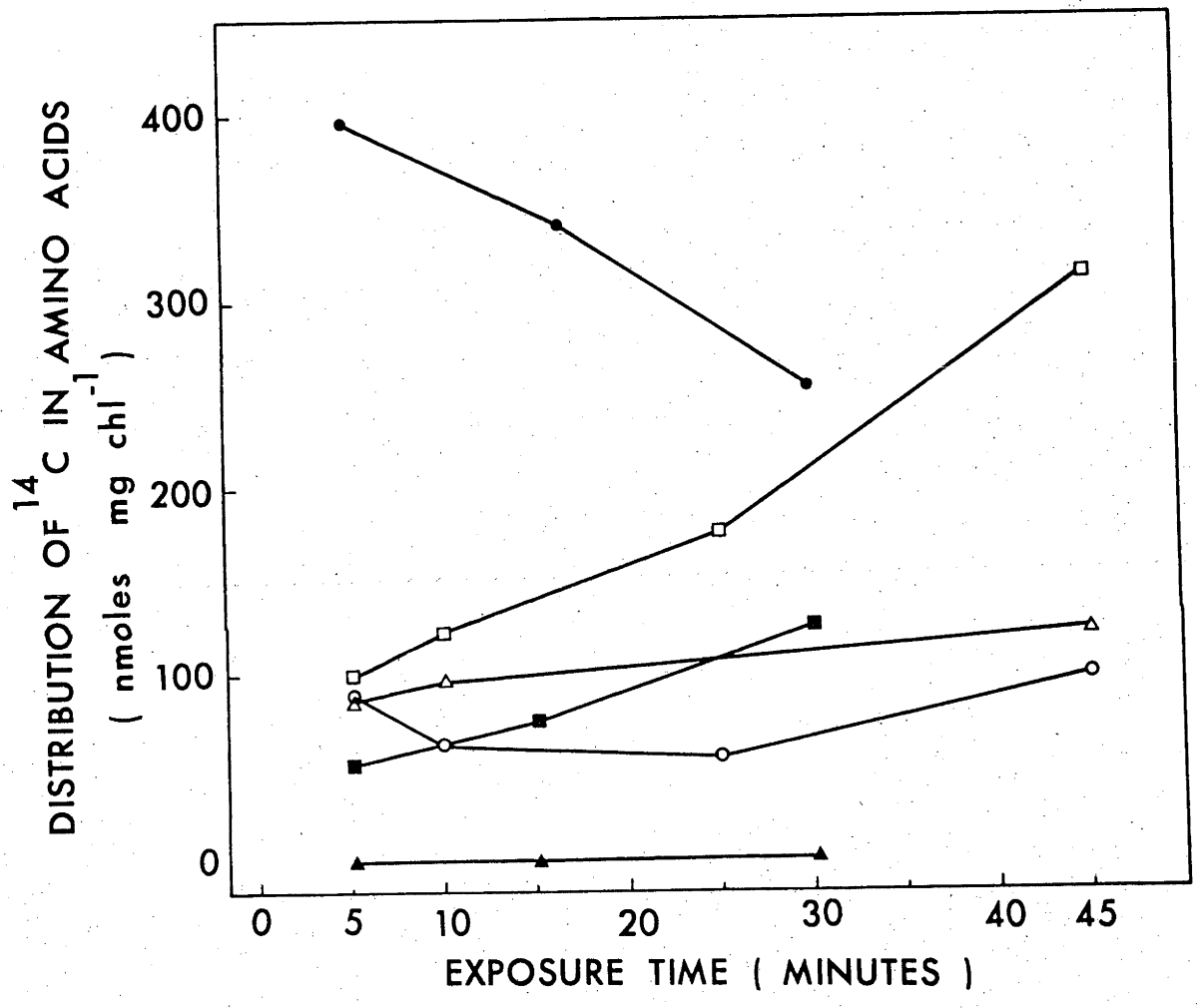
DISTRIBUTION OF ^{14}C IN AMINO ACIDS
(nmoles mg chl^{-1})
400
300
200
100
0
0
5
10
20
30
40
45
EXPOSURE TIME (MINUTES)

patula and with deacidified *Kalanchoe daigremontiana* leaf strips undergoing steady state photosynthesis. In both these studies phosphorylated compounds and sugars were the major labelled metabolites and little label was observed in malate, citrate and in the amino acids. The authors concluded that RuP_2 carboxylase was the principal carboxylating enzyme. That is, in the case of the CAM tissue, PEP carboxylase was in some way inhibited or PEP was limiting. Another possibility is that PEP carboxylase is indeed functioning but the malate is rapidly being decarboxylated. This is not a possibility in investigations by Osmond and Allaway as they used a pulse-chase technique. Although I cannot unequivocally dismiss this possibility in my experiments, there is reasonable *in vitro* evidence that it is unlikely to be of major importance.

Partially purified PEP carboxylase is competitively inhibited by malate and possibly by pyruvate (Kluge and Osmond, 1972). If the vacuolar malate efflux during deacidification is a passive process and thus the cytoplasmic malate concentration more or less reflects the vacuolar concentration, then one would expect that the cytoplasmic malate concentration during deacidification would be many times greater than the K_i (malate), observed by Kluge and Osmond, of 3 mM. Indeed, recent experiments (K. Winter, unpublished) with PEP carboxylase from *Aloe* and *Mesembryanthemum* suggest that the K_i (malate) during deacidification is much lower than previously thought and may even be less than 1 µM.

In *Kalanchoe*, malate appears to saturate at around 0.7-0.8 µmoles ^{14}C mg chl^{-1} after about 20 minutes exposure. This suggests that there

is effectively no mixing of the cytoplasmic and vacuolar malate pools. The observation (Figure 2.10) that malate is labelled before there is substantial labelling in citrate, fumarate and succinate is also relevant to the question of compartmentation. Increases in the label in fumarate and succinate and, to a lesser extent, citrate are not paralleled by an increase in the ^{14}C content of malate, which suggests firstly that there may be an exchange of malate between the cytoplasm and the mitochondrion and secondly that malate in the mitochondrion maybe turning over rapidly. It is tempting to speculate that some malate from the cytoplasm enters the mitochondria where it is decarboxylated by NAD malic enzyme and the resulting pyruvate is transported out of the mitochondria. Isolated mitochondria from the same *Kalanchoe* population have been shown to convert malate to pyruvate at about half the rates of deacidification observed in intact tissue (D. Day, personal communication). It also appears that very little of the pyruvate is metabolised within the mitochondria if the pH of the external medium is below about pH 7.4.

The present investigations do not, however, indicate whether the TCA cycle *per se* is, or is not, functioning in the light. Certainly if it is functional, it metabolises little label from $^{14}CO_2$. Oxygen exchange studies using *Aloe* leaf slices showed that net oxygen evolution during deacidification was inhibited 80% by 1.5 mM amytal, 10 mM fluoroacetate and 10 mM diethyl malonate, all inhibitors of mitochondrial electron transport and the TCA cycle (Denius and Homann, 1972). The authors concluded that both electron transport and the TCA cycle functioned in the light and provided energy for decarboxylation. However, it is puzzling that the same inhibitors had no effect on dark respiration.

2.2.4 Conclusions

Both *Kalanchoe* and *Stapelia* appear to have similar CO_2 fixing mechanisms in the light and the dark. Presumably PEP is not limiting in the dark. The rates of light CO_2 fixation by deacidifying leaf slices are adequate to account for fixation of all CO_2 produced even during times of maximum deacidification. RuP_2 carboxylase seems to be the major primary carboxylase although PEP carboxylase may account for some of the $^{14}CO_2$ fixation. It is hard to assess how this compares with the *in vivo* situation as fixation of external CO_2 is very low during deacidification because the stomates are tightly closed. The only report in the literature of short-term $^{14}CO_2$ labelling of deacidifying detached leaves suggests that possibly 10-15% of the CO_2 was fixed by PEP carboxylase (Avadhani *et al.*, 1971). *In vitro* experiments, in which malate inhibition of PEP carboxylase have been studied, suggest that the contribution of PEP carboxylase to carbon fixation during deacidification should be less than this. One can conclude that it is uncertain whether the apparent PEP carboxylase activity truly represents the *in vivo* situation or whether it is, at least in part, an experimentally produced artefact. Certainly refixation of carbon by PEP carboxylase during deacidification is a futile and energetically wasteful cycle.

There appears to be little mixing of cytoplasmic and vacuolar malate but some mixing of cytoplasmic and mitochondrial malate. Fumarate and succinate, the mitochondrial pools of which are most probably smaller than citrate and isocitrate, are more rapidly labelled than citrate plus isocitrate. This observation suggests that citrate and isocitrate are not precursors of fumarate and succinate, and indicates that the label may enter the latter compounds from malate which may, in turn, enter the

mitochondria from the cytoplasm. It is unlikely that ^{14}C-pyruvate derived from photosynthetic products is a major source of label for the TCA cycle acids since labelling of citrate plus isocitrate and fumarate plus succinate continues to increase over a period of at least 45 minutes, long after photosynthetic intermediates and non-vacuolar malate pools are saturated.

2.3 Pyruvate Metabolism in Deacidifying CAM Tissue

2.3.1 Introduction

Pyruvate is an important biological intermediate. It is the only substrate common to the EMP pathway and the TCA cycle; it is closely associated with fat metabolism, nitrogen metabolism and alcoholic fermentation. Pyruvate is also the product of malate decarboxylation by NADP and NAD malic enzymes in CAM plants. In intact *Bryophyllum crenata* and *B. calycinum* leaves the pyruvate pools are small but increase during deacidification from 50 to 100 nmoles g^{-1} fr. wt. and from 200 to 350 nmoles g^{-1} fr.wt., respectively, although between 100 and 150 µmoles malate g^{-1} fr.wt. is decarboxylated during the same period (Milburn *et al.* 1968). Obviously the pyruvate formed during decarboxylation is rapidly metabolised.

Tissues of CAM plants appear to be capable of metabolising pyruvate by at least four pathways in the light. Pyruvate may be oxidised by the TCA cycle and the CO_2 so produced may be refixed by the PCR cycle (Champigny *et al.*, 1958; Moyse *et al.*, 1958). Pyruvate may be converted to alanine (Walker and Ranson, 1958) or to PEP. If it is converted to PEP via pyruvate, Pi dikinase (Kluge and Osmond, 1971; Sugiyama and Laetsch, 1975) the PEP may be subsequently converted to glucan by gluconeogenesis (Haidri, 1955a) or be carboxylated to malate via PEP carboxylase. The latter

possibility is probably only of minor importance during deacidification (Phase 3) since there is a wealth of evidence which shows that all four carbons of malate are converted to carbohydrate in the light (Wolf, 1938; Pucher *et al.*, 1949a, 1949b; Vickery, 1954b; Haidri, 1955a; Sutton, 1974), and that PEP carboxylase activity is most probably inhibited during deacidification (Kluge and Osmond, 1972).

One way of studying the fate of pyruvate during deacidification in the light is to feed ^{14}C labelled pyruvate to deacidifying CAM tissues and to observe the products of incorporation. In Sections 2.1 and 2.2 it was shown that acidified leaf slices from various malic enzyme and PEPCK CAM plants deacidify in the light, and possess CO_2 assimilation characteristics similar to those previously reported for intact tissues. Deacidifying leaf slices thus appear to be a useful experimental system in which to examine the metabolism of ^{14}C pyruvate. Experiments in which 1-^{14}C-, 2-^{14}C- and 3-^{14}C-pyruvate were fed in the light to deacidifying leaf slices from CAM plants, and also to leaf slices from C_3 plants, will be described in this section. The aim was to examine the short-term products as likely indicators of any gross differences in the pathways of metabolising pyruvate in a number of photosynthetic tissues containing different pathways of carbon assimilation viz. *Kalanchoe daigremontiana*, a malic enzyme CAM plant, *Stapelia gigantea*, a PEPCK CAM plant, C_3 and CAM *Mesembryanthemum crystallinum* and *Spinacia oleracea*, a C_3 plant. The advantages of using the aforementioned tissues is that comparisons of the metabolism of ^{14}C pyruvate can be made both between C_3 and CAM tissues and between CAM tissues containing different decarboxylating enzymes. One might expect that if, in CAM tissues, pyruvate is converted to glucan via

gluconeogenesis (see Chapter 1.4), then differences in pyruvate metabolism may not only exist between CAM and C_3 plants, but may also exist between malic enzyme CAM plants, which produce pyruvate during deacidification and PEPCK CAM plants which produce PEP.

Mesembryanthemum crystallinum is particularly suited to comparative studies as the pathway of carbon assimilation in mature leaves may be altered from exclusively C_3 to C_3 + CAM by changing the growth conditions. Any changes which may occur in the metabolism of pyruvate during the change from C_3 to C_3 + CAM will most likely be related to changes in the pathway of carbon assimilation rather than to other factors which may complicate interpretations of interspecific comparisons.

1,4-^{14}C- and 2,3-^{14}C-succinate were also fed to deacidifying leaf slices of *Kalanchoe*, a malic enzyme CAM plant, and *Aloe*, a PEPCK CAM plant, in an attempt to gather information on the operation of the TCA cycle in the light, and to assess whether a significant amount of carbon other than CO_2 is exported from the mitochondria.

2.3.2 Materials and methods

2.3.2.1 *Experimental material*

Plants were grown and leaf slices prepared as described in Section 2.1.2. Tissue was harvested between 40 and 90 minutes after illumination. The malate content was measured at harvest and at the beginning, midpoint and endpoint of each experiment as described in Section 2.1.2.

1-^{14}C-, 2-^{14}C- and 3-^{14}C-pyruvate (sodium salts), and 1,4-^{14}C- and 2,3-^{14}C-succinate were obtained from the Radiochemical Centre, Amersham, U.K.

2.3.2.2 *^{14}C-pyruvate labelling and extraction*

Acidified leaf slices were suspended in 3 ml of a medium containing 25 mM MES-NaOH, pH 6.0 and 0.1 mM $CaSO_4$. Pyruvate labelled in (1-^{14}C), (2-^{14}C) or (3-^{14}C) position was mixed with unlabelled carrier pyruvate and added after a 10 minutes preincubation in the light to give a final concentration of 2 mM (6 µmoles in 100 µl; specific activity 1.5-2.0 x 10^6 dpm µmole^{-1}, unless specified otherwise).

After various intervals, the tissue was flushed from the vials with H_2O, quickly washed with two changes of H_2O and plunged into 20 ml of a boiling solution of 0.1% (w/v) 2,4 dinitophenylhydrazine (2,4 DNPH) in 85% EtOH (v/v) acidified with 0.5 N formic acid. Approximately 15-20 seconds elapsed between removal of the tissue from the vials and killing the tissues. During this time the slices were exposed to low laboratory light. The slices were boiled for 3-4 minutes, cooled to room temperature and ground in a 15 ml Ten-Broek glass homogeniser. The extract was allowed to stand at room temperature for 30 minutes. The residue, which had settled, was resuspended by gently swirling the flasks and the extract was filtered, under vacuum, through a 5.5 cm diameter glass microfibre filter paper (Whatman GF/C, 5.5 cm). The filter paper was washed with 10 ml EtOH, 2 ml $CHCl_3$, 2 ml EtOH, 5 ml H_2O and 2 ml EtOH respectively. These filtrates were combined as the "ethanolic extract".

The glass fibre disc which contained the residue, was boiled in H_2O for 15 minutes. The disc was then removed and spun dry in a centrifuge tube. The combined aqueous extracts were again filtered through a glass fibre disc and washed.

The "aqueous filtrate", with the "ethanolic extract", were later extracted with chloroform. The insoluble residues on the two glass fibre discs were dried and counted.

2.3.2.3 *^{14}C-succinate labelling and extraction*

1,4-^{14}C- and 2,3-^{14}C-succinate were fed under similar conditions to those described for ^{14}C-pyruvate labelling. The suspension medium contained 1 mM succinate. (The specific activity of 1,4-^{14}C-succinate was 2.5×10^6 dpm μmole^{-1}; the specific activity of 2,3-^{14}C-succinate was 1.6×10^6 dpm μmole^{-1}). The tissue was killed in boiling EtOH, rather than 2,4 DNPH.

2.3.2.4 *Chloroform separation*

The aqueous filtrates and ethanolic extracts were extracted with chloroform to remove lipids, waxes, chlorophyll and, when present, 2,4 DNP hydrazones and unreacted 2,4 DNP hydrazine.

Water or ethanol was added to bring the fractions to the same volume. They were then pooled in a 250 ml glass separating column and chloroform was added to give a 1:1:1 ratio. The column was shaken and the two phases allowed to separate for 10-20 minutes. If phase separation was not complete a small amount of either H_2O or EtOH was added and the column was reshaken. The lower chloroform phase was decanted and the upper phase was re-extracted with EtOH and $CHCl_3$. The resulting clear upper layer was placed in a 250 ml rotary evaporation flask and further clarified by storage overnight at -20°C. Any precipitate was carefully removed with a pippette and the supernatant was spun at 12,000 x g for 10 minutes at 0-4°C. The supernatant was decanted, rotary evaporated to dryness, and resuspended in 10 ml of 10% (v/v) isopropanol.

2.3.2.5 *Separation and identification of compounds*

Methods used for the separation and identification of labelled and unlabelled metabolites were identical to those described in Sections 2.2.2.3 to 6.

The identity of three of the most heavily labelled amino acids, glutamate, alanine and aspartate was verified from mass spectra of their n-butyl esters (prepared after Darbre, 1978) using a gas chromatograph mass spectrometer.

2,4 DNP hydrazine and hydrazones were identified using one dimensional, descending paper chromatography (Whatman 3 mM paper, 46 cm x 57 cm). The samples were run for 7 hours in Butanol/EtOH/0.5 N NH_4CH (7:1:2)(Block *et al.*, 1958).

2.3.2.6 *Evaluation of labelling and extraction methods*

The tissue suspension medium was kept at acid pH because it is well documented that alkaline solutions of α-keto acids undergo aldol type condensation to form polymers (cf. Von Korff, 1964). The polymerisation of pyruvate to form a dimer, parapyruvate (γ-methyl-γ-hydroxy-α-keto glutarate), which has been reported to inhibit α-ketoglutarate dehydrogenase and to interrupt TCA oxidations, is catalysed by alkaline pH and tends to be autocatalytic (Montgomery and Webb, 1956; Von Korff, 1964). Sodium pyruvate is more unstable than pure pyruvic acid, particularly when frozen at -20°C. However, at acidic pH the formation of parapyruvate is greatly reduced. Consequently in all experiments involving ^{14}C-pyruvate labelling, fresh ^{14}C-pyruvate stock solution was prepared between 30 to 60 minutes before labelling.

A second reason for keeping the suspension medium at acid pH is that membranes are more permeable to associated acids than to disassociated acids. It is not feasible, however, to feed associated pyruvate as the pKa pyruvate is 2.5. Lüttge and Ball (1977) have shown that below pH 4.5 *K. daigremontiana* leaf slices are wilted, appear to lack turgor and begin to lose anthocyanin from the vacuoles. Malate uptake by *K. daigremontiana* leaf slices from an external solution is independent of pH above 5 as well as being independent of the osmotic pressure of the medium between 0 and -5 bar.

The pyruvate concentration of the external medium was kept low (2 mM) although one might expect that pyruvate uptake would increase exponentially with increasing external pyruvate concentration in a manner similar to that reported for malate uptake (Lüttge and Ball, 1977b). Since pyruvate uptake is very slow and, in the present study, the products were being examined over relatively short time periods it was important to feed the maximum amount of tissue with pyruvate of very high specific activity. This is also the reason for the high tissue to volume ratio (0.6 - 1.0 g in 3 ml) used in this study. Furthermore, high external pyruvate concentrations can result in the internal production of ethanol, CO_2 and, occasionally, lactate which cause large increases in the respiratory quotient (Neal and Beevers, 1960). Stimulation of O_2 uptake has also been observed (Laties, 1949a, 1949b). According to Neal and Beevers 2 mM pyruvate is well below this level for *B. calycinum* leaf tissue.

The purity of the variously labelled ^{14}C-pyruvates was checked by comparing the 2,4 DNP hydrazones of ^{14}C-pyruvate with authentic pyruvate

2,4 DNP hydrazones (Figure 2.12). The two major labelled spots correspond to the cis and trans forms of the hydrazones. The identity of the minor labelled spot, which contained less than 0.05% of the label, is unknown. The three labelled spots correspond exactly with three coloured spots on both the test and the control chromatograms. A fourth coloured spot which was unlabelled and ran with the solvent front in both chromatograms corresponds to unreacted 2,4 DNPH.

In ^{14}C-pyruvate labelling experiments large amounts of ^{14}C-pyruvate remained in the tissue extracts even after washing the slices prior to killing. It is probable that this residual ^{14}C-pyruvate is located in the intercellular spaces and is not unmetabolised intracellular ^{14}C-pyruvate, since, as mentioned beforehand, pyruvate is rapidly metabolised and the internal pyruvate pools are small even during maximum deacidification. This residual ^{14}C-pyruvate interfered with assimilation measurements and tended to swamp chromatograms. Consequently tissue was killed in a 2,4 DNPH solution and the pyruvate and other keto-acid hydrazones were extracted in $CHCl_3$. Chloroform extraction removed pigments such as chlorophyll and lipids, which also interefere in chromatography. Conversely, nearly all PCR, TCA and glycolytic pathway intermediates are insoluble in $CHCl_3$. Keto acids such as OAA and α-ketoglutarate, which would be removed with pyruvate, are unlikely to contain large amounts of label.

Both 2,4 DNP hydrazine and its hydrazones strongly interfere with ^{14}C determination by scintillation counting as a result of both colour quenching and chemiluminescence. It is thus very important to remove all the 2,4 DNP hydrazones and unreacted hydrazine from the extract.

Figure 2.12 The distribution of radioactivity and colour in a chromatographed sample of the 2,4 DNP hydrazone of 2-^{14}C-pyruvate.

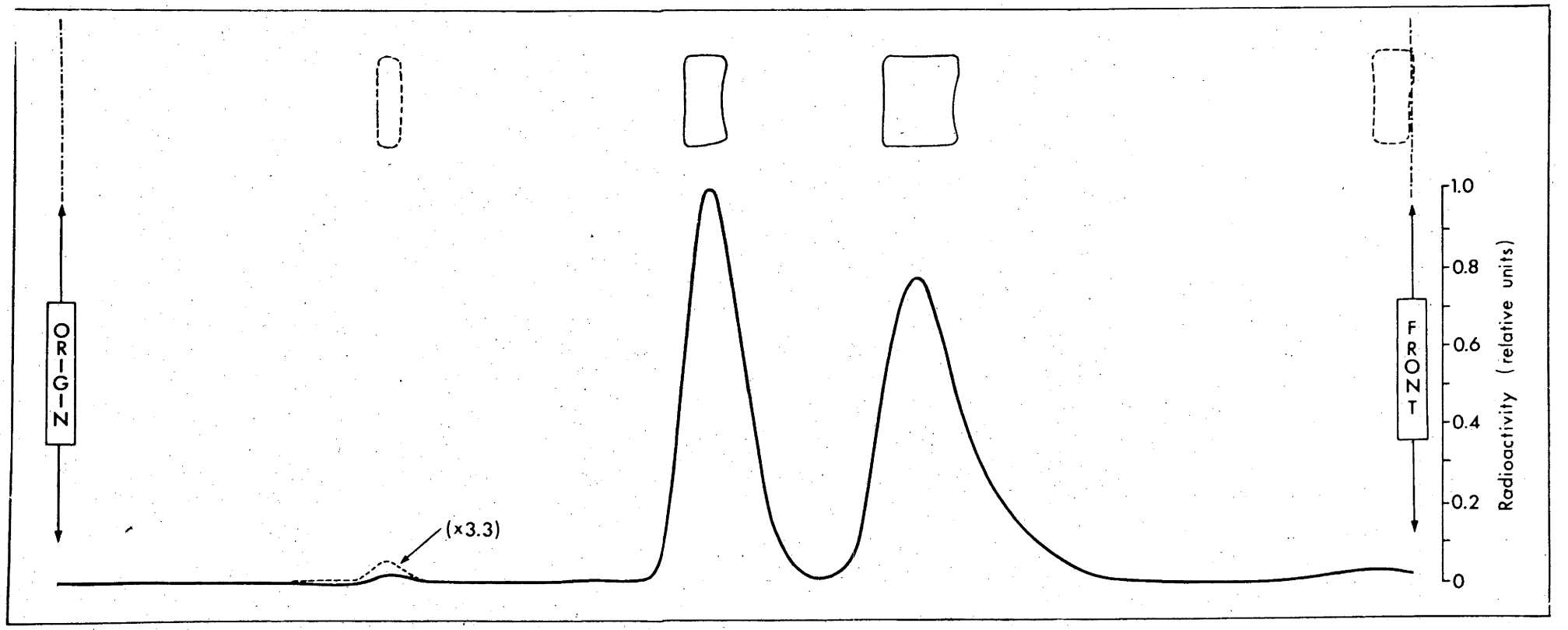
ORIGIN
(×3.3)
FRONT
1.0
0.8
0.6
0.4
0.2
0
Radioactivity (relative units)

It is also necessary to show that the products of ^{14}C labelling in tissue killed in EtOH/2,4 DNPH are similar to the products in tissue killed in boiling EtOH and that the subsequent chloroform extraction only removes unwanted compounds. The EtOH/2,4 DNPH extraction solution was acidified with formic acid, not with HCl as is more commonly used, because the HCl salt which remained after rotary evaporation interfered with subsequent chromatography.

Although the total ^{14}C incorporated was the same when *Kalanchoe* tissue was fed $^{14}CO_2$ and killed either in boiling 80% EtOH or in boiling EtOH/2,4 DNPH a greater percentage of the label was in the insoluble fraction in the EtOH/2,4 DNPH killed tissue. However, when the insoluble fractions were re-extracted in boiling H_2O and refiltered as described in Section 2.3.2.2, the distribution between aqueous and insoluble fractions was similar for both treatments (Table 2.2).

Perchloric acid extraction of the insoluble residue (as described by Sutton, 1974) from tissue labelled with 3-^{14}C-pyruvate showed that after 30 minutes exposure 93-95% of the label in the residue was in starch and acid soluble carbohydrate i.e. glucan (Table 2.3). For convenience, throughout the rest of this study the term carbohydrate will refer to the label in the insoluble residue fraction plus the label in the neutral sugar fraction, whilst the term glucan will be used solely to refer to the insoluble fraction.

When 3-^{14}C-pyruvate labelled *Stapelia* tissue was killed in EtOH and extracted with $CHCl_3$ prior to ion exchange chromatography, the acid fraction contained a large amount of ^{14}C, the majority of which proved to

Table 2.2 Effect of killing *Kalanchoe* leaf slices in EtOH and in 2,4 DNP hydrazine and re-extracting the insoluble fraction in boiling H_2O on the percentage distribution of products of $^{14}CO_2$ fixation.

Treatment	Exposure (min)	Distribution in original fractions (%)		Distribution in re-extracted fractions (%)	
		Soluble	Insoluble	Soluble	Insoluble
EtOH killed	1	96.7	3.3	98.6	1.4
	3	93.6	6.4	97.6	2.3
	7	78.1	21.9	90.4	9.7
2,4 DNP hydrazine killed	1	89.3	10.7	96.5	3.5
	3	83.1	16.9	93.7	5.5
	7	79.4	20.6	90.5	9.5

Table 2.3 Distribution of ^{14}C in the initial and in the perchloric extract of the insoluble residue from deacidifying *Stapelia* and *Kalanchoe* leaf slices fed 3-^{14}C-pyruvate in the light.

Species	Exposure time (min)	Initial residue	Perchloric acid extraction Soluble	Insoluble	Recov.
			µmoles mg chl^{-1}		%
Kalanchoe	30	0.098	0.091	0.002	95
	60	0.122	0.113	0.005	97
	120	0.337	0.321	0.009	98
Stapelia	30	0.297	0.269	0.007	93
	60	0.403	0.379	0.012	97
	120	0.891	0.847	0.026	98

be in pyruvate (Table 2.4). The amount of ^{14}C in the acid fraction was not related to the time of exposure. However, when *Stapelia* tissue was fed with 3-^{14}C- pyruvate and then extracted in EtOH/2,4 DNPH, the majority of the ^{14}C was in the chloroform fraction (Table 2.4). Chromatography showed that over 98% of the label was present as pyruvate hydrazones. In contrast, the acid fraction contained small amounts of ^{14}C, the amounts being proportional to the time of exposure. Chromatography of this fraction showed no ^{14}C-pyruvate or ^{14}C-pyruvate hydrazones. Similar observations were made for ^{14}C-pyruvate labelled *Kalanchoe* tissue.

The above data are reinforced by the observations presented in Table 2.5 which show the partitioning of various ^{14}C-labelled compounds between residue, $CHCl_3$ and aqueous fractions after EtOH/2,4 DNPH extraction and $CHCl_3$ separation. Only pyruvate is present in the $CHCl_3$ fraction. Some F-6-P and F-1,6-P_2 adheres to the residue. This particular experiment, however, was performed before the residue was routinely re-extracted in boiling H_2O, as suggested previously in this section, and it is probable that with further extraction these sugar phosphates would be solubilised.

2.3.3 Results

2.3.3.1 *Metabolism of 3-^{14}C-pyruvate*

The incorporation of 3-^{14}C-pyruvate in the light by deacidifying *Kalanchoe* and *Stapelia* leaf slices, and by spinach leaf slices, was linear with exposure time and tissue weight (Figure 2.13). The chlorophyll content of the tissues varied but, on average, *Kalanchoe* contained about 0.4-0.45 mg chl g^{-1} fr.wt., *Stapelia* contained about 0.2-0.25 mg chl g^{-1} fr.wt., and spinach contained about 1.3 mg chl g^{-1} fr.wt. The

Table 2.4 Effect of chloroform extraction on the distribution of ^{14}C(a) in *Stapelia gigantea* leaf slices fed 3-^{14}C-pyruvate and killed in either 80% EtOH or 2,4 DNP hydrazine.

Exposure time (min)	Chloroform fraction	Residue + neutral	Acid fraction	Amino acids	Total ^{14}C in non-chloroform fraction
			n moles mg^{-1} chl		
a) EtOH killed tissue					
5	4.9	16.7	2443	2.8	2463
10	3.2	29.7	2264	2.0	2296
20	9.5	68.0	3553	7.9	3629
40	8.4	67.0	2083	9.5	2160
b) Distribution of label in 2,4 DNP hydrazine killed tissue					
10	6473	54.3	155.6	44.1	254.0
30	9564	112.9	198.9	29.7	341.5
60	15624	230.5	369.5	49.0	649.0
120	7945	513.7	360.0	70.9	944.6

(a) The uptake rates are not strictly comparable as the EtOH killed tissue was fed 0.7 mM 3-^{14}C-pyruvate (sp act $\simeq$ 3.2 x 10^6 dpm $\mu mole^{-1}$) and the 24 DNPH killed tissue was fed 3 mM 3-^{14}C-pyruvate (1.1 x 10^6 dpm $\mu mole^{-1}$)

Table 2.5 Effect of 2,4 DNP hydrazine extraction and chloroform separation on the partitioning of various ^{14}C-labelled compounds between residue, chloroform and aqueous fractions.[a]

Compound	Concentration mM	Chloroform %	Residue %	Aqueous %
3-^{14}C-pyruvate	3.0	96.3	0.3	3.5
U-^{14}C-malate	2.5	ND	1.4	98.6
U-^{14}C-aspartate	2.5	ND	2.2	97.8
D-(U-^{14}C)-glucose	2.5	ND	0.2	99.8
L-(U-^{14}C)-3-PGA	2.5	ND	6.3	93.7
D-(U-^{14}C)-F-6-P[b]	2.5	TRACE	32.5	77.5
D-(U-^{14}C)-F-1,6-P_2	2.5	TRACE	21.0	79.0

a the ^{14}C-labelled compounds were extracted with previously killed unlabelled tissue and treated as described in Section 2.3.2

b separate experiment

Figure 2.13 Incorporation of 3-^{14}C-pyruvate in the light by deacidifying *Kalanchoe daigremontiana* (●), *Stapelia gigantea* (o) and by spinach (Δ) leaf slices.

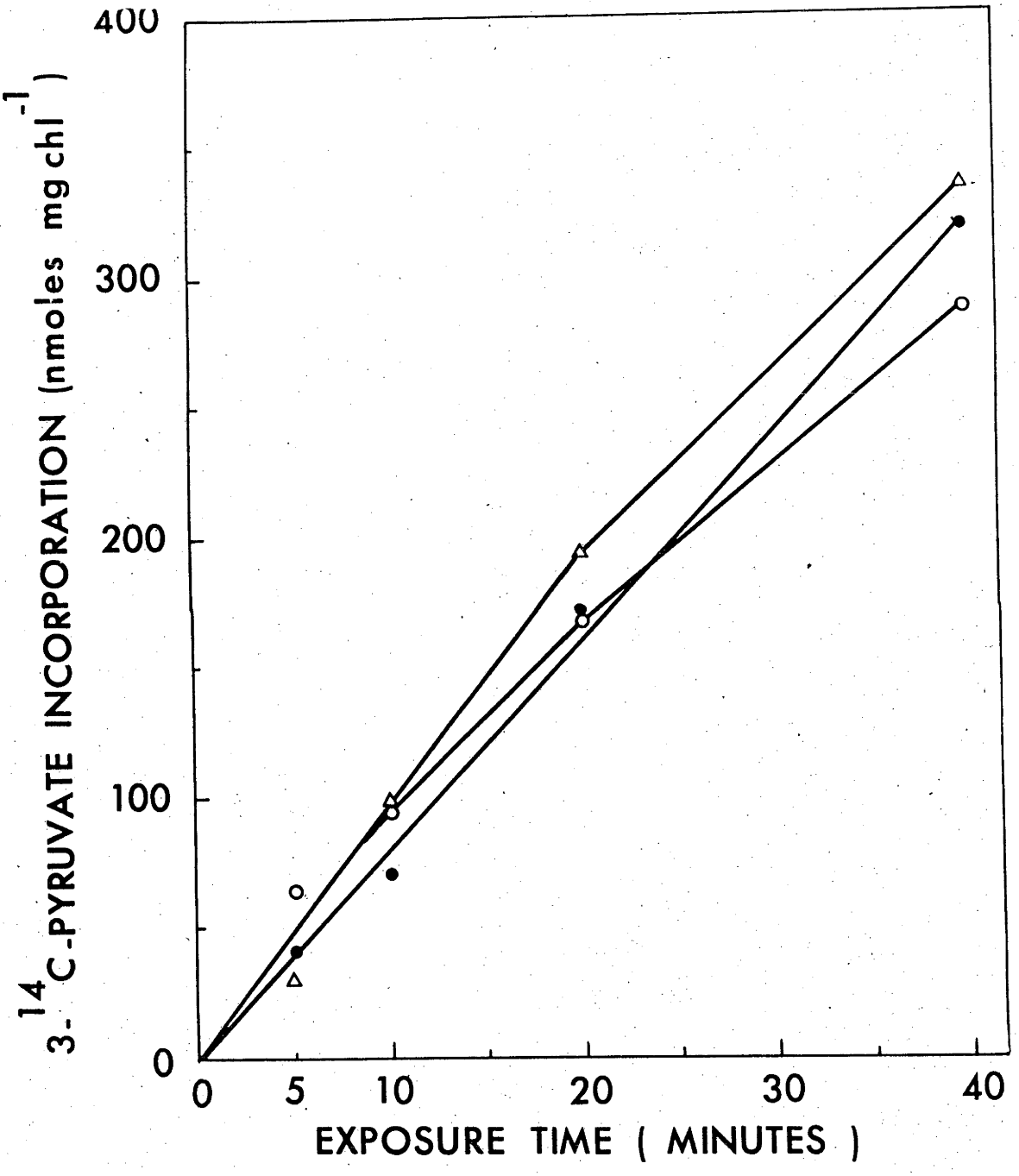
400
300
200
100
0
3-^{14}C-PYRUVATE INCORPORATION (nmoles mg chl^{-1})
0
5
10
20
30
40
EXPOSURE TIME (MINUTES)

chlorophyll content of *Stapelia* is probably an underestimate due to differing amounts of chlorophyll-less pith tissue which remained attached to the slices. However, as shown in Table 2.6, ^{14}C-pyruvate is not incorporated into pith tissue.

The rates of pyruvate incorporation, of about 0.5 µmoles mg chl^{-1} hr^{-1} in all tissues studied, are comparable to those reported for malate and $^{36}Cl^-$ influx in *Kalanchoe* (≃ 0.4 µmoles mg chl^{-1} hr^{-1}) but less than that reported for $K^+/^{86}Rb^+$ influx (≃ 1.5 µmoles mg chl^{-1} hr^{-1})(Lüttge and Ball, 1974b, 1977). They are, however, very low when compared with the rates of deacidification and CO_2 fixation, of 26-100 µmoles mg chl^{-1} hr^{-1} and 80-110 µmoles mg chl^{-1} hr^{-1} respectively, observed in the CAM tissues used in this study (Sections 2.1 and 2.2). Since the rates of pyruvate incorporation are linear, but well below the activities of the pyruvate consuming mechanisms (Milburn *et al.*, 1968), it can be assumed that ^{14}C-pyruvate incorporation is limited by the rate of pyruvate entry into the cells. Pyruvate entry into the cells will depend upon the length of the diffusion pathways and upon the rates of diffusion of pyruvate (1) across the boundary layers surrounding the leaf slices, (2) through the unstirred intercellular spaces, and (3) across the plasmalemma.

Although detailed quantitative interpretation of the labelling data is made difficult by the low rates of 3-^{14}C-pyruvate incorporation (due presumably to low uptake), certain distinct patterns can be distinguished in the distribution of label amongst the products of ^{14}C-pyruvate metabolism in the different tissues. The major difference in the distribution of label between *Kalanchoe* and *Stapelia* tissues was in the proportion of label in the organic acid and carbohydrate fractions. In *Kalanchoe*, label from

Table 2.6 Incorporation of 3-^{14}C-pyruvate into leaf slices and pith tissue from *Stapelia gigantea* during the light.

Tissue	10 minutes		30 minutes	
	Residue	Aqueous[a]	Residue	Aqueous[a]
	(n moles mg^{-1} chl)			
Leaf slices	4.9	119.2	42.0	202.8
Pith slices	ND[b]	ND	ND	< 0.1

a after chloroform extraction

b ND - not detected

3-^{14}C-pyruvate was rapidly incorporated into carbohydrates (Figures 2.14 and 2.15). The initial rate of incorporation of label into carbohydrates and phosphorylated compounds was about 3 to 4 times more rapid than in *Stapelia*. In the latter species, organic acids (mainly malate and citrate/isocitrate) were the major initial products of pyruvate metabolism and were labelled twice as rapidly as in *Kalanchoe*. These differences are clearly demonstrated in Figure 2.16 which shows the proportion of label in organic acids and in carbohydrates observed in a number of experiments.

The relative contributions of labelled glucan and sugars (mostly sucrose), to the total carbohydrate fraction varied considerably, but was not significantly different between the two species. There may be a trend for proportionally more label to be in the sugar fraction in *Stapelia* and proportionally more label to be in the glucan fraction in *Kalanchoe* (Figure 2.17).

Label in phosphorylated compounds in *Stapelia* was negligible but in *Kalanchoe* this fraction contained 13% of the label after 5 minutes, declining to 3% after 40 minutes. In both species the initial proportion of label in amino acids was similar, about 25%, but declined to only 11% at the end of the experiment (Figures 2.14 and 2.15).

Differences were also observed in the distribution of label in the products of 3-^{14}C-pyruvate metabolism by C_3 and CAM *Mesembryanthemum*. Incorporation of 3-^{14}C-pyruvate was linear and, for 20 minutes at least, similar on a chlorophyll basis (Figures 2.18). The CAM tissue contained about 10% more chlorophyll per gram fresh weight than the C_3 tissue.

Figure 2.14 A. Incorporation of 3-^{14}C-pyruvate in the light by deacidifying *Kalanchoe daigremontiana* leaf slices into carbohydrates (●), organic acids (▲), phosphorylated compounds (■) and amino acids (Δ).

B. Incorporation of 3-^{14}C-pyruvate in the light by deacidifying *Stapelia gigantea* leaf slices into carbohydrates (●), organic acids (▲) and amino acids (Δ).

C. Incorporation of 3-^{14}C-pyruvate in the light by spinach leaf slices into carbohydrates (●), organic acids (▲) and amino acids (Δ).

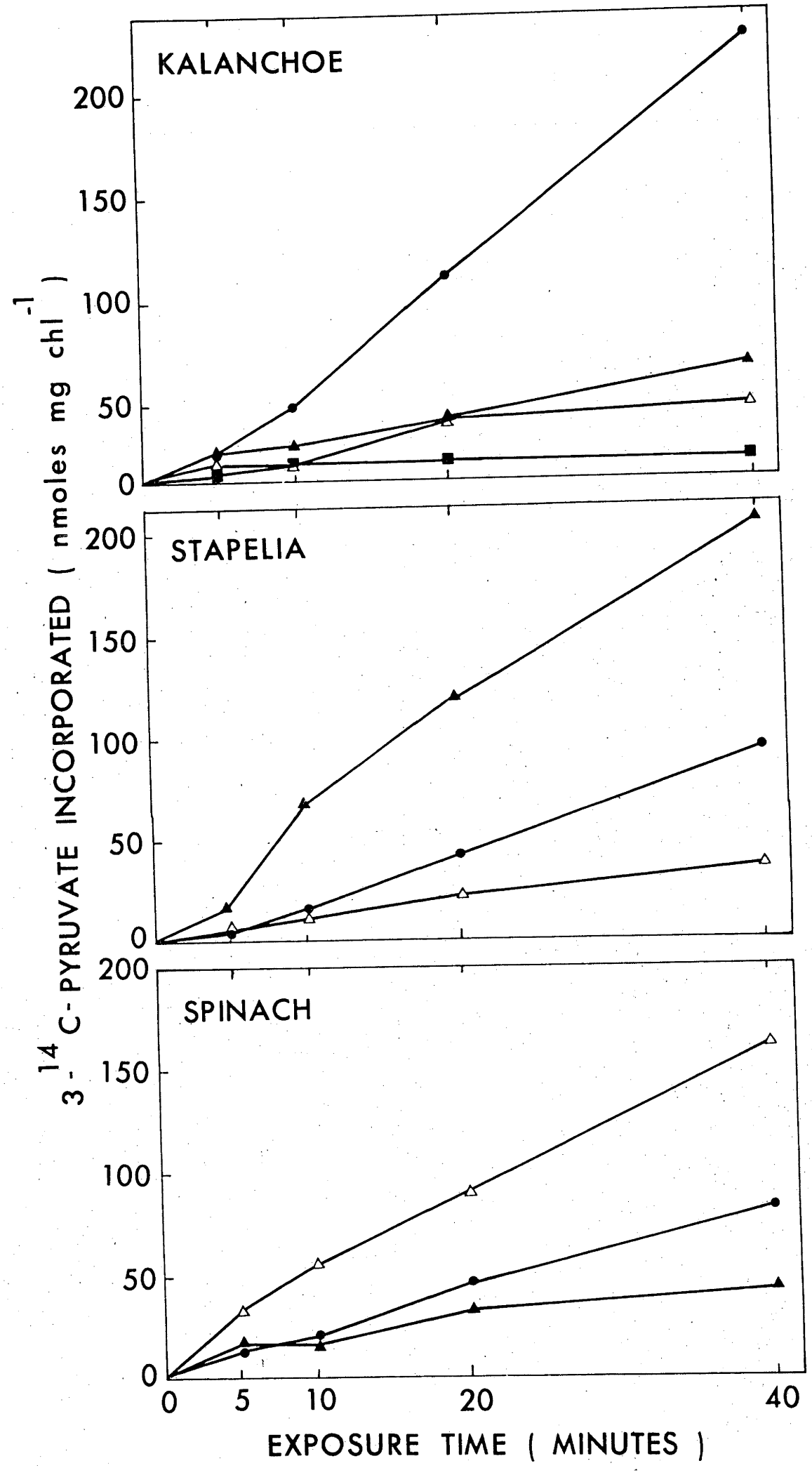
KALANCHOE
STAPELIA
SPINACH
200
150
100
50
0
0
5
10
20
40
3-^{14}C-PYRUVATE INCORPORATED (nmoles mg chl^{-1})
EXPOSURE TIME (MINUTES)

Figure 2.15 A. Percentage distribution of ^{14}C in the products of 3-^{14}C-pyruvate incorporation in the light by deacidifying *Kalanchoe daigremontiana* leaf slices. Carbohydrates (●) organic acids (▲), phosphorylated compounds (□), amino acids (▽).

B. Percentage distribution of ^{14}C in the products of 3-^{14}C-pyruvate incorporation in the light by deacidifying *Stapelia gigantea* leaf slices. Carbohydrates (●), organic acids (▲), amino acids (▽).

C. Percentage distribution of ^{14}C in the products of 3-^{14}C-pyruvate incorporation in the light by spinach leaf slices. Carbohydrates (◎), organic acids (▲), amino acids (▽).

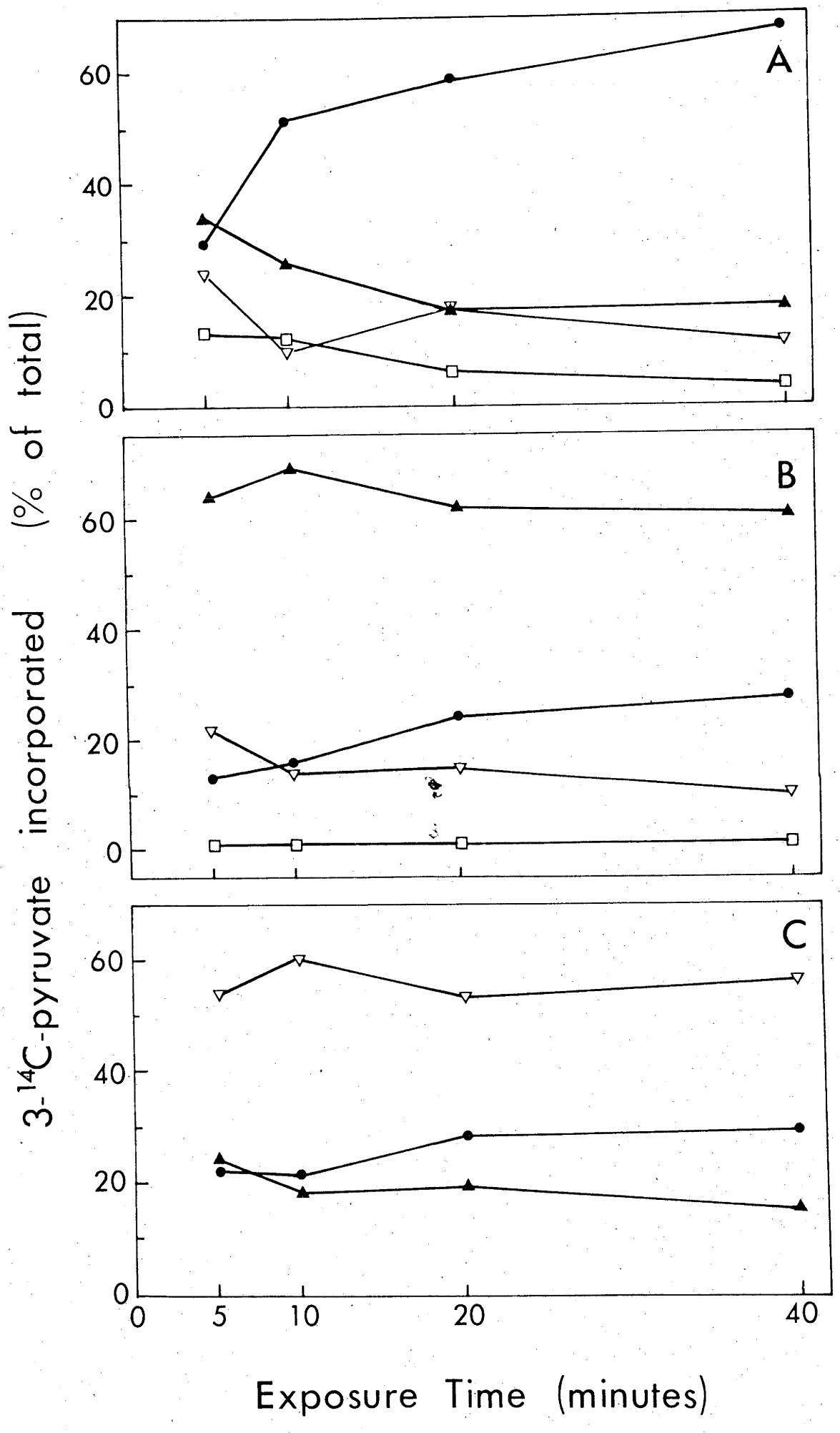
A
B
C
60
40
20
0
0
5
10
20
40
3-14C-pyruvate incorporated (% of total)
Exposure Time (minutes)

Figure 2.16 A. The distribution of ^{14}C, expressed as a percentage of the total 3-^{14}C-pyruvate incorporated in the carbohydrate fractions from deacidifying *Kalanchoe daigremontiana* (●) and *Stapelia gigantea* (o) leaf slices fed 3-^{14}C-pyruvate in the light.

B. The distribution of ^{14}C, expressed as a percentage of the total 3-^{14}C-pyruvate incorporated, in organic acids in deacidifying *Kalanchoe daigremontiana* (●) and *Stapelia gigantea* (o) leaf slices fed 3-^{14}C-pyruvate in the light.

NB. Data from 4 experiments with *Stapelia* and 2 experiments with *Kalanchoe* tissue. All data points are the mean of duplicates.

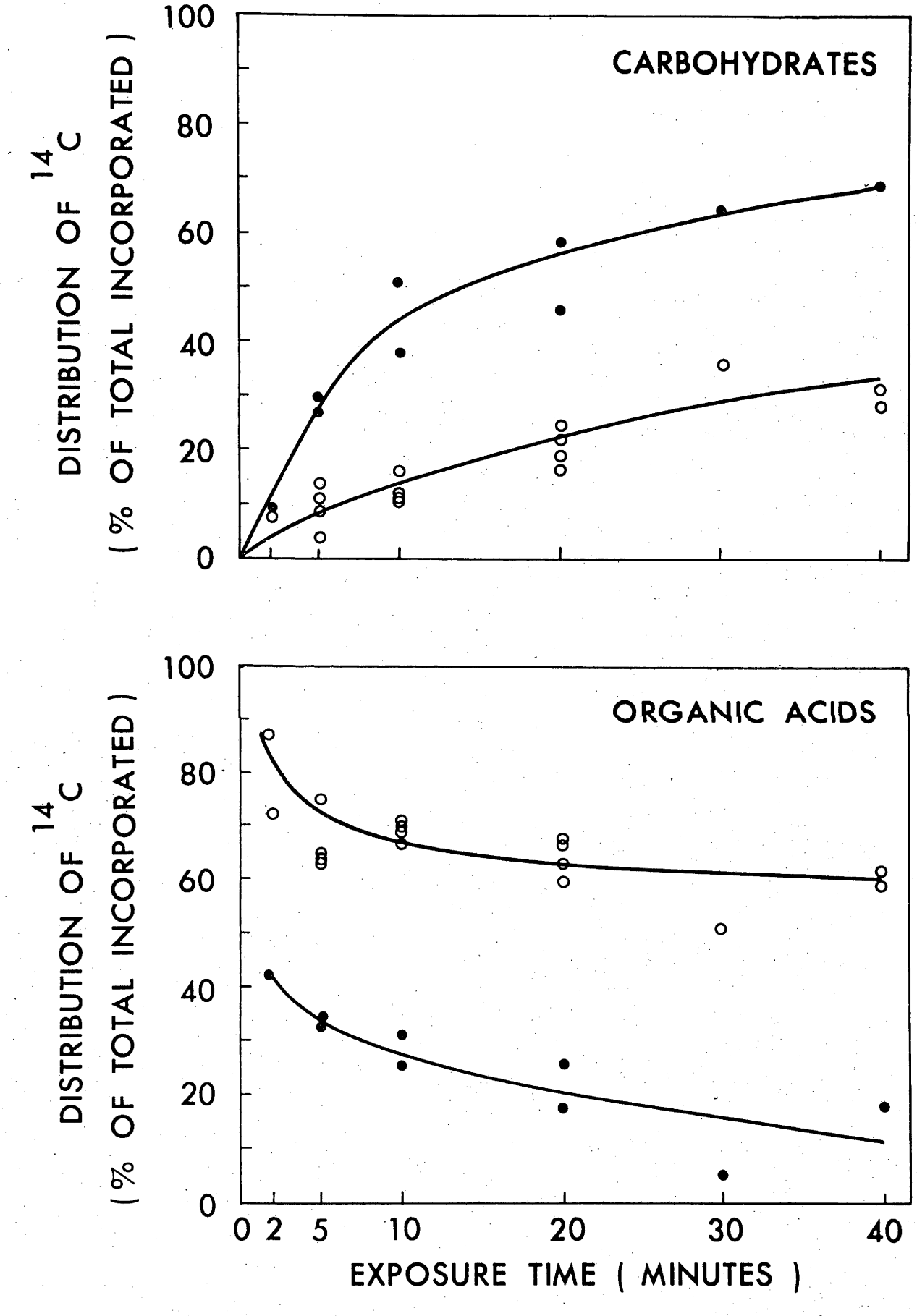
CARBOHYDRATES
ORGANIC ACIDS
DISTRIBUTION OF ^{14}C
(% OF TOTAL INCORPORATED)
100
80
60
40
20
0
0 2 5 10 20 30 40
EXPOSURE TIME (MINUTES)

Figure 2.17 A. Distribution of ^{14}C expressed as a percentage of the total 3-^{14}C-pyruvate incorporated, in glucan (●) and in soluble sugar (o) fraction from *Stapelia gigantea*.

B. Distribution of ^{14}C, expressed as a percentage of the total 3-^{14}C-pyruvate incorporated, in glucan (●) and soluble sugar (o) fractions from *Kalanchoe daigremontiana*.

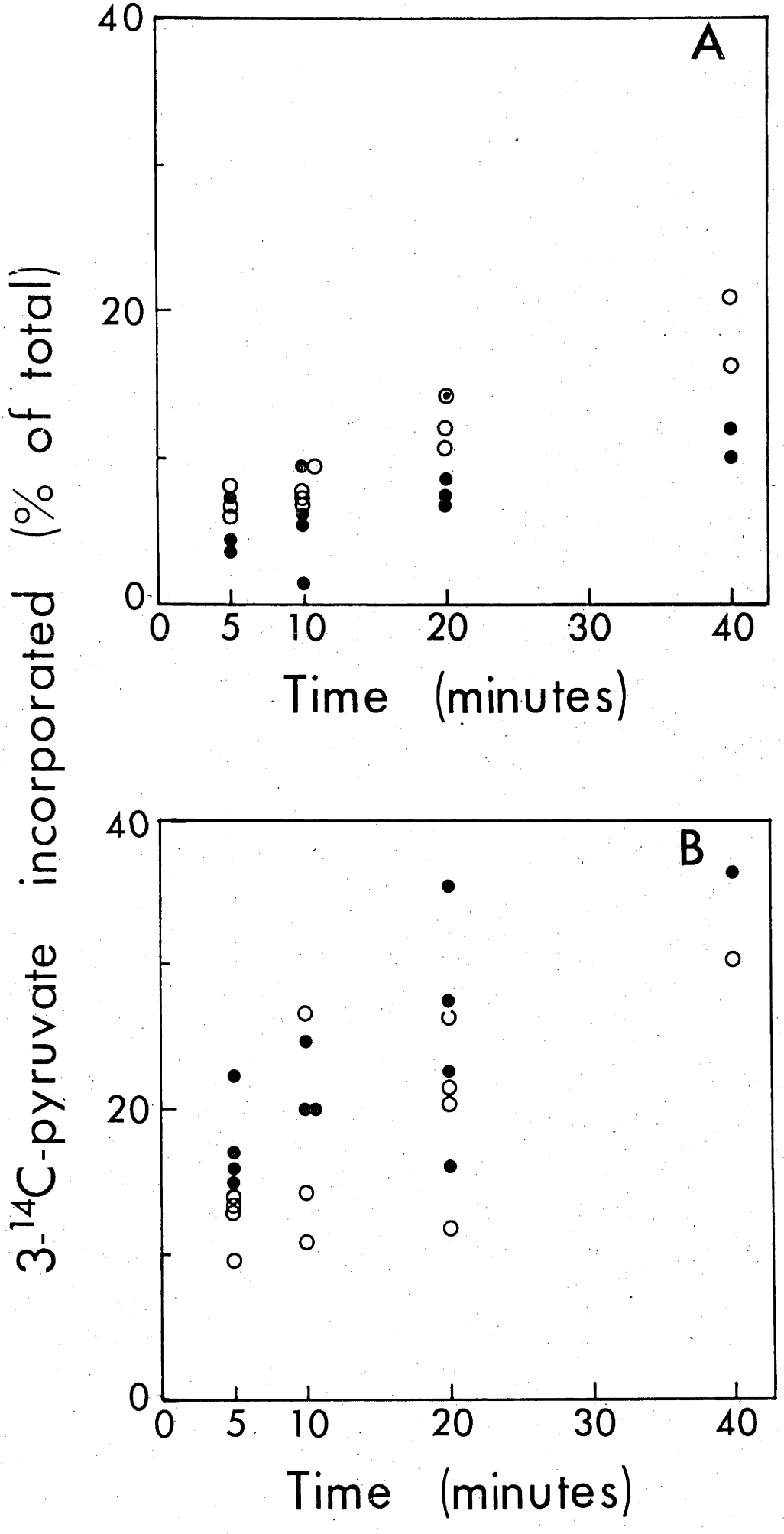
A
B
40
20
0
0
5
10
20
30
40
Time (minutes)
3-14C-pyruvate incorporated (% of total)

Figure 2.18 A. Incorporation of 3-^{14}C-pyruvate in the light by C_3 (100 mM NaCl grown) (o) and CAM (400 mM NaCl grown)(●) *Mesembryanthemum crystallinum*.

B. Incorporation of 3-^{14}C-pyruvate in the light by C_3 (100 mM NaCl grown) *Mesembryanthemum crystallinum* leaf slices into carbohydrates (●), organic acids (▲), phosphorylated compounds (□), and amino acids (▽).

C. Incorporation of 3-^{14}C-pyruvate in the light by CAM (400 mM NaCl grown) *Mesembryanthemum crystallinum* leaf slices into carbohydrates (●), organic acids (▲) phosphorylated compounds (□) and amino acids (▽).

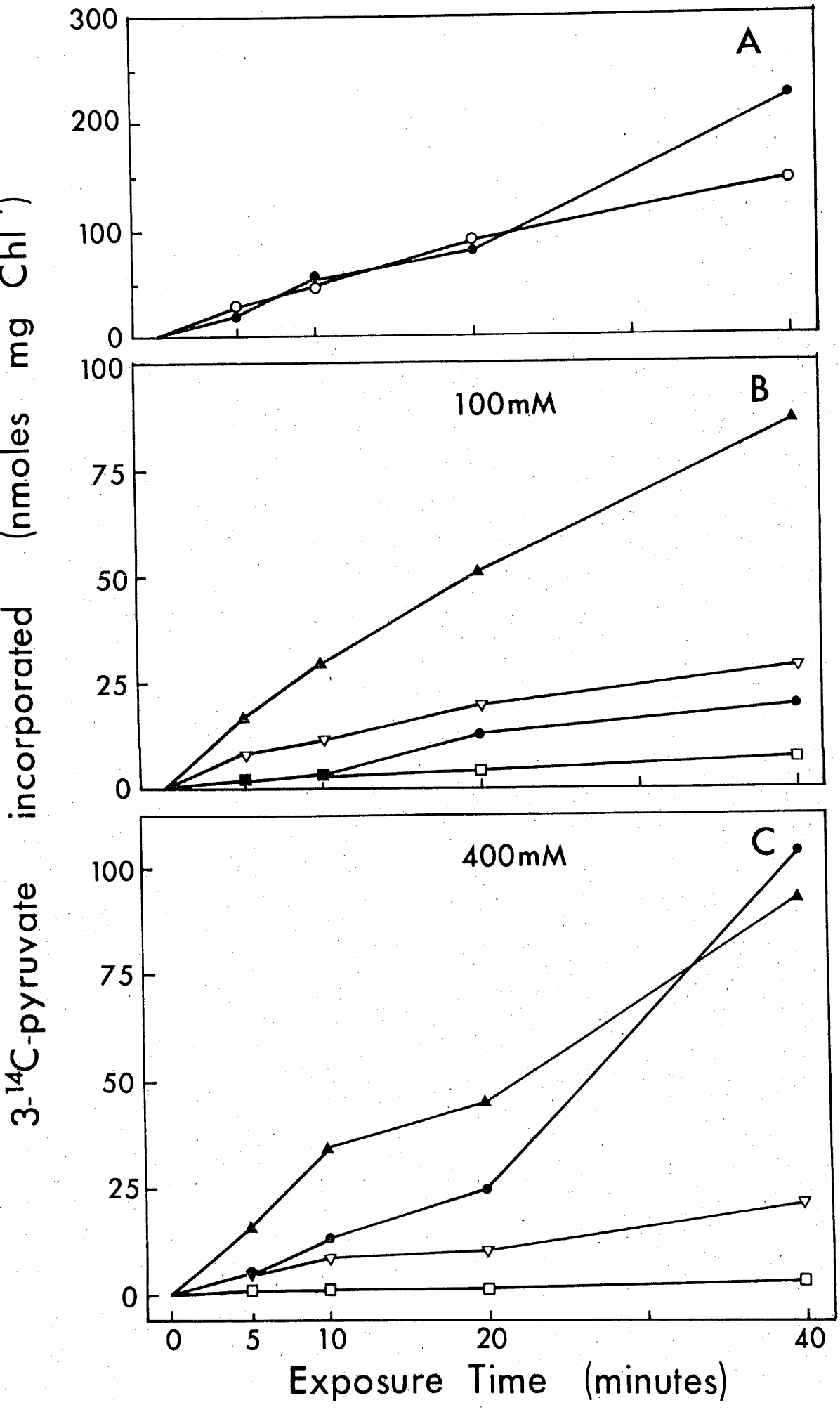
A
B
100mM
C
400mM
300
200
100
0
100
75
50
25
0
100
75
50
25
0
0
5
10
20
40
Exposure Time (minutes)
3-14C-pyruvate incorporated (nmoles mg Chl-1)

Although in both *Mesembryanthemum* tissues organic acids (mostly malate and citrate/isocitrate) were the major early labelled products, the CAM tissue accumulated label in carbohydrates about 3 times more rapidly than did the C_3 tissue (Figures 2.18 and 2.19). In both tissues the phosphorylated compounds never contained more than 5% of the total ^{14}C incorporated, and the distribution of label in amino acids was similar to that observed in *Kalanchoe* and *Stapelia*.

In the C_3 plant spinach, 3-^{14}C-pyruvate is rapidly and continuously incorporated into amino acids (Figures 2.14 and 2.15). The principal amino acids being alanine and glutamate, and to a lesser extent aspartate, serine and glycine. Label is converted to carbohydrate, initially about 1.3 times as rapidly as *Stapelia*, but less than half the rate observed in *Kalanchoe*. Similarly organic acids were initially labelled at about one half and one third the rates observed in *Kalanchoe* and *Stapelia* respectively.

The gluconeogenic conversion of ^{14}C-pyruvate to carbohydrate requires the initial conversion of ^{14}C-pyruvate to triose and hexose phosphates followed by accumulation of ^{14}C in carbohydrates. The observation that phosphorylated compounds and carbohydrates are much more rapidly labelled in *Kalanchoe* than in *Stapelia* is consistent with the operation of a gluconeogenic pathway in *Kalanchoe*. If ^{14}C-pyruvate is metabolised via the TCA cycle, label should initially appear in TCA cycle acids and only slowly appear in phosphorylated compounds and in carbohydrates, after $^{14}CO_2$ evolved during the second turn of the TCA cycle is refixed via the PCR cycle. Such a pattern was observed in *Stapelia* and in C_3 *Mesembryanthemum*. Although in CAM *Mesembryanthemum* the distribution of label between organic

Figure 2.19 Distribution of ^{14}C expressed as a percentage of the total ^{14}C incorporated, in the carbohydrate and organic acid fractions from C_3 and CAM *Mesembryanthemum crystallinum* leaf slices fed 3-^{14}C-pyruvate in the light.

Key

	100 mM	400 mM
carbohydrate	●	■
organic acids	o	□

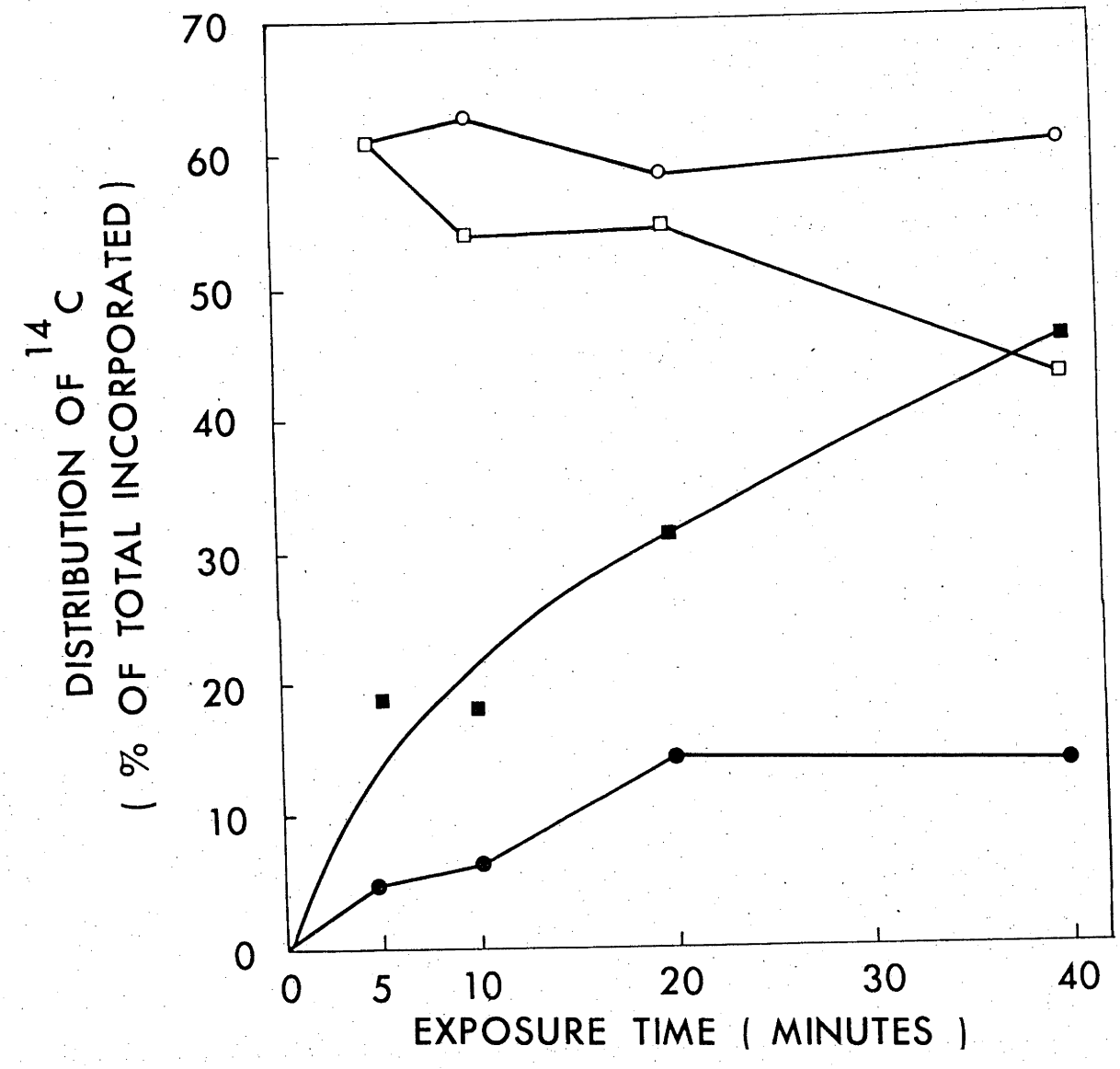
70
60
50
40
30
20
10
0
0
5
10
20
30
40
DISTRIBUTION OF ^{14}C
(% OF TOTAL INCORPORATED)
EXPOSURE TIME (MINUTES)

acids and carbohydrates is intermediate between that observed for *Kalanchoe* and *Stapelia*, 3-^{14}C-pyruvate is converted to carbohydrate 3 times more rapidly in the CAM tissue than in the C_3 tissue. This difference is unlikely to be due to differences in pool sizes of the intermediates since, if this were so, one would expect the CAM tissue to have smaller pools of phosphorylated compounds and the C_3 tissue to have large TCA cycle acid pools. Although nothing is known about the phosphorylated compound pool sizes in C_3 and CAM *Mesembryanthemum* , in C_3 and CAM *K. blossfeldiana* the pool sizes of triose and hexose phosphates involved in glycolysis and the PCR cycle are either similar or slightly larger in the CAM tissue during deacidification (Pierre and Queiroz, 1979). Malate is obviously present in a larger pool in CAM *Mesembryanthemum*. There is no reason to suspect that the pool sizes of the other TCA cycle acids are smaller in CAM than in C_3 *Mesembryanthemum*, although they have not been measured. The possible effects of the different capacities of glycolytic enzymes in C_3 and CAM *Mesembryanthemum* will be discussed in Section 4.3.

It is important to consider the effect of the dilution of exogenously supplied ^{14}C-pyruvate by internally produced unlabelled pyruvate in relation to the amounts and relative proportions of label incorporated into organic acids and carbohydrates in the various tissues studied. Dilution of ^{14}C-pyruvate within a cell will depend upon the rate of entry of ^{14}C-pyruvate into the cell, the internal pyruvate pool size, the rate at which endogenous pyruvate is synthesised, and the rate at which pyruvate is metabolised (Figure 2.20). Since, as stated previously, the rates of ^{14}C-pyruvate incorporation are much slower than the known capacities of the various tissues to metabolise pyruvate (Milburn *et al.*, 1968; Kluge

Figure 2.20 Scheme showing the relationship between the uptake of ^{14}C-pyruvate, the internal pyruvate pool, and the major internal sources and sinks of pyruvate in deacidifying CAM tissue.

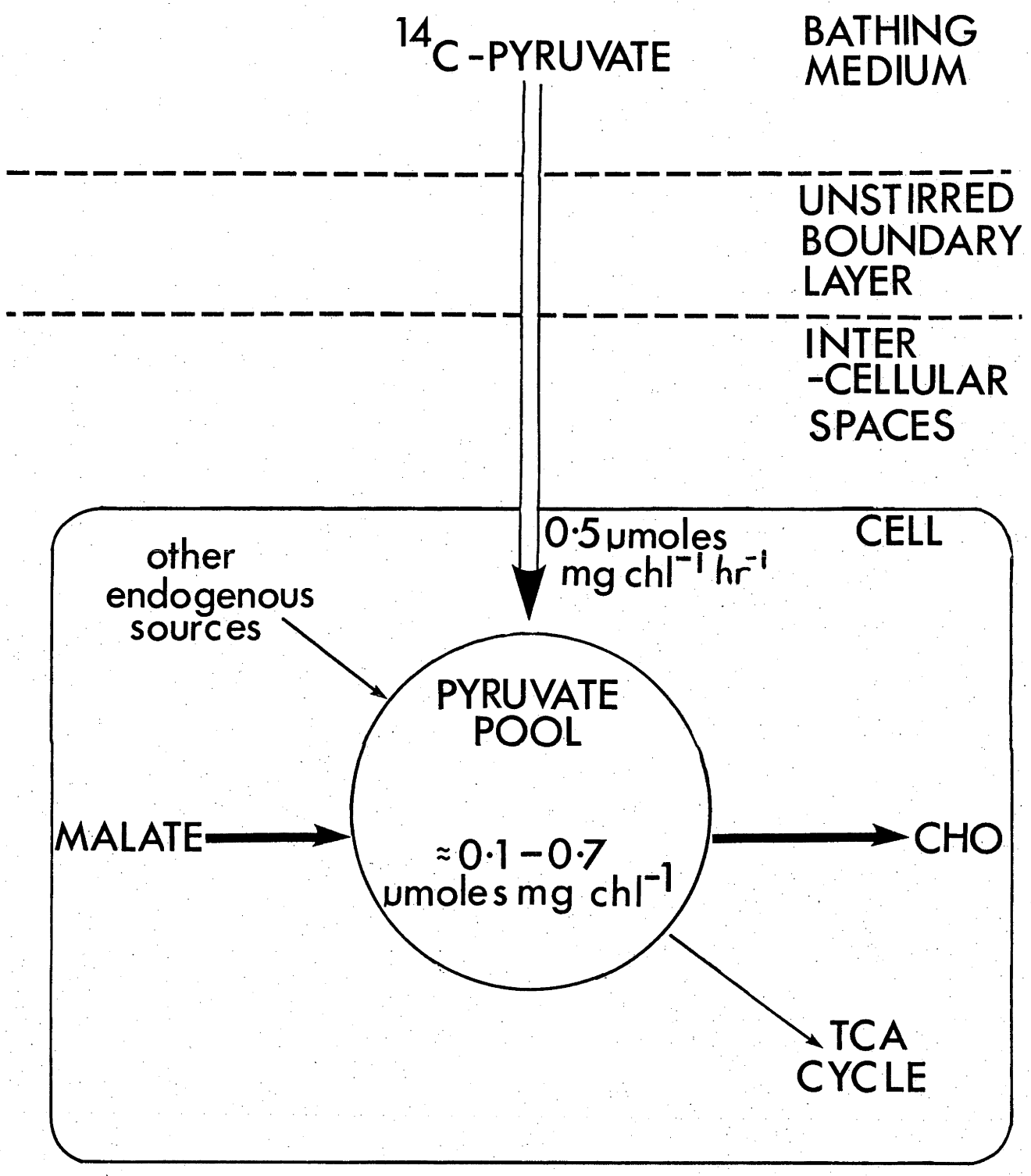
^{14}C-PYRUVATE
BATHING MEDIUM
UNSTIRRED BOUNDARY LAYER
INTER-CELLULAR SPACES
CELL
0·5 μmoles mg chl^{-1} hr^{-1}
other endogenous sources
PYRUVATE POOL
≈0·1–0·7 μmoles mg chl^{-1}
MALATE
CHO
TCA CYCLE

and Osmond, 1971; see also Chapters 4.1 and 4.3), it is reasonable to assume that the observed rates of ^{14}C-pyruvate incorporation are limited by the rates of ^{14}C-pyruvate entry into the tissue. This deduction is further supported by the observation that the rates of ^{14}C-pyruvate incorporation were similar in all C_3 and CAM tissues studied, irrespective of their relative capacities to produce and metabolise pyruvate.

If we accept that the low ^{14}C-pyruvate incorporation rates reflect low ^{14}C-pyruvate uptake rates, then we would expect to see a lag in the rate of ^{14}C incorporation which should last until the internal pyruvate pools reach their maximum attainable specific activities. This lag period was not observed in the present experiments (Figures 2.13 and 2.21), most probably because internal pyruvate pools are small. These small pools, of about 0.1 to 0.7 μmoles mg chl^{-1} in 3 species of Crassulaceae (Milburn *et al.*, 1968; Cockburn and McAulay, 1977), have short turnover times and had presumably already reached their maximum attainable specific activities by the time the first samples were taken (2-5 minutes after exposure to ^{14}C-pyruvate). Shorter sampling times were not feasible because the amount of ^{14}C incorporated was low and because residual 2,4 DNPH in the extracts introduced errors in scintillation counting.

Since the internal pyruvate pools are small and the ^{14}C-pyruvate uptake rates are low, the specific activity of the ^{14}C-pyruvate being metabolised within the tissue will be determined by the flux of endogenous pyruvate. However, as long as uptake of exogenous ^{14}C-pyruvate and the pyruvate pool sizes remain constant, the rate of accumulation of ^{14}C in the end-products of ^{14}C-pyruvate metabolism will be the same irrespective of any changes in the rate of endogenous pyruvate production. This is because any

increase or decrease in the rate of endogenous pyruvate production will result in a respective decrease or increase in the specific activity of the internal pyruvate pool.

During deacidification in *Kalanchoe* and in CAM *Mesembryanthemum*, up to 44 μmoles pyruvate mg chl^{-1} hr^{-1} and 26 μmoles pyruvate mg chl^{-1} hr^{-1}, respectively, is produced endogenously. However, in *Stapelia*, PEP is probably the main decarboxylation product, and endogenous pyruvate production would be much lower. Thus, although the ^{14}C-pyruvate incorporation rates are similar for the 3 CAM tissues the amount of label in the end products is probably derived from ^{14}C-pyruvate of very different specific activities. If the dilution of exogenous ^{14}C-pyruvate by endogenous pyruvate is taken into account, and if we assume that (1) the pyruvate pool sizes are small and more or less similar in all tissues, (2) no pyruvate is produced by malic enzyme in *Stapelia*, a PEPCK CAM plant, and (3) the rate of production of endogenous pyruvate from other, non-decarboxylation sources is similar in all tissues; then it is possible to estimate the rate of transfer of pyruvate into carbohydrates and other end-products (Table 2.7). *Kalanchoe* and CAM *Mesembryanthemum*, both malic enzyme CAM plants, convert pyruvate to carbohydrates more rapidly than *Stapelia*, a PEPCK CAM plant, and C_3 *Mesembryanthemum*. *Kalanchoe* converts pyruvate to carbohydrate over 200 times more rapidly than *Stapelia*, and the rate of conversion by CAM *Mesembryanthemum* is over 400 times faster than that by C_3 *Mesembryanthemum*. The CAM *Mesembryanthemum* rate is also over 40 times more rapid than the *Stapelia* rate.

2.3.3.2 *The metabolism of 2-^{14}C- and 3-^{14}C-pyruvate*

A major advantage of feeding tissues differentially labelled pyruvates is that comparisons can be made of the labelling patterns within a single

Table 2.7 Effect of the dilution of 3-^{14}C-pyruvate by endogenous unlabelled pyruvate on the apparent rate of conversion of 3-^{14}C-pyruvate into carbohydrate and organic acids in deacidifying *Kalanchoe*, *Stapelia* and C_3 and CAM *Mesembryanthemum* leaf slices in the light.

	Stapelia		*Kalanchoe*		*Mesembryanthemum crystallinum* C_3		*Mesembryanthemum crystallinum* CAM	
	Organic acids	Carbo-hydrate	Organic acids	Carbo-hydrate	Organic acids	Carbo-hydrate	Organic acids	Carbo-hydrate
Observed rate[1]	0.196	0.094	0.056	0.212	0.086	0.020	0.091	0.105
Calculated rate[2]	0.196[3]	0.094[3]	5.17	19.59	0.086[3]	0.020[3]	7.34	8.46

1 Rate measured after 40 minutes 3-^{14}C-pyruvate incorporation

2 Rate = $\frac{\text{Malate decarboxylated } (\mu\text{moles mg chl}^{-1}\ \text{hr}^{-1})}{3\text{-}^{13}\text{C-pyruvate incorporated } (\mu\text{moles mg chl}^{-1}\ \text{hr}^{-1})}$ x ^{14}C in product (μmoles mg chl^{-1} hr^{-1})

3 Assuming no internal pyruvate production

tissue. Such comparisons minimise the uncertainties, due to factors such as differing rates of pyruvate utilisation and different pool sizes, when comparing the labelling patterns of tissues from different species.

If pyruvate is oxidised via TCA cycle reactions, then the distribution of label between organic acids and carbohydrates should vary depending upon the position of ^{14}C within the pyruvate molecules. The ^{14}C in 1-^{14}C-pyruvate will be released as $^{14}CO_2$ immediately the pyruvate enters the TCA cycle, whereas the label from 2- and 3-^{14}C-pyruvate will be released at a slower rate. Label from 3-^{14}C-pyruvate will be released more slowly than label from 2-^{14}C-pyruvate. Conversely, if the pyruvate is metabolised gluconeogenically, the distribution of label amongst the products should be independent of the position of ^{14}C in the pyruvate skeleton since condensation of two complete pyruvate molecules is involved rather than the evolution of $^{14}CO_2$.

Unfortunately, up to 1.9% of the 1-^{14}C-pyruvate was non-enzymatically decarboxylated after 30 minutes (Tables 2.8 and 9). This decarboxylation was more rapid than observed by Neal and Beevers (1960) who noted that a maximum of 0.35% of 1-^{14}C-pyruvate was spontaneously decarboxylated after 24 hours at pH 5.0. In the present study a greater amount of $^{14}CO_2$ was evolved in flasks containing 1-^{14}C-pyruvate and boiled *Stapelia* mesophyll cells (see Section 3.2 for details of preparation) than was evolved in the dark or in the light by living material (Table 2.8). Similarly, a large amount of ^{14}C, in the form of $^{14}CO_2$, was evolved from flasks containing boiled *Kalanchoe* leaf slices than was incorporated into non-organic acid fractions by living tissue (Table 2.9). Obviously both externally evolved $^{14}CO_2$ and 1-^{14}C-pyruvate will be metabolised by the slices. The incorporation

Table 2.8 Evolution of $^{14}CO_2$ from 1-^{14}C-pyruvate by isolated *Stapelia gigantea* mesophyll cells in the light and in the dark compared with $^{14}CO_2$ evolution by boiled cells.

Exposure time (min)	Boiled cells		Living cells	
	$^{14}CO_2$ evolved	Evolved $^{14}CO_2$ as % of total 1-^{14}C-pyruvate in medium	Light	Dark
	cpm x 10^4		cpm x 10^4	
5	5.7	0.6	0.9	2.3
10	11.6	1.2	1.4	2.8
30	19.0	1.9	3.8	3.8

Table 2.9 Evolution of $^{14}CO_2$ from 1-^{14}C-pyruvate by boiled *Kalanchoe daigremontiana* leaf slices compared with the amount of ^{14}C incorporated in non-organic acid fractions by deacidifying leaf slices in the light.

Exposure time (min)	Boiled tissue		Living tissue
	$^{14}CO_2$ evolved	Evolved $^{14}CO_2$ as % of total 1-^{14}C-pyruvate in medium	^{14}C in non organic acid fractions
	cpm x 10^4		cpm x 10^4
10	9.6	0.8	3.9
20	14.9	1.2	-
30	17.8	1.9	10.8

of $^{14}CO_2$ by deacidifying leaf slices is, as shown earlier, much more rapid than the observed rates of ^{14}C-pyruvate uptake. The rapid refixation of this externally produced $^{14}CO_2$ combined with the slow rate of ^{14}C-pyruvate uptake precluded the collection of meaningful data from 1-^{14}C-pyruvate feeding experiments. In spite of this, comparisons of the products of 2-^{14}C- and 3-^{14}C-pyruvate metabolism remain relevant.

The incorporation of 2-^{14}C- and 3-^{14}C-pyruvate was linear with time in both *Kalanchoe* and *Stapelia* (Figure 2.21). The distribution of ^{14}C in the carbohydrate and organic acid fractions from both tissues is shown in Figures 2.22.

In *Kalanchoe*, fed with either 2-^{14}C- or 3-^{14}C-pyruvate, the amount and distribution of ^{14}C in the carbohydrate fractions was similar (Figure 2.22A). The organic acid fractions contain slightly more label when fed 3-^{14}C-pyruvate but the difference is marginal, particularly when expressed on a chlorophyll basis (Figure 2.22C). In contrast, there were appreciable differences in the amount and distribution of label in the carbohydrate and organic acid fractions from *Stapelia* labelled with 2-^{14}C- or 3-^{14}C-pyruvate (Figures 2.22B and D). After 40 minutes exposure 56% of the label incorporated from 2-^{14}C-pyruvate was in carbohydrates compared with 31% when fed 3-^{14}C-pyruvate. Conversely, in 2-^{14}C-pyruvate labelled tissue only 34% of the label was in organic acids compared with 61% in the 3-^{14}C-pyruvate labelled tissue.

These data are interpreted as follows. If 3-^{14}C-pyruvate is metabolised via the TCA cycle, it will enter the cycle as carbon-2 of citrate which is not released as CO_2 during the first two turns of the cycle. However due to

Figure 2.21 A. Incorporation of 2-^{14}C-pyruvate (o) and 3-^{14}C-pyruvate (•) in the light by deacidifying *Kalanchoe daigremontiana* leaf slices.

B. Incorporation of 2-^{14}C-pyruvate (o) and 3-^{14}C-pyruvate (•) in the light by deacidifying *Stapelia gigantea* leaf slices.

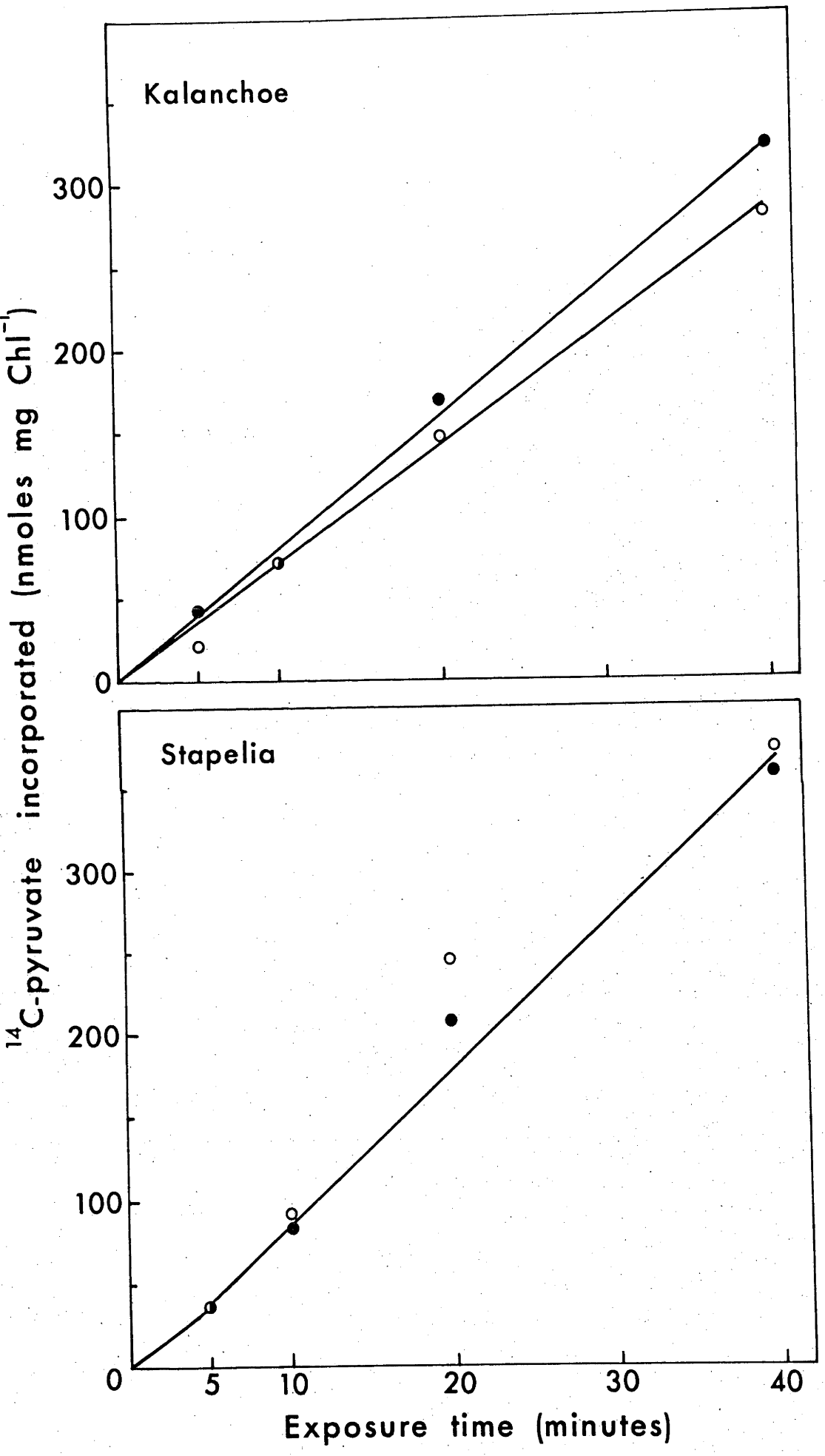
Kalanchoe
Stapelia
300
200
100
0
5
10
20
30
40
^{14}C-pyruvate incorporated (nmoles mg Chl^{-1})
Exposure time (minutes)

Figure 2.22 A. Incorporation of 2-^{14}C-pyruvate (o) and 3-^{14}C-pyruvate (•) into carbohydrates in the light by deacidifying *Kalanchoe daigremontiana* leaf slices.

B. Incorporation of 2-^{14}C-pyruvate (o) and 3-^{14}C-pyruvate (•) into carbohydrates in the light by deacidifying *Stapelia gigantea* leaf slices.

C. Incorporation of 2-^{14}C-pyruvate (o) and 3-^{14}C-pyruvate (•) into organic acids in the light by deacidifying *Kalanchoe daigremontiana* leaf slices.

D. Incorporation of 2-^{14}C-pyruvate (o) and 3-^{14}C-pyruvate (•) into organic acids in the light by deacidifying *Stapelia gigantea* leaf slices.

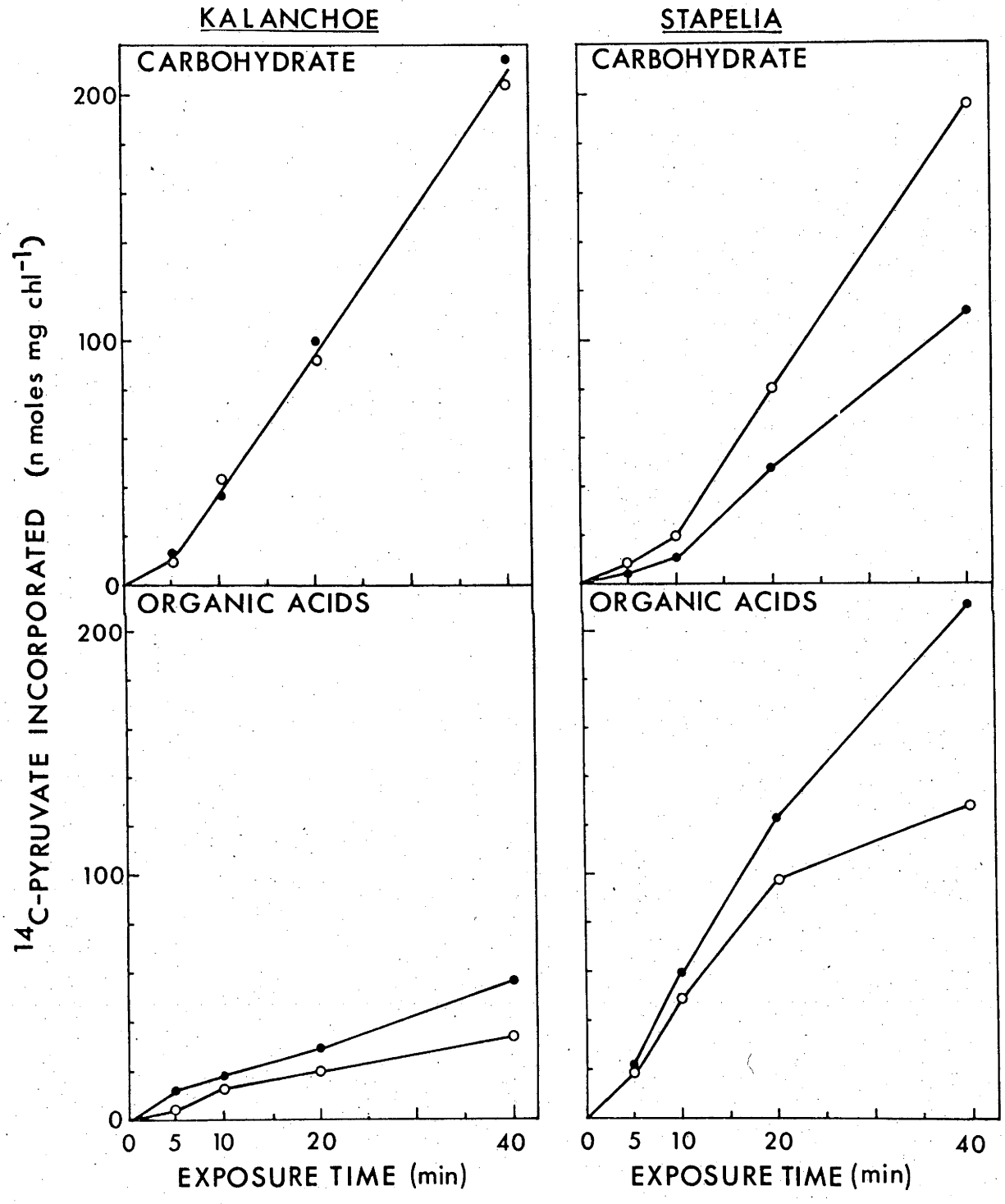
KALANCHOE
STAPELIA
CARBOHYDRATE
CARBOHYDRATE
ORGANIC ACIDS
ORGANIC ACIDS
200
100
0
200
100
0
0 5 10 20 40
0 5 10 20 40
EXPOSURE TIME (min)
EXPOSURE TIME (min)
^{14}C-PYRUVATE INCORPORATED (n moles mg chl^{-1})

randomisation of the 1 and 4 carbons of succinate and fumarate by succinic thiokinase and fumarase, half the ^{14}C will be evolved during the third turn of the cycle by isocitrate dehydrogenase and α-ketoglutarate dehydrogenase, and half the remainder will be evolved during each successive turn. 2-^{14}C-pyruvate will enter the cycle as the terminal carbon-1 which is liberated as CO_2 by isocitrate dehydrogenase and α-ketoglutarate dehydrogenase during the second turn of the cycle. Therefore, until the TCA cycle acids are saturated with ^{14}C from 3-^{14}C-pyruvate, $^{14}CO_2$ will be evolved more rapidly when 2-^{14}C-pyruvate is metabolised via the TCA cycle than when 3-^{14}C-pyruvate is metabolised. Consequently, in tissue in which pyruvate is predominantly metabolised via the TCA cycle, carbohydrates would be expected to be more rapidly labelled when fed 2-^{14}C-pyruvate than when fed 3-^{14}C-pyruvate. Moreover, until the acid pools became saturated, a greater proportion of the label would appear in TCA cycle acids in 3-^{14}C-pyruvate labelled tissue than in 2-^{14}C-pyruvate labelled tissue. This is precisely the pattern observed in deacidifying *Stapelia* tissue (Figures 2.22D). The amount of label in the TCA cycle acids in the 3-^{14}C-pyruvate fed tissue had not saturated by the end of the experiments, whilst the amount of label in the acid pools in the 2-^{14}C-pyruvate fed tissue appeared to be reaching saturation.

Gluconeogenic metabolism of pyruvate involves the condensation of complete pyruvate molecules. Therefore no differences would be expected in the distribution of label in the products of 2-^{14}C- or 3-^{14}C-pyruvate metabolism. This is what is observed in *Kalanchoe* (Figure 2.22A and C).

2.3.3.3 *Metabolism of 1,4-^{14}C- and 2,3-^{14}C-succinate*

Labelled succinate was fed to deacidifying *Kalanchoe* and *Aloe* leaf slices in an attempt to confirm indications that the TCA cycle may be

active in the light and to ascertain whether there was any export of carbon, in a form other than CO_2, out of the mitochondria. Succinate is thought to be metabolised exclusively in the mitochondria (Chapman and Osmond, 1974). If ^{14}C-succinate is metabolised via the TCA cycle then ^{14}C from I,4-^{14}C-succinate will be released during the first turn of the cycle (Figure 2.23). No ^{14}C from 2,3-^{14}C-succinate will be released during the first turn,however 50% will be released during the second turn and 50% of the remainder will be released during each subsequent turn.

The incorporation of 1,4-^{14}C and 2,3-^{14}C-succinate by *Kalanchoe* leaf slices and of 1,4-^{14}C-succinate by *Aloe* leaf slices in the light is shown in Figure 2.24. Succinate incorporation was linear after an initial phase of rapid incorporation but the absolute rates varied between treatments. I have no explanation for the variation observed in the incorporation of 1,4-^{14}C- and 2,3-^{14}C-succinate by *Kalanchoe* tissue, although it may be due merely to differences in the leaf tissue used in the two experiments. The rates of ^{14}C-succinate incorporation were very low and were between one sixth and one third of those observed for ^{14}C-pyruvate incorporation.

The distribution of label amongst the products of ^{14}C-succinate metabolism is shown in Table 2.10. Although the data must be interpreted cautiously due to the irregular rates of incorporation certain generalisations can be made. Label from both 1,4-^{14}C- and 2,3-^{14}C-succinate is almost equally converted to carbohydrates. Since, in *Kalanchoe*, label from 1,4-^{14}C-succinate is converted to carbohydrates more slowly than from 2,3-^{14}C-succinate, it is possible that ^{14}C is being exported from the

Figure 2.23 Scheme showing the predicted transfer of ^{14}C from I,4-^{14}C-succinate within the TCA cycle.

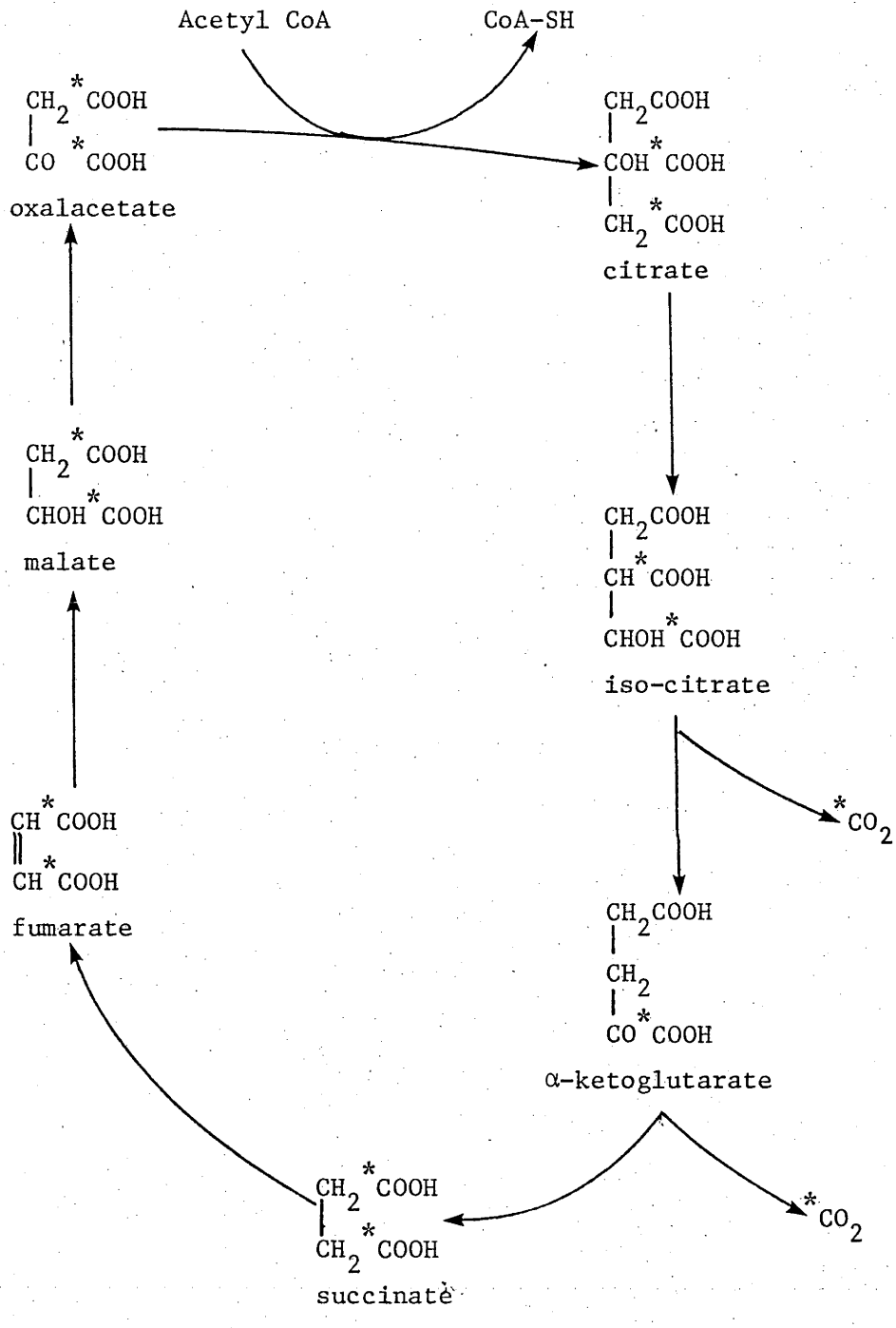
Acetyl CoA
CoA-SH
CH2*COOH
CO*COOH
oxalacetate
CH2COOH
COH*COOH
CH2*COOH
citrate
CH2*COOH
CHOH*COOH
malate
CH2COOH
CH*COOH
CHOH*COOH
iso-citrate
*CO2
CH*COOH
CH*COOH
fumarate
CH2COOH
CH2
CO*COOH
α-ketoglutarate
CH2*COOH
CH2*COOH
succinate
*CO2

Figure 2.24 The incorporation of 1,4-^{14}C-succinate (●) and 2,3-^{14}C-succinate (o) by deacidifying *Kalanchoe* leaf slices and of 1,4-^{14}C-succinate (▲) by deacidifying *Aloe* leaf slices in the light.

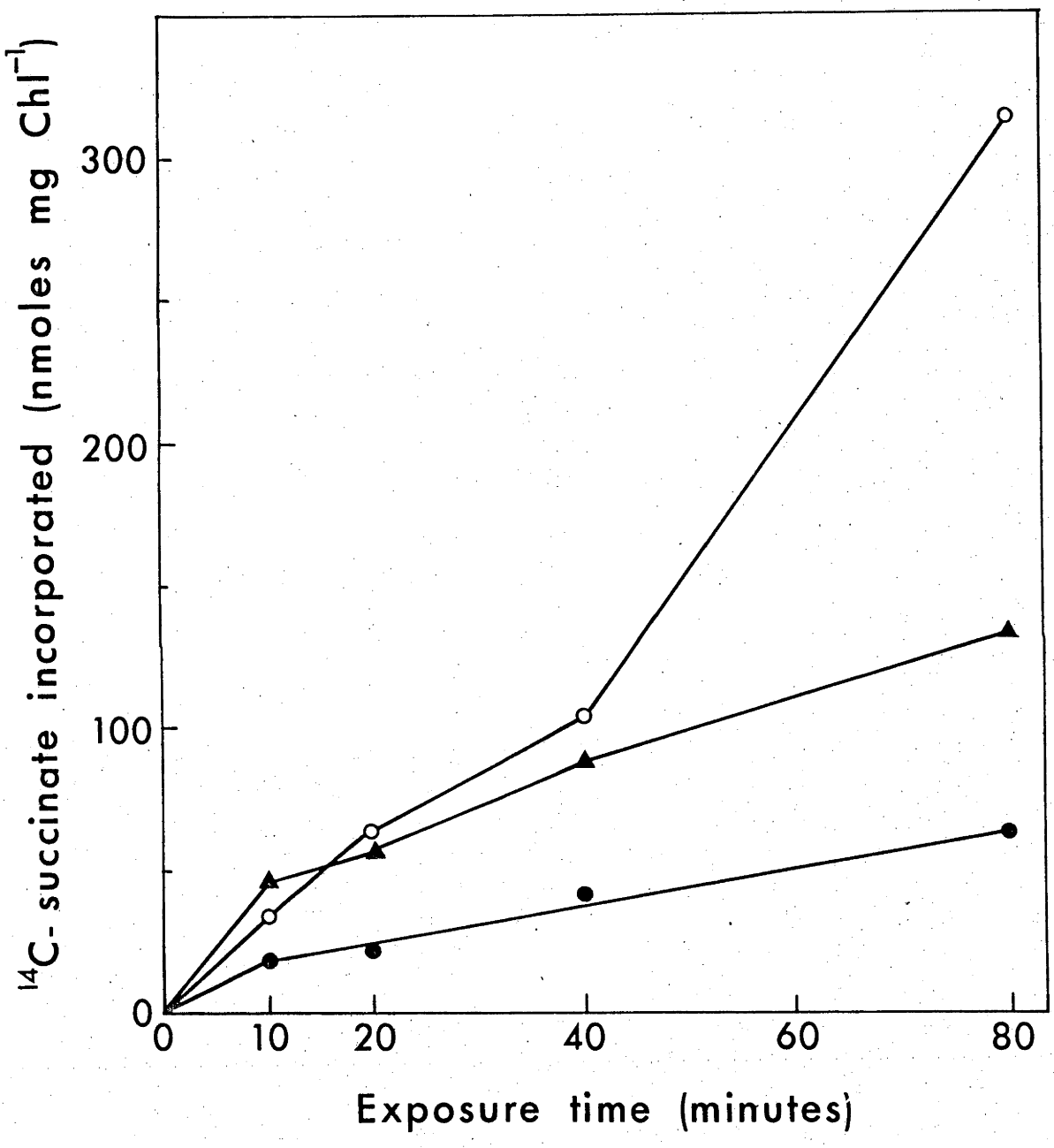
^{14}C- succinate incorporated (nmoles mg Chl^{-1})
300
200
100
0
0
10
20
40
60
80
Exposure time (minutes)

Table 2.10 Distribution of ^{14}C in deacidifying *Kalanchoe* and *Aloe* leaf slices exposed to 1,4-^{14}C- or 2,3-^{14}C- succinate in the light.

Compound	10 minutes exposure			80 minutes exposure		
	Aloe	*Kalanchoe*		*Aloe*	*Kalanchoe*	
	1,4-^{14}C-succinate	1,4-^{14}C-succinate	2,3-^{14}C-succinate	1,4-^{14}C-succinate	1,4-^{14}C-succinate	2,3-^{14}C-succinate
	(% of succinate metabolised)					
Carbohydrate (glucan + sugars)	13	22	37	56	50	72
Malate	33	37	30	21	26	15
Citrate + isocitrate	Tr	Tr	Tr	Tr	Tr	Tr
Fumarate	38	26	23	27	13	6
Glycine + serine	16	14	7	7	6	6
Aspartate	1	1	3	2	5	1
Glutamate	-	-	-	Tr	Tr	Tr
Total ^{14}C-succinate metabolised (nmoles mg chl^{-1})	48	20	32	140	60	320

Tr = trace amounts

- = not detected

mitochondria in a metabolite rather than as $^{14}CO_2$. The low amount of label in citrate/isocitrate and the absence of label in glutamate suggest that succinate does not proceed to citrate and α-ketoglutarate. It appears likely that the route of carbohydrate labelling from succinate does not involve the complete cycling of carbon through the TCA cycle. As malate and fumarate, but not citrate/isocitrate, contain substantial amounts of ^{14}C it is possible that malate, OAA, or some derivative of malate or OAA such as pyruvate, is labelled from ^{14}C-succinate and exported from the mitochondria.

The data broadly agree with the observations of Chapman and Osmond (1974) who fed 1,4-^{14}C- and 2,3-^{14}C-succinate in the light and in the dark to leaf slices of the NAD malic enzyme C_4 plant, *Atriplex spongiosa*. Both 1,4-^{14}C- and 2,3-^{14}C-succinate were converted to sucrose and other photosynthetic products at about equal rates in the light. This conversion was however, considerably more rapid than the rate of $^{14}CO_2$ release in the dark and it was suggested that even if $^{14}CO_2$ release continued unabated in the light the refixation of $^{14}CO_2$ during photosynthesis could not account for the observed labelling patterns, particularly in the case of 2,3-^{14}C-succinate. The authors concluded that the most plausible explanation, as it seems to be in the present study, was that ^{14}C-succinate was not metabolised beyond ^{14}C-malate or ^{14}C-OAA in the TCA cycle. Presumably malate can either be decarboxylated by NAD malic enzyme in the mitochondria or it can be exported to the cytoplasm and decarboxylated there.

2.3.4 Discussion

The distribution of label in the products of ^{14}C-pyruvate metabolism is consistent with the conversion of pyruvate to carbohydrate via a gluconeogenic

mechanism in *Kalanchoe* and probably also in CAM *Mesembryanthemum*. The data does not support the gluconeogenic conversion of pyruvate to carbohydrates in *Stapelia*, C_3 *Mesembryanthemum* or in spinach. It is possible that *Stapelia*, a PEPCK CAM plant which produces PEP but not pyruvate during deacidification, can convert PEP to carbohydrate but is unable to convert pyruvate to carbohydrate. The conversion of pyruvate to PEP as the first step in gluconeogenesis requires an enzyme such as pyruvate, Pi dikinase to reverse the physiologically irreversible pyruvate kinase reaction $PEP \xrightarrow[ATP]{ADP} PYRUVATE$. Pyruvate, Pi dikinase has been reported to be present in *Kalanchoe* (Kluge and Osmond, 1971; Sugiyama and Laetsch, 1975) but, as will be shown in Chapter 4.1, is absent from *Stapelia*.

In *Stapelia*, and to a lesser extent in *Kalanchoe*, a substantial proportion of the label from 3-^{14}C-pyruvate rapidly appears in the organic acid fraction, principally in malate and citrate/isocitrate. The differences in the amount of radioactivity in the carbohydrate and organic acid fractions from tissues fed either 2-^{14}C- or 3-^{14}C-pyruvate suggests that, in *Stapelia*, TCA cycle reactions may be important in pyruvate metabolism. The distribution of label in the fractions from *Kalanchoe* indicates that only a small proportion is metabolised by this means. In spinach, the bulk of the label from ^{14}C-pyruvate was in alanine and glutamate which suggests that pyruvate was metabolised principally via transamination, not by the TCA cycle or gluconeogenesis.

This interpretation of the distribution of ^{14}C in products of ^{14}C-pyruvate metabolism is, however, based on two assumptions. The first is that during

^{14}C-pyruvate feeding, ^{14}C-pyruvate is the only labelled compound fed to the tissue. The second is that ^{14}C is only exported from the mitochondria as $^{14}CO_2$.

The 1-^{14}C-pyruvate data suggests that a small proportion of external pyruvate is non-enzymatically decarboxylated. The most probable 2-carbon product is ^{14}C-acetate. Acetate is rapidly taken up by tissues and is metabolised within the mitochondria. It is thus possible that a small proportion of the initial label in TCA cycle acids and subsequently in both acids and carbohydrate is due to the incorporation of ^{14}C-acetate, not ^{14}C-pyruvate. A small amount of ^{14}C-acetate incorporation does not significantly alter the interpretation of the data. In *Kalanchoe*, allowance for ^{14}C-acetate incorporation suggests that a greater proportion of the label from ^{14}C-pyruvate was converted directly to carbohydrates than was initially indicated i.e. it strengthens the evidence for a gluconeogenic mechanism. In *Stapelia*, although any allowance for ^{14}C-acetate incorporation would lower the initial apparent amount of label from ^{14}C-pyruvate in the organic acid fraction, the acids are still easily the heaviest labelled fraction. In fact, the metabolism of ^{14}C-acetate by TCA cycle reactions should be almost identical to the mitochondrial metabolism of ^{14}C-pyruvate and the relative proportions of label in the acid and carbohydrate fractions should remain constant.

Both the ^{14}C-succinate data and observations with isolated CAM mitochondria, mentioned earlier, suggest that malate, pyruvate and OAA (as well as aspartate, α-ketoglutarate and glutamate) can cross the mitochondrial membrane. If such export occurs then the labelling pattern observed in *Kalanchoe* would only be observed if the exported metabolite was rapidly

converted *in toto* to carbohydrate, which again implicates a gluconeogenic pathway. The distribution of label in the products of ^{14}C-pyruvate metabolism in *Stapelia* could only occur if the exported metabolite was decarboxylated and the $^{14}CO_2$, but not the 3-carbon skeleton, was converted to carbohydrate. If the 3-carbon skeleton was directly converted to carbohydrate one would not expect to observe either such a large proportion of the label in organic acids, or a distribution of ^{14}C amongst the products of ^{14}C-pyruvate which is dependent upon the position of the ^{14}C in the labelled pyruvate. This evidence plus the observations that PEPCK plants have low malic enzyme activities (Dittrich *et al.*, 1973; Dittrich, 1976) suggests that any $^{14}CO_2$ produced internally from ^{14}C-pyruvate is done so in the mitochondria, most probably from TCA cycle reactions.

Unfortunately, due to the uncertainties caused by the internal dilution of ^{14}C-pyruvate, it is difficult to estimate the relative rates of TCA cycle activity in *Stapelia* and *Kalanchoe*. The observation that label in ^{14}C-succinate is exported from the mitochondria suggests that if the TCA cycle is to function as a cycle then a TCA cycle carbon acceptor must replace the carbon which is exported. Since PEPCK seems to be the principal decarboxylating enzyme in *Stapelia* it is possible that the activity of the TCA cycle may be adequate to oxidise the small amounts of pyruvate which may be produced during deacidification by NADP malic enzyme. However, the slow rate of conversion of ^{14}C-pyruvate to carbohydrates and the low activity of pyruvate kinase in CAM plants (Sutton, 1974, 1975b) make it unlikely that the PEP formed during the same period is converted to pyruvate then oxidised.

It is also possible that some exogenously supplied ^{14}C-pyruvate may be directly converted to malate in the cytoplasm. In *Kalanchoe* this could

occur via pyruvate, Pi dikinase and PEP carboxylase if the latter enzyme retains any activity, although such a conversion would result in a futile cycle. It is hard to envisage how this would occur in *Stapelia* particularly when one considers the differences in the distribution of label from 2-^{14}C- and 3-^{14}C- fed tissue.

The distribution of ^{14}C amongst the products of 3-^{14}C-pyruvate metabolism in C_3 *Mesembryanthemum* is similar to that observed in *Stapelia*, whilst the distribution of ^{14}C in CAM *Mesembryanthemum* is intermediate between *Stapelia* and *Kalanchoe*. However, when the internal dilution of ^{14}C-pyruvate is taken into account CAM *Mesembryanthemum* quite obviously has a far greater capacity to convert pyruvate to carbohydrate than C_3 *Mesembryanthemum*. This capacity is not matched by the rates of dark respiration observed in leaf slices (Winter, personal communication).

It is difficult to understand why the organic acid fractions were so heavily labelled in CAM *Mesembryanthemum*. Interpretation is complicated by the high NaCl content of the tissue which interfered with the chromatography of malate and citrate in particular, and which made the two acids run as a single spot. It is possible that PEP carboxylase may have been still significantly active and may have converted PEP, which could be formed from pyruvate (see Chapter 4.3), to malate. Unfortunately, for purely circumstantial reasons, I was unable to distinguish between respiratory and non-respiratory pyruvate metabolism by feeding 2-^{14}C- and 3-^{14}C-pyruvate to both C_3 and CAM tissues. It is probably reasonable to state that, in lieu of a more detailed investigation, the CAM tissue has a far greater capacity to convert 3-^{14}C-pyruvate to carbohydrate than the C_3 tissue and this observation, coupled with the relatively lower

respiration rates, suggests that pyruvate is rapidly converted to carbohydrate in CAM *Mesembryanthemum* by a non-respiratory process. Such a process will most likely involve a gluconeogenic mechanism.

3 ISOLATION AND METABOLISM OF INTACT MESOPHYLL CELLS

3.1 Introduction

Isolated mesophyll cells are a useful experimental system for investigating some physiological and biochemical processes in plant tissues. Photosynthetically active leaf mesophyll cells and protoplasts have been enzymatically isolated from C_3 and C_4 plants (cf. Kanai and Edwards, 1973), however, it is only recently that intact cells have been isolated from CAM tissue. Mechanically isolated mesophyll cells from the malic enzyme CAM plant *Sedum telephium*, required the addition of phosphorylated compounds before significant $^{14}CO_2$ incorporation was observed (Rouhani, 1972; Rouhani *et al.*, 1973). In subsequent studies with enzymatically isolated *Sedum telephium* protoplasts and cells, high rates of $^{14}CO_2$ incorporation of 30-70 μmoles mg chl^{-1} hr^{-1} at 30°C were observed without the addition of any substrates (Kanai and Edwards, 1973; Spalding and Edwards, 1978). The cells exhibited high, linear rates of oxygen evolution, and ratios of oxygen evolution to CO_2 incorporation of close to unity. $^{14}CO_2$ incorporation rates of 56-73 μmoles mg chl^{-1} hr^{-1} at 30°C, which were also independent of added substrates, have been reported for mesophyll cells isolated from *Opuntia polycantha* and *Opuntia monocantha*(Gerwick *et al.*, 1978). To date there have been no reports of cells isolated from any PEPCK CAM plants.

In this section some of the properties of intact and photosynthetically active mesophyll cells, enzymatically isolated from the malic enzyme CAM plant *Kalanchoe daigremontiana*, and from the PEPCK CAM plant *Stapelia gigantea* will be investigated. In particular, evidence will be sought for a difference in the response of these cells to externally added pyruvate.

The gluconeogenic hypothesis presented in Section 1.4 and experiments reported in Section 2.3 predict that *Kalanchoe* mesophyll cells should convert pyruvate to PEP *in vivo* more effectively than *Stapelia* cells, and this may be reflected in the rates of CO_2 assimilation via PEP carboxylase in the light.

3.2 Materials and Methods

3.2.1 Experimental material

Plants were grown as described in Section 2.1.2. For *Kalanchoe* the second expanded leaf was used. It was important to use young actively growing tissue since the cell yield diminished with increasing tissue age.

3.2.2 Isolation of cells

Deacidified *Kalanchoe* and *Stapelia* tissue was cut with a sharp razor blade into 0.5-1 mm thick slices and suspended (about 5 g in 50 ml) in an isolating medium containing 50 mM MES-NaOH pH 5.5, 0.3 M mannitol, 5 mM $MgCl_2$, 1 mM K_2HPO_4, 0.1 mM $CaSO_4$, 0.5% (w/v) PVP-40 and 0.5% (w/v) Macerase (1.0% Macerase was used for *Kalanchoe* tissue). The slices were vacuum infiltrated for 5 second periods until they no longer floated. This usually required three or four infiltrations. A piece of gauze on the surface of the isolation medium ensured that the slices were completely submerged throughout the infiltration.

The tissue was digested at room temperature with occasional shaking, for 1-2 hours before being placed, together with a magnetic flea, in the central well of a two compartment chamber similar to that described by Rehfeld and Jensen (1973). The well was covered with coarse mesh (1 mm) nylon gauze and the chamber filled with isolation medium to

a level 0.5-1.0 cm above the lip of the centre well. The suspension was stirred for up to 45 minutes, depending upon both the species and the cell yield. The stirring speed was adjusted so that the vortex created was just sufficient to push any separated cells upwards through the gauze and outwards. The cells which settled in the unstirred outer well were transferred using a wide mouthed pippette to a test tube containing 5-10 ml (depending upon the cell yield) of resuspension medium consisting of 25 mM HEPES-NaOH, 25 mM MES-NaOH pH 7.5, 0.25 M mannitol, 5 mM $MgCl_2$ and 0.1 mM $CaSO_4$. After settling for 5-10 minutes the cells were resuspended in 5 to 10 ml of the resuspension medium. This resuspension was repeated before storing the cells at room temperature until used (1-3 hours).

I was unable to isolate photosynthetically active cells from *Ananas comosus* (pineapple), *Aloe arborescens* or *Hoya carnosa*. Cells from the latter two species appeared to have been ruptured by crystals which were abundant in the tissues. Cells which evolved O_2 at low rates were isolated from *Bryophyllum pinnatum*, *Escheveria glauca* and *Sanseveria trifasciata*. Cells of varying activity were also isolated from C_3 and CAM *Mesembryanthemum crystallinum*.

3.2.3 Incorporation of $^{14}CO_2$

$^{14}CO_2$ fixation was assayed at room temperature (21°C) in sealed scintillation vials. Cells (200-400 µg chlorophyll in 200 µl) were suspended in 0.7 ml of assay medium containing 25 mM HEPES-NaOH pH 7.8, 0.25 M mannitol, 5 mM $MgCl_2$, 1 mM K_2HPO_4 and 0.1 mM $CaSO_4$. The vials were illuminated with a quantum flux density of 1,200 µeinstein m^{-2} s^{-1} at vial-top height from a 1000 W Philips HPLR high pressure mercury vapour

fluorescent lamp through a 5 cm water filter. The cells were preincubated for 10 minutes in a mechanical shaker (≃ 20 strokes min^{-1}) with or without substrates before 10 µmoles $NaH^{14}CO_3$ in 0.1 ml was added (1-2 x 10^6 dpm/µmole). After appropriate intervals the cells were killed with 200 µl of 20% trichloroacetic acid. The suspension was blown to dryness and acid-stable counts were determined by liquid scintillation counting. Products of $^{14}CO_2$ fixation were separated and identified as described in Section 2.2.2, but chromatography of soluble sugars proved impracticable due to the high concentration of mannitol in the reaction mixture which coeluted from the Dowex resin with the neutral fraction.

3.2.4 Oxygen exchange measurements

Oxygen exchange was measured at 25°C using a Clark-type Rank electrode. Cells (100-250 µg chl in 0.1 ml) were suspended in 2.9 ml of buffer identical to that used for $^{14}CO_2$ incorporation except that the buffer was CO_2 free. "CO_2 free" buffer was prepared by heating the buffer close to boiling point whilst bubbling with N_2 in an Erlenmeyer flask. A tube containing Carbosorb was placed in the flask and the flask was sealed and allowed to cool.

The reaction vessel was illuminated by a 150 W projector lamp which provided 1000-1200 µeinstein m^{-2} s^{-1} at the vessel centre. When a red filter was used, the light intensity dropped to about 800 µeinstein m^{-2} s^{-1}.

3.2.5 Estimation of intactness of cells

The intactness of cells was routinely verified by light microscopy. (Fig.3.
To examine for intact cells a small amount of Evans Blue in 0.3 M mannitol

Figure 3.1 A. Isolated mesophyll cells from *Stapelia gigantea*. Smaller chloroplast deficient cells are pith cells.

B. Exclusion of Evans Blue by isolated mesophyll cells from *Stapelia gigantea*.

C. Mesophyll cell from *Stapelia gigantea*. The orientation of chloroplasts on the periphery of the cell indicates that the tonoplast and plasmalemma are intact.

D. Mesophyll cells isolated from *Kalanchoe daigremontiana*.

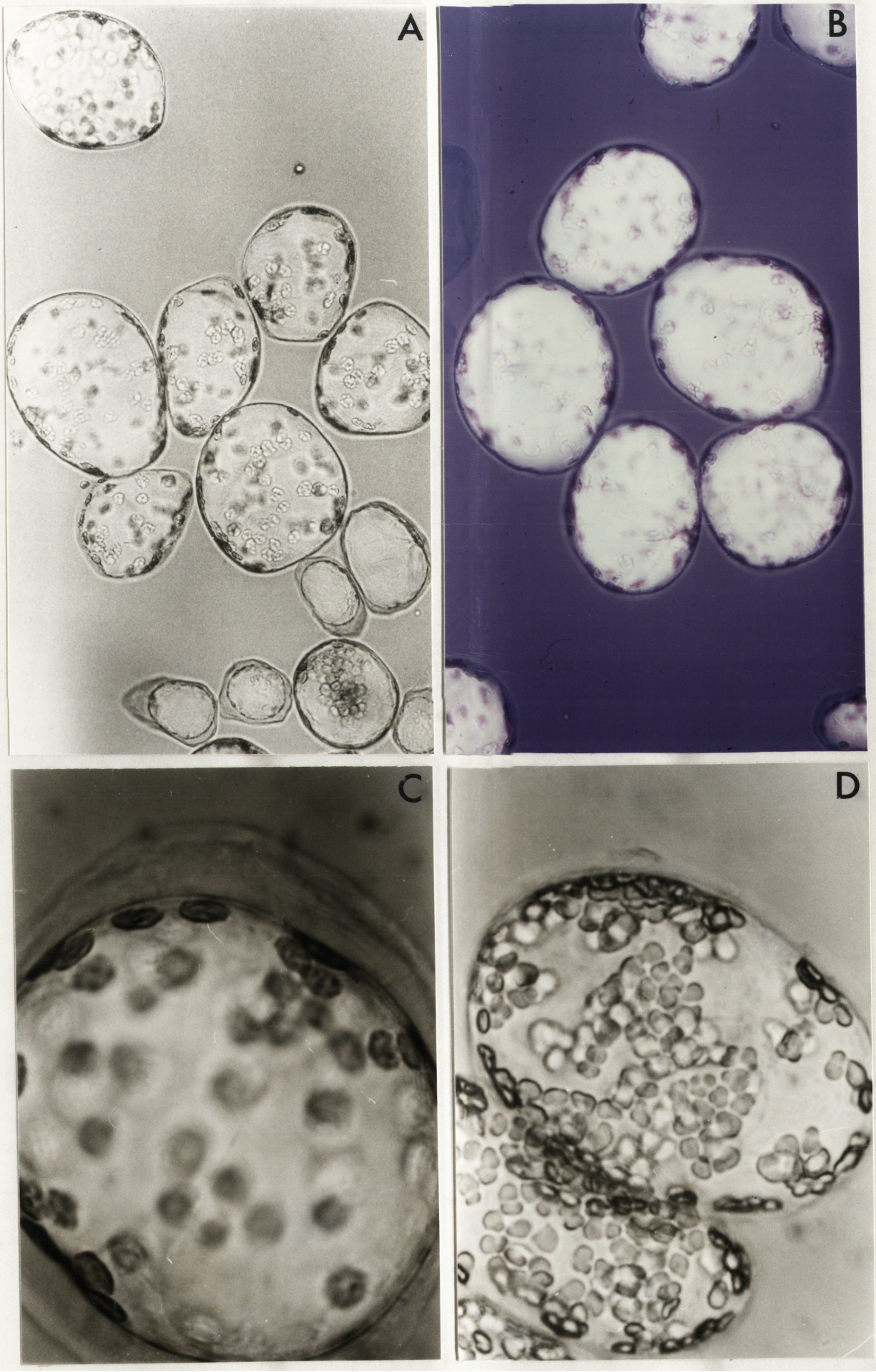
A
B
C
D

was mixed with the cell preparation on a microscope slide and examined under a light microscope for exclusion of the dye. Evans Blue is a water soluble dye (M.wt ≃ 900) which is excluded by intact semipermeable membranes (Figure 3.1)(Gaff and Okong'o-Ogloa, 1971).

3.2.6 Chlorophyll estimation

A 1 ml aliquot of cells was shaken with 4 ml of 100% acetone and spun for 5 min at maximum speed (about 4,000 x g) in a clinical centrifuge. The chlorophyll content of the supernatant was assayed after Arnon (1949) as described in Section 2.1.2.4.

3.3 Results

The mannitol concentration required for production of intact cells was determined in a number of preliminary experiments. It appeared that the cells were more viable when isolated in a slightly plasmolysed state. Hence cells were extracted in 0.3 M mannitol and assayed in 0.25 M mannitol.

Cells were more easily obtained from *Stapelia* than from *Kalanchoe*. *Stapelia* tissue usually required only about 15 minutes stirring to produce a high yield of cells that were regularly 75-90% intact before purification. The cells were considered physically intact if they actively excluded Evans Blue. The yield of cells from *Kalanchoe* was less predictable as both the percentage of intact cells and the total yield varied between experiments. Cells from *Kalanchoe* were not used unless they were at least 60% intact before purification. The cells remaining after purification were about 75-85% intact. Cells of older *Kalanchoe* leaves

were less easily separated than those from young leaves. Tissue age had no effect on cell separation from *Stapelia* tissue although the older cells had less chlorophyll.

3.3.1 Oxygen evolution and consumption

Isolated *Kalanchoe* and *Stapelia* mesophyll cells exhibited high rates of light dependent O_2 evolution which were linear for at least 15 minutes and proportional to the amount of chlorophyll present (Figure 3.2). Intactness of the cell chloroplasts is indicated by the observation that O_2 evolution was not stimulated by ferricyanide (Table 3.1). The ratio of O_2 evolution to DCMU sensitive $^{14}CO_2$ incorporation is close to unity which indicates that the PCR cycle is functional and coupled to the photosystems (Table 3.2).

Oxygen evolution in both species, although requiring exogenous CO_2 for maximum activity, was only partially dependent upon external CO_2 (Table 3.1). Both the external CO_2 dependent and the independent components were completely inhibited by 4 μM DCMU (Table 3.3). Although the maximum observed rates of O_2 evolution were similar for each species (20-50 μmoles mg chl^{-1} hr^{-1} in *Kalanchoe* and 50-70 μmoles mg chl^{-1} hr^{-1} in *Stapelia*) the proportion contributed by the external CO_2 independent component varied considerably between extractions. Similar external CO_2 independent oxygen evolution has been observed in *Aloe* leaf slices and in isolated *Sedum telephium* cells (Denius and Homann, 1972; Spalding and Edwards, 1978). In *Aloe* leaf slices, external CO_2 independent O_2 evolution is proportional to the tissue malate content and is most probably due to CO_2 being produced internally via malate decarboxylation. Spalding and Edwards (1978) reached the same conclusions regarding the external CO_2 independent O_2 evolution observed in *Sedum* cells.

Figure 3.2 O_2 evolution in the light by isolated mesophyll cells from *Kalanchoe daigremontiana* (○) and *Stapelia gigantea* (●) expressed as a function of chlorophyll content. Results of two experiments.

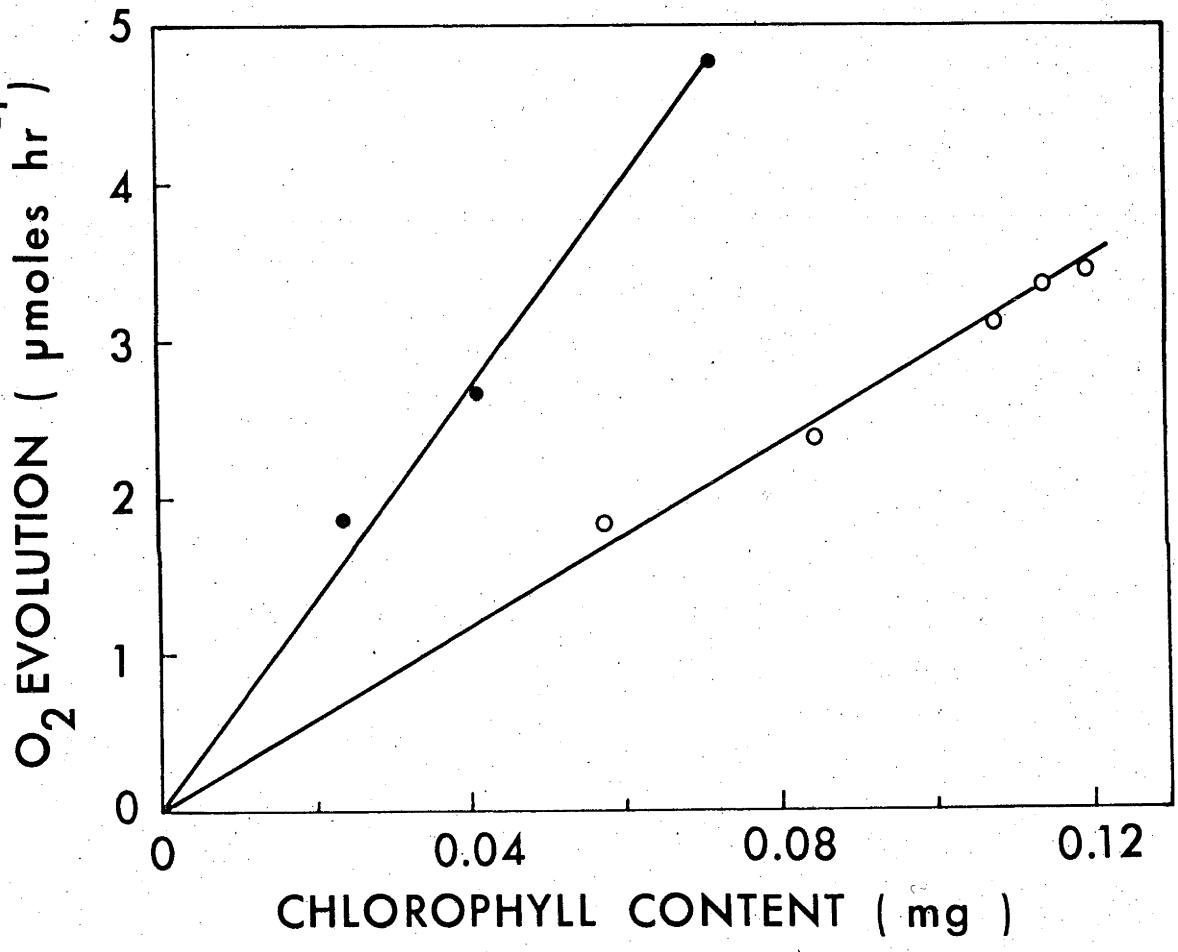
5
4
3
2
1
0
O_2 EVOLUTION (μmoles hr^{-1})
0
0.04
0.08
0.12
CHLOROPHYLL CONTENT (mg)

Table 3.1 Effect of ferricyanide on net oxygen exchange and oxygen evolution in isolated *Kalanchoe* and *Stapelia* mesophyll cells.

Species	Treatment	Net O_2 exchange (μmoles mg chl^{-1} hr^{-1})	O_2[a] evolution (μmoles mg chl^{-1} hr^{-1})
Stapelia	light on[b]	23.2	34.8
	+ ferricyanide [1 mM]	21.8	33.4
	+ $NaHCO_3$ [10 mM]	33.4	45.0
	+ DCMU [4 μM]	-11.6	0
	light on[b]	9.4	32.8
	+ $NaHCO_3$ [10 mM]	39.8	63.9
	light off	-23.4	0
	light on	37.5	60.9
	+ ferricyanide [1 mM]	37.5	60.9
Kalanchoe	light on[b]	4.0	14.5
	+ $NaHCO_3$ [10 mM]	15.6	25.6
	+ ferricyanide [1 mM]	15.6	25.6
	+ light off	-10.5	0

a Apparent O_2 evolution calculated by assuming the basal dark O_2 uptake rate was equivalent to zero O_2 evolution

b All cells initially in CO_2 free buffer

Table 3.2 Relationship between $^{14}CO_2$ assimilation and oxygen evolution in isolated *Kalanchoe* and *Stapelia* mesophyll cells in the light.[a]

Species	$^{14}CO_2$ incorporation[b]	$^{14}CO_2$ minus DCMU insensitive[c]	O_2 evolution[d]	$\frac{O_2 \text{ Evoln.}}{^{14}CO_2 \text{ Incorpn.}}$	$\frac{O_2 \text{ Evoln.}}{^{14}CO_2 - \text{DCMU sensitive}}$
		(μmoles mg Chl^{-1} hr^{-1})			
Kalanchoe	36.5(±3.0)	31.6(±3.0)	31.9(±4.9)	0.87	1.01
Stapelia	59.5(±2.1)	49.4(±2.7)	53.7(±7.5)	0.90	1.09

a Both O_2 evolution and $NaH^{14}CO_3$ incorporation in the presence of 10 mM $NaHCO_3$. Assay conditions as described in methods

b Mean of 4 determinations plus standard deviation

c Mean of 3 determinations plus standard deviation. 5 μM DCMU used

d Mean of 6 determinations plus standard deviation

Table 3.3 Effect of DCMU on net oxygen exchange and oxygen evolution in isolated *Kalanchoe* and *Stapelia* mesophyll cells.

Species	Treatment	Net O_2 exchange (μmoles mg chl^{-1} hr^{-1})	O_2[a] evolution
Kalanchoe	dark[b]	-7.0	0
	light on	-4.1	2.9
	+ $NaHCO_3$ [10 mM]	20.8	27.8
	+ $NaHCO_3$ + DCMU [4 μM]	-7.0	0
Stapelia	dark[b]	-10.0	0
	light on	21.1	31.1
	+ $NaHCO_3$ [10 mM]	35.0	45.0
	+ $NaHCO_3$ + DCMU [4 μM]	-9.6	0.4

a Apparent O_2 evolution calculated by assuming the basal dark O_2 uptake rate was equivalent to zero O_2 evolution

b All cells initially in CO_2 free buffer

The addition of malate in the absence of external CO_2 did not increase O_2 evolution to the levels observed in CO_2 fed cells (Table 3.4). This suggests that either malate is not entering the cells or, if it is, the rate of malate decarboxylation was already saturated. Since the $^{14}CO_2$ feeding data presented in the following section indicates that the cells are permeable to PEP and to a lesser extent to PGA and pyruvate, it is most unlikely that they are impermeable to malate.

Accurate measurements of dark respiration were not obtained. Although very high rates of dark O_2 uptake were observed, it is unlikely that the uptake was of respiratory origin as it was insensitive to a range of respiratory and other inhibitors even when exposed to very high concentrations viz. 10 mM KCN, 0.5 mM antimycin-A, 0.4 mM oligomycin and 1 mM DCMU. Similarly, light dependent O_2 uptake observed in the presence of 4 μM DCMU, was insensitive to KCN, antimycin and oligomycin. Light dependent O_2 uptake was observed in boiled cells from both species. It is possible that this is a similar phenomenon to that observed by Denius and Homann (1972) in *Aloe* leaf slices and is due to photo-oxidation of light absorbing pigments. Obviously there are also other factors involved which require further investigation.

3.3.2 Light and dark $^{14}CO_2$ fixation

Cells isolated from deacidified *Kalanchoe* and *Stapelia* mesophyll tissue fix $^{14}CO_2$ more rapidly in the light than in the dark and $^{14}CO_2$ fixation is linear for at least 30 minutes. The distribution of label in the products of 30 minutes light and dark $^{14}CO_2$ incorporation by *Stapelia* cells (Table 3.5) is similar to the distribution observed in

Table 3.4 Effect of malate, PEP and pyruvate on net oxygen exchange and oxygen evolution in isolated *Kalanchoe* and *Stapelia* mesophyll cells.

Treatment	*Kalanchoe*		*Stapelia*	
	net O_2 exchange	O_2[a] evolution	net O_2 exchange	O_2[a] evolution
	(μmoles mg chl^{-1} hr^{-1})			
dark[b]	-6.4	0	-22.0	0
light on	-3.2	3.2	6.0	28.0
light + malate [10 mM]	5.5	11.9	11.5	33.5
light + malate + $NaHCO_3$ [10 mM]	22.3	28.7	34.4	56.4
dark[b]	-5.7	0	-23.0	0
light on	5.2	10.9	6.6	29.6
light + PEP [10 mM]	8.8	14.6	8.6	31.6
light + PEP + $NaHCO_3$ [10 mM]	29.6	35.3	30.7	53.7
dark[b]	-9.7	0	-[c]	-
light on	-1.0	8.6	-	-
light + $NaHCO_3$ [10 mM]	26.9	36.6	-	-
light + $NaHCO_3$ + PEP [10 mM]	30.5	40.1	-	-
dark[b]	-7.0	0	-	-
light on	-2.5	4.5	-	-
light + pyruvate [10 mM]	-1.2	5.8	-	-
light + pyruvate + $NaHCO_3$ [10 mM]	21.8	28.7	-	-
dark[b]	-	-	-20.1	0
light on	-	-	9.8	29.9
light + $NaHCO_3$ [10 mM]	-	-	37.6	57.7
light + $NaHCO_3$ + pyruvate [10 mM]	-	-	37.6	57.7

a Apparent O_2 evolution calculated by assuming the basal dark O_2 uptake rate was equivalent to zero O_2 evolution

b All cells initially in CO_2 free buffer

c - not determined

Table 3.5 Distribution of ^{14}C in the products of 30 minutes light and dark $^{14}CO_2$ fixation by isolated *Stapelia* mesophyll cells.[a]

Labelled metabolites	Light (%)	Dark
Insolubles	15.6	1.1
Soluble sugars	54.9	15.8
Phosphorylated compounds	3.2	1.9
Malate plus citrate[b]	20.9	68.4
Other acids[c]	0.9	0.9
Amino acids	4.9	12.0
Total counts incorporated (dpm)	1.2×10^6	1.9×10^4

a $NaH^{14}CO_3$ specific activity - 1.2×10^6 dpm µmole

b Citrate fraction | also contains isocitrate

c Fumarate, succinate and possibly aconitate

deacidified *Stapelia* and *Kalanchoe* leaf slices (see Section 2.2) and in intact tissue (Kluge, 1969c; Osmond and Allaway, 1974). After 40 minutes incorporation less than 3% of the total counts were in the bathing solution.

The addition of 10 mM PEP stimulated light $^{14}CO_2$ fixation between 1.7 and 2.1 times in both species, presumably by providing a substrate for PEP carboxylase activity (Table 3.6). This interpretation is confirmed by the observation that in *Kalanchoe*, PEP stimulated $^{14}CO_2$ fixation is insensitive to DCMU whereas the basal $^{14}CO_2$ fixation is inhibited by DCMU (Table 3.6). Such a response would be expected if the original rates are due to RuP_2 carboxylase activity which is dependent upon the light reactions, for provision of substrate. PEP carboxylase has no such direct light energy requirement if PEP is supplied exogenously. Table 3.6 also indicates that in the isolated cells the PEP supply is limited and this may explain why, in intact deacidified tissue (Phase 4), CO_2 appears to be mainly incorporated by RuP_2 carboxylase not PEP carboxylase (Osmond and Allaway, 1974).

Dark $^{14}CO_2$ fixation was increased 2.5 fold in *Stapelia* and 4 fold in *Kalanchoe* by the addition of 5 mM 3-PGA, presumably due to the conversion of 3-PGA to PEP catalysed by enolase and 3-PGA mutase (Table 3.7). However, although 10 mM PEP stimulated light $^{14}CO_2$ fixation in *Kalanchoe* by over 100%, 3-PGA had no effect. This suggests that in the light in *Kalanchoe*, 3-PGA is not converted to PEP.

Although the addition of 10 mM pyruvate had no significant effect on dark $^{14}CO_2$ fixation in both species, pyruvate stimulated light $^{14}CO_2$

Table 3.6 Effect of DCMU and PEP on light $^{14}CO_2$ fixation[a] by isolated *Kalanchoe* and *Stapelia* mesophyll cells.

Treatment	*Kalanchoe*		*Stapelia*	
	(μmoles mg chl^{-1} hr^{-1})			
None	56		58	
+ DCMU [5 mM]	5	51	10	48
+ PEP [10 mM]	95	90	110	100
+ DCMU + PEP	28		37	

a Rate observed over 20 minutes linear $^{14}CO_2$ fixation, duplicate samples for each time point

Table 3.7 The effect of the addition of 5 mM 3-PGA on $^{14}CO_2$ fixation by isolated *Kalanchoe* and *Stapelia* mesophyll cells.

Treatment	Light		Dark	
	Kalanchoe	*Stapelia*	*Kalanchoe*	*Stapelia*
	(μmoles mg chl^{-1} hr^{-1})			
None	30	61	2	9
3-PGA [5 mM]	31	-	8	23
PEP [10 mM]	63	111	19	26

fixation by up to 50% in *Kalanchoe* but had no effect on light fixation in *Stapelia* (Table 3.8). This is consistent with the hypothesis that if gluconeogenesis occurs in malic enzyme plants such as *Kalanchoe*, pyruvate must be converted to PEP.

3.4 Discussion

Isolated *Kalanchoe* and *Stapelia* mesophyll cells appear to be intact as judged by a number of criteria. They actively exclude Evans Blue, O_2 evolution is not stimulated by 1 mM ferricyanide, and more than 97% of the products of 40 minutes $^{14}CO_2$ fixation remain in the cells. Although the cells exclude Evans Blue, they appear to be more permeable to exogenous substrates than leaf slices (cf. Section 2.3, Lüttge and Ball, 1977). This is unlikely to be due to a leaky plasmalemma since, as already stated, there is no significant leakage of labelled products of $^{14}CO_2$ fixation into the bathing medium even after 40 minutes. It is probable that this is due to the reduced diffusive resistance present in cell suspensions as compared to leaf slice suspensions. The higher pyruvate concentrations used in the cell experiments may also facilitate pyruvate uptake. This is supported by the observation that in cell and leaf slice suspensions the rates of incorporation of $^{14}CO_2$, which rapidly diffuses into both cells and leaf slices, are similar.

Confirmation of the integrity of the light reactions, the PCR cycle and of the dark carbon fixing pathway is provided by a number of observations. Firstly, 4 µM DCMU inhibited O_2 evolution and basal $^{14}CO_2$ fixation but does not affect PEP stimulated $^{14}CO_2$ fixation; secondly, the ratio of O_2 evolution to DCMU sensitive $^{14}CO_2$ incorporation

Table 3.8 The effect of the addition 10 mM pyruvate on $^{14}CO_2$ fixation by isolated *Kalanchoe* and *Stapelia* mesophyll cells.

Treatment		Light		Dark	
		Kalanchoe	*Stapelia*	*Kalanchoe*	*Stapelia*
		(μmoles mg chl^{-1} hr^{-1})			
Expt 1	None	18	49	-	-
	Pyruvate [10 mM]	23	44	-	-
Expt 2	None	30	61	2	9
	Pyruvate [10 mM]	44	63	4	9
	PEP [10 mM]	63	111	19	26

is close to unity, and thirdly, the distribution of products of light and dark $^{14}CO_2$ fixation are similar to those observed in deacidified leaf slices and in deacidified intact tissue (Kluge, 1969c;Osmond and Allaway, 1974).

Both in the light and in the dark, $^{14}CO_2$ fixation by PEP carboxylase is limited by the PEP supply. As exogenous PEP causes a greater stimulation of light $^{14}CO_2$ fixation than observed in the dark it seems probable that one or more other components may limit dark fixation. PEP carboxylase activity, for example, may be subject to end product inhibition by malate if the external osmotic pressures are not condusive to vacuolar malate uptake, or OAA reduction may be limited by the supply of NADH. Nonetheless, the PEP stimulated dark fixation rate in both species is higher than that needed to account for the rates of acidification measured in intact tissue.

Gas exchange and $^{14}CO_2$ labelling studies with deacidified intact tissue in the light have shown that CO_2 is fixed principally via RuP_2 carboxylase (Kluge, 1969b;Osmond and Allaway, 1974). In the present experiments it is evident that PEP carboxylase was also active in cells of deacidified tissue if PEP was provided. Because no significant labelling of the C_4 acids was observed in the $^{14}CO_2$ fixation experiments, one must conclude that the supply of PEP was limiting. This conclusion is supported by the observation that although 3-PGA stimulates dark $^{14}CO_2$ fixation in both *Kalanchoe* and in *Stapelia*, in *Kalanchoe* 3-PGA has no effect on light $^{14}CO_2$ fixation even though 10 mM PEP doubles the fixation rate. Presumably 3-PGA is not converted to PEP.

In contrast, 10 mM pyruvate stimulates light fixation in *Kalanchoe* by up to 50% but does not affect light fixation in *Stapelia* or dark fixation in either species. Since *Kalanchoe* possesses pyruvate, Pi dikinase and *Stapelia* is deficient in this enzyme (Section 4.1), and as the enzyme is known to be light activated, it is quite possible that the light stimulated $^{14}CO_2$ fixation in *Kalanchoe* is due to the conversion of pyruvate to PEP which acts as a substrate for PEP carboxylase.

Rouhani *et al.* (1973) reported an 8 fold increase in $^{14}CO_2$ fixation in cells which had been supplied both pyruvate (3 mM) and ATP (1 mM), although the addition of each compound separately caused no stimulation. Presumably this is the same phenomena as that observed in *Kalanchoe* cells with the exception that the *Sedum* cells used in the above study were not as intact as the cells used in these experiments and required ATP.

Both the pyruvate and 3-PGA data presented in this section support the gluconeogenic hypothesis (proposed in Section 1.4 and tested in Section 2.3) that pyruvate is converted to PEP *in vivo* in *Kalanchoe* and that, for some reason, 3-PGA is not. The latter observation suggests that the reverse reaction namely PEP → 3-PGA is favoured in the light. The conversion of 3-PGA to starch in the light is well documented in plant tissues (cf. Hatch, 1976).

4 THE CAPACITY OF CAM PLANTS TO SYNTHESISE CARBOHYDRATES FROM MALATE IN THE LIGHT

4.1 The Activity of Enzymes Involved in the Production and Metabolism of Pyruvate and PEP

4.1.1 Introduction

Until the early 1970's information on the activities of the enzymes involved in CAM was, at best, fragmentary. Recently a number of authors have studied the activities of PEP and RuP_2 carboxylases, PEPCK, NAD and NADP malic enzymes, pyruvate, Pi dikinase, alanine and aspartate aminotransferases, and various glycolytic and pentose phosphate pathway enzymes in a range of species (Kluge and Osmond, 1971, 1972; Morel and *et al.*, 1972; Dittrich *et al.*, 1973; Sutton, 1974; Sugiyama and Laetsch, 1975; Dittrich, 1976; Herbert *et al.*, 1979, Pierre and Queiroz, 1979; Spalding *et al.*, 1979). With the exception of *K. blossfeldiana*, which has been extensively studied by Queiroz and co-workers, and *K. daigremontiana* which has been studied in a number of different laboratories, the information on enzyme activities has been spread thinly over a number of species.

In this section the activity of 9 enzymes involved in acidification, deacidification, and pyruvate metabolism in 4 malic enzyme and 3 PEPCK CAM plants are described and compared with the observed *in vivo* rates of acidification, deacidification and pyruvate utilisation. These observations are discussed in relation to the ^{14}C-pyruvate and $^{14}CO_2$ labelling data reported in Chapters 2 and 3, and in relation to the capacities of CAM plants to perform gluconeogenesis.

4.1.2 Materials and methods

4.1.2.1 *Extraction methods*

Plants were grown as described in Section 2.1.2.1. Deacidified tissue was weighed, and illuminated for 30 minutes under 1200 μE m^{-2} s^{-1} before extraction. The tissue to volume ratio of the extraction media was between 5 and 10 for most tissues. In *Opuntia inermis* this ratio was reduced to 30 and only young pads were used in an unsuccessful attempt to avoid problems with mucilage in the extracts.

All extractions were performed at 0-4°C in the presence of acid-washed sand in a mortar and pestle. In the case of pyruvate, Pi dikinase, although the extraction was carried out at 0-4°C, all subsequent operations were performed at room temperature.

The extraction procedures were as follows:

PEP carboxylase and NAD malate dehydrogenase were extracted in a buffer containing 50 mM Bicine-NaOH, 50 mM HEPES-NaOH, pH 8.0, 2 mM $MgCl_2$, 5 mM DTT, and 1% (w/v) PVP 40. The brei was filtered through two layers of Miracloth and an aliquot was taken for chlorophyll determination. The remaining extract was centrifuged for 10 minutes at 12,000 x g. The supernatant was either directly assayed for enzyme activity or was passed through a column (0.5 cm x 15 cm) of G-25 Sephadex previously equilibrated with a buffer composed of 25 mM Bicine-NaOH, 25 mM HEPES-NaOH, pH 8.0, 1 mM $MgCl_2$ and 1 mM DTT.

NADP malate dehydrogenase and NADP malic enzyme were extracted in a buffer containing 100 mM HEPES-NaOH, pH 7.5, 2 mM $MgCl_2$, 2 mM EDTA, 10 mM DTT, and 1% (w/v) PVP 40. After filtration and centrifugation the extract

was passed through a column (0.5 cm x 15 cm) of G-25 Sephadex previously equilibrated with 50 mM HEPES-NaOH pH 7.5, 2.5 mM DTT, and 2.5 mM EDTA.

PEP carboxykinase and pyruvate, Pi dikinase were extracted in a medium containing 100 mM HEPES-NaOH pH 7.5, 10 mM $MgCl_2$, 10 mM $MnCl_2$, 1 mM EDTA, 5 mM DTT, 2.5 mM pyruvate, 2 mM K_2HPO_4, 0.5% (w/v) ascorbate, 0.5% (w/v) BSA, and 1% (w/v) PVP 40. The brei was filtered through Miracloth and spun at room temperature at 4000 x g for 10 minutes. The supernatant was divided into two fractions, one which was kept at 0°C and used for PEPCK determinations and the other which was kept at room temperature and used for pyruvate, Pi dikinase determinations. Depending on the particular experiment, the fractions were either subjected to gel filtration through G-25 Sephadex or to $(NH_4)_2\ SO_4$ fractionation.

The fraction to be tested for PEPCK activity was passed through a G-25 Sephadex column equilibrated with 25 mM HEPES-NaOH pH 7.5, 5 mM $MgCl_2$, 5 mM $MnCl_2$ and 1 mM DTT. The dikinase fraction was passed through a column equilibrated with 25 mM HEPES-NaOH pH 7.5, 5 mM $MgCl_2$ and 1 mM DTT. Both enzymes were present in the protein fraction which precipitated out between 30-60% $(NH_4)_2SO_4$ saturation. The PEPCK fraction was desalted by passing the resuspended precipitate through a G-25 Sephadex column equilibrated as described above. The pyruvate, Pi dikinase fraction was resuspended in the buffer used to equilibrate the Sephadex column described above but was not desalted, as desalting caused a reduction in activity of about 10-20%.

Alanine and aspartate aminotransferases were extracted in a buffer containing 100 mM HEPES-NaOH, pH 7.5, 10 mM DTT, 8 µM pyridoxal phosphate, 1 mM DTT, and 1% (w/v) PVP 40. After filtration and centrifugation the supernatant was passed through a column (0.5 cm x 15 cm) of G-25 Sephadex equilibrated with 25 mM HEPES-NaOH pH 7.5, 2 mM DTT and 4 µM pyridoxal phosphate.

4.1.2.2 *Enzyme assays*

With the exception of PEPCK which was measured either using a radioisotopic method or by following the extinction of OAA at 280 nm, all enzymes were measured at room temperature (21°C) by following the change in absorbance of a pyridine nucleotide at 340 nm, in a 3 ml reaction mix, using either a Varian Series 634 or a Perkin Elmer 124 double beam spectrophotometer.

The enzymes were assayed in the following reaction mixtures. The given concentrations are the final concentrations in the cuvette and in each case the last listed compound was added to initiate the reaction.

PEP carboxylase - (Orthophosphate: oxaloacetate carboxy-lyase (phosphorylating), E.C. 4.1.1.31) (modified from Kluge and Osmond, 1972) 25 mM Bicine-NaOH, 25 mM HEPES-NaOH pH 8.0, 10 mM $KHCO_3$, 2 mM $MgCl_2$, 0.2 mM NADH, 6 units MDH, 1 mM G-6-P, 100 µl extract, and 3 mM PEP. ✓

NAD malate dehydrogenase (L-malate: NAD oxidoreductase, E.C. 1.1.1.37) (modified from Kluge and Osmond, 1972) 25 mM Bicine-NaOH, 25 mM HEPES-NaOH, pH 8.0, 2 mM $MgCl_2$, 0.2 mM NADH, 25 µl extract, and 2 mM OAA.

NADP malate dehydrogenase (modified from Johnson and Hatch, 1970) 25 mM Bicine-NaOH, 25 mM-NaOH pH 8.0, 1 mM EDTA, 0.2 NADPH, 100 µl extract, and 1 mM OAA.

NADP malic enzyme (L-malate: NADP oxidoreductase (decarboxylating), E.C. 1.1.1.40) (modified from Garnier-Dardart and Queiroz, 1974) 50 mM HEPES-NaOH, pH 7.5, 3 mM $MgCl_2$, 0.25 mM NADP, 100 µl extract, and 3 mM malate.

PEP carboxykinase (ATP: oxaloacetate carboxy-lyase (transphosphorylating), E.C. 4.1.1.32) Spectrophotometric assay: (modified from Hatch, 1973) 50 mM HEPES-NaOH, pH 7.5, 2.5 mM $MgCl_2$, 2.5 mM $MnCl_2$, 6 units pyruvate kinase, 100 µl extract, 1 mM OAA and 0.2 mM ATP. The OAA stock solution was made daily according to the procedure of Hatch (1973). The extinction co-efficient for OAA was also determined daily and varied with pH, $MgCl_2$ and $MnCl_2$ concentrations.

Exchange reaction: (modified from Mazelis and Vennesland, 1957) The assays were performed in scintillation vials and the total volume of the reaction mix as 1 ml. The reaction mix contained 50 mM HEPES-NaOH, pH 7.5, 1 mM $MgCl_2$, 1 mM $MnCl_2$, 0.2 mM ATP, 10 mM $NaH^{14}CO_3$, 100 µl extract and 1 mM OAA. Blank samples without ATP were measured to assess ATP independent incorporation of ^{14}C. After various intervals the reaction was killed with 0.2 ml of 20% (w/v) trichloroacetic acid and

bubbled with CO_2 for 5 minutes before 9 ml scintillation fluor (consisting of a 2:1 ratio of 5 g l^{-1} toluene and Teric x 100) was added. The acid stable radioactivity was counted in a scintillation counter.

Pyruvate, Pi dikinase (ATP: pyruvate, orthophosphate phosphotransferase, E.C. 2.7.9.1) (modifed from Sugiyama and Laetsch, 1975) 50 mM HEPES-NaOH, pH 8.0, 10 mM $MgCl_2$, 0.1 mM EDTA, 50 mM $KHCO_3$, 0.2 mM NADH, 2 units PEP carboxylase, 3 units MDH, 100 µl extract, 2.5 mM pyruvate, 1.25 mM ATP, and 2.5 mM K_2HPO_4.

Aspartate aminotransferase (L-Aspartate: 2-oxoglutarate aminotransferase E.C. 2.6.1.1)(modified from Hatch and Mau, 1973) 25 mM HEPES-NaOH, 25 mM MES-NaOH, pH 7.5, 12 µM pyridoxal phosphate, 2.5 mM α-ketoglutarate, 2 mM EDTA, 0.2 mM NADH, 6 units MDH, 100 µl extract and 2.5 mM L-aspartat

Alanine aminotransferase (L-Alanine: 2-oxoglutarate aminotransferase E.C. 2.6.1.2) (modified from Hatch and Mau, 1973) 25 mM HEPES-NaOH, 25 mM MES-NaOH, pH 6.5, 12 µM pyridoxal phosphate, 2. 5 mM α-keto-glutarate, 2 mM EDTA, 0.2 NADH, 6 units LDH, 100 µl extract, and 10 mM alanine.

4.1.2.3 *Chlorophyll estimation*

Chlorophyll content was estimated using the method of Arnon (1949) as described in Chapter 2.1.2.4.

4.1.2.4 *Aspartate estimation*

At various times during the day/night cycle, 2 leaves from different plants within the same population were harvested, quickly weighed, and extracted in 100 ml of boiling 80% EtOH and then in 50 ml of boiling H_2O, The extracts were pooled, filtered through glass wool, and spun at 12,000 x g

for 10 minutes at 0-4°C. Aspartate and other amino acids were removed from the supernatant on a cation column equilibrated as described in Section 2.2.2.2. The effluent was frozen and later assayed for malate content as described in Section 2.1.2.3 using the method of Hohorst (1963). The amino acids were eluted from the column with 10% (v/v) NH_4OH and evaporated to dryness. Preliminary tests with authentic aspartic acid showed that 2-5% of the aspartic acid was lost during this step. The amino acids were then resuspended in 5 ml of 100 mM HEPES-NaOH, pH 7.5 and the aspartate content was determined spectrophotometrically by following the change of absorbance at 340 nm in the assay mixture which consisted of 100 mM HEPES-NaOH pH 8.0, 12 µM pyridoxal phosphate, 2.5 mM α-ketoglutarate, 2 mM $MgCl_2$, 0.2 mM NADH, 6 units aspartate aminotransferase, 12 units MDH and 0.2 ml extract. Due to the reversability of the aminotransferase reaction, the reaction did not quite reach end point. However, preliminary experiments showed that after 45 minutes about 90% of the aspartate was converted to malate plus glutamate.

4.1.2.5 *3-mercaptopicolinic acid (3-MPA) feeding experiments*

Leaf slices of acidified *Kalanchoe* and *Aloe* were prepared as described in Chapter 2.1.2.2. The slices were illuminated for 10 minutes prior to the addition of 3-MPA. After various time periods the tissue was killed and the malate was extracted and determined as described in Chapter 2.1.2.3.

4.1.3 Results

4.1.3.1 *Enzymes involved in dark acidification*

In all species the activities of PEP carboxylase and NAD malate dehydrogenase were far in excess of those required to account for the maximum rates of acidification observed in intact tissues (Table 4.1).

Table 4.1 A comparison of the activities of various enzymes involved in acidification and deacidification, and the rates of acidification and deacidification, in seven species of CAM plants.

	Kalanchoe daigremontiana	*Bryophyllum pinnatum*	*Bryophyllum tubiflorum*	*Opuntia inermis*	*Aloe arborescens*	*Hoya carnosa*	*Stapelia gigantea*
				µmoles mg chl^{-1} min^{-1}			
Enzymes Involved in Acidification							
PEP carboxylase	8.1	7.3	5.3	3.0	17.4	10.7	9.3
NAD malate dehydrogenase	116	146	159	327	117	158	212
Maximum rate of acidification[a]	0.4	0.5	0.4	0.3[b]	0.6	0.3	0.6
Enzymes Involved in Deacidification							
NADP malic enzyme	2.4	1.1	1.2	9.5	1.1	0.3	1.5
NAD malic enzyme[c]	2.7	-	-	-	-	0.1	-
PEP carboxykinase	-[d]	-	-	ND	3.0	4.7	6.5
Pyruvate, Pi dikinase	1.1	0.9	0.5[e]	ND[f]	-	-	-
RuP_2 carboxylase[g]			2.2	ND	2.2	2.7	1.3
Maximum rate of deacidification[a]	0.5	0.6	0.6	0.7[b]	1.9	0.6	1.3
Other Enzymes							
NADP malate dehydrogenase	2.5	0.6	0.8	ND	3.0	1.5	1.8
Alanine aminotransferase	1.3	5.1	1.7	ND	4.4	2.2	1.7
Aspartate aminotransferase	5.0	3.5	3.3	ND	1.4	2.3	1.9

a µmoles mg chl^{-1} min^{-1}

b From Osmond *et al* (1979)

c From Dittrich (1976)

d - not detected

e Some activity lost since $(NH_4)_2SO_4$ protein did not form a proper pellet

f ND not determined

g From Dittrich *et al* (1973)

4.1.3.2 *Enzymes involved in deacidification*

NADP malic enzyme: The activity of NADP malic enzyme at one pH value is a function of the malate, Mg^{2+} and NADP concentrations (Garnier-Dardart and Queiroz, 1974). Under the conditions used in this study the enzyme had a pH optimum of about 7.2 (Figure 4.1). At the pH optimum *Kalanchoe daigremontiana, Bryophyllum pinnatum, Bryophyllum tubiflorum* and *Opuntia inermis* all had at least twice the activity required for maximum deacidification (Table 4.1). *Stapelia gigantea* had just sufficient activity, whilst the activities in *Aloe arborescens* and *Hoya carnosa* were well below those required.

PEP carboxykinase: Initial attempts to measure PEPCK using the exchange reaction, first used by Vennesland *et al.* (1947), resulted in rates well below those reported by Dittrich *et al.* (1973) for the same species of plants, and well below those measured using the spectrophotometric method developed by Hatch (1973). The problem was traced to non-enzymatic decarboxylation of OAA by both $MnCl_2$ and $MgCl_2$ (Figure 4.2). Although previous workers studying PEPCK in CAM plants have used 10 mM $MgCl_2$ and 10 mM $MnCl_2$ in their assay media (Dittrich *et al.* 1973), Figures 4.2 and 4.3 show that maximum activity is attained with about 0.25-0.5 mM $MgCl_2$ and $MnCl_2$. When low $MgCl_2$ and $MnCl_2$ assay concentrations are used (1-2 mM) the rates measured for the exchange reaction approach those measured by the spectrophotometric assay (Table 4.2). PEPCK lost about 30-40% activity during desalting but the activity appeared to increase by about 10% during $(NH_4)_2SO_4$ fractionation. The pH optimum for both the exchange and spectrophotometric assays was between 7.0 and 8.0 (Figure 4.4 which, although similar, is broader than that reported for the partially purified enzyme from *Ananas comosus* (pineapple)(Daley *et al.*, 1976).

Figure 4.1 Activity of NADP malic enzyme, isolated from *Kalanchoe daigremontiana*, as a function of pH.

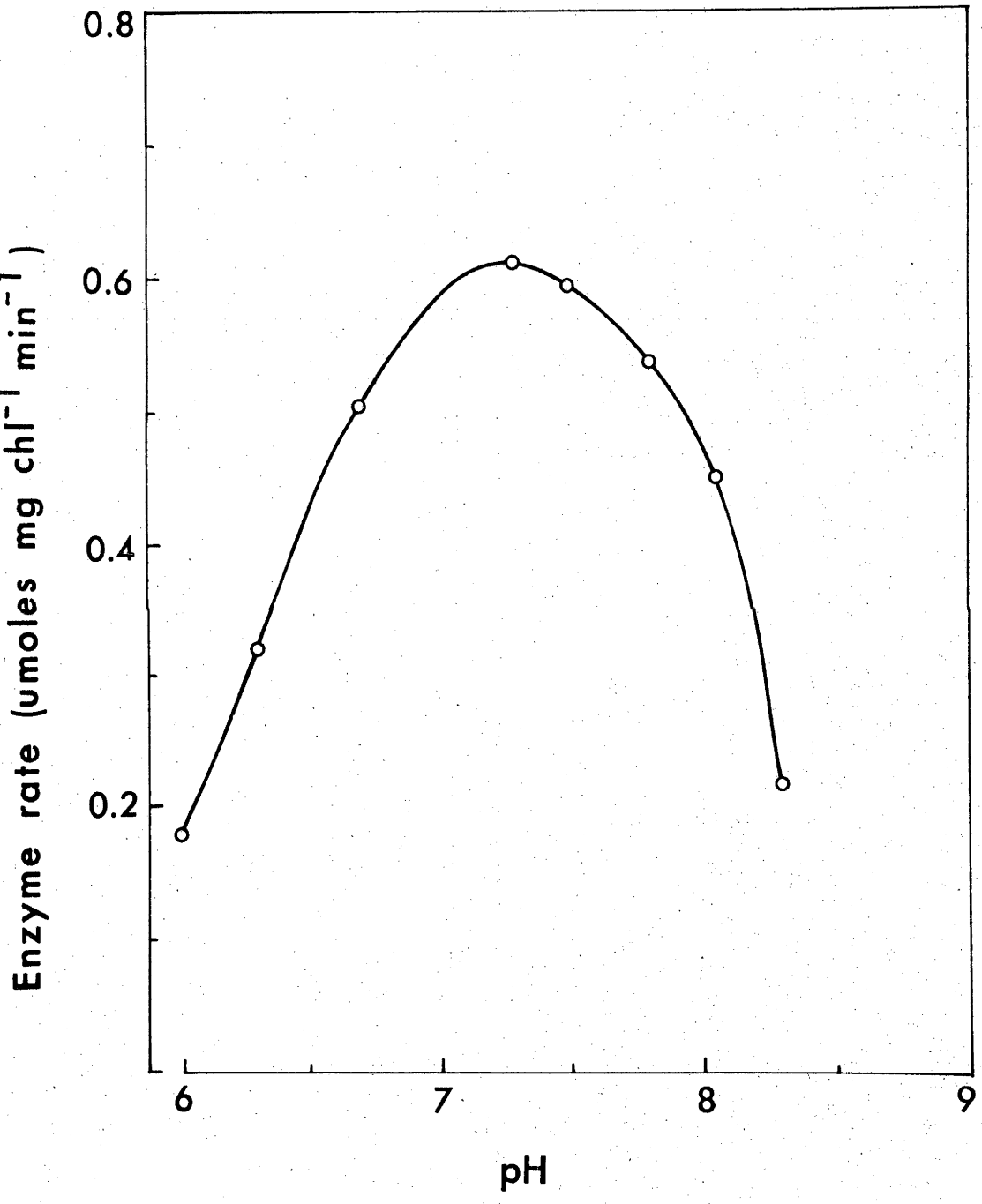
0.8
0.6
0.4
0.2
Enzyme rate (umoles mg chl^{-1} min^{-1})
6
7
8
9
pH

Figure 4.2 Non-enzymatic decarboxylation of 4-^{14}C-OAA in the presence of varying concentrations of $MgCl_2$ and/or $MnCl_2$.

A. Decarboxylation in the presence of 2 mM $MgCl_2$ (● —— ●), 5 mM $MgCl_2$ (o —— o) and 10 mM $MgCl_2$ (□——□).

B. Decarboxylation in the presence of 2 mM $MnCl_2$ (● —— ●), 5 mM $MnCl_2$ (o —— o) and 10 mM $MnCl_2$ (□——□).

C. Decarboxylation in the presence of 0 mM $MgCl_2$ plus 0 mM $MnCl_2$ (Δ--- Δ), 2 mM $MgCl_2$ plus 2 mM $MnCl_2$ (● —— ●), 5 mM $MgCl_2$ plus 5 mM $MnCl_2$ (o —— o), and 10 mM $MgCl_2$ plus 10 mM $MnCl_2$ (□——□).

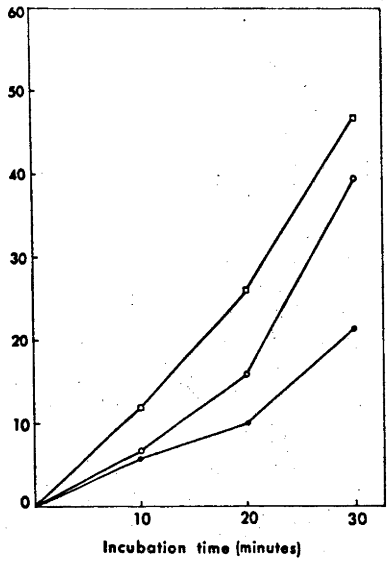
60
50
40
30
20
10
0
10
20
30
Incubation time (minutes)

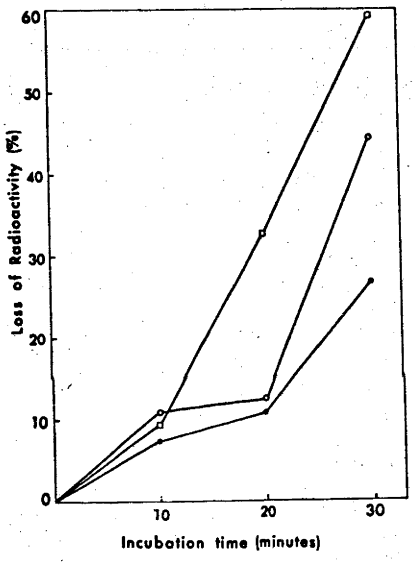
Loss of Radioactivity (%)
60
50
40
30
20
10
0
10
20
30
Incubation time (minutes)

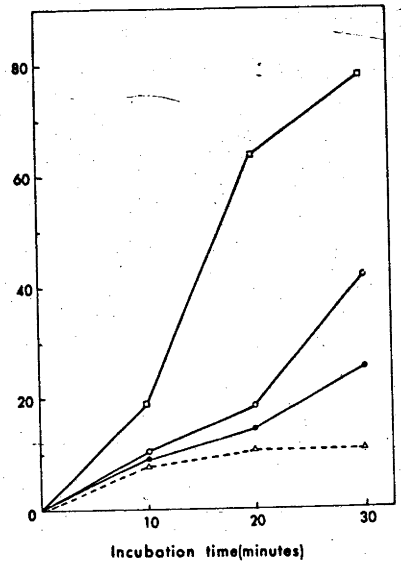
80
60
40
20
0
10
20
30
Incubation time(minutes)

Figure 4.3 Incorporation of ^{14}C from $NaH^{14}CO_3$ into ^{14}C-OAA via the PEPCK exchange reaction. All points are for 2 minute assays.

A. The effect of $MgCl_2$ in the absence of $MnCl_2$, on the rate of ^{14}C exchange. Assay without ATP (o —— o), with ATP (● —— ●).

B. The effect of $MnCl_2$, in the absence of $MgCl_2$, on the rate of ^{14}C exchange. Assay without ATP (o —— o), with ATP (● —— ●).

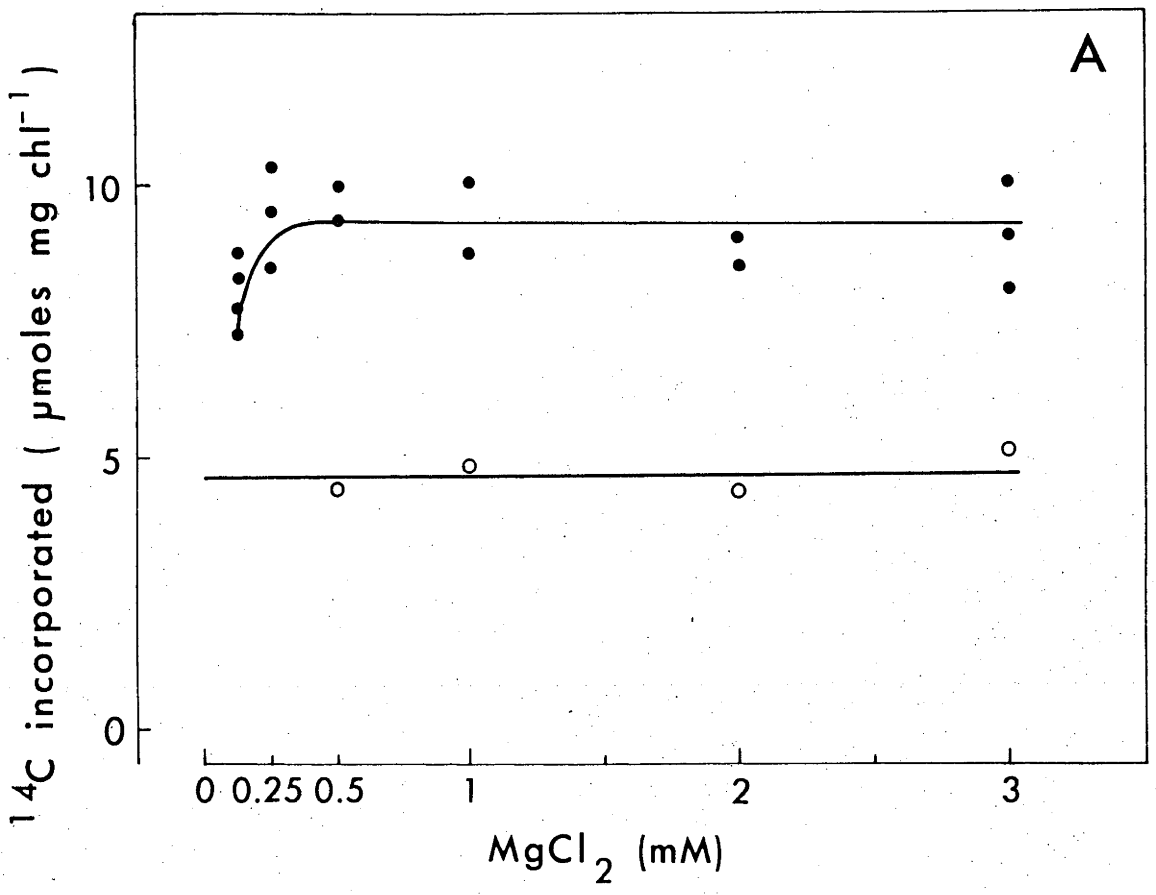
A
^{14}C incorporated (μmoles mg chl^{-1})
10
5
0
0 0.25 0.5 1 2 3
$MgCl_2$ (mM)

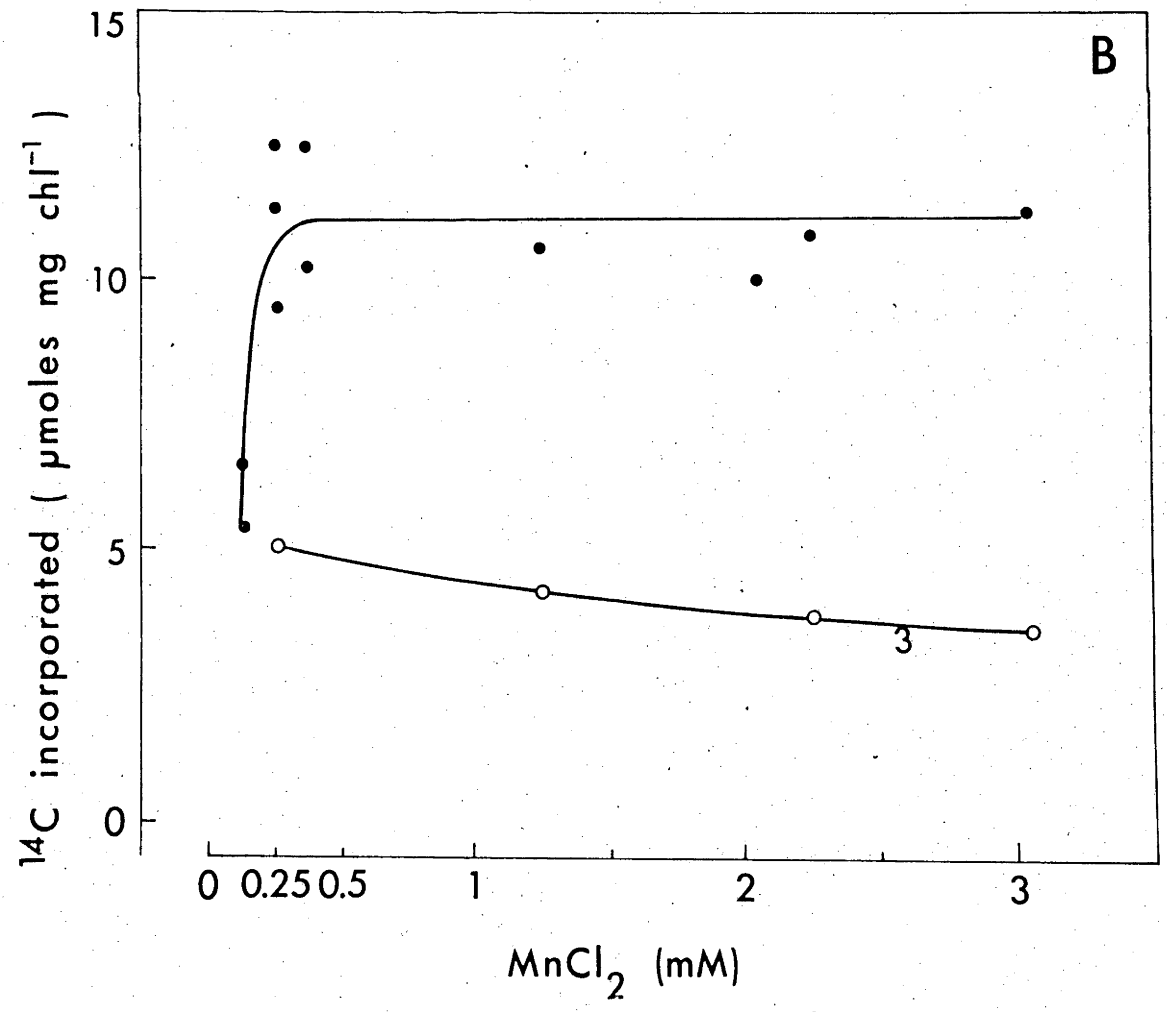
B
^{14}C incorporated (μmoles mg chl^{-1})
15
10
5
0
3
0 0.25 0.5 1 2 3
$MnCl_2$ (mM)

Table 4.2 PEP carboxykinase activity from two species of CAM plant measured using an isotopic and a spectrophotometric method.

Treatment	*Aloe arborescens*		*Bryophyllum pinnatum*	
	Exchange reaction	Spectro. assay	Exchange reaction	Spectro. assay
	µmoles mg chl^{-1} hr^{-1} [a]			
Crude extract	126	145	-[b]	-
Sephadexed extract	80	ND[c]	-	ND
$(NH_4)_2SO_4$ fractionation				
0- 30% fraction	-	-	-	-
30- 60% fraction	142	160	-	< 1
30-100% fraction	-	< 5	-	-

a µmoles ^{14}C incorporated in the case of the exchange reaction, and µmoles OAA metabolised in the case of the spectrophotometric assay

b not detected

c ND-not determined

Figure 4.4 The activity of PEPCK, isolated from *Aloe arborescens*, as a function of pH. Activity was measured using the exchange reaction (●) or by spectrophotometrically following the metabolism of OAA (o).

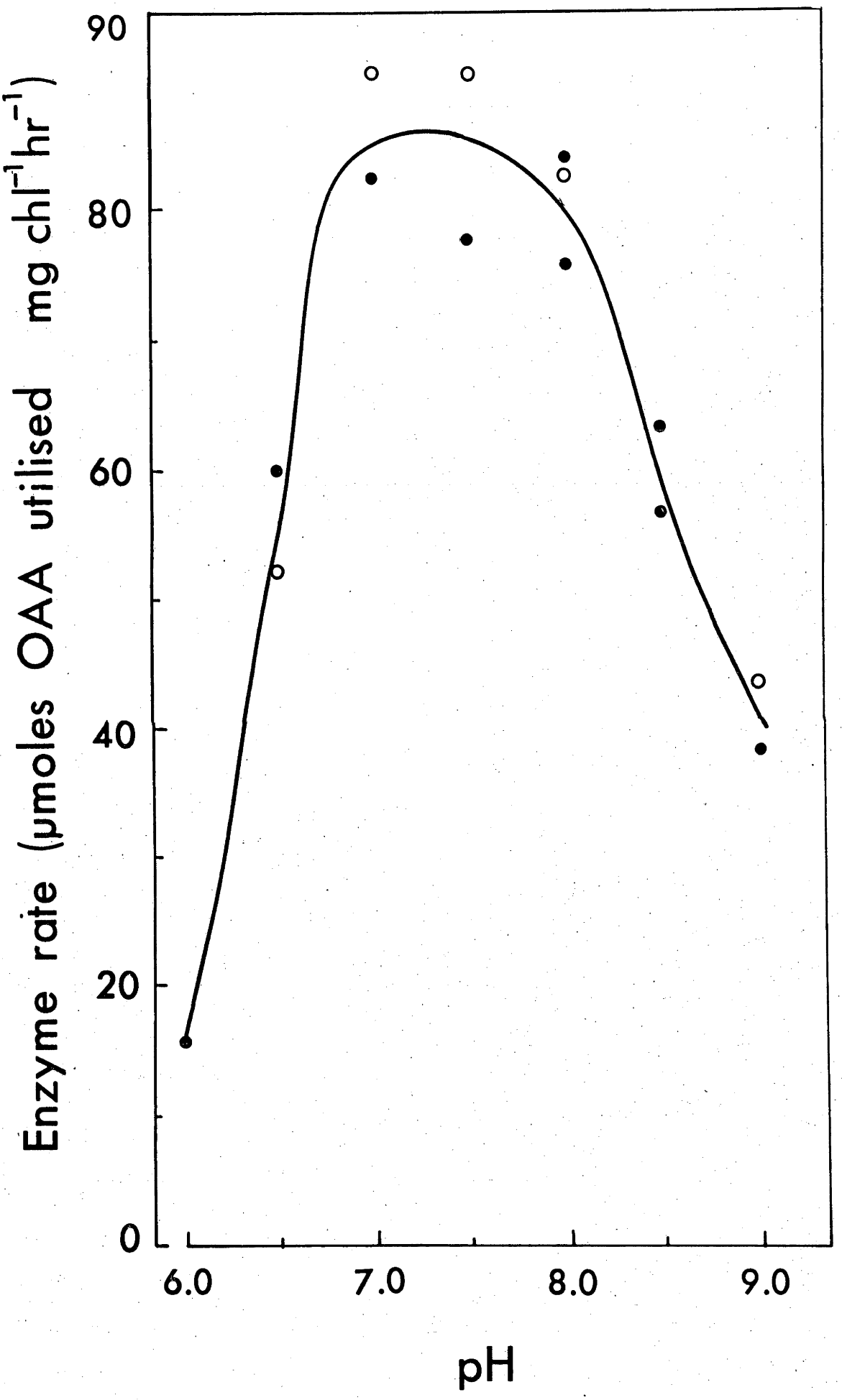
Enzyme rate (μmoles OAA utilised mg chl^{-1}hr^{-1})
90
80
60
40
20
0
6.0
7.0
8.0
9.0
pH

It was important to add BSA to the extraction medium and to perform the PEPCK measurements as rapidly as possible because activity declined rapidly after isolation. Daley *et al.* (1976) have observed that PEPCK from *Ananas* is attacked by a protease.

Pyruvate, Pi Dikinase: Pyruvate,Pi dikinase was present in the three malic enzyme plants *K. daigremontiana, B. pinnatum* and *B. tubiflorum*, but was not present in *Aloe, Hoya* and *Stapelia*, the three PEPCK species studied (Table 4.1). Although the dikinase activities were low they were sufficient to account for the maximum observed rates of deacidification. Furthermore, the estimates of dikinase capacity are minimum estimates since they represent rates measured in 30-60% $(NH_4)SO_4$ fractions and almost certainly some of the enzyme was lost during fractionation. Fractionation was necessary to concentrate the enzyme since the rates in the crude extracts were very low.

The enzyme had a pH optimum of about 7.7 (Figure 4.5). The rates were proportional to the amount of enzyme added (Figure 4.6), and were also Pi dependent (Figure 4.7). The basal Pi independent rate, shown in Figure 4.7, is possibly due to LDH activity. The stimulation of dikinase activity in $(NH_4)_2SO_4$ fractions is probably due to activation by ammonium ions, a phenomena which has also been reported for the maize leaf and bacterial enzymes (Reeves *et al.*, 1961; Evans and Wood, 1971; Sugiyama, 1973).

4.1.3.3 *Other enzymes*

NADP malate dehydrogenase: In contrast with the enzyme from C_4 plants which possess a single pH optimum around pH 8.5 (Johnson and Hatch, 1970), the NADP malate dehydrogenase from *Kalanchoe* exhibited two

Figure 4.5 The activity of pyruvate, Pi dikinase isolated from *Kalanchoe daigremontiana*, as a function of pH.

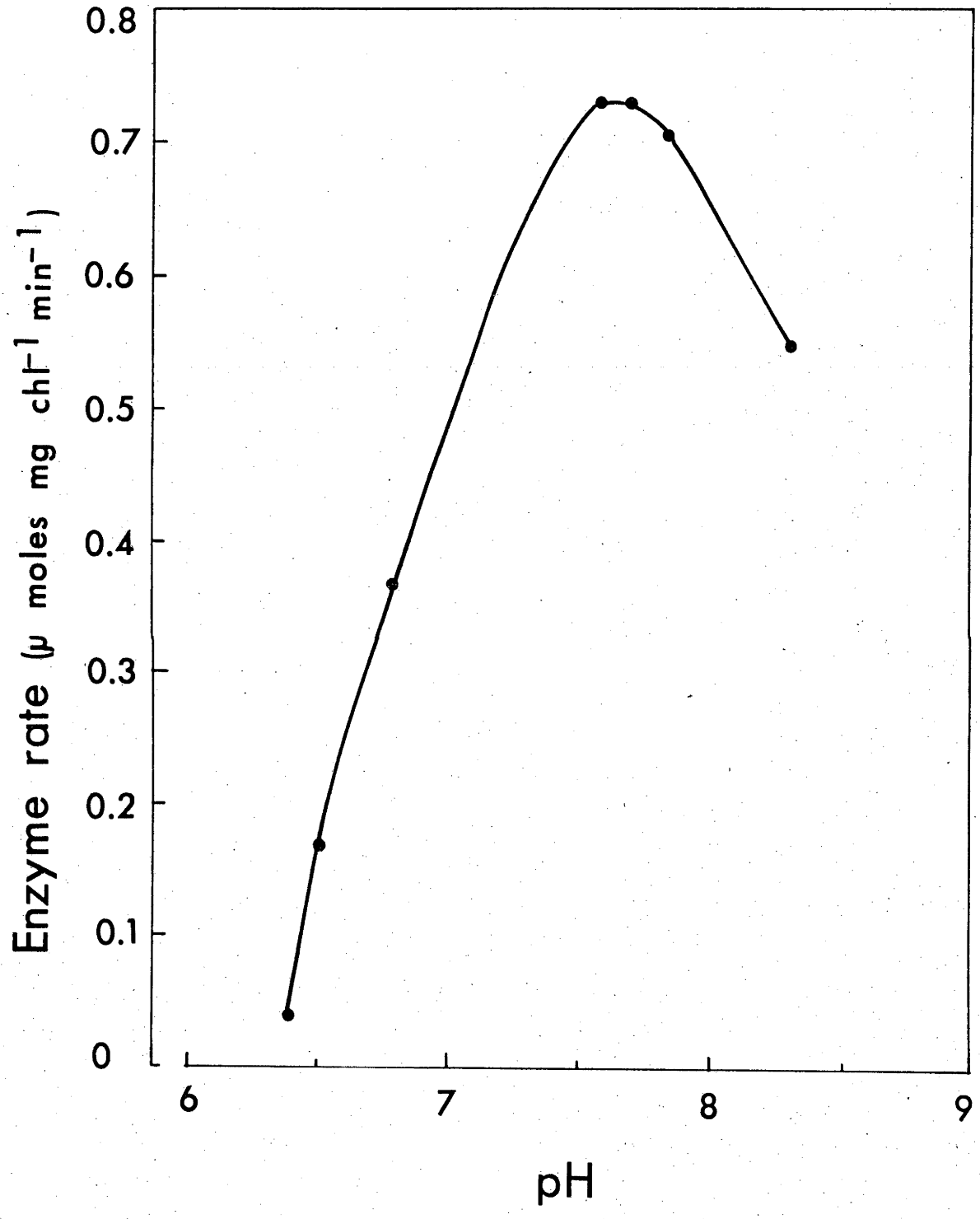
0.8
0.7
0.6
0.5
0.4
0.3
0.2
0.1
0
Enzyme rate (μ moles mg chl^{-1} min^{-1})
6
7
8
9
pH

Figure 4.6 Pyruvate, Pi dikinase activity as a function of the amount of enzyme in the assay.

Figure 4.7 The dependence of pyruvate, Pi dikinase activity on K_2HPO_4 (2.5 mM).

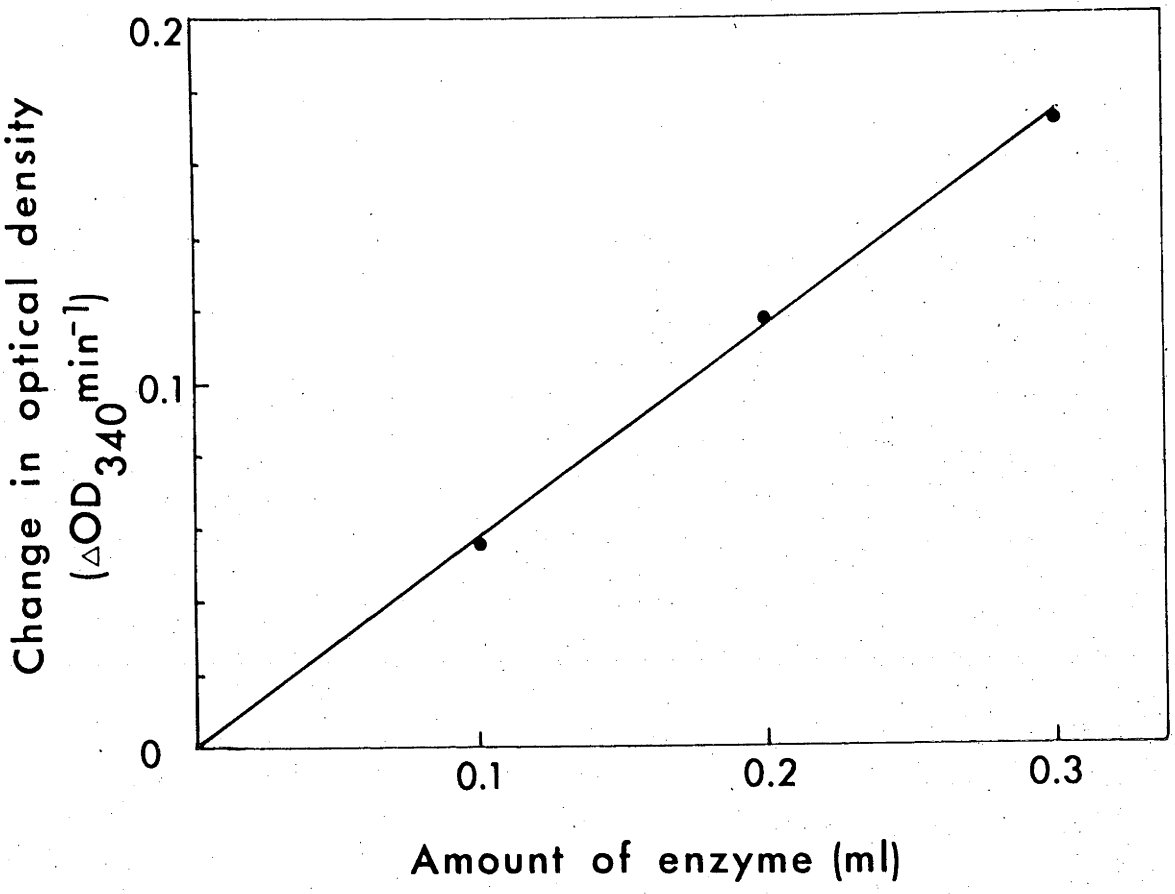
Change in optical density
($\Delta OD_{340} min^{-1}$)
0.2
0.1
0
0.1
0.2
0.3
Amount of enzyme (ml)

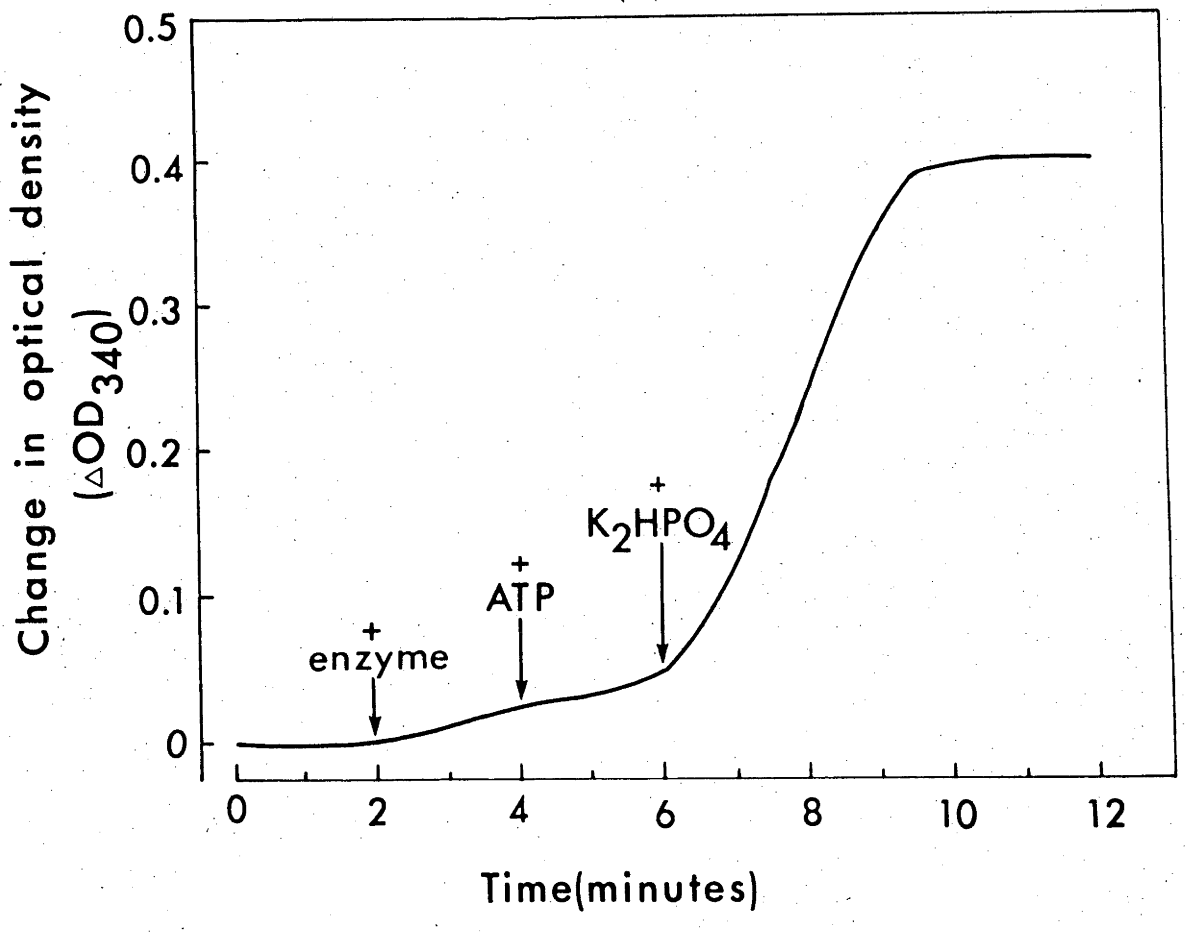
Change in optical density
(ΔOD_{340})
0.5
0.4
0.3
0.2
0.1
0
+ enzyme
+ ATP
+ K_2HPO_4
0
2
4
6
8
10
12
Time(minutes)

pH optima, one at pH 6.0 and the other at pH 8.0 (Figure 4.8). The activities of the enzyme at the two optima were similar.

Alanine and aspartate aminotransferase: Alanine and aspartate aminotransferase had broad pH optima around pH 6.5 and pH 7.0-8.0, respectively (Figures 4.9 and 4.10). There is no correlation between the possession of high aminotransferase activity and the possession of PEPCK (Table 4.1) as has been observed in C_4 plants (Guttierez *et al.*, 1974; Hatch *et al.*, 1975).

Aspartate is the major C_4 acid found in C_4 plants which possess high aspartate aminotransferase activities and either high PEPCK or high NAD malic enzyme activities, however, Figure 4.11 shows that in *Kalanchoe*, a malic enzyme CAM plant, and in *Hoya*, a PEPCK CAM plant, malate not aspartate was the major storage acid during the dark period. This, of course, does not rule out the possibility that aspartate is an intermediate in the CO_2 fixing metabolism but if it is then it is rapidly converted to malate. $^{14}CO_2$ labelling patterns which indicate this sort of exchange have been observed by Winter *et al.* (1974) in CAM *M. crystallinum*.

4.1.3.4 *Inhibition of deacidification by 3-mercaptopicolinic acid (3-MPA)*

3-MPA has been shown to be a potent specific inhibitor, both *in vitro* and *in vivo*, of PEPCK from animals and C_4 plants (DiTullio *et al.*, 1974; Robinson and Oei, 1975; Jomain-Baum *et al.*, 1976; Ray and Black, 1976b, 1977). Ray and Black (1977) have shown that both NAD and NADP malic enzyme from C_4 plants are insensitive to up to 2 mM 3-MPA.

In the present study 3-MPA was fed in the light to deacidifying leaf slices of *Kalanchoe daigremontiana*, which possesses both NAD and NADP malic enzyme, and *Aloe arborescens*, which possesses high PEPCK activity but low NAD

Figure 4.8 The activity of NADP malic dehydrogenase, isolated from *Kalanchoe daigremontiana*, as a function of pH.

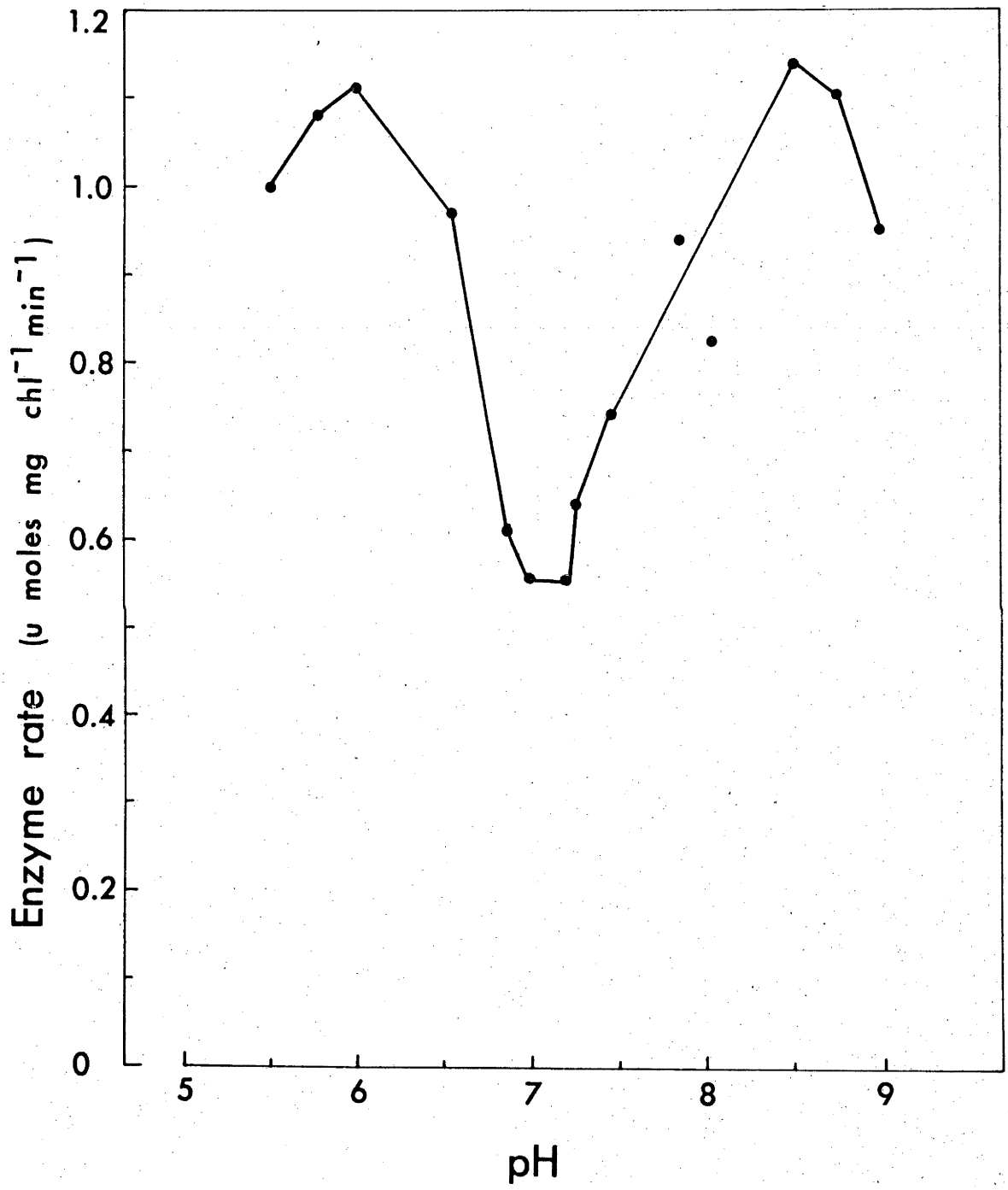
1.2
1.0
0.8
0.6
0.4
0.2
0
Enzyme rate (u moles mg chl^{-1} min^{-1})
5
6
7
8
9
pH

Figure 4.9 The activity of alanine aminotransferase, isolated from *Kalanchoe daigremontiana* (●), *Bryophyllum pinnatum* (▲), *Bryophyllum tubiflorum* (□), *Aloe arborescens* (○) and *Stapelia gigantea* (■) as a function of pH.

Figure 4.10 The activity of aspartate aminotransferase, isolated from *Kalanchoe daigremontiana* (○), *Bryophyllum pinnatum* (▲), *Bryophyllum tubiflorum* (□), *Aloe arborescens* (○) and *Stapelia gigantea* (■) as a function of pH.

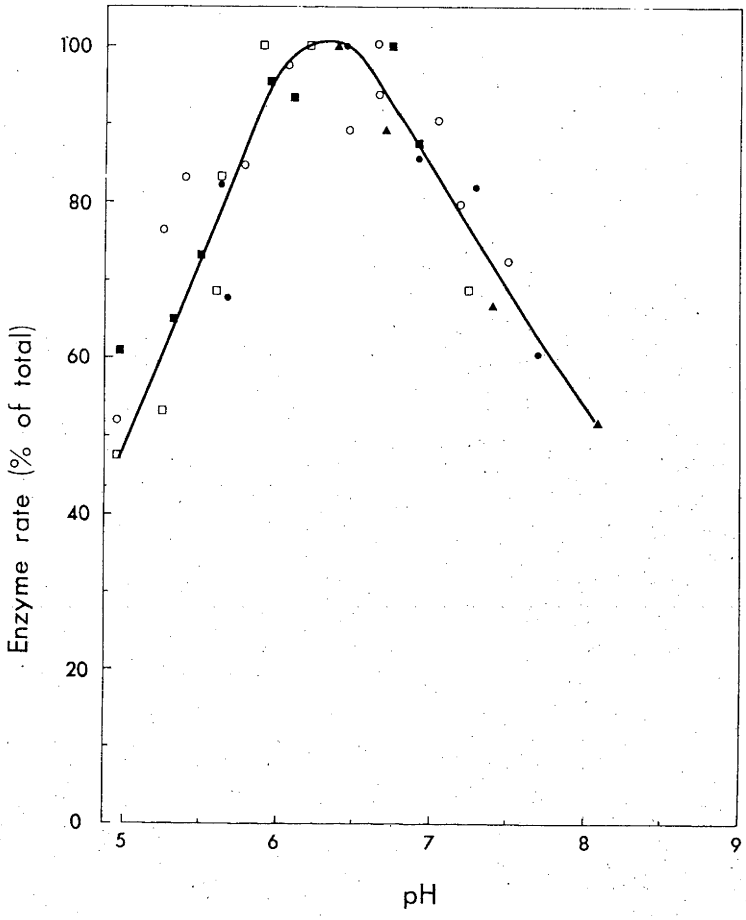
Enzyme rate (% of total)
100
80
60
40
20
0
5
6
7
8
9
pH

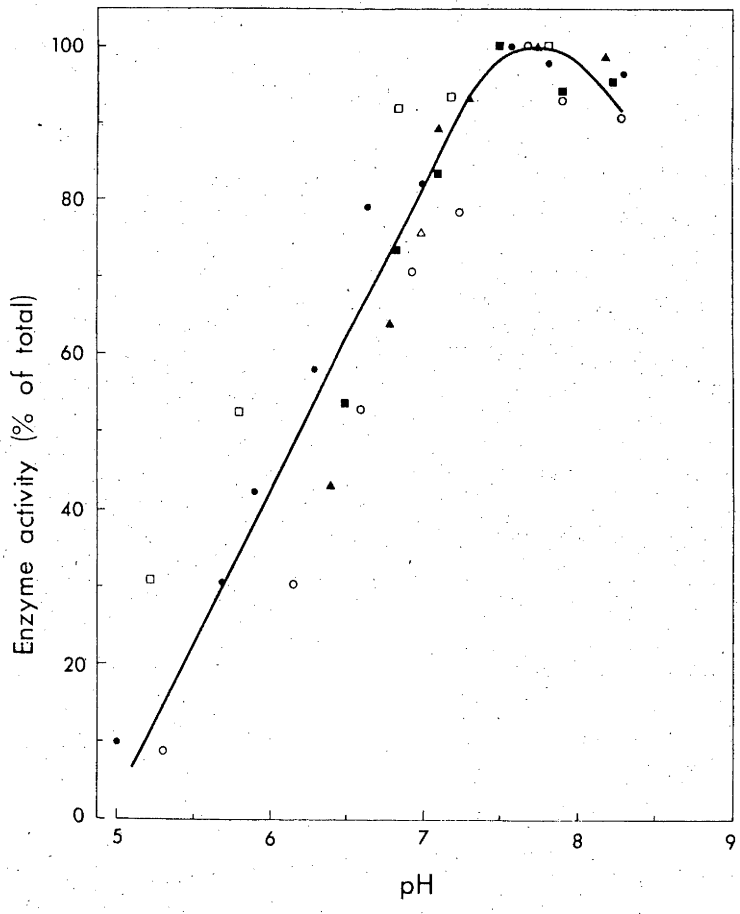
Enzyme activity (% of total)
100
80
60
40
20
0
5
6
7
8
9
pH

Figure 4.11 A. Fluctuation of malic acid (o) and aspartate (•) in *Hoya carnosa*, a PEPCK CAM plant, during a 24 hour day/night cycle.

B. Fluctuation of malic acid (o) and aspartate (•) in *Kalanchoe daigremontiana*, a malic enzyme CAM plant, during a 24 hour day/night cycle.

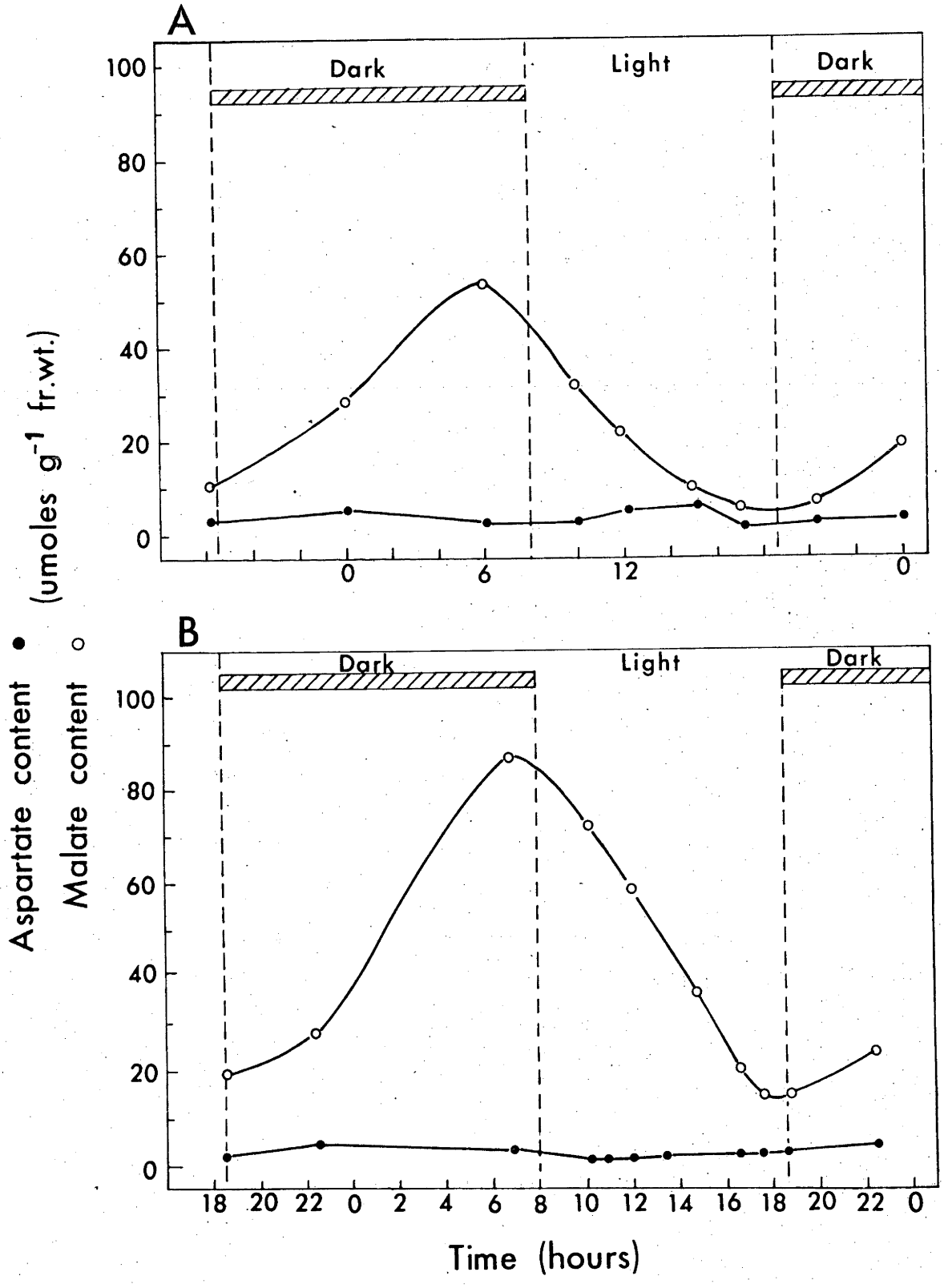
A
Dark
Light
Dark
100
80
60
40
20
0
0
6
12
0
B
Dark
Light
Dark
100
80
60
40
20
0
18
20
22
0
2
4
6
8
10
12
14
16
18
20
22
0
Time (hours)
Aspartate content •
Malate content ○
(umoles g-1 fr.wt.)

and NADP malic enzyme activities. 0.1 mM 3-MPA caused substantial inhibition of deacidification in *Aloe* but not in *Kalanchoe*. However, 0.5 mM 3-MPA resulted in a similar inhibition in *Kalanchoe* (Figure 4.12).

4.1.4 Discussion

Table 4.1 shows that pyruvate, Pi dikinase was not present in the 3 CAM plants which possessed PEPCK but was present in those species which did not possess PEPCK. The dikinase activities, although low, were sufficient to account for the conversion of pyruvate to PEP at the rates required by deacidification. The presence of the dikinase in malic enzyme CAM plants but not in PEPCK CAM plants is consistent with paths of pyruvate metabolism proposed in Section 1.4. Malic enzyme plants produce pyruvate during deacidification and an enzyme is required to convert pyruvate to PEP if gluconeogenesis is to take place. CAM plants which possess PEPCK however, have no requirement for such an enzyme since they produce PEP as a direct product of deacidification.

The possession of pyruvate, Pi dikinase by *Kalanchoe* but not by *Stapelia* also explains some of the phenomena observed in Chapters 2 and 3. Deacidifying *Kalanchoe* leaf slices were able to convert ^{14}C pyruvate $\longrightarrow$ CHO whereas *Stapelia* leaf slices were unable to do so (Figure 2.16). Presumably this was because the *Stapelia* tissue was unable to convert ^{14}C-pyruvate to ^{14}C-PEP. Similarly, pyruvate stimulated $^{14}CO_2$ fixation in isolated deacidified *Kalanchoe* mesophyll cells but had no effect on $^{14}CO_2$ fixation by *Stapelia* cells (Table 3.8). Presumably in the *Kalanchoe* cells exogenous pyruvate enters the cells and is converted to PEP which acts as a substrate for $^{14}CO_2$ fixation by PEP carboxylase. In the *Stapelia* cells pyruvate is not converted to PEP so $^{14}CO_2$ fixation is not stimulated. Pyruvate

Figure 4.12 A. Deacidification by *Aloe* leaf slices in the presence of 0 mM 3-MPA (● —— ●), 0.1 mM 3-MPA (Δ——Δ), 0.2 mM 3-MPA (o —— o) and 0.5 mM 3-MPA (□—— □).

B. Deacidification by *Kalanchoe* leaf slices in the presence of 0 mM 3-MPA (● —— ●), 0.1 mM 3-MPA (Δ——Δ), 3 mM 3-MPA (o —— o) and 5 mM (□——□).

C. Deacidification by *Kalanchoe* leaf slices in the presence of 0 mM 3-MPA (● —— ●), 0.01 mM 3-MPA (Δ——Δ), 0. 1 mM 3-MPA (o —— o) and 0.5 mM 3-MPA (□——□).

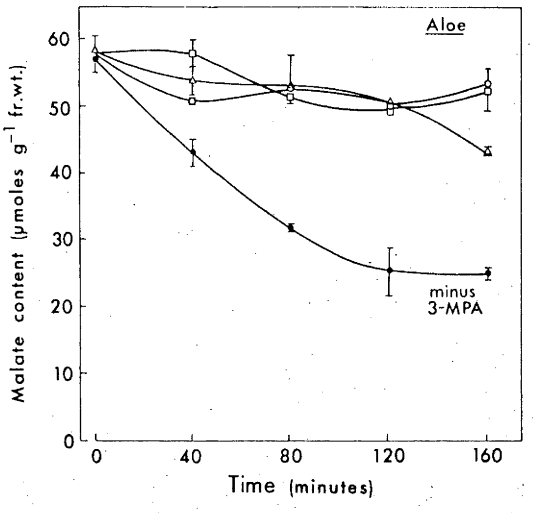
Aloe
Malate content (μmoles g⁻¹ fr.wt.)
60
50
40
30
20
10
0
minus
3-MPA
0
40
80
120
160
Time (minutes)

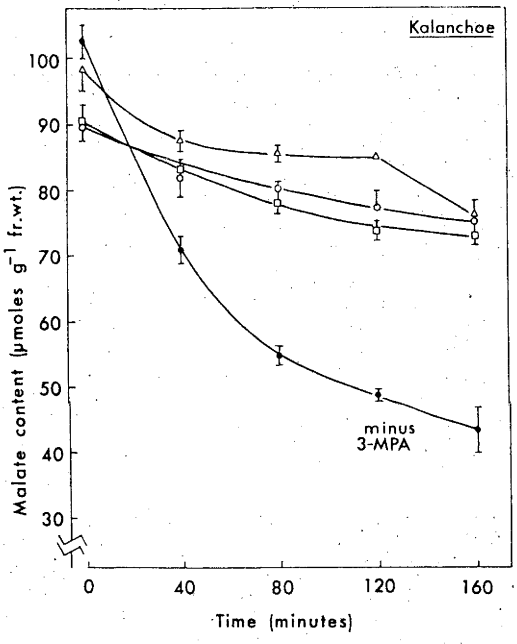
Kalanchoe
Malate content (μmoles g⁻¹ fr.wt.)
100
90
80
70
60
50
40
30
minus
3-MPA
0
40
80
120
160
Time (minutes)

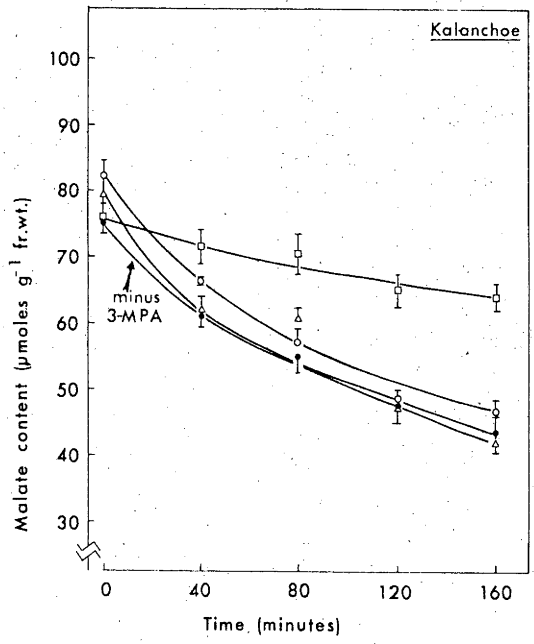
Kalanchoe
Malate content (μmoles g⁻¹ fr.wt.)
100
90
80
70
60
50
40
30
minus
3-MPA
0
40
80
120
160
Time (minutes)

Pi dikinase is essential for the operation of gluconeogenesis in CAM plants which do not possess PEPCK.

The activity of PEP carboxylase and NAD malate dehydrogenase are sufficient to account for the *in vivo* rates of dark CO_2 fixation and malate accumulation observed in all species examined.

RuP_2 carboxylase activity was not measured in this study but data from Dittrich *et al.* (1973) indicate that the rates are sufficient to account for the internal reassimilation of CO_2 released during deacidification (Table 4.1).

The activity of NADP malic enzyme in *K. daigremontiana, B. pinnatum, B. tubiflorum* and *O. inermis* is sufficient to account for the rates of deacidification observed in these species. The presence of NAD malic enzyme in these 4 species will obviously increase their capacity for pyruvate production. The activity of NADP malic enzyme and NAD malic enzyme (the latter enzyme was not measured in this study, data from Dittrich, 1973), in plants possessing PEPCK is either insufficient or barely sufficient to account for the observed rates of deacidification. The PEPCK activities however, are far greater than required.

3-MPA, allegedly a specific inhibitor of both animal and plant PEPCK (Robinson and Oei, 1975; Ray and Black, 1976b) was fed to leaf slices of *Aloe,* a PEPCK plant, and *Kalanchoe*, a malic enzyme plant, in an attempt to assess the contribution of malic enzyme to deacidification in the PEPCK plant. It was hoped that an estimation could then be made of the amount of pyruvate being produced during deacidification in PEPCK CAM plants. The effect

of 3-MPA was non-specific and, at concentrations greater than 0.1 mM, inhibited deacidification in both tissues by at least 70%. However, when tissues were exposed to 0.1 mM 3-MPA, no inhibition of deacidification was observed in *Kalanchoe*, the malic enzyme species, whilst deacidification was inhibited by over 70% in *Aloe*, the PEPCK species. The 3-MPA data is not accurate enough to enable a precise measurement of the contribution of NAD and NADP malic enzyme to deacidification in the PEPCK plant *Aloe*. It does indicate however, that despite the fact that the extractable NADP malic enzyme activity is about 1/3 that of the extractable PEPCK activity, the contribution of NADP malic enzyme to deacidification is minimal i.e. there is not a large flow of carbon through pyruvate during deacidification. This observation supports the assumption, proposed in Chapter 2.3, that exogenous ^{14}C-pyruvate was considerably diluted in the malic enzyme plant *Kalanchoe*, but was diluted much less so in the PEPCK plant *Stapelia*.

The effect of 3-MPA on deacidification in *Kalanchoe* is puzzling. Ray and Black (1976b) observed that 0.5 mM 3-MPA had no effect on either NADP malic enzyme from *Sorghum halpense* or on NAD malic enzyme from *Atriplex spongiosa*, yet 0.5 mM 3-MPA inhibited deacidification in *Kalanchoe* leaf slices by about 70%. This suggests that NADP or NAD malic enzyme from *Kalanchoe* is more sensitive to 3-MPA or, alternatively, that 3-MPA affects some other process involved with deacidification. One possibility is that 3-MPA may affect the transfer of malate across the tonoplast. This is supported to some extent by ^{14}C labelling studies with the C_4 plant *Panicum maximum* (Ray and Black, 1977) in which 5 mM 3-MPA fed to intact leaves prevented the transfer of ^{14}C from malate and aspartate into 3-PGA and sugars. This was ascribed to the inhibition

of PEPCK by 3-MPA but may also have been partly due to the inhibition of the transfer of aspartate or malate into the bundle sheath cells.

NADP malate dehydrogenase activity was similar in the six species measured. The roles of both the double pH optimum, which was observed in *Kalanchoe* and in *B. pinnatum* the only two species in which it was looked for, and the observed NADP malate dehydrogenase capacities are unknown.

In contrast to the reports for short day treated *K. blossfeldiana* (Morel *et al.*, 1972; Morel, pers. comm.), the aspartate aminotransferase activities of the 6 species measured in this study were always considerably smaller than those observed for PEP carboxylase. There was no correlation between the activity of alanine and aspartate aminotransferases and the presence of PEPCK or NAD malic enzyme in CAM plants as has been observed in C_4 plants (Hatch and Kagawa, 1974a; Hatch *et al.*, 1975). Furthermore, isolated *K. daigremontiana* mitochondria possess low aspartate aminotransferase activities (D. Day, personal communication), in contrast to NAD malic enzyme C_4 plants which possess high capacities of both cytoplasmic and mitochondrial isoenzymes (Hatch and Kagawa, 1974b). The observation that aspartate does not accumulate in the two CAM plants examined argues against any direct involvement of aspartate aminotransferase in dark malate accumulation. Some OAA may, of course, be converted to aspartate as a side reaction. These differences suggest that the roles of aspartate aminotransferase in C_4 and in CAM plants may be very different.

Although alanine aminotransferase activities are up to 5 times greater than the pyruvate, Pi dikinase activities in the same tissues,

and are greater than the TCA cycle rates in the light in both types of CAM plants, comparatively little label was observed in alanine and glutamate in ^{14}C-pyruvate feeding experiments (cf. Chapter 2.3). Moreover, although over 70% of the label in spinach was observed in alanine and glutamate, in C_3 *Mesembryanthemum* the pattern of labelling of amino acids was similar to that observed in CAM *Mesembryanthemum* and in other CAM species fed ^{14}C-pyruvate. The role of alanine aminotransferases in these CAM plants is by no means clear.

One can conclude firstly, that the *in vitro* activites of the various enzymes required for acidification and deacidification are sufficient to account for the observed rates *in vivo*. Secondly, that malic enzyme CAM plants have the capacity to convert pyruvate ⟶ PEP at rates comparable to the rate of pyruvate production during deacidification; and thirdly, CAM plants in which PEPCK is the major decarboxylase have no detectable pyruvate, Pi dikinase. Since PEP, not pyruvate, is the major product of deacidification in these CAM plants, they have no requirement for this enzyme. The activities of enzymes involved in the conversion of PEP to glucan via gluconeogenesis is considered in the next section.

4.2 The Capacity of CAM Plants to Metabolise Pyruvate and PEP via Gluconeogenesis

4.2.1 Introduction

The direct conversion of the C_3 compounds remaining from malate decarboxylation to glucan, requires that the activity of the gluconeogenic enzymes be at least equivalent to the measured flux of carbon from malic acid to glucan during deacidification in the light.

Sutton (1974, 1975b,c) demonstrated that the activities of the enzymes of glycolysis and glucan breakdown in two CAM species, *Kalanchoe daigremontiana* and *Bryophyllum pinnatum*, were adequate to account for the measured flux of carbon from glucan to malic acid during dark acidification. In this section I shall report the *in vitro* activities of PGA kinase, NAD and NADP G-3-P dehydrogenase, alkaline FDPase and phosphohexose isomerase when assayed in the gluconeogenic direction, in extracts from 3 malic enzyme and 2 PEPCK CAM plants. Enolase and phosphofructokinase activities were measured in the glycolytic direction and PGA mutase activity was measured in both directions. Each enzyme assay was optimised with respect to the pH and substrate concentrations required for maximum *in vitro* activity.

4.2.2 Materials and methods

4.2.2.1 *Extraction methods*

Plants were grown in a growth cabinet under conditions previously described in Chapter 2.1.2.1. Deacidified leaf tissue was harvested 4-5 hours after illumination and was illuminated for 15 minutes with a quantum flux density of 1200 μeinstein m^{-2} s^{-1} from a 1000 W Philips HPLR high pressure mercury vapour fluorescent lamp through a 5 cm water filter. Between 5 and 15 g of photosynthetic tissue was ground with a small amount of acid washed sand, in a mortar and pestle, with 3-5 volumes of buffer containing 100 mM HEPES-NaOH, pH 8.0, 5 mM $MgCl_2$, 5 mM DTT, 0.5 mM EDTA, 0.5% (w/v) BSA, and 1% (w/v) PVP 40.

The brei was filtered through two layers of Miracloth and two 2 ml aliquots were taken for chlorophyll determinations. The remaining extract was centrifuged at 12,000 x g for 10 minutes at 0-4°C. The supernatant was decanted and either immediately used for assays, or a 1 ml aliquot was passed through a small column of G-25 Sephadex (0.5 cm x 15.0 cm)

equilibrated, at room temperature, with the following buffer; 25 mM HEPES-NaOH, pH 8.0, 5 mM $MgCl_2$, and 5 mM DTT.

Pyruvate kinase was extracted in a buffer containing 50 mM Bicine-NaOH, 50 mM HEPES-NaOH, pH 8.0, 5 mM $MgCl_2$, 5 mM DTT, 1 mM EDTA, 0.5% (w/v) BSA, and 1% (w/v) PVP 40. After filtration and centrifugation the supernatant was passed through a column of G-25 Sephadex (0.5 cm x 15 cm) equilibrated with 25 mM Bicine-NaOH, 25 mM HEPES-NaOH, pH 8.0, 10 mM $MgCl_2$ and 1 mM DTT.

4.2.2.2 *Enzyme assays*

All enzymes were assayed by following the change of absorbance at 340 nm, of a 3 ml reaction mix in a 1 cm glass cuvette, at 20°C using either a Varian Series 634 or a Perkin Elmer 124 double beam spectrophotometer.

The enzymes were assayed in the following reaction mixtures. The given concentrations are the final concentrations in the cuvette and in each case the last listed compound was added to initiate the reaction.

Pyruvate kinase (ATP: Pyruvate 2-O-phosphotransferase, E.C. 2.7.1.40)(Sutton, 1975b) 25 mM MES-NaOH, 25 mM HEPES-NaOH, pH 7.5, 6 units glucose-6-phosphate dehydrogenase, 0.06 mM NADP, 6 units hexokinase, 0.7 mM D-glucose, 200 µl extract, 8 mM $MgSO_4$, 75 mM KCl, 0.4 mM ADP and 1.0 mM PEP.

Enolase (2-phospho-D-glycerate hydro-lyase, E.C. 4.2.1.11), 25 mM MES-NaOH, 25 mM HEPES-NaOH, pH 7.0, 2 mM $MgCl_2$, 0.08 mM NADH, 50 mM $KHCO_3$, 3 units MDH, 6 units PEP carboxylase, 200 µl extract and 2 mM 2-PGA.

Phophoglycerate mutase (2,3-bisphospho-D-glycerate; 2-phospho-D-glycerate transferase E.C. 2.7.5.3)(Grisola, 1962) Glycolytic direction: 25 mM MES-NaOH, 25 mM HEPES-NaOH, pH 7.0, 2 mM $MgCl_2$, 0.08 mM NADH, 6 units enolase 3 units MDH, 6 units PEP carboxylase, 50 mM $KHCO_3$, 200 µl extract and 3 mM 3-PGA. The 3-PGA contained about 2% (w/w) of the cofactor 2,3 diphosphoglyceric acid.

Gluconeogenic direction: 25 mM MES-NaOH, 25 mM HEPES-NaOH, pH 7.0, 2 mM $MgCl_2$, 0.2 mM 2,3 diphosphoglyceric acid, 0.08 mM NADH, 1 mM ATP, 6 units phosphoglycerate kinase, 6 units NADH G-3-P dehydrogenase, and 3 mM 2-PGA. After 3-PGA, which was a contaminant in the 2-PGA, was metabolised the reaction was initiated with 200 µl of extract.

Phosphoglycerate kinase (ATP: 3-phospho-D-glycerate 1-phosphotransferase E.C. 2.7.2.3)(modified from Sutton, 1975b) 25 mM Bicine-NaOH, 25 mM HEPES-NaOH, pH 9.0, 2 mM $MgCl_2$, 0.08 mM NADH, 9 units NADH G-3-P dehydrogenase, 200 µl extract, 2 mM 3-PGA and 1 mM ATP.

NAD glyceraldehyde-3-phosphate dehydrogenase (D-glyceraldehyde-3-phosphate: NAD^+ oxidoreductase (phosphorylating), E.C. 1.2.1.12)(modified from Latzko and Gibbs, 1968) 25 mM Bicine-NaOH, 25 mM HEPES-NaOH, pH 7.5, 2 mM $MgCl_2$, 0.08 mM NADH, 9 units phosphoglycerate kinase, 200 µl extract, 3 mM 3-PGA and 1 mM ATP.

NADP glyceraldehyde-3-phosphate dehydrogenase (D-glyceraldehyde-3-phosphate: $NADP^+$ oxidoreductase (phosphorylating) E.C. 1.2.1.13)(modified from Latzko and Gibbs, 1968) 25 mM Bicine-NaOH, 25 mM HEPES-NaOH, pH 9.0, 2 mM $MgCl_2$, 0.08 mM NADPH, 2 mM DTT, 9 units phosphoglycerate, 200 µl extract, 3 mM 3-PGA and 1 mM ATP.

Phosphofructokinase (ATP: D-fructose-6-phosphate 1-phosphotransferase E.C. 2.7.1.11)(Sutton, 1975b) 25 mM Bicine-NaOH, 25 mM HEPES-NaOH, pH 8.5, 2 mM $MgCl_2$, 0.08 mM NADH, 3 units fructose bisphosphate aldolase, 6 units triose phosphate isomerase, 9 units glycerol-3-phosphate isomerase, 1 mM ATP, 200 µl extract and 2 mM fructose-6-phosphate.

Fructose-1,6-diphosphatase (D-fructose-1,6-diphosphate 1-phospho-hydrolase, E.C. 3.1.3.11) (modified from Baier and Latzko, 1975) 25 mM Bicine-NaOH, 25 mM HEPES-NaOH, pH 9.0, 10 mM $MgCl_2$, 2 mM EDTA, 2 mM DTT, 0.2 mM NADP, 6 units phosphohexose isomerase, 6 units glucose-6-phosphate dehydrogenase, and 2 mM fructose-1,6-diphosphate. The reaction was allowed to proceed until F-6-P which was a contaminant in the F-1,6-P_2, was metabolised before 200 µl of extract was added.

Phosphohexose isomerase (D-glucose-6-phosphate ketol-isomerase, E.C. 5.3.1.9) (modified from Sutton, 1975b) 25 mM Bicine-NaOH, 25 mM HEPES-NaOH, pH 9.0, 10 mM $MgCl_2$, 2 mM EDTA, 0.2 mM NADP, 6 units glucose-6-phosphate dehydrogenase, 200 µl extracts and 2 mM fructose-6-phosphate.

Glucose-6-phosphate dehydrogenase (D-glucose-6-phosphate $NADP^+$ 1-oxido-reductase, E.C. 1.1.1.49) (modified from Sutton, 1975b) 25 mM Bicine-NaOH, 25 mM HEPES-NaOH, pH 9.0, 4 mM $MgCl_2$, 0.2 mM NADP, 200 µl extract, and 2 mM glucose-6-phosphate.

Hexokinase (ATP: D-glucose 6-phosphotransferase E.C. 2.7.1.2) (modified from Sutton, 1975b) 25 mM Bicine-NaOH, 25 mM HEPES-NaOH, pH 8.5, 3 mM $MgCl_2$, 0.07 nM NADP, 3 units glucose-6-phosphate dehydrogenase, 200 µl extract, 2 mM glucose and 1 mM ATP.

4.2.2.3 *Chlorophyll estimation*

4 ml of acetone was added to 1 ml of uncentrifuged leaf extract. Chlorophyll was determined as described in Section 2.1.2.4.

4.2.3 Results

Pyruvate kinase activities could not be measured due to interference in the coupled assay by high adenylate kinase activity (about 8 μmoles mg chl^{-1} min^{-1} in *Kalanchoe*). This activity gave a large ADP dependent, but PEP and KCl independent, change in absorbance. The change of absorbance which resulted from the subsequent addition of PEP and KCl was very small compared to the background. Sutton (1974) experienced similar problems, but estimated that in *Kalanchoe* the pyruvate kinase activity was in the region of 0.1 μmole mg chl^{-1} min^{-1}.

Enolase was assayed in the glycolytic direction because the reverse reaction suffers interference from PEP carboxylase which competes for the common substrate PEP. Nevertheless since enolase is a freely reversible enzyme with a Keq of about 3, activity of the enzyme in the glycolytic direction also indicates the activity in the reverse direction. The enzyme had a pH optimum around 7.0 (Figure 4.13). Enolase activity decreased considerably during gel filtration and thus the rates reported in Table 4.3 are those observed in crude extracts.

PGA mutase was assayed in both the glycolytic and gluconeogenic directions. The maximum activities were between 2 and 10 times greater in the gluconeogenic direction than in the glycolytic direction. This might be expected since, for the yeast enzyme, the $\Delta G'$ for the reaction 3-PGA $\longrightarrow$ 2-PGA is +1,050 cal.mol.$^{-1}$ pH 7.0 and 25°C and the reaction has a Keq of 0.17 (Conn and Stumpf, 1972). The pH optimum for the CAM enzyme was about 7.0 in both directions (Figure 4.14). This agrees with the observation of Spalding *et al.* (1979) that PGA mutase is a cytoplasmic enzyme in *Sedum praealtum*. The apparent Km (2-PGA) of 1.8-3.6 x 10^{4} mM

Figure 4.13 The activity of enolase isolated from *Kalanchoe daigremontiana*, as a function of pH. Enolase was assayed in crude extracts as the enzyme lost activity during gel filtration.

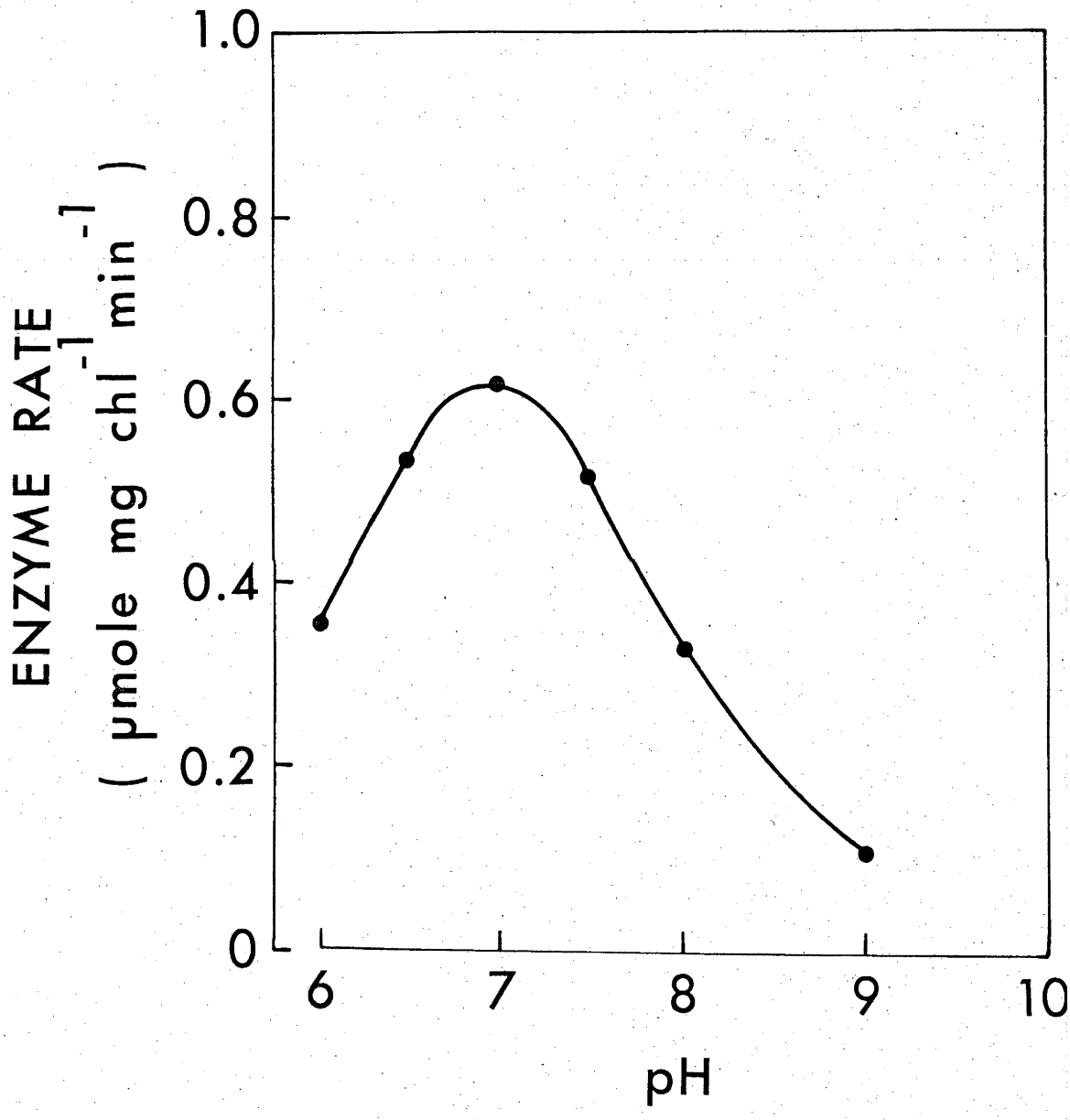
ENZYME RATE
(μmole mg chl^{-1} min^{-1})
1.0
0.8
0.6
0.4
0.2
0
6
7
8
9
10
pH

Figure 4.14 A. The activity of PGA mutase, isolated from *Kalanchoe daigremontiana* as a function of 2-PGA concentration (a) and pH (b) when assayed in the direction of 3-PGA formation (gluconeogenic direction).

B. The activity of PGA mutase, isolated from *Kalanchoe daigremontiana* as a function of 3-PGA concentration (a) and pH (b) when assayed in the direction of 2-PGA formation (glycolytic direction).

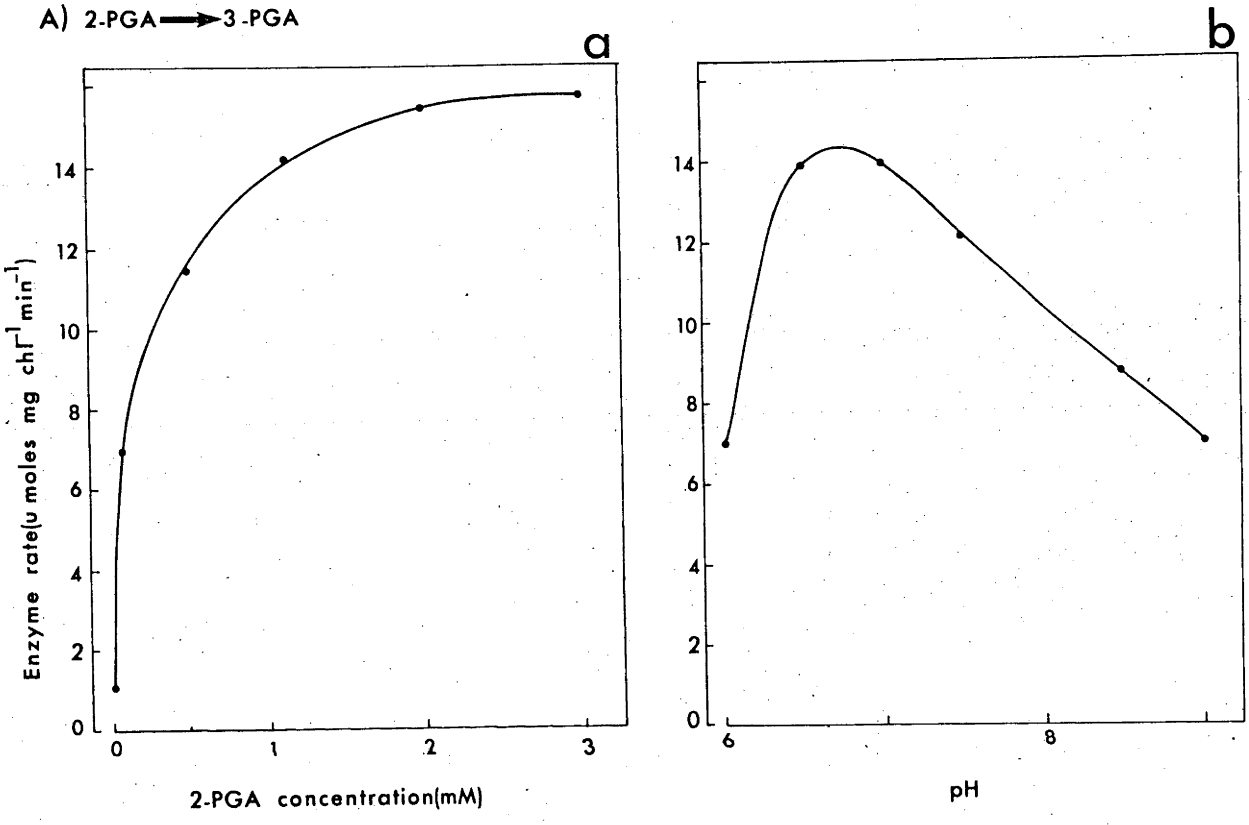
A) 2-PGA ⟶ 3-PGA
a
b
Enzyme rate(μ moles mg chl^{-1} min^{-1})
0
2
4
6
8
10
12
14
0
1
2
3
2-PGA concentration(mM)
6
8
pH

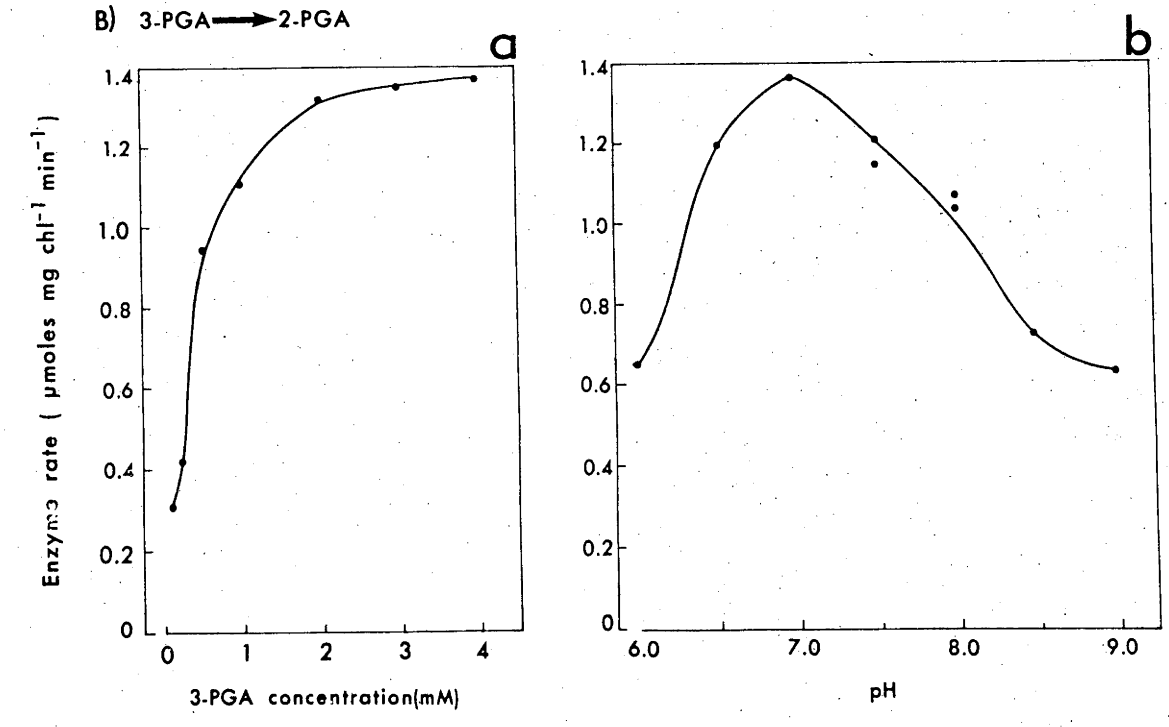
B) 3-PGA ⟶ 2-PGA
a
b
Enzyme rate (μmoles mg chl^{-1} min^{-1})
0
0.2
0.4
0.6
0.8
1.0
1.2
1.4
0
1
2
3
4
3-PGA concentration(mM)
6.0
7.0
8.0
9.0
pH

was similar to the apparent Km (3-PGA) of 2.4 x 10^{-4} mM (Figure 4.14). The maximum activity in the glycolytic direction was not attained until 1-2 minutes after adding the substrate. This lag phase was not slowed by adding extra coupling enzymes, co-factor, or substrate.

No distinction was made between the 2,3-DPGA dependent and 2,3-DPGA independent PGA mutases which have been reported in yeast and in wheat germ respectively (Grisola, 1962). As 3-PGA contains about 0.2% 2,3-DPGA and the 2,3-DPGA independent enzyme is sensitive to 2,3-DPGA only at very high 2,3-DPGA concentrations, it was not possible to establish whether the reaction assayed in these experiments was catalysed by one or both enzymes. The addition of 2,3-DPGA had little effect on the reaction rates.

PGA kinase was present in high activities and had a pH optimum around 9.0. Substantial activity was still present at pH 7.0 (Figure 4.15). The reaction was saturated by 2.0 mM 3-PGA, 1.0 mM ATP and 2 mM $MgCl_2$. A requirement for 80 mM $MgSO_4$, previously reported for the enzyme from *Kalanchoe* (Sutton, 1974), was not observed. In fact 80 mM $MgSO_4$ was found to be inhibitory.

NAD and NADP G-3-P dehydrogenase were assayed by adding PGA kinase to the reaction mix and using 3-PGA as the substrate because the real substrate, 1,3-DPGA, is unstable. NAD G-3-P dehydrogenase had a pH optimum of 7.0-7.5, whilst the NADP enzyme had a broad pH optimum of around 8.5-9.0 (Figure 4.16). 3-PGA was saturating at about 3 mM for the NAD enzyme and about 2 mM for the NADP enzyme. Whereas the NAD mediated reaction was linear, the NADP mediated reaction exhibited an initial non-linear rate which declined for 1-2 minutes before assuming linearity. I was unable to stabilise the initial high rate

Figure 4.15 The activity of PGA kinase, isolated from *Kalanchoe daigremontiana* and assayed in the gluconeogenic direction, as a function of (A) pH, (B) 3-PGA concentration, and (C) ATP concentration.

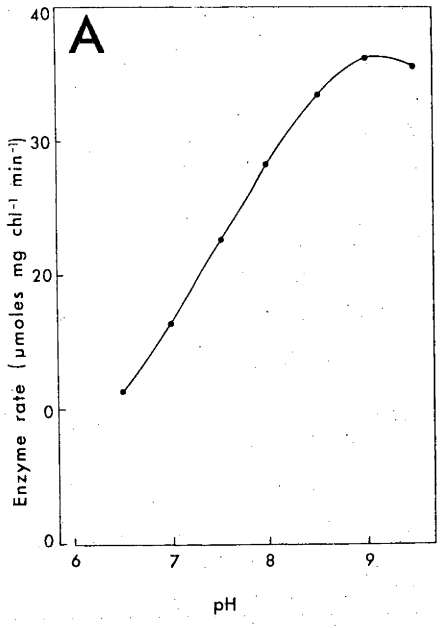
A
Enzyme rate (μmoles mg chl⁻¹ min⁻¹)
40
30
20
0
6
7
8
9
pH

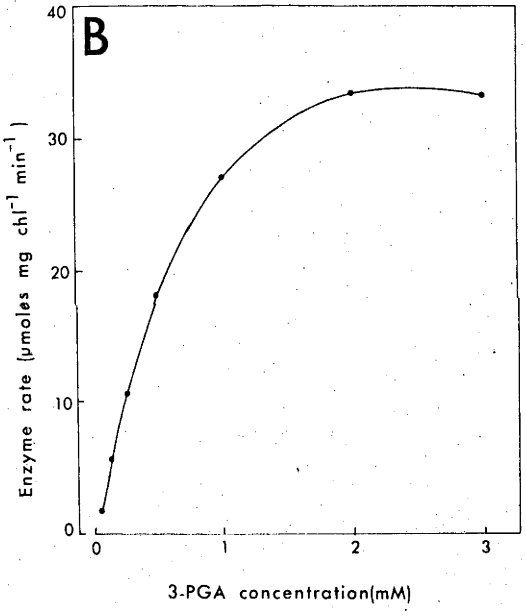
B
Enzyme rate (μmoles mg chl⁻¹ min⁻¹)
40
30
20
10
0
0
1
2
3
3-PGA concentration(mM)

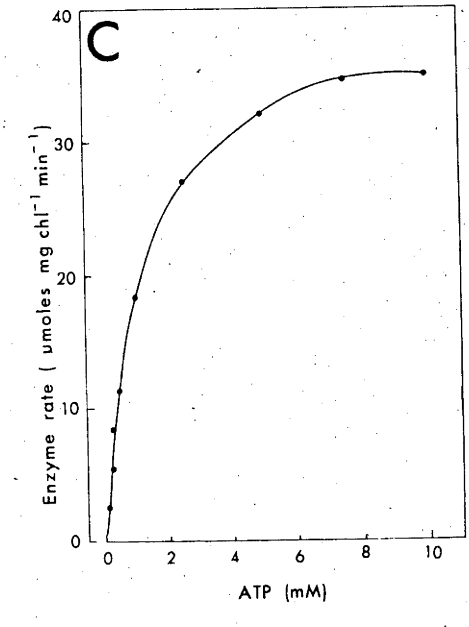
C
Enzyme rate (μmoles mg chl⁻¹ min⁻¹)
40
30
20
10
0
0
2
4
6
8
10
ATP (mM)

Figure 4.16 A. The activity of NAD G-3-P dehydrogenase, isolated from *Kalanchoe daigremontiana* and assayed in the gluconeogenic direction as a function of 3-PGA concentration (a) and pH (b).

B. The activity of NADP G-3-P dehydrogenase, isolated from *Kalanchoe daigremontiana* and assayed in the gluconeogenic direction, as a function of 3-PGA concentration (a) and pH (b).

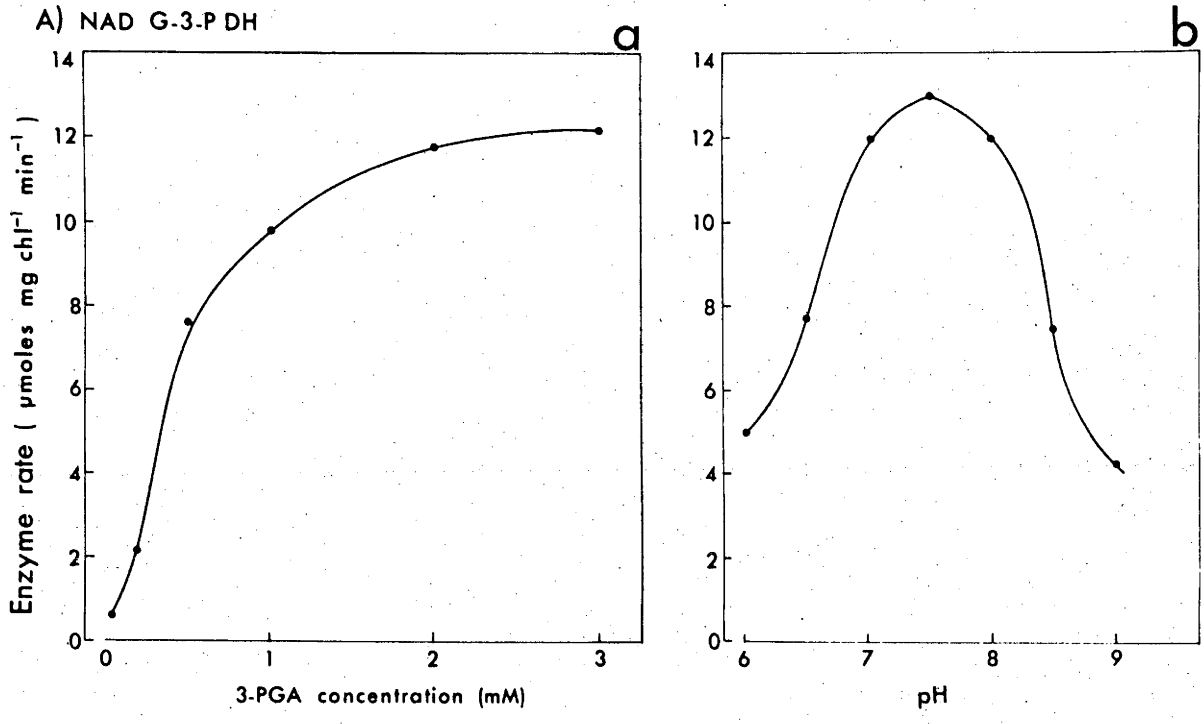
A) NAD G-3-P DH
a
b
Enzyme rate (μmoles mg chl^{-1} min^{-1})
3-PGA concentration (mM)
pH

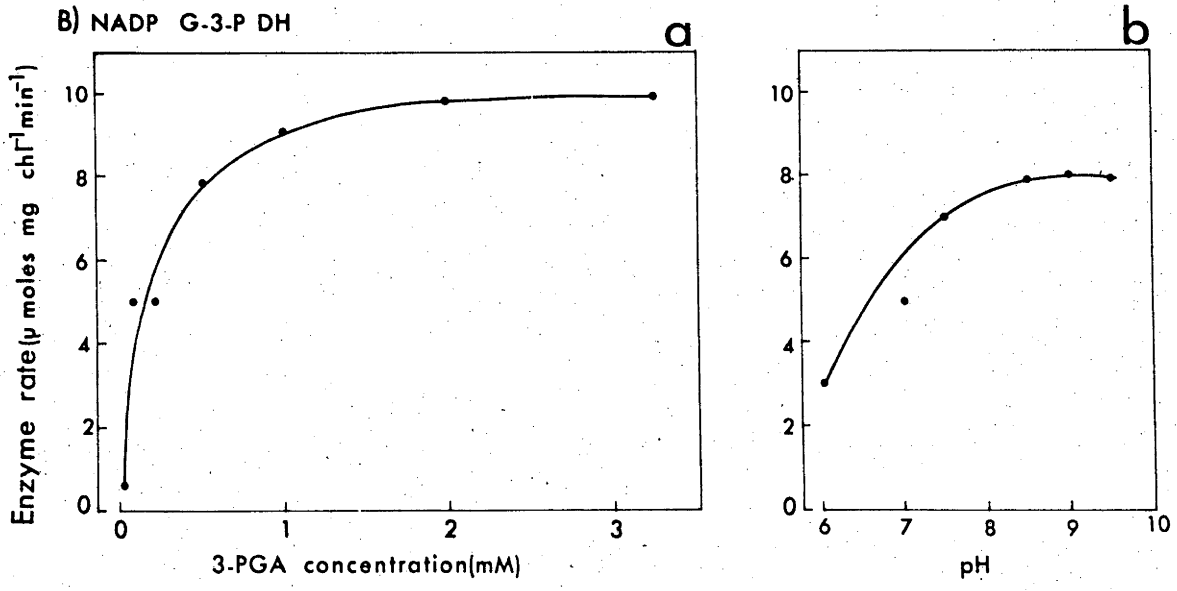
B) NADP G-3-P DH
a
b
Enzyme rate(μ moles mg chl^{-1}min^{-1})
3-PGA concentration(mM)
pH

and thus have expressed the rates for this enzyme as the average rate observed over the initial 3 minutes of assay. This phenomenon of non-linearity of the NADP G-3-P dehydrogenase reaction is commonly observed and the reasons are unknown (G. Kelly, personal communication). It is possible a proportion of the NAD G-3-P dehydrogenase activity was actually due to NAD activity of the NADP enzyme (Cerff, 1978). Neither enzyme was activated further by 50 mM glycine nor 50 mM alanine which have been reported to activate NAD and NADP G-3-P dehydrogenase from *Chlorella*, *Scenedesmus* and spinach leaves (Tomova *et al.*, 1972a, 1972b). In fact, 50 mM glycine inhibited the NAD enzyme by about 70%.

Fructose-1,6-diphosphatase exhibited two pH optima, one at pH 9.0 and one at pH 7.0 (Figure 4.17a). The enzyme was routinely assayed at pH 9.0 as it was assumed that the pH 9.0 peak represented the maximum activity of the photosynthetic alkaline FDPase whilst the pH 7.0 peak was that of an acid FDPase. F-1,6-P_2, the substrate for FDPase, was contaminated with F6P so, as in the PGA mutase assay, the plant extract was added last after all the F6P was metabolised by the coupling enzymes and there was no further change in absorbance. The reaction was saturated by about 2 mM F-1,6-P_2 (Figure 4.17b). Almost half the FDPase activity was routinely lost during gel filtration so the activities expressed in Table 4.3 are for crude extracts. Each unit of FDPase activity represents the conversion of 2 units of pyruvate.

Phosphofructokinase was assayed in the glycolytic direction using substrate concentrations which have been shown by Sutton (1974a, 1975b, 1975c) to be optimal for the *Kalanchoe daigremontiana* enzyme. The enzyme had a pH optimum of about pH 8.5-9.0 (Figure 4.18).

Figure 4.17 The activity of fructose-1,6-diphosphatase, isolated from *Kalanchoe daigremontiana*, as a function of (A) pH, and (B) [F-1,6-P_2].

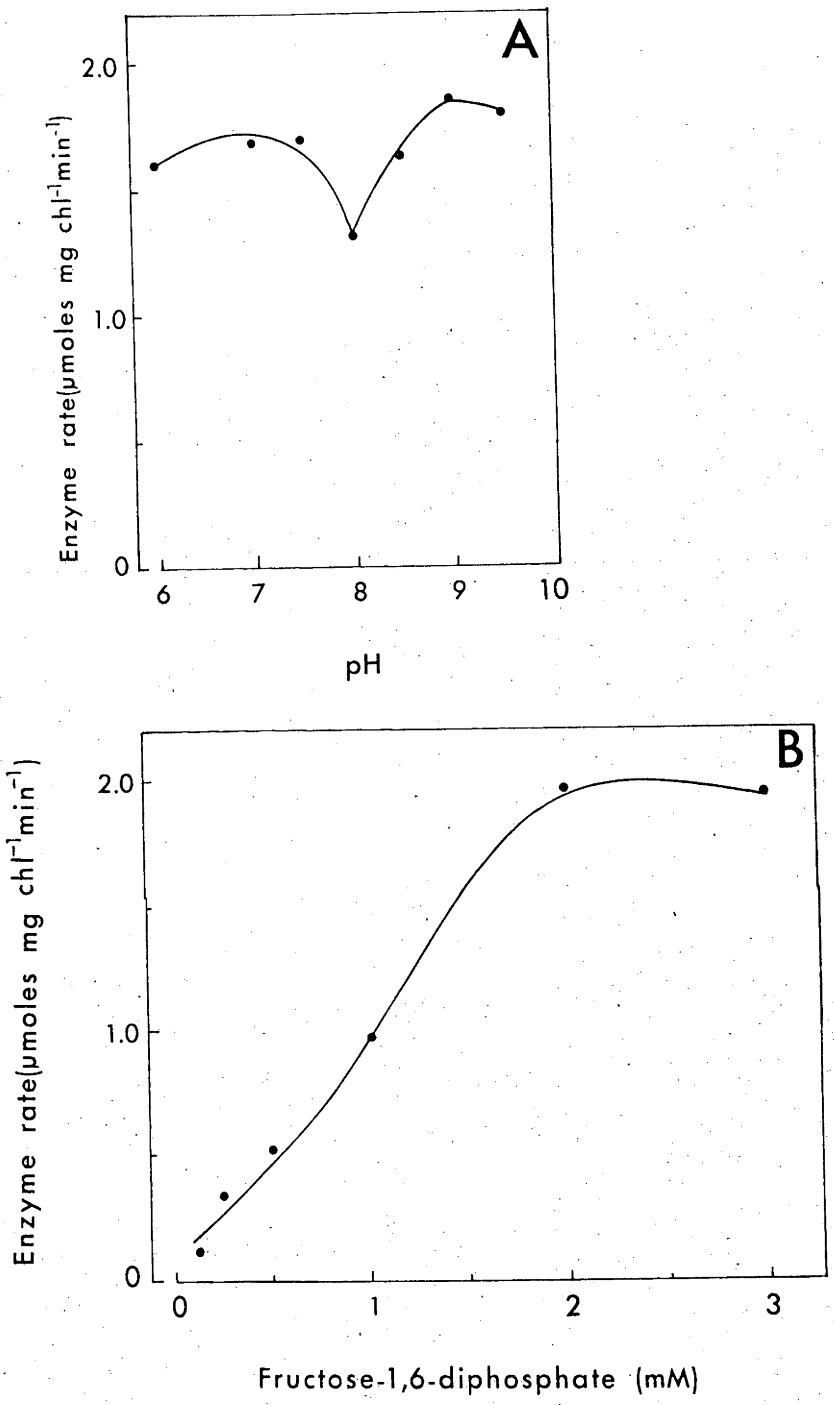
A
2.0
1.0
0
Enzyme rate(μmoles mg chl^{-1}min^{-1})
6
7
8
9
10
pH
B
2.0
1.0
0
Enzyme rate(μmoles mg chl^{-1}min^{-1})
0
1
2
3
Fructose-1,6-diphosphate (mM)

Figure 4.18 The activity of phosphofructokinase, isolated from *Kalanchoe daigremontiana*, as a function of pH.

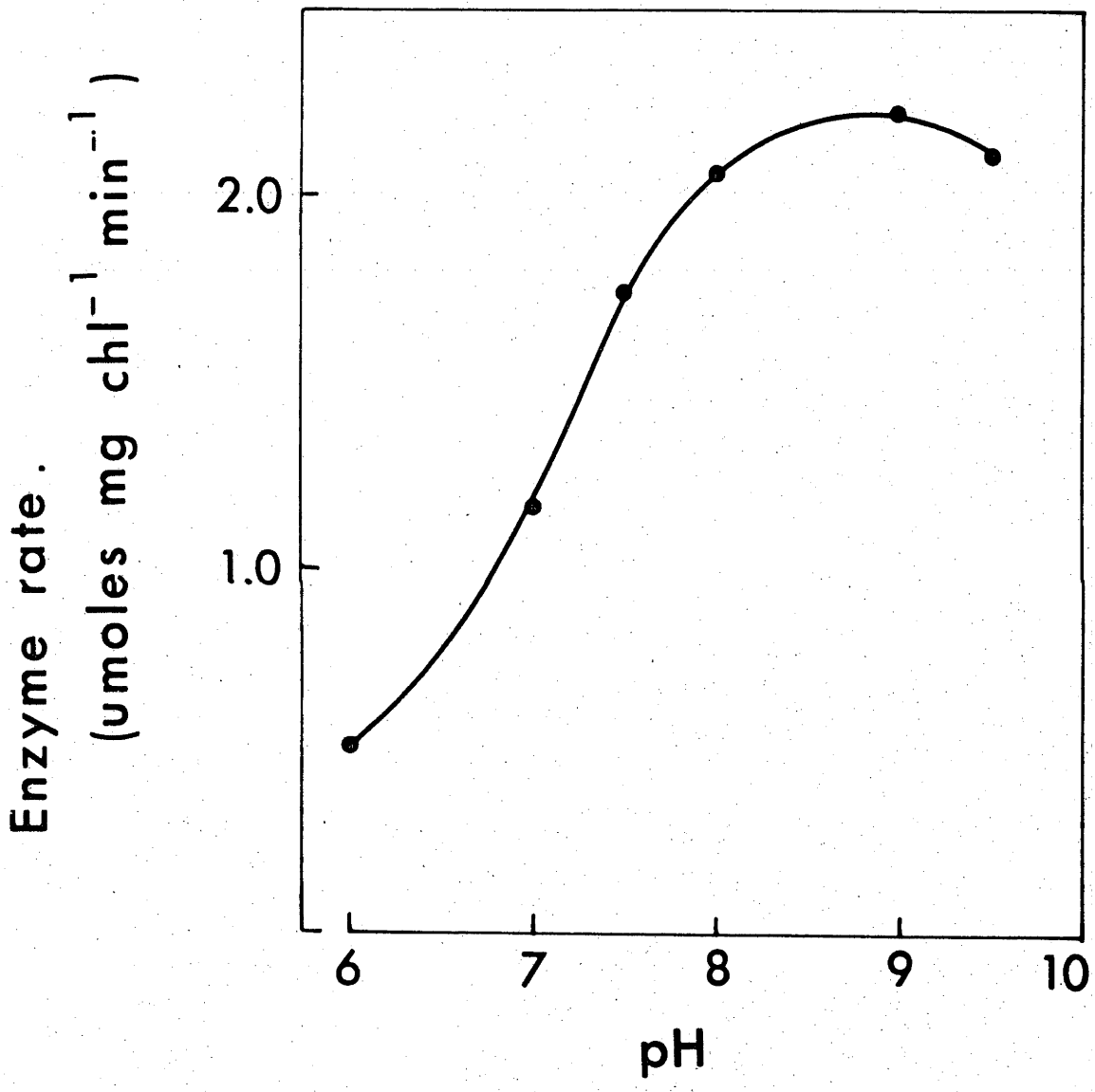
Enzyme rate.
(umoles mg chl^{-1} min^{-1})
2.0
1.0
6
7
8
9
10
pH

Phosphohexose isomerase had a pH optima between 8.0 and 9.0, with maximal activity around 9.0. The reaction was saturated by 1 mM F6P and had an apparent Km (F6P) of about 1.0×10^{-4} mM (Figure 4.19).

Table 4.3 shows the maximum activities of the various glycolytic enzymes in 3 malic enzyme species and in 3 PEPCK species, and compares these rates with the observed rates of deacidification in intact tissue. The rates are adequate to sustain the flow of carbon produced during deacidification.

4.2.4 Discussion

Table 4.3 shows that the activities of the various glycolytic enzymes, when assayed in the reverse direction, are greater than the rate of malate decarboxylation and hence are sufficient to account for the conversion of PEP to CHO via gluconeogenesis. Triose phosphate isomerase, FDP aldolase, and phosphoglucomutase were not measured but are known to be readily reversible and are present in CAM tissue in high activities (Sutton, 1974, 1975b). FDPase and, in malic enzyme plants, enolase and pyruvate, Pi dikinase appear to be the rate limiting steps.

Of the enzymes involved in glycolysis, 4 catalyse exergonic reactions which are not readily reversible. Although there is little information available on the properties of these enzymes in CAM plants some data is available for C_3 plants. Hexokinase catalyses

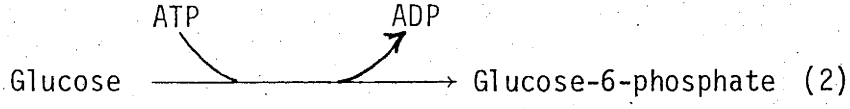

(2)

Most leaf tissues, including CAM tissues, have low hexokinase activities (Sutton, 1974, 1975b) but possess high activities of chloroplastic and cytosolic phosphoglucomutase, a freely reversible enzyme which catalyses the reaction

Figure 4.19 The activity of phosphohexose isomerase, isolated from *Kalanchoe daigremontiana* and assayed in the gluconeogenic direction, as a function of (A) pH and (B) [F-1,6-P_2].

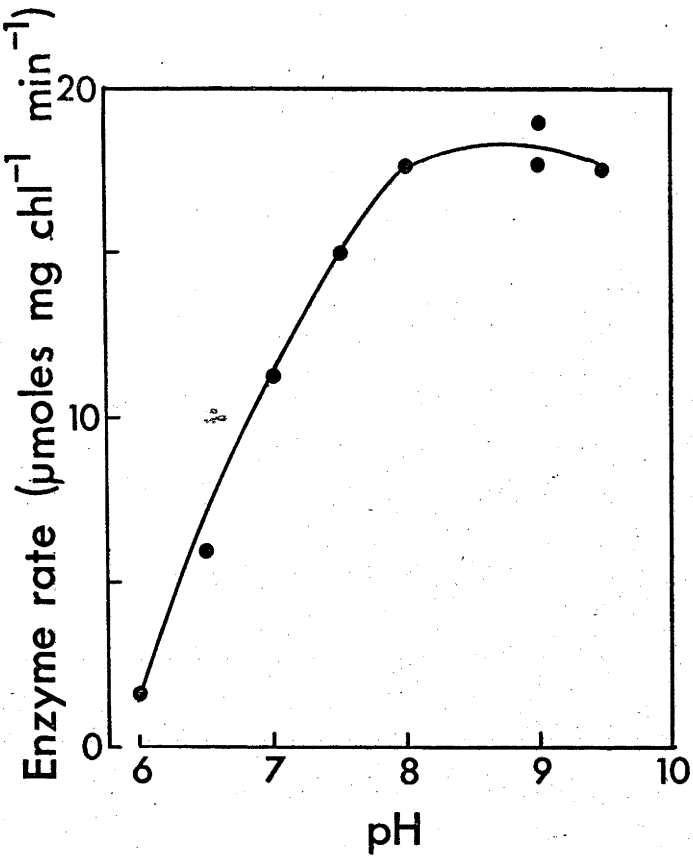
Enzyme rate (μmoles mg chl^{-1} min^{-1})
20
10
0
6
7
8
9
10
pH

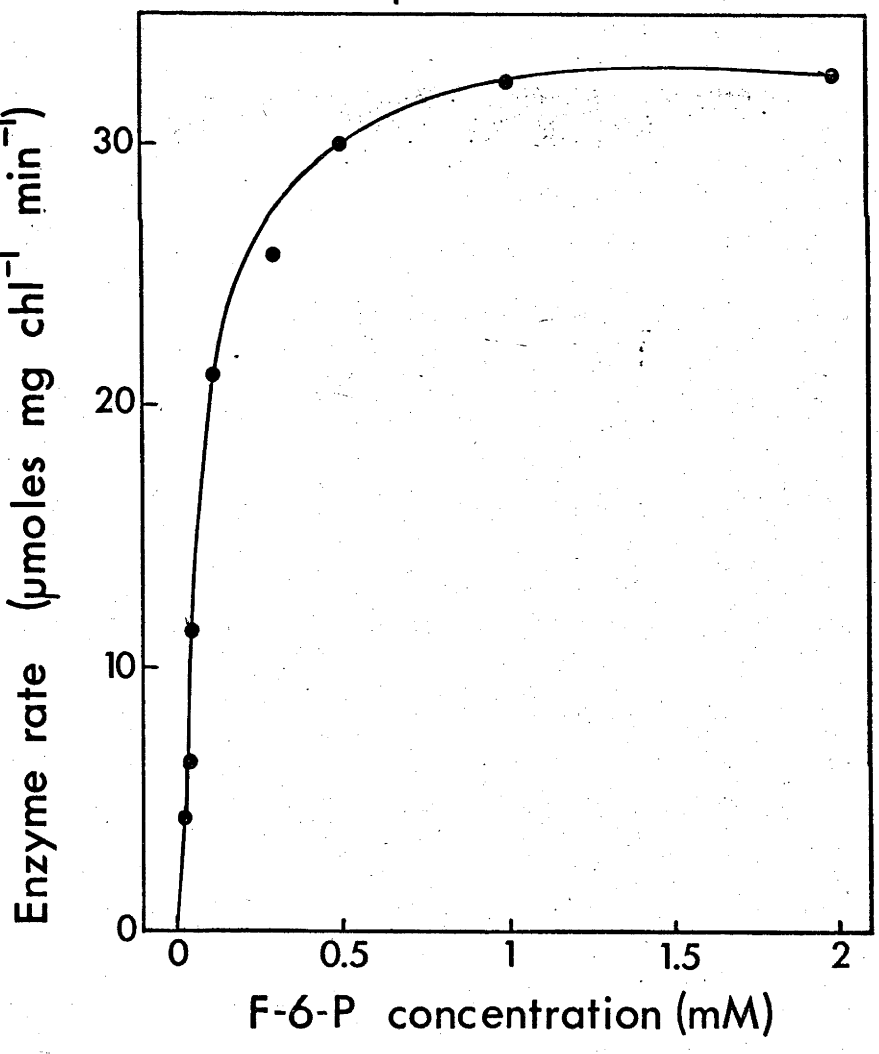
Enzyme rate (μmoles mg chl^{-1} min^{-1})
30
20
10
0
0
0.5
1
1.5
2
F-6-P concentration (mM)

Table 4.3 Relationship between the maximum observed rates of deacidification and the maximum *in vitro* activities of various glycolytic enzymes mostly assayed in the gluconeogenic direction, in 5 species of CAM plants.

Enzyme	Assay direction	Malic enzyme plants			PEPCK plants	
		Kalanchoe daigremontiana	*Bryophyllum pinnatum*	*Bryophyllum tubiflorum*	*Aloe arborescens*	*Stapelia gigantea*
Phosphohexose isomerase	↑[b]	13.6[a]	5.5	3.5	58.3	11.6
Phosphofructokinase	↓[c]	3.6	2.2	0.1(!)	3.5	2.9
Fructose-1,6-diphosphatase	↑	2.6	1.2	0.4	3.3	0.5
NADP G-3-P dehydrogenase	↑	10.0	-[d]	8.2	-	7.8
NAD G-3-P dehydrogenase	↑	18.5	-	13.2	13.7	64.6
PGA kinase	↑	39.7	-	25.9	82.5	76.5
PGA mutase	↑	7.9	-	5.6	20.8	11.3
PGA mutase	↓	0.8	-	1.3	9.1	3.4
Enolase	↓	0.6	-	0.8	4.1	3.5
Pyruvate Pi,dikinase[e]	↑	1.1	0.9	0.5	ND[f]	ND
Required flux predicted by deacidification[g]		≃ 0.73	≃ 0.75	≃ 0.75	≃ 1.85	≃ 1.7

a All activities are the mean of at least two determinations

b ↑ assayed in gluconeogenic direction

c ↓ assayed in glycolytic direction

d - not measured

e Data from Section 4.1

f ND not detected

g Data from Table 2

$$\text{Glucose-6-phosphate} + \text{glucose-1,6-diphosphate} \rightleftharpoons \text{Glucose-1-phosphate} + \text{glucose-1,6-diphosphate} \quad (3)$$

(Mühlbach and Schnarrenberger, 1978; Sutton, 1974; 1975b; Herbert *et al.*, 1979). The product, glucose-1-phosphate, is considered to be the precursor for chloroplast starch formation via ADP-glucose pyrophosphorylase and ADP-glucose-starch synthase shown in reaction 4.

$$\text{Glucose-1-phosphate} \xrightleftharpoons[\text{ADP-glucose pyrophosphorylase}]{\text{ATP} \;\; \text{PPi}} \text{ADP-Glucose} \xrightarrow[\text{ADP-glucose starch synthase}]{} \text{Starch} \quad (4)$$

(Preiss and Kosuge, 1970; Turner and Turner, 1975; Kelly *et al.*, 1976). The second physiologically irreversible reaction is the conversion of

$$\text{Fructose-6-phosphate} \xrightarrow{\text{ATP} \;\; \text{ADP}} \text{Fructose-1,6-diphosphate} \quad (5)$$

catalysed by phosphofructokinase, an enzyme formerly thought to be restricted to the cytoplasm but which has now been found in chloroplasts (Kelly and Latzko, 1975, 1977a, 1977b). Most tissues including CAM tissues (Satta and Sisini, 1964), contain acid and alkaline FDPases which catalyse the reverse reaction.

$$\text{Fructose-1,6-diphosphate} \xrightarrow{\text{Pi}} \text{Fructose-6-phosphate} \quad (6)$$

The activity of alkaline FDPase in CAM plants is similar to that of the phosphofructokinase (Table 4.3). It is unlikely, however, that phosphofructokinase competes for the products of FDPase in the chloroplast during gluconeogenesis since about 70% of the total alkaline FDPase activity, in spinach and in *Pisum*, is restricted to the chloroplast (Latzko and Gibbs, 1968; Baier and Latzko, 1975; Latzko *et al.*, 1974), whereas over 90% of the

phosphofructokinase activity is cytoplasmic (Kelly and Latzko, 1975). This might suggest that, depending upon the level of regulatory metabolites such as ATP, Pi, a PEP and malate, there is little transfer of carbon directly into sucrose within the cytoplasm during deacidifcation.

The third exergonic reaction

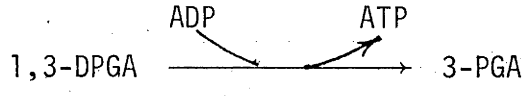

(7)

is mediated by PGA kinase. Although the thermodynamics favour ATP formation, the reaction will be reversed if the ratio of 3-PGA to 1,3-PGA exceeds 200:1 and if the adenylate energy charge is in the region 0.85-1.0 (Conn and Stumpf, 1972; Pacold and Anderson, 1973). Most photosynthetic tissues contain substantial amounts of 3-PGA in the light; spinach chloroplasts contain about 4 mM 3-PGA and the CAM plant *K. blossfeldiana* contains about 0.9 µmoles 3-PGA g^{-1} dry weight (about 0.3 µmoles mg chl^{-1})(Pierre and Queiroz, 1979). 1,3-DPGA concentrations are so low that under physiological conditions their direct estimation has not been possible (Bücher, 1947; Negelein, 1963). When the adenylate energy charge is high in the light it seems likely that this reaction would function adequately in the gluconeogenic direction.

The fourth physiologically irreversible reaction

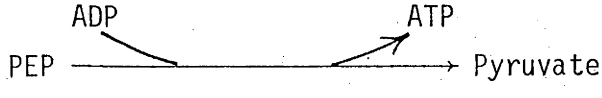

(8)

is mediated by pyruvate kinase. As discussed in the previous section malic enzyme CAM plants possess pyruvate, Pi dikinase, a light activated enzyme which circumvents this reaction.

The other glycolytic enzymes are freely reversible and present no real problems with respect to the operation of gluconeogenesis as long as their respective substrate and co-factors are present in adequate quantities. So if we assumed that the glycolytic enzymes found in CAM tissues are not radically different to the C_3 enzymes, in terms of substrate affinities and sensitivity to intermediates, then in actively deacidifying CAM plants in the light the flow of carbon from pyruvate and PEP to glucan, appears to be feasable.

As the enzymes measured in this study were from crude extracts no distinction was made between isoenzymes or compartmentally separated enzymes which catalyse identical reactions, except in the case where there was a clear distinction in pH optima between the acid and alkaline FDPases. All the glycolytic enzymes, with the exception of hexokinase, have been reported to be present, to various degrees, in both the chloroplast and the cytoplasm, (Kelly *et al.*, 1976). The evidence for chloroplastic PGA mutase, enolase and pyruvate kinase is indirect, and no PGA mutase or enolase was found in chloroplasts from the CAM plant *Sedum praealtum* (Spalding *et al.*, 1979). The possible importance of compartmentation and direct of indirect light activation of enzymes is discussed more fully in Chapter 5.

4.3 A Comparison of the Capacities of Photosynthetic and Glycolytic Enzymes in C_3 and CAM *Mesembryanthemum crystallinum*

4.3.1 Introduction

In the previous section CAM plants were shown to have the enzymes and activities needed to convert C_3 compounds to carbohydrates. More detailed work is required to determine what particular characteristics of particular enzymes are unique or essential to CAM. *Mesembryanthemum crystallinum*

represents a useful system in which some of these questions may be investigated, since CAM can be readily induced in expanded, mature leaves by water stress (Winter, 1973b, 1974). In this section the activities of a range of photosynthetic and glycolytic enzymes were compared in C_3 and CAM *Mesembryanthemum*. The activity of several enzymes involved in acidification, deacidification and glycolysis were also measured at 1-3 day intervals, over a 13 day period, during which CAM was induced in C_3 plants by increasing the NaCl concentration of the nutrient medium. The data will be discussed with reference to the functions of the particular enzymes in CAM and to the capacity of *Mesembryanthemum* to perform CAM.

4.3.2 Materials and methods

4.3.2.1 *Extraction methods*

Experimental material was grown in culture solution containing 100 mM NaCl as described in Section 2.1.2.1. The third and fourth foliar leaves, which were expanded before the NaCl concentration was increased, were used in all experiments (cf. Winter, 1973a). Two leaves were harvested 4 hours after the beginning of the light period and were illuminated for 20 minutes with 1,200 $\mu E\ m^{-2}\ s^{-1}$ supplied (Total area, - 36.2 cm^2) were then cut from the leaves with a cork borer and ground in a mortar and pestle with 15 ml of ice cold buffer containing 100 mM HEPES-NaOH, pH 8.0, 5 mM DTT, 0.5% (w/v) BSA and 0.5% (w/v) PVP 40. The brei was passed through two layers of Miracloth and 10 ml was transfered to a test tube to which 5 mM $MgCl_2$ was added. Samples were taken from both fractions for chlorophyll determinations. After 5 minutes centrifugation at 10,000 x g and 0-4°C, each supernatant was split into two fractions, one of which was immediately used for assays and the second was passed through a column (0.5 cm x 15.0 cm) of G-25 Sephadex

previously equilibrated at 0°C with a buffer containing 25 mM Bicine 25 mM HEPES - NaOH pH 8.0, 2 mM DTT and with or without 2 mM $MgCl_2$. The extract without $MgCl_2$ was used in the assay of NADP MDH to minimise interference from NADP malic enzyme which has a magnesium requirement.

When pyruvate, Pi dikinase was to be measured the tissue was extracted, after illumination, in 15 ml of ice cold buffer containing 100 mM HEPES-NaOH, pH 8.0, 2.5 mM K_2HPO_4, 2.5 mM pyruvate, 5 mM DTT, 1 mM EDTA, 10 mM $MgCl_2$, 0.5% (w/v) ascorbate and 0.5% (w/v) PVP 40. Subsequent filtration, centrifugation, ammonium sulphate fractionation and gel filtration were performed at room temperature as described in Section 4.1.2.1.

For RuP_2 carboxylase measurements the tissue was extracted at 0°C in 10 ml of buffer containing 100 mM Bicine-NaOH 25 mM TES-NaOH, pH 8.0, 5 mM $MgSO_4.7H_2O$, 1 mM EDTA, 10 mM $NaHCO_3$ and 0.5 mM DTT. The extract was centrifuged for 5 minutes at 4000 x g and immediately assayed.

4.3.2.2 *Assay methods*

With the exception of RuP_2 carboxylase which was measured using a radioisotope method and PEP carboxykinase which was measured by following the extinction of OAA at 280 nm, all enzymes were measured at 25°C by following the change of absorbance at 340 nm in a 3 ml reaction mix containing a pyridine nucleotide, using methods described in Section 4.1 and 4.2.

RuP_2 carboxylase (3-phospho-D-glycerate carboxy-lyase (dimerising), E.C. 4.1.1.39), RuP_2 carboxylase was routinely measured using a radioisotope assay, however a spectrophotometric assay was used as a

double check. The resultant RuP_2 carboxylase activities were within 3% of each other.

Radioisotope assay: 25 µl or 50 µl of crude extract was added to a buffer containing 25 mM TES-NaOH, 25 mM Bicine-NaOH, pH 8.0, 20 mM $MgCl_2$ and 20 mM $NaH^{14}CO_3$ in a scintillation vial. The reaction was initiated with 1 mM RuP_2 (to give a total volume of 0.5 ml) and killed after various intervals with 20% trichloroacetic acid. The reaction mix was then blown dry prior to counting in a scintillation counter.

Spectrophotometric assay (adapted from Lilley and Walker, 1974):

50 mM HEPES-NaOH, pH 7.8, 15 mM $MgCl_2$, 1 mM EDTA, 5 mM DTT, 5 mM ATP, 1 mM NADH, 10 mM $NaHCO_3$, 2.5 units G-3-P dehydrogenase, 4 units PGA kinase, 5 mM phosphocreatine, 1 unit creatine phosphokinase and extract. The reactions were started after 5 minutes preincubation by the addition of 5 mM ribose-5-P.

4.3.3 Results

The *in vitro* activities of various photosynthetic and glycolytic enzymes in C_3 and CAM *Mesembryanthemum* leaves are shown in Table 4.4. The activities are expressed on both a chlorophyll and a leaf area basis since the CAM tissues contain about 1.5 times as much chlorophyll per gram fresh weight as the C_3 tissue. In general the enzymes from the CAM tissues have higher activities on both chlorophyll and leaf area bases. The exceptions are G-6-P dehydrogenase which is slightly more active in the C_3 tissue and hexokinase, RuP_2 carboxylase and phosphofructokinase the

Table 4.4 Activities of various photosynthetic and glycolytic enzymes in C_3 and CAM *Mesembryanthemum crystallinum*.[a]

Enzyme	Assay direction	*Mesembryanthemum crystallinum* C_3	CAM	C_3	CAM
		µmoles mg chl^{-1} min^{-1}		µmoles cm^{-2} min	
Carboxylases					
PEP carboxylase (pH 7.0)		0.4	17.9	0.016	0.645
RuP_2 carboxylase[b]		2.1	2.1	0.067	0.076
Decarboxylases					
NADP malic enzyme		0.1	0.4	0.010	0.023
PEP carboxykinase		ND[c]	ND	ND	ND
Other photosynthetic enzymes					
NAD malate dehydrogenase		53.4	195.4	-[d]	-
NADP malate dehydrogenase (pH 8.0)		0.1	1.8	0.005	0.065
Aspartate aminotransferase		0.5	1.1	-	-
Alanine aminotransferase		1.5	2.1	-	-
Pyruvate, Pi dikinase		ND	1.0	ND	0.037
Glycolytic enzymes					
Pyruvate kinase	↓	ND	ND	ND	ND
Enolase[e]	↓	2.1	4.2	0.073	0.148
PGA mutase	↓	1.7	3.6	0.059	0.127
PGA mutase	↑	1.6	17.9	0.054	0.634
PGA kinase	↑	18.0	28.0	0.624	0.991
NAD G-3-P dehydrogenase[e]	↑	10.1	44.1	0.350	1.561
NADP G-3-P dehydrogenase	↑	6.1	8.5	0.211	0.300
Fructose-1,6-bisphosphate[e,f]	↑	0.3	0.53	0.010	0.019
Phosphofructo kinase[f]	↑	1.0	1.0	0.033	0.036
Phosphohexose isomerase[f]	↓	7.5	27.0	0.256	0.956
G-6-P dehydrogenase[f]	↑	0.3	0.1	-	-
Hexokinase[f]	↓	< 0.2	< 0.2	-	-
Maximum observed rate of deacidification		ND	0.43	ND	0.015

a Each figure, with the exception of PEP carboxykinase G-6-P dehydrogenase, pyruvate kinase and hexokinase is the mean of at least 2 determinations on two separate occasions.

b Assayed using spectrophotometric method

c ND not detected

d - not determined

e Data for crude, unsephadexed extracts

f Each mole of activity represents the formation or breakdown of 2 moles of pyruvate.

activities of which on a chlorophyll basis, are the same in both C_3 and CAM tissues although the latter two enzymes have slightly higher activities in the CAM tissue on a leaf area basis.

Pyruvate, Pi dikinase was found in the CAM tissue, but not in the C_3 tissue, and PEP carboxykinase was absent from both tissues. Adenylate kinase interferred with pyruvate kinase assays as reported for *Kalanchoe* in Section 4.1.

In a subsequent experiment, the capacities of most of the same enzymes were measured at regular intervals during the development of CAM. This was induced by increasing the NaCl concentration of the growth medium from 100 mM to 400 mM and was complete about 13 days after the initial increase in the NaCl concentration (cf. Greenway *et al.*,1978). The plants gradually developed the large day/night fluctuations in malate content which are characteristic of CAM tissues (Figure 4.20) and the malate concentration at the end of the light period also increased up until about the seventh day.

The activities of PEP carboxylase, NADP MDH, NADP malic enzyme, pyruvate, Pi dikinase, PGA mutase, NAD G-3-P dehydrogenase and phosphohexose isomerase increased markedly during the induction of CAM whilst NADP G-3-P dehydrogenase and FDPase activities increased only marginally (Figures 4.21 to 4.26).

PEP carboxylase activity increased over 70 fold from about 0.25 to 18.0 μmoles mg chl^{-1} min^{-1} (Figure 4.21). Although maximum dark acidification was not achieved until about the 12th day after increasing the NaCl concentration, the PEP carboxylase activity at day 2 was

Figure 4.20 The effect of increased NaCl concentration of the growth medium on day/night malate fluctuations in *M. crystallinum*. The open circles (o) represent the malate content of the leaves at the end of the light period, and the closed circles (●) represent the malate content at the end of the dark period.

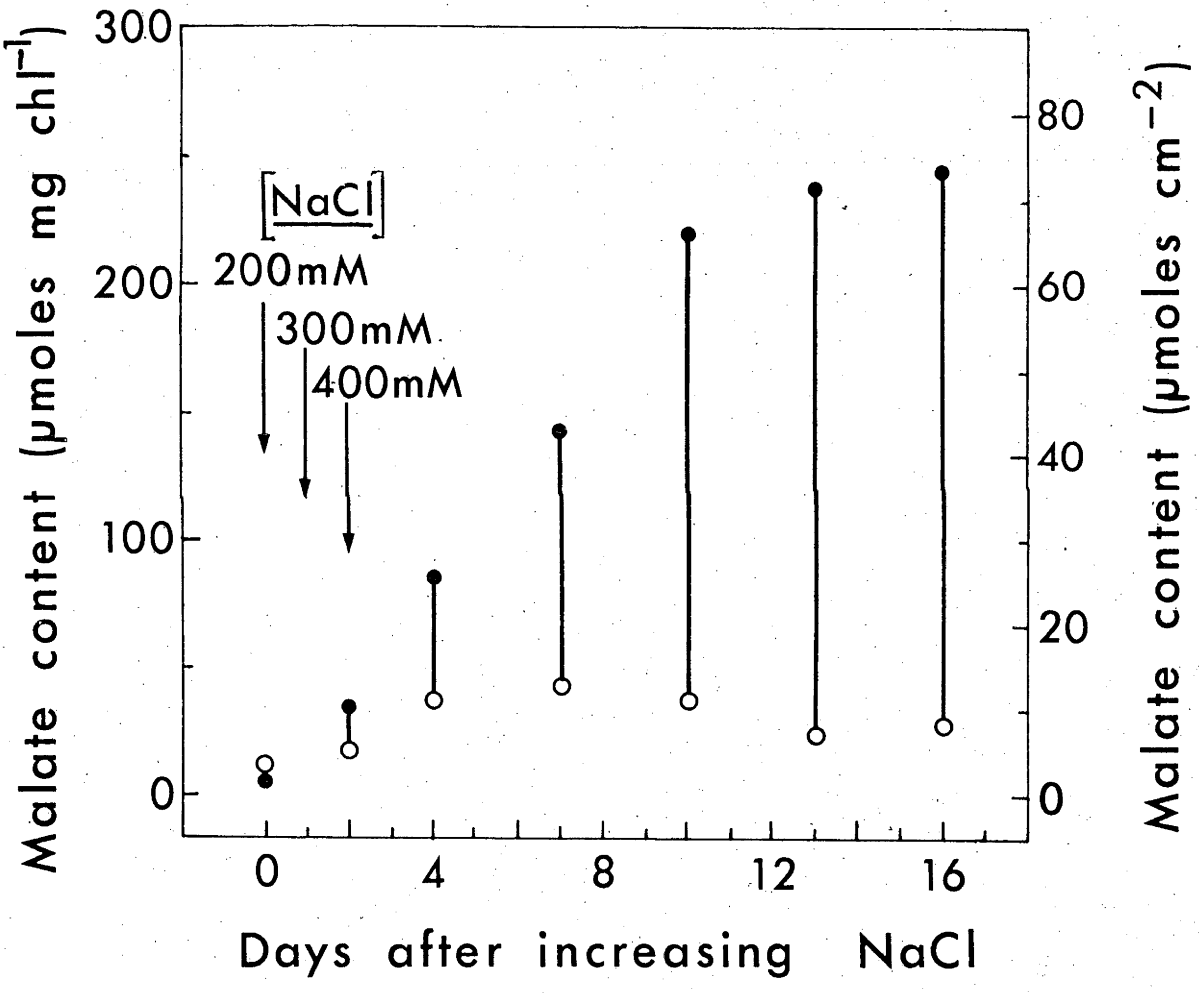
Malate content (μmoles mg chl^{-1})
300
200
100
0
[NaCl]
200mM
300mM
400mM
0
4
8
12
16
Days after increasing NaCl
80
60
40
20
0
Malate content (μmoles cm^{-2})

Figure 4.21 Change in the extractable activity of PEP carboxylase during the induction of CAM in *M. crystallinum*. Crude extracts (▲ —— ▲), extracts filtered through G-25 Sephadex (● —— ●).

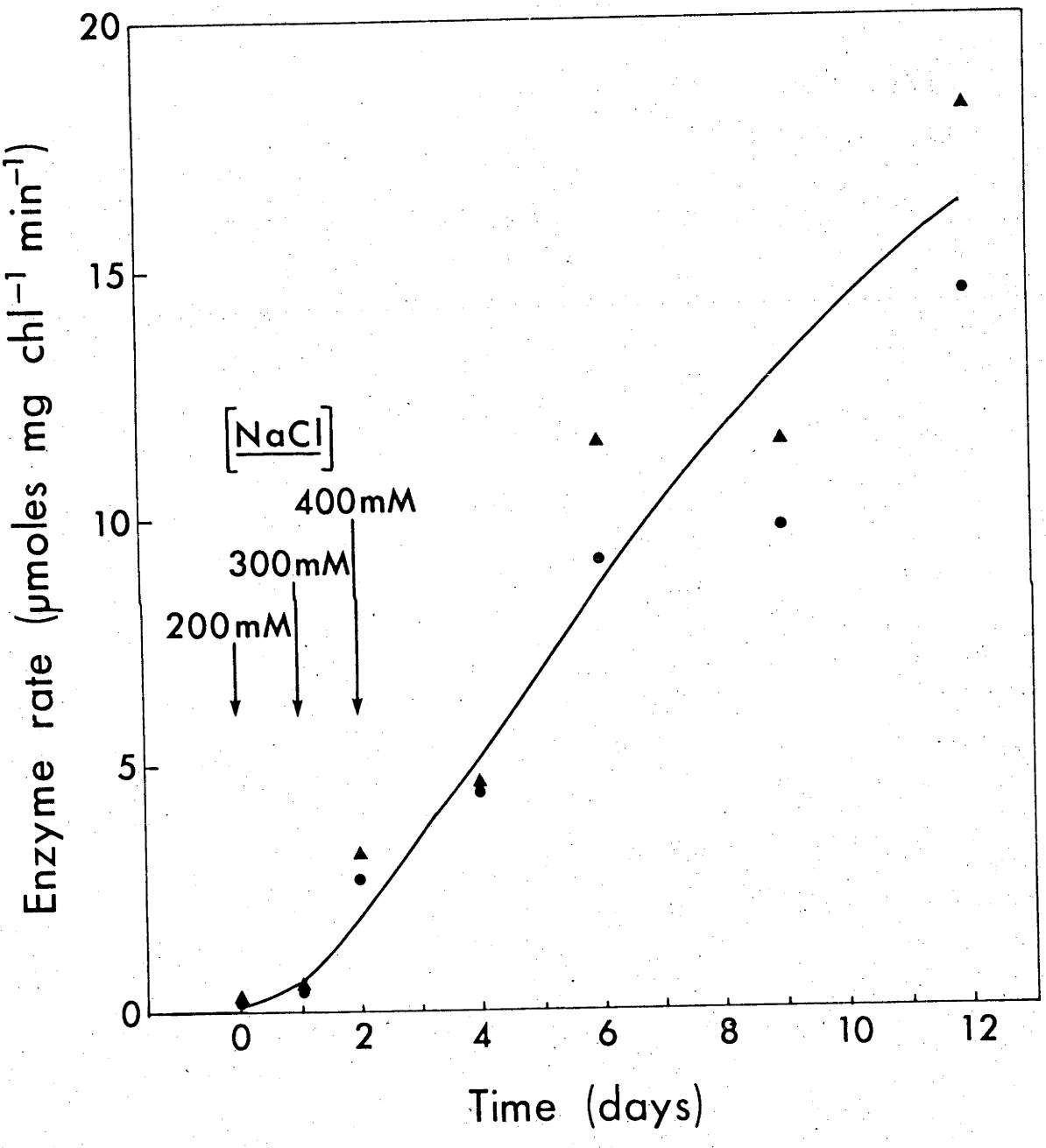
20
15
10
5
0
Enzyme rate (μmoles mg chl^{-1} min^{-1})
[NaCl]
400mM
300mM
200mM
0
2
4
6
8
10
12
Time (days)

sufficient to account for the maximum rates of acidification observed in the CAM tissue even when the difference between the night acidification temperature (17°C) and the assay temperature (25°C) was taken into account (PEPC has a Q_{10} of about 2.7; Greenway *et al.*, 1978).

Pyruvate, Pi dikinase activity was low or absent in the C_3 tissue but gradually increased during the induction period until, by about day 9, the activity was sufficient to account for the maximum observed rates of deacidification (Figure 4.22). Final pyruvate, Pi dikinase activity was only about 1/30th of that observed for PEP carboxylase and a little over a half that observed for pyruvate, Pi dikinase in earlier experiments (Table 4.4).

NADP malic enzyme capacity increased from about 0.2 to 0.5 µmoles mg chl^{-1} min^{-1} during the induction of CAM (Figure 4.23). This increase was smaller than that observed in preliminary experiments and in the literature (Greenway *et al.*, 1978; Winter and Greenway, 1978). The enzyme was present in marginally sufficient capacity to account for the maximum rates of deacidification. The enzyme activity appeared to be greater in extracts which had been filtered through G-25 Sephadex.

Surprisingly, NADP MDH from C_3 *Mesembryanthemum* exhibited a pH optimum at about pH 6, however the enzyme from the CAM tissue exhibited two optima, one at pH 6 and a slightly smaller optimum at pH 8 (Figure 4.24A). The activity at pH 6.0 did not change during the induction of CAM but the activity at pH 8.0 increased 10 fold from 0.015 to 0.15 µmoles mg chl^{-1} min^{-1} (Figure 4.24B and C). Preliminary tests indicated that malate was the product of NADPH oxidation at both pH 6.0 and 8.0.

Figure 4.22 Change in the activity of pyruvate, Pi dikinase during the induction of CAM in *M. crystallinum*. The dotted line (---) represents the maximum rate of deacidification observed in leaf slices.

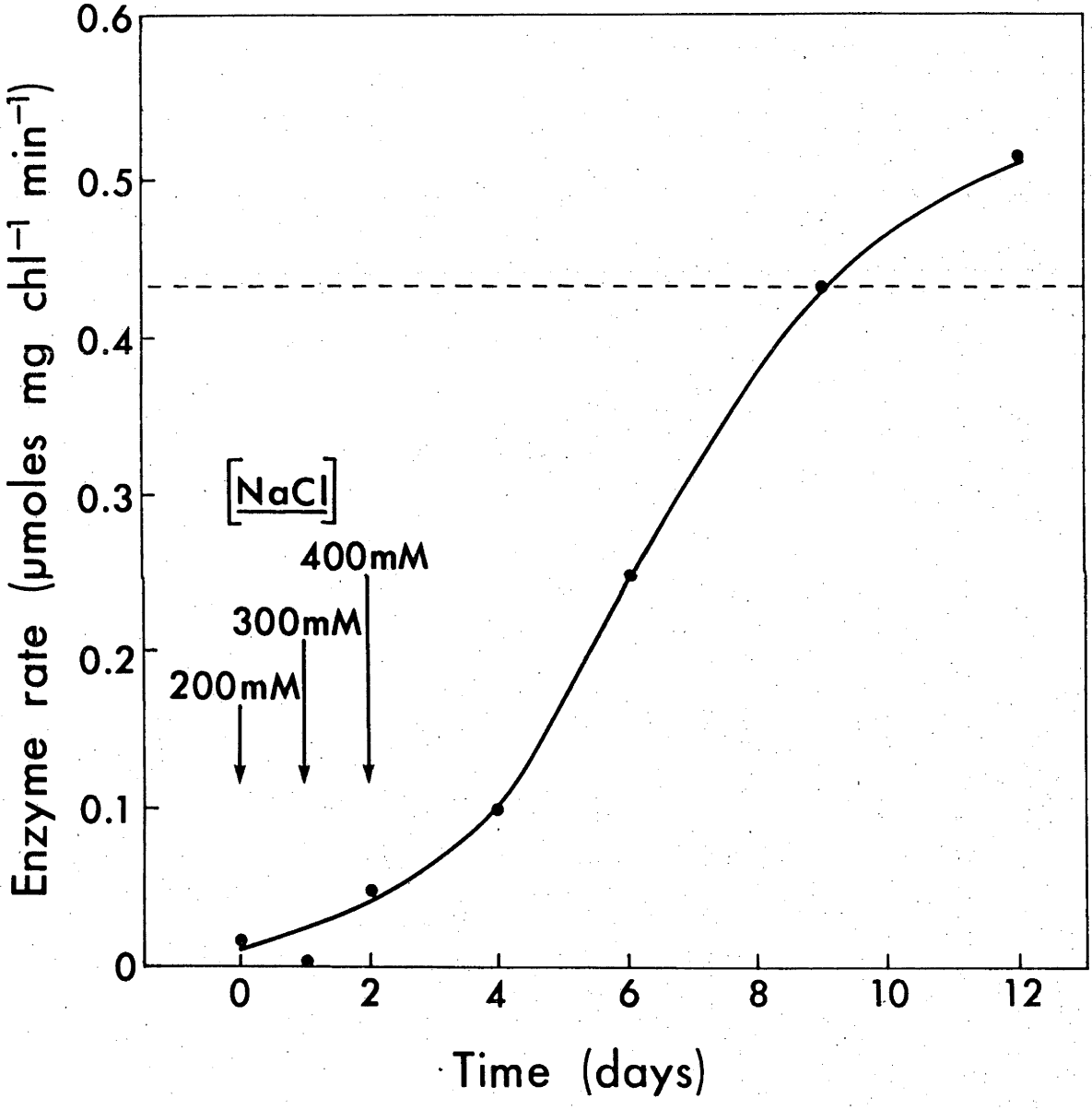
0.6
0.5
0.4
0.3
0.2
0.1
0
Enzyme rate (μmoles mg chl^{-1} min^{-1})
[NaCl]
400mM
300mM
200mM
0
2
4
6
8
10
12
Time (days)

Figure 4.23 Change in the extractable activity of NADP malic enzyme during the induction of CAM in *M. crystallinum*. Crude extracts (▲ —— ▲) extracts filtered through G-25 Sephadex (● —— ●). The dotted line represents the maximum rate of deacidification observed in leaf slices.

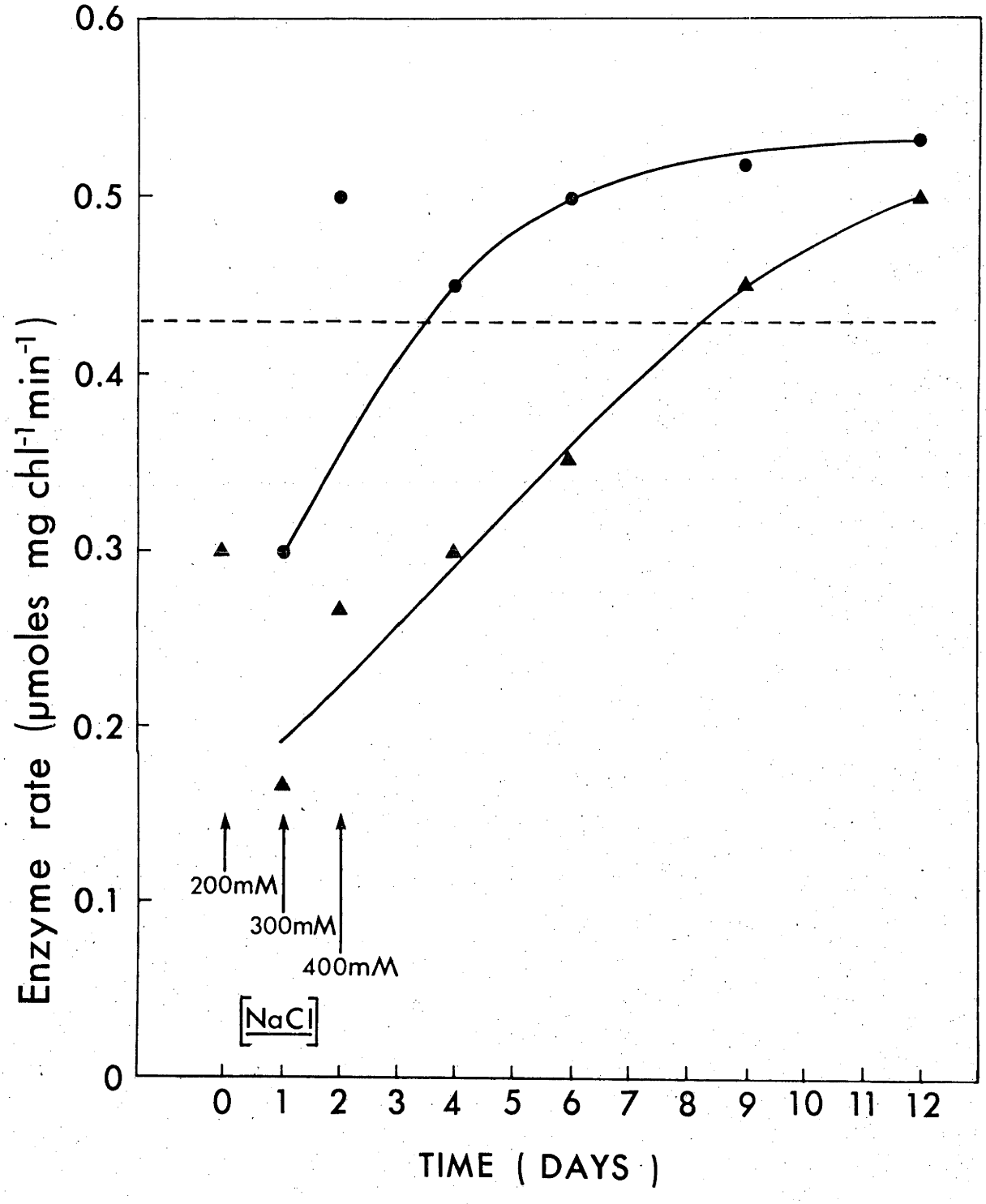
0.6
0.5
0.4
0.3
0.2
0.1
0
Enzyme rate (μmoles mg chl^{-1} min^{-1})
200mM
300mM
400mM
[NaCl]
0 1 2 3 4 5 6 7 8 9 10 11 12
TIME (DAYS)

Figure 4.24 A. pH response of NADP MDH from C_3 *M. crystallinum* (day 1, o —— o) and from CAM *M. crystallinum* (day 12, ● —— ●).

B. Activity of NADP MDH, assayed at pH 6.0, during the induction of CAM.

C. Activity of NADP MDH, assayed at pH 8.0, during the induction of CAM.

Crude extracts (▲ —— ▲), extracts filtered through G-25 Sephadex (● —— ●). Dotted line (---) indicates the maximum rate of deacidification observed in leaf slices.

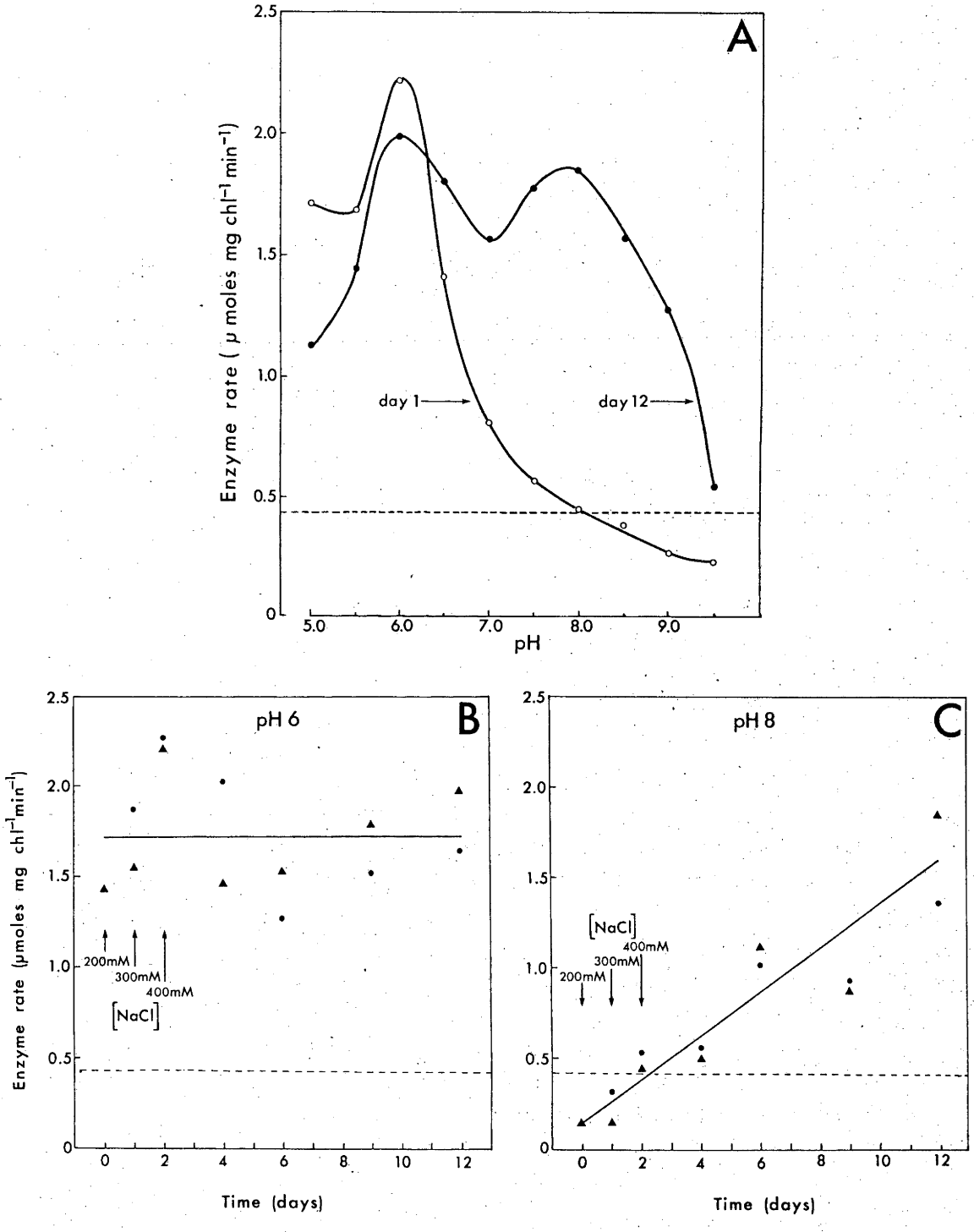
A
Enzyme rate (μ moles mg chl⁻¹ min⁻¹)
pH
day 1
day 12
B
pH 6
Enzyme rate (μmoles mg chl⁻¹min⁻¹)
200mM
300mM
400mM
[NaCl]
Time (days)
C
pH 8
[NaCl]
200mM
300mM
400mM
Time (days)

The activity of PGA mutase from C_3 *Mesembryanthemum* was similar when measured in the glycolytic and gluconeogenic directions, however during the induction of CAM the gluconeogenic activity increased about 13 fold whilst the glycolytic activity increased by only 3 fold (Figure 4.25).

NAD G-3-P dehydrogenase activity in crude extracts increased about 4-fold during the induction period, however considerable activity was lost during gel filtration and the filtered extracts showed only a 2-fold increase (Figure 4.26). Nevertheless, even in the C_3 tissue, the NAD G-3-P dehydrogenase activity was at least 20-fold greater than the maximum required during deacidification.

In contrast to NAD G-3-P dehydrogenase, the NADP activity increased by only about 20% during the induction of CAM (Figure 4.26). As with the NAD enzyme the NADP activity was at least 10 fold greater than that required during deacidification.

As with NAD G-3-P dehydrogenase, FDPase activity in gel filtered extracts was much lower than that observed in crude extracts (Figure 4.27). Whereas the filtered extracts exhibited no change in activity on a chlorophyll basis, the FDPase activity in the crude extracts increased from about 0.35 to 0.55 μmoles mg chl^{-1} min^{-1} during the induction of CAM.

Phosphohexose isomerase activity remained unchanged until day 2 after whicl it increased from 7.5 μmoles mg chl^{-1} to about 28.5 μmoles mg chl^{-1} min^{-1} by day 12 (Figure 4.27). The phosphohexose isomerase activity in the C_3 tissue was 30 fold higher than that required for maximum deacidification.

Figure 4.25 Change in the extractable activity of PGA mutase during the induction of CAM in *M. crystallinum*. The enzyme was assayed in the gluconeogenic direction (crude extract, ▲ —— ▲, extract filtered through G-25 Sephadex ● —— ●) and in the glycolytic direction (crude extract Δ —— Δ, extract filtered through G-25 Sephadex o —— o). The dotted line represents the maximum rate of deacidification observed in leaf slices.

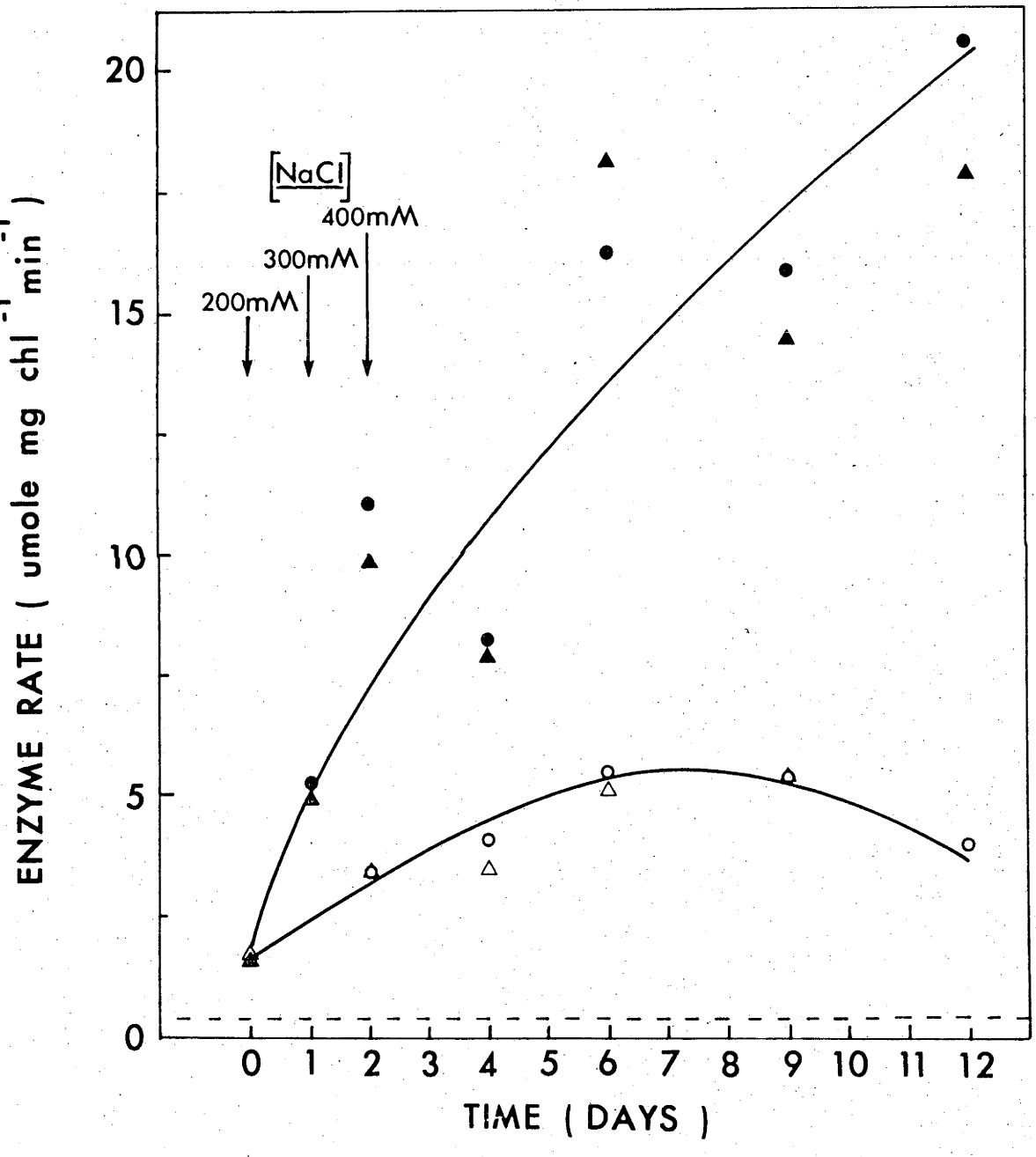
ENZYME RATE (umole mg chl^{-1} min^{-1})
TIME (DAYS)
[NaCl]
200mM
300mM
400mM
0
5
10
15
20
0 1 2 3 4 5 6 7 8 9 10 11 12

Figure 4.26 A. Change in the gluconeogenic activity in NADP G-3-P dehydrogenas observed during the induction of CAM in *M. crystallinum*.

B. Change in the gluconeogenic activity in NAD G-3-P dehydrogenase

Crude extracts (▲ —— ▲), extracts filtered through G-25 Sephadex (● —— ●). Dotted line (---) indicates the maximum rate of deacidification observed in leaf slices.

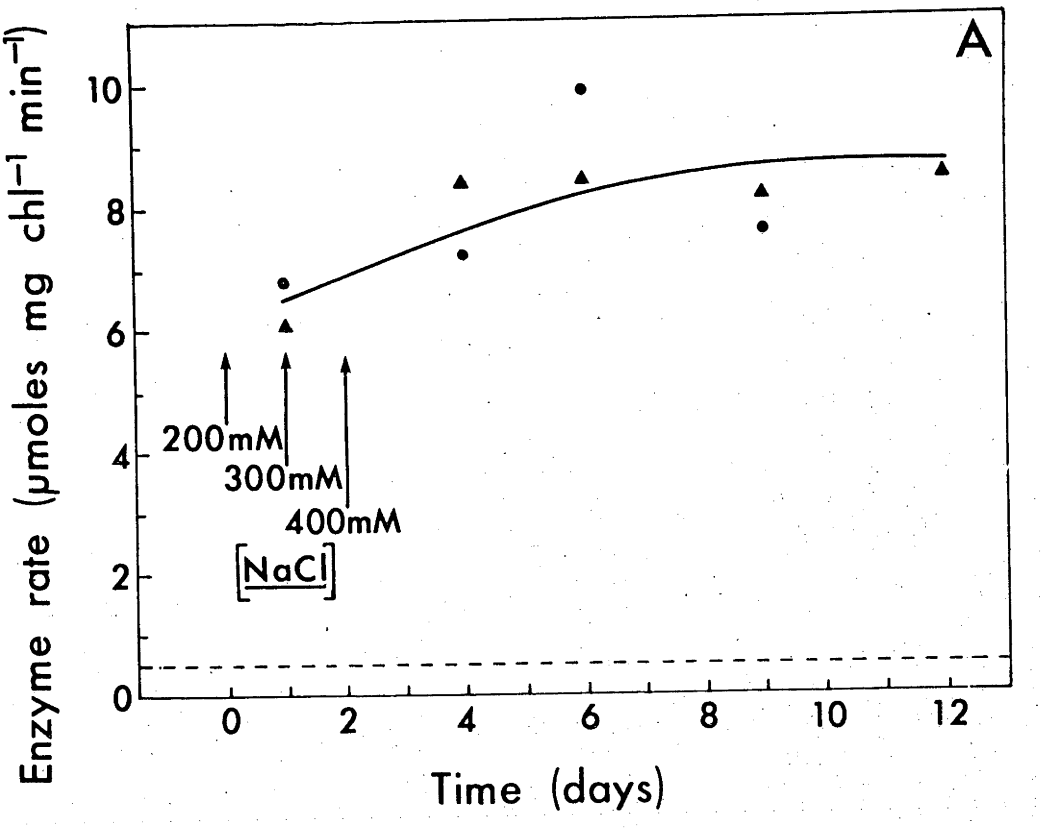
A
Enzyme rate (μmoles mg chl^{-1} min^{-1})
10
8
6
4
2
0
200mM
300mM
400mM
[NaCl]
0
2
4
6
8
10
12
Time (days)

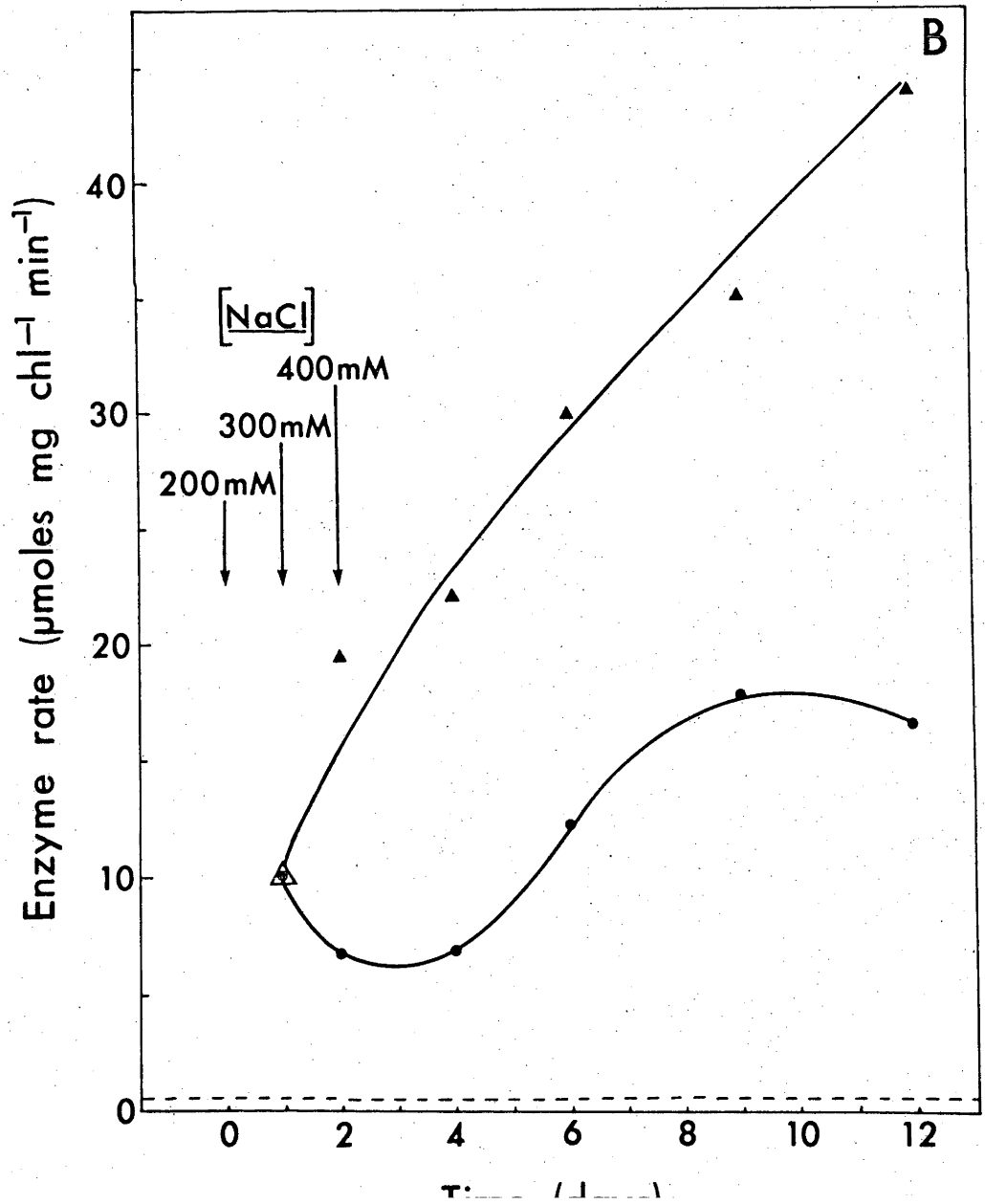
B
Enzyme rate (μmoles mg chl^{-1} min^{-1})
40
30
20
10
0
[NaCl]
400mM
300mM
200mM
0
2
4
6
8
10
12

Figure 4.27 A. Change in activity of alkaline FDPase during the induction of CAM in *M. crystallinum*.

B. Change in gluconeogenic activity of phosphohexose isomerase during the induction of CAM in *M. crystallinum*.

Crude extract (▲ —— ▲), extract filtered through G-25 Sephadex (● —— ●). Dotted line (---) indicates the maximum rate of deacidification observed in leaf slices.

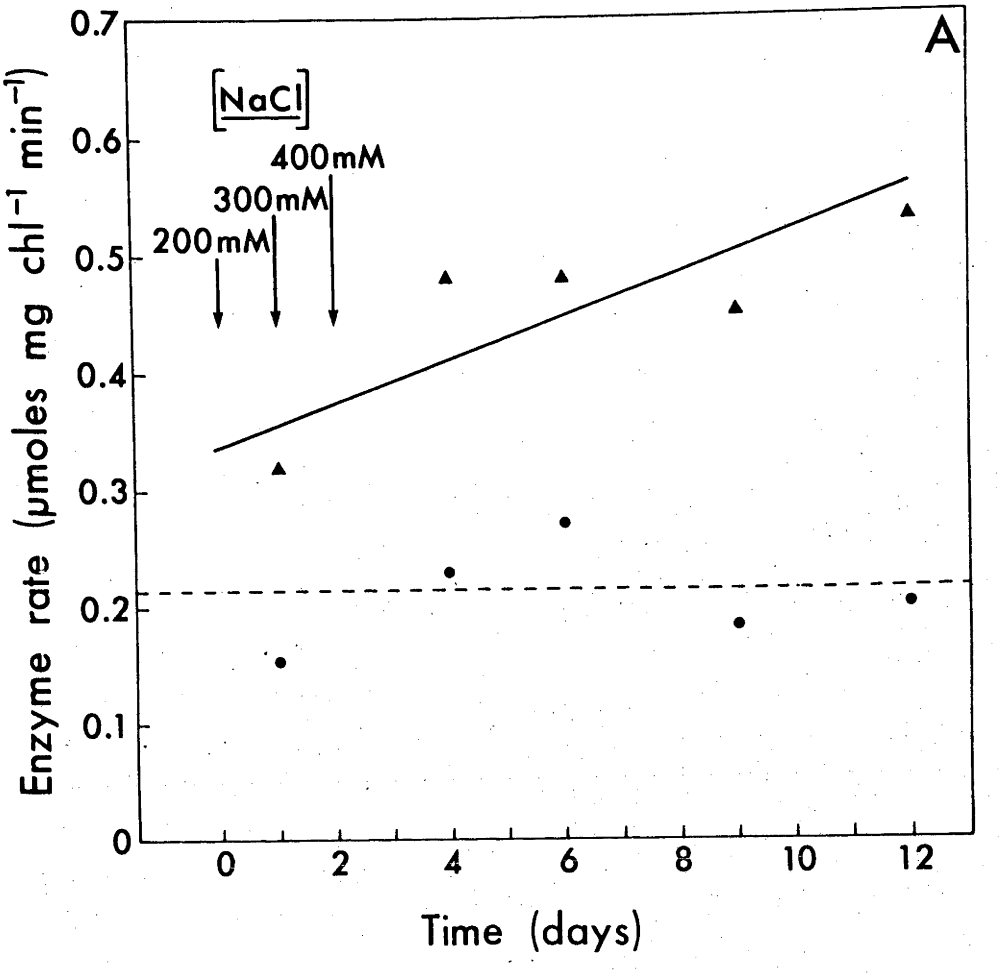
A
[NaCl]
200mM
300mM
400mM
Enzyme rate (μmoles mg chl⁻¹ min⁻¹)
0.7
0.6
0.5
0.4
0.3
0.2
0.1
0
0
2
4
6
8
10
12
Time (days)

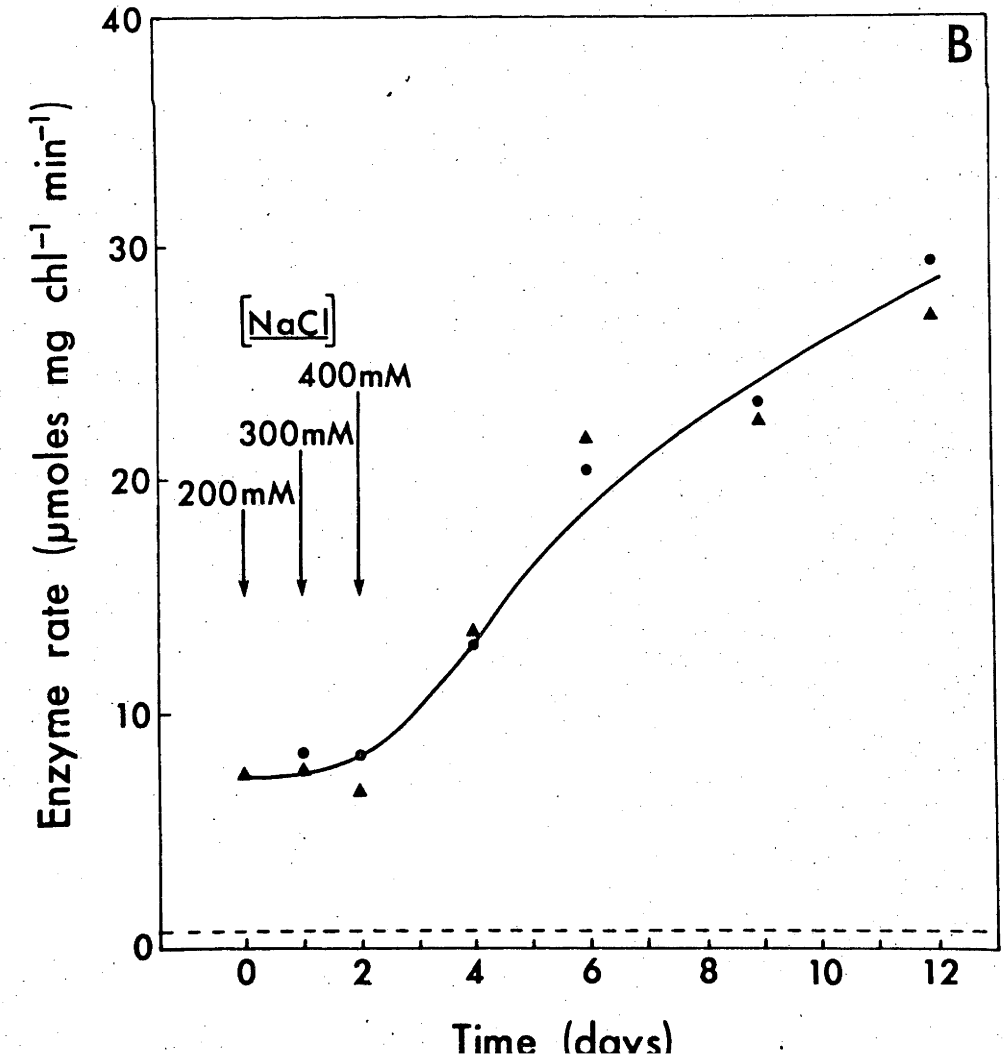
B
[NaCl]
200mM
300mM
400mM
Enzyme rate (μmoles mg chl⁻¹ min⁻¹)
40
30
20
10
0
0
2
4
6
8
10
12
Time (days)

In the preliminary experiment no differences were observed in the activities of FDPase, phosphofructokinase, NADP malic enzyme and PGA mutase (assayed in both directions) isolated from C_3 *Mesembryanthemum* in the late light period and in the dark.

4.3.4 Discussion

The induction of CAM in *M. crystallinum* involves changes in many physiological processes, such as nocturnal stomatal opening and a capacity for malic acid transport into cell vacuoles, as well as changes in biochemical systems (Winter and Lüttge, 1976). Only the latter have been studied here and it is evident that the induction of CAM is accompanied by changes in enzymes responsible for malic acid synthesis in the dark, as well as for its utilisation in the light.

The activities of PEP carboxylase, NADP malic enzyme and NADP MDH increased from levels below those necessary for maximum rates of malate synthesis and decarboxylation to levels adequate to support these processes. *M. crystallinum* had no detectable PEPCK activity before or after the induction of CAM, but it is not known whether CAM *Mesembryanthemum* also possess substantial NAD malic enzyme activity in common with some other NADP malic enzyme plants, notably those from the family Crassulaceae.

The increase in pyruvate, Pi dikinase activity which accompanied the induction of CAM in *M. crystallinum* is consistent with the observation that malic enzyme (NADP or NAD) and not PEPCK is the principal decarboxylase of CAM in this species. Although the activities are low, the activities are greater than the maximum rates of deacidification observed in intact tissue. The low activity of this enzyme suggests that the conversion of pyruvate to PEP following malate decarboxylation may be important in the regulation of CAM in *M. crystallinum*.

Several other enzymes of gluconeogenesis increased in activity during the induction of CAM. However, the activity of these enzymes, even before the induction of CAM, is very much in excess of the carbon fluxes through CAM, and it is difficult to assess the significance of the changes observed.

The activities of PEP carboxylase, NADP malic enzyme and pyruvate, Pi dikinase increase much more rapidly than does the capacity of the intact tissue to synthesise and degrade malic acid. It is possible that acidification is limited by some other factor(s) such as PEP supply, or the tissue may not have fully developed the ability to store malic acid in the vacuole which might result in malate inhibition of PEP carboxylase (Greenway *et al.*, 1978).

The responses of some of the other enzymes to the induction of CAM are harder to interpret. The pH optimum for NADP MDH of pH 6.0 is surprisingly low compared with the enzyme from C_3 and C_4 plants which has an optimum of about pH 8.0-8.9 depending upon the OAA concentration (Johnson and Hatch, 1970). However, during the induction of CAM in *Mesembryanthemum* the activity at pH 8.0 increases although there is no change of activity at pH 6.0. A similar double peak was observed for the *Kalanchoe* enzyme described in Section 4.2. It appears quite possible that an isoenzyme of NADP MDH is synthesised during the induction process. A particular role for this enzyme is not evident in present models of the biochemistry of CAM in malic enzyme plants, but it may well be needed to sustain dicarboxylate shuttles between compartments (Chapter 5).

It is similarly difficult to assess the relevance of the large increases in the gluconeogenic activities of PGA kinase, NAD G-3-P dehydrogenase, phosphohexose isomerase, the large increase of the activity

of PGA mutase in gluconeogenic direction, but not in the glycolytic direction, and the small increases in the capacities of enolase, NADP G-3-P dehydrogenase and FDPase. It is possible that the high capacity of PGA mutase to operate in the gluconeogenic direction enables enolase to function in the gluconeogenic direction and to compete more effectively with any residual PEP carboxylase activity for PEP.

The increase in FDPase activity is small and probably not directly related to the presence of CAM. The low FDPase activity, however, suggests that FDPase may play a regulatory role similar to that proposed for pyruvate, Pi dikinase. FDPase from chloroplasts is activated by Mg^{2+}, DTT, F-1,6-P_2 and possibly by reduced ferredoxin and a small protein factor (Baier and Latzko, 1975; Buchanan *et al.*, 1971). As a result the enzyme is thought to be active in the light but inactive in the dark.

Pierre and Queiroz (1979) have reported large increases in the capacities of phosphofructokinase, aldolase, NAD G-3-P dehydrogenase, PGA mutase and enolase (all measured in the glycolytic direction) during the induction of CAM in *Kalanchoe blossfeldiana*. In *K. blossfeldiana*, CAM was induced by altering the photoperiod, not by increasing water stress. As in *Mesembryanthemum*, the activities of these enzymes before induction of CAM were much higher than that required for maximum acidification and deacidification in CAM. In *K. blossfeldiana* the leaves which performed C_3 photosynthesis are small and immature and expand considerably during the induction of CAM (unlike in *Mesembryanthemum*). Some of the differences in enzyme capacities in *K. blossfeldiana* may thus be the result of developmental differences. Regretably, these authors did not include controls which would enable us to distinguish changes in activity associated with CAM from those associated with leaf development.

4.4 General Conclusion

The data presented in Sections 4.1-3, support the hypothesis proposed in Section 1.4 for the conversion of pyruvate and PEP to carbohydrate and also support the data presented in Chapters 2 and 3. The presence of pyruvate, Pi dikinase in malic enzyme CAM plants and not in PEPCK CAM plants explains why exogenous ^{14}C-pyruvate was not readily metabolised to carbohydrate in *Stapelia*.

CAM plants have the capacity to convert pyruvate or PEP to carbohydrate via gluconeogenesis during deacidification in the light at the rates observed for starch accumulation. It should not be assumed, however, that this capacity is altogether peculiar to CAM tissues. All tissues which possess the PCR cycle have the ability to perform at least partial gluconeogenesis in the light since the reactions involved in the transfer of carbon from 3-PGA to carbohydrates are similar, and may even involve the same enzymes in the same organelle. CAM tissues appear to differ with respect to their ability to convert pyruvate or PEP to 3-PGA. This difference is partly a result of the different carbon sources in C_3 and CAM plants. In C_3 plants CO_2 is the sole source of carbon during the light whilst in CAM plants, during deacidification, carbon from pyruvate, PEP and CO_2 is converted to carbohydrate. Data presented in this chapter are used to prepare schemes for carbon metabolism in CAM plants during malate decarboxylation outlined in the next chapter.

5 DISCUSSION

The data presented in this study are consistent with the operation of gluconeogenesis in the light during deacidification in CAM plants. Two schemes for gluconeogenesis, one for malic enzyme CAM plants and one for PEPCK CAM plants, which are based on the present understanding of enzyme complement, enzyme capacities, enzyme localisation, and metabolite transport, are presented in Figure 5.1 and 5.2. Each scheme is accompanied by a balance sheet showing the overall equation and energy cost of the reactions involved in converting malate to glucan in the light.

Although the schemes are obviously incomplete, they illustrate the problem areas in the biochemistry of CAM. They also serve to indicate why gluconeogenesis is favoured over other possible fates of pyruvate metabolism in the light, and why starch synthesis is favoured over sucrose synthesis during deacidification.

5.1 Schemes for Gluconeogenesis During Deacidification

5.1.1 Enzyme localisation

The overall formats of the proposed schemes are dictated by current concepts of enzyme localisation in CAM plants. The literature on enzyme localisation in CAM tissues is, as discussed in the introductory chapter, one of contradictory reports which may reflect the different enzyme localisation in different species, but which is more likely to reflect imprecise organelle separations. Recent evidence suggests that PEPCK, NADP malic enzyme, enolase and PGA mutase are exclusively cytoplasmic (Spalding *et al.*, 1979; Dittrich, unpublished), NAD malic enzyme is mitochondrial (Dittrich, 1976; Spalding *et al.*, 1979; Day, unpublished), and RuP_2 carboxylase and pyruvate, Pi dikinase are restricted

Figure 5.1 Scheme showing the proposed pathway by which malate is converted to glucan in the light in CAM plants possessing NADP malic enzyme. The overall equations and the metabolic costs converting the products of malate decarboxylation to glucan are given below.

GLUCONEOGENESIS

$$6\times MALATE + 6\times NADP + 6\times NADPH + 6\times H_2O + 15\times ATP + 3[glucosyl]_n - glucose$$
$$\longrightarrow 6\times CO_2 + 6\times AMP + 9\times PPi + 3\times Pi + 6\times NADP + 9\times ADP + 3[glucosyl]_{n+I}glucose$$

$$6 \times NADPH \longrightarrow 9\times PPi + 9\times H_2O \longrightarrow 18\times Pi$$

$$6 \times ATP + 6\times AMP \longrightarrow 12\times ADP$$

photophosphorylation:-

$$21 \times ADP + 21\times Pi \longrightarrow 21\times ATP + 21\times H_2O$$

$$6\times NADP + 6\times H_2O \longrightarrow 6\times NADPH + 6\times H^+ + 3\times O_2$$

Sum:

$$6\times MALATE + 6\times NADP + 6\times H_2O + 3[glucosyl]_n\text{-}glucose$$
$$\longrightarrow 6\times CO_2 + 3\times O_2 + 6\times NADPH + 6\times H^+ + 3[glucosyl]_{n+I}glucos$$

PHOTOSYNTHETIC CARBON REDUCTION CYCLE

$$6\times CO_2 + 19\times ATP + 12\times NADPH + 12\times H^+ + I[glucosyl]_n\text{-}glucose$$
$$\longrightarrow 6\times O_2 + 19\times ADP + 17\times Pi + PPi + 12\times NADP + 7\times H_2O +$$
$$I[glucosyl]_{n+I}glucos$$

$$PPi + H_2O \longrightarrow 2\times Pi$$

photophosphorylation:-

$$19\times ADP + 19\times Pi \longrightarrow 19\times ATP + 19\times H_2O$$

$$12\times NADP + 12\times H_2O \longrightarrow 12\times NADPH + 12\times H^+ + 6\times O_2$$

Sum:

$$6\times CO_2 + 6\times H_2O + I[glucosyl]_n\text{-}glucose \longrightarrow 6\times O_2 + I[glucosyl]_{n+I}glucose$$

GRAND TOTAL:

$$6\times MALATE + 12\times H_2O + 6\times NADP + 4[glucosyl]_n\text{-}glucose$$
$$\longrightarrow 9\times O_2 + 6\times NADPH + 6\times H^+ + 4[glucosyl]_{n+I}glucose$$

$$\frac{ATP}{NADPH} = \frac{40}{18} = 2.2$$

$$\frac{O_2 \text{ evolved}}{\text{malate decarb}^d} = \frac{9}{6} = 1.5$$

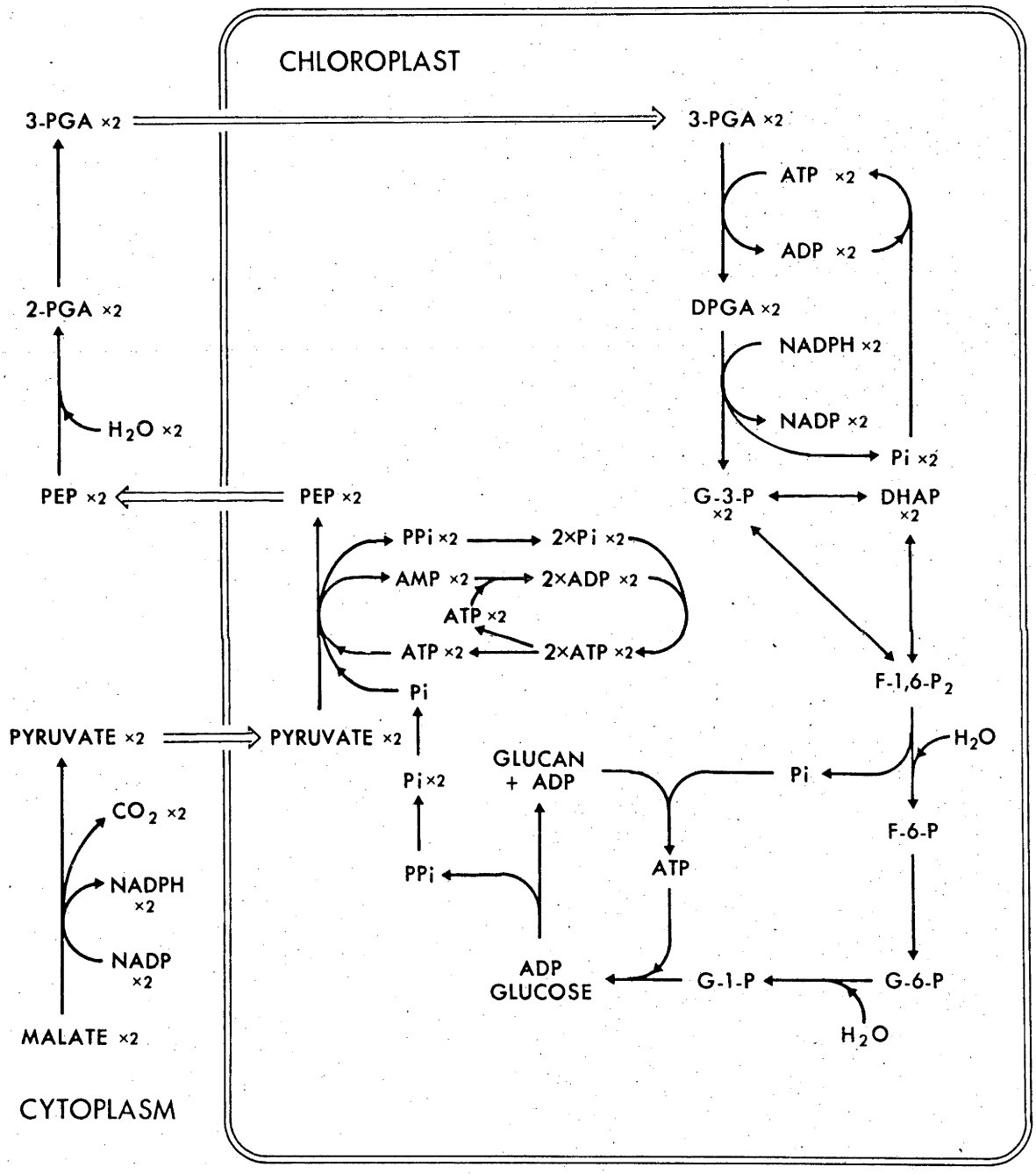
CHLOROPLAST
3-PGA ×2
3-PGA ×2
ATP ×2
ADP ×2
DPGA ×2
NADPH ×2
NADP ×2
Pi ×2
2-PGA ×2
H2O ×2
PEP ×2
PEP ×2
G-3-P ×2
DHAP ×2
PPi ×2
2×Pi ×2
AMP ×2
2×ADP ×2
ATP ×2
ATP ×2
2×ATP ×2
Pi
F-1,6-P2
PYRUVATE ×2
PYRUVATE ×2
H2O
GLUCAN + ADP
Pi
Pi ×2
F-6-P
CO2 ×2
NADPH ×2
NADP ×2
PPi
ATP
ADP GLUCOSE
G-1-P
G-6-P
H2O
MALATE ×2
CYTOPLASM

Figure 5.2 Scheme showing the proposed pathway by which malate is converted to glucan in the light in CAM plants possessing PEPCK. The overall equations and the metabolic costs of converting the products of malate decarboxylation to glucan are given below.

GLUCONEOGENESIS

$$6\text{xMALATE} + 6\text{xNAD} + 15\text{x}H_2O + 15\text{xATP} + 6\text{xNADPH} + 6\text{x}H^+ + 3[\text{glucosyl}]_n\text{-glucose}$$
$$\longrightarrow 6\text{x}CO_2 + 15\text{xADP} + 6\text{xNADH} + 6\text{ X NADP} + 15\text{xPi} + 3[\text{glucosyl}]_{n+I}\text{glucose}$$

photophosphorylation:- $9\text{xADP} + 9\text{xPi} \longrightarrow 9\text{xATP} + 9\text{x}H_2O$

$6\text{xNADP} + 6\text{x}H_2O \longrightarrow 6\text{xNADPH} + 6\text{x}H^+ + 3\text{x}O_2$

Sum:

$$6\text{xMALATE} + 6\text{xNAD} + 12\text{x}H_2O + 6\text{xATP} + 3[\text{glucosyl}]_n\text{-glucose}$$
$$\longrightarrow 6\text{x}CO_2 + 3\text{x}O_2 + 6\text{xNADH} + 6\text{xADP} + 6\text{xPi} + 3[\text{glucosyl}]_{n+I}\text{glucose}$$

PHOTOSYNTHETIC CARBON REDUCTION CYCLE

$$6\text{x}CO_2 + 19\text{xATP} + 12\text{xNADPH} + 12\text{x}H^+ + 12\text{x}H_2O \longrightarrow 6\text{x}O_2 + 19\text{xADP} + 17\text{xPi} + \text{PPi} +$$
$$12\text{xNADP} + 1[\text{glucosyl}]_n\text{-glucose} + 1[\text{glucosyl}]_{n+I}\text{glucose} + 19H_2O$$
$$\text{PPi} + H_2O \longrightarrow 2\text{xPi}$$

photophosphorylation:- $19\text{xADP} + 19\text{xPi} \longrightarrow 19\text{xATP} + 19\text{x}H_2O$

$12\text{xNADP} + 12\text{x}H_2O \longrightarrow 12\text{xNADPH} + 12\text{x}H^+ + 6\text{x}O_2$

Sum:

$$6\text{x}CO_2 + 6\text{x}H_2O + 1[\text{glucosyl}]_n\text{-glucose} \longrightarrow 6\text{x}O_2 + 1[\text{glucosyl}]_{n+I}\text{glucose}$$

GRAND TOTAL:

$$6\text{xMALATE} + 6\text{xNAD} + 18\text{x}H_2O + 6\text{xATP} + 4[\text{glucosyl}]_n\text{-glucose}$$
$$\longrightarrow 9\text{x}O_2 + 6\text{xNADH} + 6\text{xADP} + 6\text{xPi} + 4[\text{glucosyl}]_{n+1}\text{ glucose}$$

$\frac{\text{ATP}}{\text{NADPH}} = \frac{28}{18} = 1.56$; or if all ADP is converted to ATP then $\frac{\text{ATP}}{\text{NADPH}} = 1.89$

$\frac{O_2 \text{ evolved}}{\text{malate decarb}^{\underline{d}}} = \frac{9}{6} = 1.5$

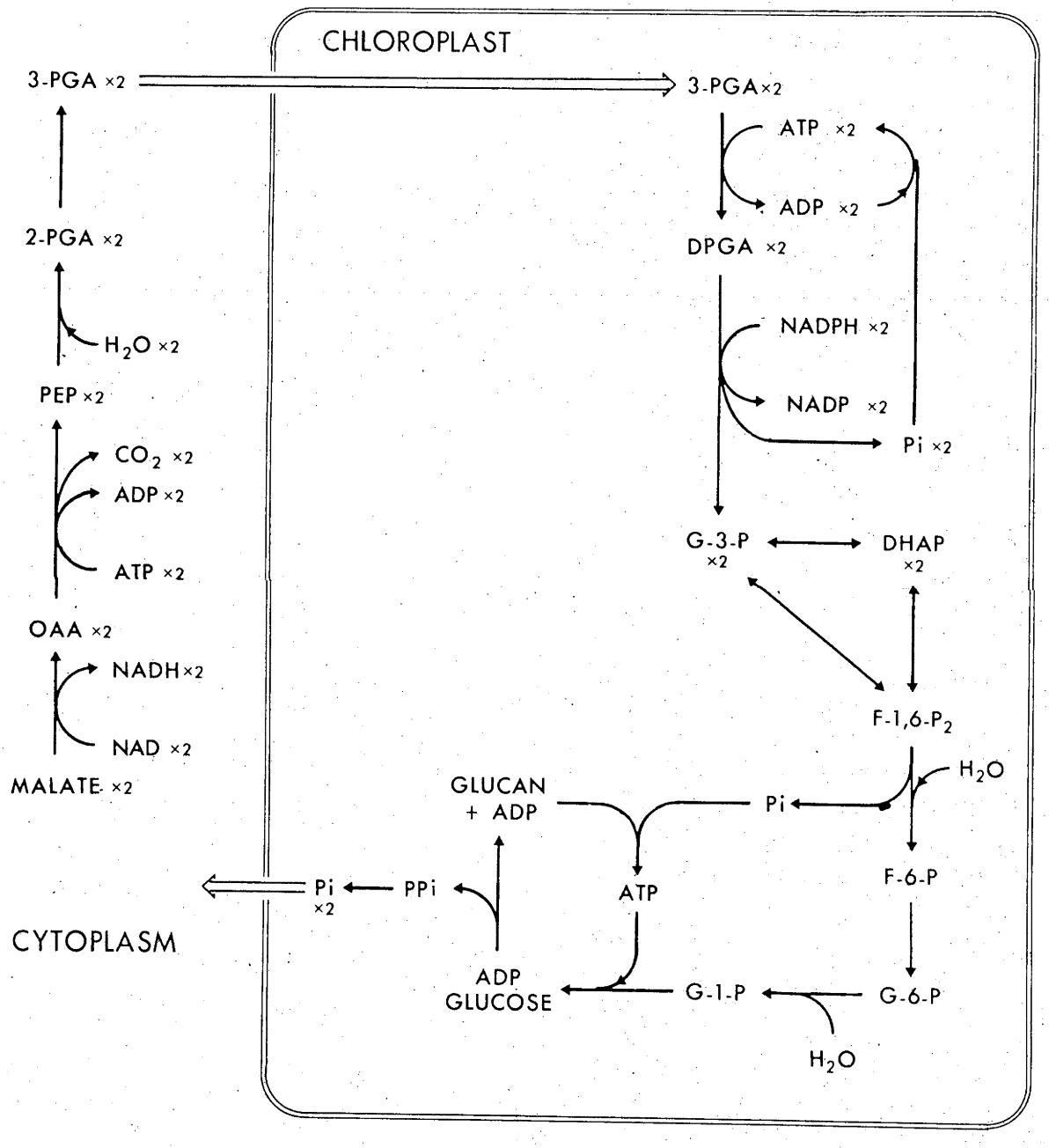
CHLOROPLAST
3-PGA ×2
3-PGA×2
ATP ×2
ADP ×2
DPGA ×2
2-PGA ×2
NADPH ×2
NADP ×2
H2O ×2
Pi ×2
PEP ×2
CO2 ×2
ADP ×2
ATP ×2
G-3-P ×2
DHAP ×2
OAA ×2
NADH×2
NAD ×2
F-1,6-P2
H2O
MALATE ×2
GLUCAN + ADP
Pi
Pi ×2
PPi
ATP
F-6-P
CYTOPLASM
ADP GLUCOSE
G-1-P
G-6-P
H2O

to chloroplasts (Hattersley *et al.*, 1977; Spalding *et al.*, 1979). The mitochondria and peroxisomes contain the normal C_3 plant complement of TCA cycle and photorespiratory enzymes (Khan *et al.*, 1970; Herbert *et al.*, 1979a; K.C. Woo, unpublished). NAD malate dehydrogenase and aspartate aminotransferase are found both in the mitochondria and in the cytoplasm (Day, unpublished; Dittrich, unpublished). Herbert *et al.* (1979b) have observed two forms of glucosephosphate isomerase, phosphoglucomutase, phosphogluconol and glucose-6-phosphate dehydrogenase in *B. calycinum*. These forms appear to be similar to the chloroplastic and cytoplasmic forms found in spinach.

Since no information is available on the localisation of other enzymes involved in glycolysis, the PCR cycle, and in starch and sucrose metabolism in CAM plants, we can only assume that the CAM enzymes are compartmented similarly to their C_3 and C_4 counterparts until proven otherwise.

5.1.2 Transport requirements

The NADP malic enzyme scheme (Figure 5.1) requires the transport of pyruvate into chloroplast followed by the export of PEP and the subsequent import of 3-PGA. The PEPCK model (Figure 5.2) requires the transport of 3-PGA into the chloroplast in return for Pi. These schemes assume chloroplast transport capabilities which have been extrapolated from C_3 and C_4 plants since physiologically active chloroplasts have not yet been isolated from CAM tissues.

Intact mesophyll chloroplasts from the C_4 plant *Digitaria sanguinalis* exhibit high rates of electrogenic, carrier-mediated pyruvate uptake

(Huber and Edwards, 1977a) in contrast to the slow rates of pyruvate transport in spinach chloroplasts (Heber, 1974). Pyruvate uptake by spinach chloroplasts may be up to two orders of magnitude slower than malate or aspartate uptake (Heldt, unpublished, cited by Heber, 1974). Net pyruvate uptake in *Digitaria* proceeds by permeation of the anion and may be dependent upon a membrane potential across the envelope. Uptake of pyruvic acid, or the equivalent pyruvate $^-$/OH^- antiport, was slow. If chloroplasts from NADP malic enzyme CAM plants possess a similar carrier system, the transport of pyruvate into the chloroplasts, and the conversion of pyruvate to PEP by pyruvate, Pi dikinase could proceed as indicated (Fig. 5.1).

The further metabolism of PEP during gluconeogenesis involves enzymes in the cytoplasm (enolase and phosphoglyceromutase), requiring that PEP be transported from the chloroplast. *Digitaria* mesophyll chloroplasts also contain a carrier which facilitates an exchange diffusion of Pi and PEP across the envelope (Huber and Edwards, 1977b). This system is probably similar in function to the phosphate translocator reported in spinach (C_3) mesophyll chloroplasts, excepting that the carrier from *Digitaria* has a higher affinity for PEP. If such a translocator is present in the chloroplast envelope of malic enzyme CAM plants, export of PEP produced from pyruvate (in exchange for Pi?) would be balanced by a subsequent import of 3-PGA from the cytoplasm (in exchange for Pi?) Whether these metabolite exchanges are mediated by Pi exchanges is not known. The Pi exchanges are not shown in Figure 5.1. Chloroplasts from NADP malic enzyme CAM plants can be envisaged to function in gluconeogenesis during deacidification as mesophyll cell chloroplasts from C_4 plants (Hatch and Osmond, 1976).

In the scheme for PEPCK CAM plants the metabolite transport requirements are simply for a Pi/3-PGA translocator in the chloroplast envelope (Figure 5.2). Whether the ATP supply for PEPCK in the cytoplasm is met by the chloroplast, via an adenylate translocator (Robinson and Wiskich, 1977), or by mitochondrion, is not clear. Either way, the Pi/3-PGA translocator in the chloroplast envelope effectively maintains phosphate balance in the cytoplasm. In the PEPCK CAM plants gluconeogenesis during deacidification could be sustained by a chloroplast with the known properties of C_3 leaf chloroplasts.

Models for both CAM plants have a requirement for the transfer of protons into the stroma i.e. both schemes appear to produce a charge imbalance. The malic enzyme scheme requires the transport of pyruvate$^-$ and 3-PGA^{3-} into the chloroplast in return for PEP^{3-} which results in a net transfer of a single negative charge per decarboxylation event into the chloroplast. The PEPCK scheme requires 3-PGA^{3-} to enter the chloroplast in return for Pi^{2-} which also results in a net transfer of a single negative charge into the chloroplast. This contrasts with the *Digitaria* mesophyll chloroplast system in which the overall transport is electroneutral since the export of PEP^{3-} is balanced by the import of pyruvate$^-$ and Pi^{2-} (Edwards and Huber, 1977). Heldt (1976) considers that it is quite possible that the counter-exchange of 3-PGA with either Pi or DHAP also involves a transfer of a proton. This would explain how in C_3 tissues, 3-PGA transport into the chloroplast might be stimulated by light induced alkalisation of the stroma. This has not, however, been proven experimentally.

5.1.3 Control of gluconeogenesis in the light and glycolysis in the dark

The above pathways for gluconeogenesis during deacidification in CAM plants in the light are reversed in the dark, when glycolysis generates PEP from glucan for malic acid synthesis (Sutton, 1974; 1975a). These reversible pathways are likely to be controlled by the following interactions:

(1) Light activation of enzymes. Pyruvate, Pi dikinase is light activated in CAM and C_4 plants (Sugiyama and Laetsch, 1975; Hatch and Osmond, 1975). Thus the reaction

$$\text{pyruvate} + \text{ATP} + \text{Pi} \longrightarrow \text{PEP} + \text{AMP} + \text{PPi} \qquad (9)$$

is inactive in the dark and the conversion of pyruvate to glucan is prevented in NADP malic enzyme CAM plants. Alkaline FDPase is light activated in C_3 plants (Kelly, Latzko and Gibbs, 1976) and presumably also in CAM plants. Inactivation of the irreversible reaction

$$\text{FDP} \xrightarrow{\text{Pi}} \text{F-6-P} \qquad (10)$$

would prevent gluconeogenesis in the dark.

(2) Inactivation of PEP carboxylase in the light. The three principal enzymes of PEP metabolism, PEP carboxylase, enolase and pyruvate kinase, are cytoplasmic enzymes and will compete for available PEP. Because PEP carboxylase is the most active, it is likely that the control of this enzyme could influence the direction of carbon traffic through PEP. Recent studies by Winter (unpublished) show that this enzyme is most sensitive to malic acid inhibition during deacidification and inhibition of PEP carboxylase at this time permits PEP to flow in the gluconeogenic direction.

(3) Energy charge. In green leaves, the adenylate energy charge ratio is high in the light and low in the dark (Santarius and Heber, 1965). This makes it unlikely that reversal of phosphofructokinase could overcome the inactivation of FDPase in the dark. Low energy charge and high F-6-P concentration in the dark (Pierre and Queiroz, 1979) presumably ensure that phosphofructokinase functions in the direction F6P → FDP required for glycolysis. By the same token, PGA kinase can function in the gluconeogenic direction only when energy charge is greater than 0.85 (Pacold and Anderson, 1973).

(4) Balance of effectors. Glucan synthesis and degradation are responsive to Pi and 3-PGA. Starch synthesis, and hence gluconeogenesis, is inhibited by high Pi and low 3-PGA (Priess, 1973), whilst high Pi stimulates phosphorylytic starch degradation in spinach chloroplasts (Steup *et al.*, 1976). In *Kalanchoe*, the phosphorylytic degradation of starch is similarly stimulated by increasing Pi whilst amylolytic degradation is inhibited (Dittrich, unpublished; Sutton, 1974; 1975c). Chloroplast Pi concentrations are higher in the dark than in the light in most photosynthetic tissues (Santarius and Heber, 1965) and the 3-PGA concentration in *K. blossfeldiana* in the dark is less than 1/4 of that in the light (Pierre and Queiroz, 1979), which suggests that starch degradation rather than formation is favoured in the dark.

5.1.4 Implications for starch and sucrose synthesis

The schemes in Figures 5.1 and 5.2 are helpful in the interpretation of data on the synthesis of starch and sucrose during CAM. During deacidification it is established that starch is stoichiometrically made from malate and that there is little increase in the soluble sugar pool (Wolf, 1938; Pucher *et al.*, 1949a; Sutton, 1974, 1975c). Moreover,

Deleens and Garnier Dardart (1977) showed that the $\delta^{13}C$ value of starch from *K. daigremontiana* confirms that malic acid formed in the dark is the main source of carbon for starch synthesis.

After deacidification is complete there is apparently a substantial shift in the fate of assimilated carbon. The major product of $^{14}CO_2$ fixation in the late afternoon is sucrose, not starch (Kluge, 1969c; Sutton, 1974). The $\delta^{13}C$ value of the free sugar pool is more negative than that of starch, consistent with an independent source involving CO_2 fixation via RuP_2 carboxylase. This apparent shift in the end product of photosynthesis occurs as the synthesis of starch from pyruvate or PEP tapers off following the completion of deacidification. The shift can be interpreted in terms of the schemes shown in Figures 5.1 and 5.2.

The enzymes involved in starch and dextrin synthesis are usually considered to be located in the chloroplast, whilst sucrose metabolism is a cytoplasmic process (Bird *et al.*, 1974; Latzko *et al.*, 1974; Kelly *et al.*, 1976), although recent evidence suggests that cytoplasmic forms of phosphorylase occur in pea and spinach (Steup and Latzko, 1979). The major regulatory enzyme involved in starch metabolism appears to be ADP-glucose pyrophosphorylase which has been shown to be variously activated by high pH, 3-PGA, F-6-P, PEP and ATP but is also strongly inhibited by Pi (Ghosh and Preiss, 1966; Preiss and Kosuge, 1970). The Pi inhibition, which should not be important in the light since Pi levels are low (Santarius and Heber, 1965), can be reversed by 3-PGA, particularly at the high pH values which are characteristic of the stroma in the light (Walker, 1976). The pyrophosphorylase reaction may also be pulled towards ADP-glucose production since the co-product, pyrophosphate, is most likely

quickly hydrolysed by a chloroplastic pyrophosphatase which has been reported in C_3 chloroplasts (Klemme and Jacobi, 1974; Kelly, *et al.*, 1976).

The schemes presented in Figures 5.1 and 5.2 suggest that 3-PGA, which stimulates starch production, will be present in high concentrations in the chloroplast during deacidification. The high 3-PGA concentration will arise because it is the major product of RuP_2 metabolism during photosynthesis at the high CO_2 concentrations which prevail in the intercellular air spaces in deacidifying CAM tissues in the light (as high as 400 $\mu l\ l^{-1}$; 4,000 ppm CO_2). It is likely that there will be reduced carbon flux through P-glycolate under these conditions (Cockburn *et al.*, 1979; Spalding *et al.*, in press). Moreover, 3-PGA is transported into the chloroplast following the conversion of pyruvate to PEP. Clearly the high 3-PGA concentration will favour starch synthesis and the pool of PEP in the chloroplast may itself stimulate ADP-glucose pyrophosphorylase.

Although the schemes suggest the cytoplasm should have an adequate source of triose phosphate in the light during deacidification, sucrose synthesis may be curtailed by low FDPase activity in the cytoplasm at acid pH. In C_3 plants the cytoplasmic FDPase capacity accounts for only about 30% of the total activity in the cell and the enzyme is unlikely to be active at all below pH 7.0 (Latzko *et al.*, 1974). If malate leaks passively from the vacuole during deacidification (Lüttge and Ball, 1974a; Lüttge *et al.*, 1975) the cytoplasmic malate concentration, and probably also the pH, should reflect the vacuolar concentration and pH and thus the cytoplasmic pH can be expected to be low enough to substantially inhibit cytoplasmic FDPase activity.

The apparent switch from glucan to sucrose synthesis which accompanies the commencement of external CO_2 fixation at the conclusion of deacidification presumably involves changes in most of these regulatory interactions. In the late afternoon, when the stored malate has been decarboxylated, the cytoplasmic pH might rise allowing FDPase to function. The cytoplasmic pool of triose phosphates is likely to decrease in the absence of the gluconeogenic flux from pyruvate or PEP to glucan. The chloroplast will then tend to export triose phosphate because the ratio of chloroplastic to cytoplasmic triose phosphate is high. In the late afternoon, the export of triose phosphate may be balanced by the import of Pi and the carbon exchanges of CAM chloroplasts are presumably similar to those of C_3 chloroplasts, leading to sucrose synthesis in the cytoplasm rather than glucan synthesis in the chloroplast (Figure 5.3).

The fate of Pi and ADP produced during sucrose synthesis in the cytoplasm is not known. It is conceivable that they could be linked to the conversion of triose phosphates to PEP via G-3-P dehydrogenase and PGA kinase. There are many reports of substantial ^{14}C incorporation into C_4 acids, as well as into sucrose (Kluge, 1969c, 1971; Osmond and Allaway, 1974). However, the stimulation of DCMU-insensitive CO_2 fixation in isolated cells of *Kalanchoe* and *Stapelia* by added PEP (Chapter 3) could not be sustained by the addition of 3-PGA.

5.2 Alternative Schemes

These schemes are obviously incomplete. The scheme for the NADP malic enzyme CAM plants (Figure 5.1) leads to net production of 1 NADPH in the cytoplasm for each malate decarboxylated. The scheme for PEPCK CAM plants (Figure 5.2) leads to the net production of 1 NADH, 1 ADP and 1 Pi per

Figure 5.3 Scheme showing proposed mechanism of sucrose production in C_3 plants and in CAM plants during the period of post-deacidification CO_2 fixation (Phase 4). (Scheme adapted from Walker and Herold, 1977).

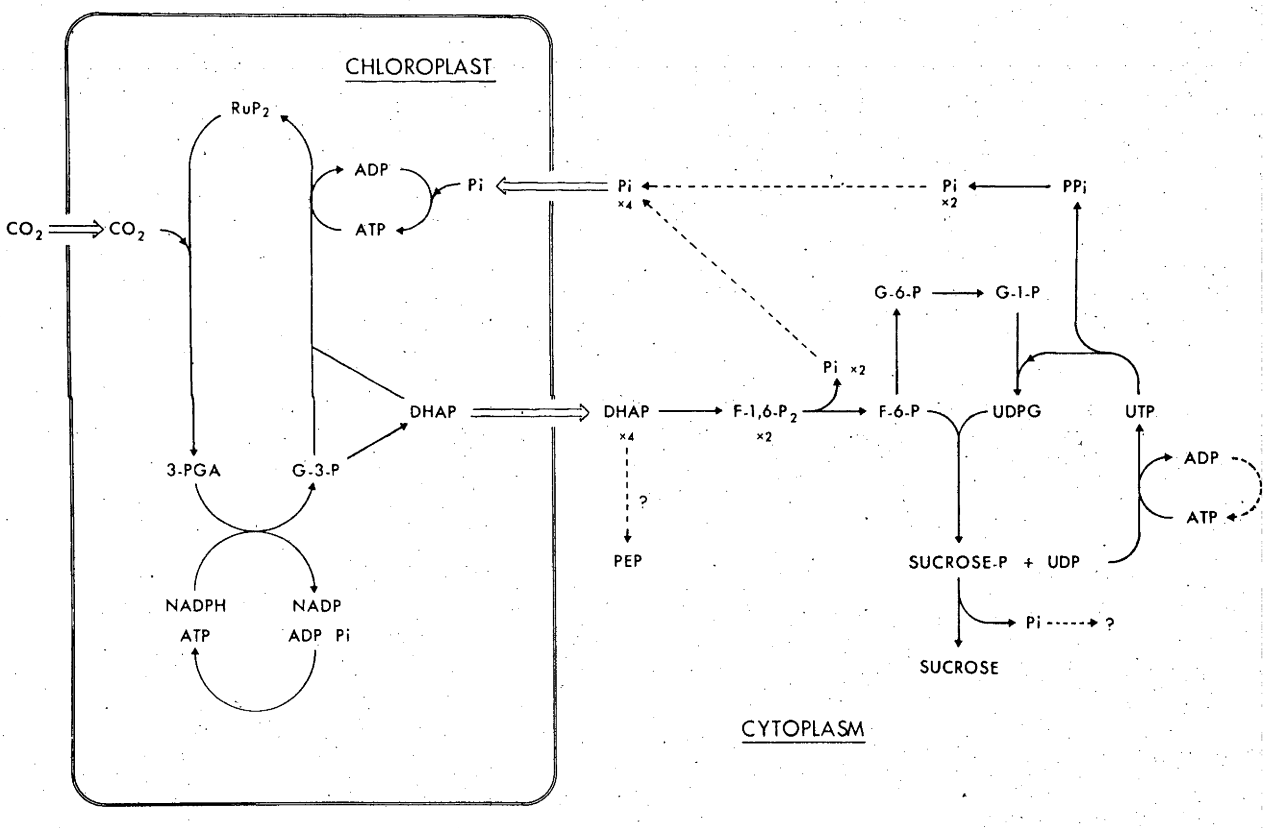
CHLOROPLAST
RuP2
ADP
Pi
ATP
CO2
CO2
DHAP
3-PGA
G-3-P
NADPH
ATP
NADP
ADP Pi
Pi ×4
Pi ×2
PPi
G-6-P
G-1-P
Pi ×2
DHAP ×4
F-1,6-P2 ×2
F-6-P
UDPG
UTP
ADP
ATP
?
PEP
SUCROSE-P + UDP
Pi
?
SUCROSE
CYTOPLASM

malate decarboxylated. Furthermore, neither scheme considers the possible roles of mitochondrial respiration and malate decarboxylation. Some alternatives, and their respective metabolic costs, for carbon flow during deacidification are shown in Figures 5.4 to 5.7.

5.2.1 Alternatives to the schemes for NADP malic enzyme CAM plants

Figure 5.4 shows that if NADP malic enzyme is inside the chloroplast, as it is in bundle-sheath chloroplasts of C_4 plants, the excess NADPH produced during decarboxylation could be regenerated by G-3-P dehydrogenase. Although this scheme solves the nucleotide balance deficiencies inherent in the scheme presented in Figure 5.1, it has other deficiencies. Firstly, as already stated, recent evidence suggests that NADP malic enzyme is located in the cytoplasm. Secondly, the scheme requires 3.3 ADP to be produced for each NADPH produced during photophosphorylation. Thirdly, the transfer of malate^{2-} and 3-PGA^{3-} into the chloroplast in return for PEP^{3-} would result in a charge$_{im}$balance caused by the transfer of two negative charges into the chloroplast per decarboxylation event. Fourthly, the scheme requires the unidirectional transport of malate, and although such a mechanism has been observed in spinach chloroplasts the rates are only about 0.2 μmoles mg chl^{-1} hour^{-1} (Lehner and Heldt, unpublished; cited by Heldt, 1976).

Figure 5.5 proposes a dicarboxylic acid shuttle to regenerate cytoplasmic NADP and requires an isoenzyme of NADP MDH in the cytoplasm. Although in C_4 and in C_3 plants NADP MDH is a chloroplastic enzyme with a pH optimum of around pH 8.5 (Johnson and Hatch, 1970), *K. daigremontiana*, *B. pinnatum* and *M. crystallinum* all possess a NADP MDH which has a low pH optimum of around pH 6.5 and which could function in the cytoplasm during

Figure 5.4 Scheme showing a possible pathway by which pyruvate, produced from the decarboxylation of malate, may be converted to glucan if NADP malic enzyme is located inside the chloroplasts of CAM plants.

The overall equations and the metabolic costs of the scheme are given below.

GLUCONEOGENESIS

$$6\text{xMALATE} + 15\text{xATP} + 12\text{x}H_2O + 3[\text{glucosyl}]_n\text{-glucose} \longrightarrow 6\text{x}CO_2 + 6\text{xAMP} + 9\text{xADP} + 3\text{xPi} + 9\text{xPPi} + 3[\text{glucosyl}]_{n+I}\text{glucose}$$

$$9\text{xPPi} + 9\text{x}H_2O \longrightarrow 18\text{xPi}$$

$$6\text{xAMP} + 6\text{xATP} \longrightarrow 12\text{xADP}$$

photophosphorylation:- $21\text{xADP} + 21\text{xPi} \longrightarrow 21\text{xATP} + 21\text{x}H_2O$

Sum:

$$6\text{xMALATE} + 3[\text{glucosyl}]_n\text{-glucose} \longrightarrow 6\text{x}CO_2 + 3[\text{glucosyl}]_{n+I}\text{glucose}$$

PHOTOSYNTHETIC CARBON REDUCTION CYCLE

$$6\text{x}CO_2 + 19\text{xATP} + 12\text{xNADPH} + 12\text{x}H^+ + 1[\text{glucosyl}]_n\text{-glucose} \longrightarrow 6\text{x}O_2 + 19\text{xADP} + 17\text{xPi} + \text{PPi} + 12\text{xNADP} + 7\text{x}H_2O + 1[\text{glucosyl}]_{n+I}\text{glucose}$$

$$\text{PPixADP} + 19\text{xPi} \longrightarrow 19\text{xATP} + 19\text{x}H_2O$$

$$12\text{xNADP} + 12\text{x}H_2O \longrightarrow 12\text{xNADPH} + 12\text{x}H^+ + 6\text{x}O_2$$

Sum:

$$6\text{x}CO_2 + 6\text{x}H_2O + 1[\text{glucosyl}]_n\text{-glucose} \longrightarrow 6\text{x}O_2 + 1[\text{glucosyl}]_{n+1}\text{glucose}$$

GRAND TOTAL:

$$6\text{xMALATE} + 6\text{x}H_2O + 4[\text{glucosyl}]_n\text{-glucose} \longrightarrow 6\text{x}O_2 + 4[\text{glucosyl}]_{n+I}\text{ glucose}$$

$$\frac{\text{ATP}}{\text{NADPH}} = \frac{40}{12} = 3.3$$

$$\frac{O_2 \text{ evolved}}{\text{malate decarb}^{\underline{d}}} = \frac{6}{6} = 1$$

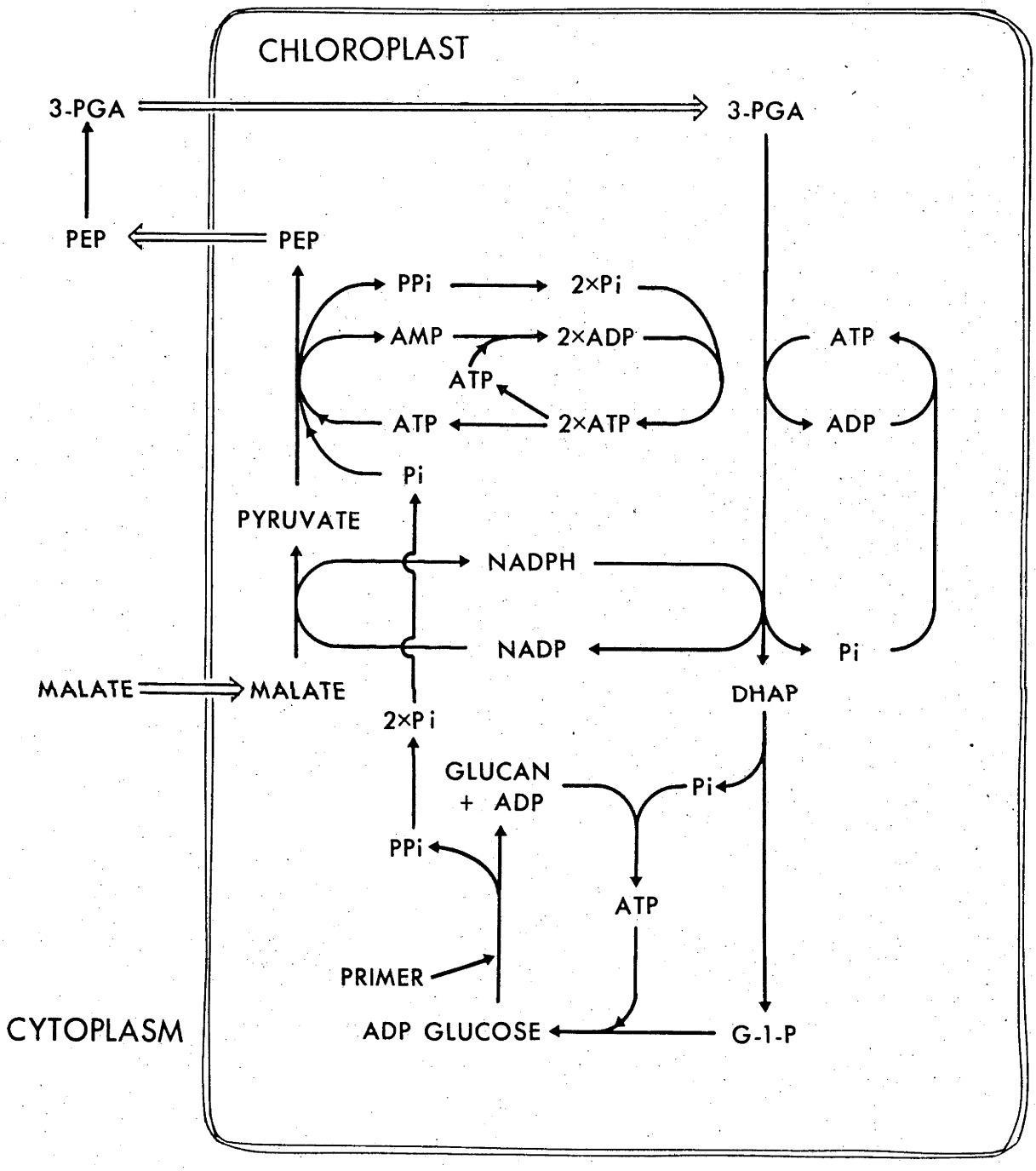
CHLOROPLAST
3-PGA
3-PGA
PEP
PEP
PPi
2×Pi
AMP
2×ADP
ATP
ATP
2×ATP
ATP
ADP
Pi
PYRUVATE
NADPH
NADP
Pi
MALATE
MALATE
DHAP
2×Pi
GLUCAN
+ ADP
Pi
PPi
ATP
PRIMER
CYTOPLASM
ADP GLUCOSE
G-1-P

Figure 5.5 Scheme showing a possible pathway by which pyruvate, produced from the decarboxylation of malate, may be converted to glucan. This scheme postulates that NADP malic enzyme is in the cytoplasm and a dicarboxylate shuttle regenerates the NADP requirement.

The overall equations and the metabolic costs of the scheme are similar to those calculated for Figure 5.4.

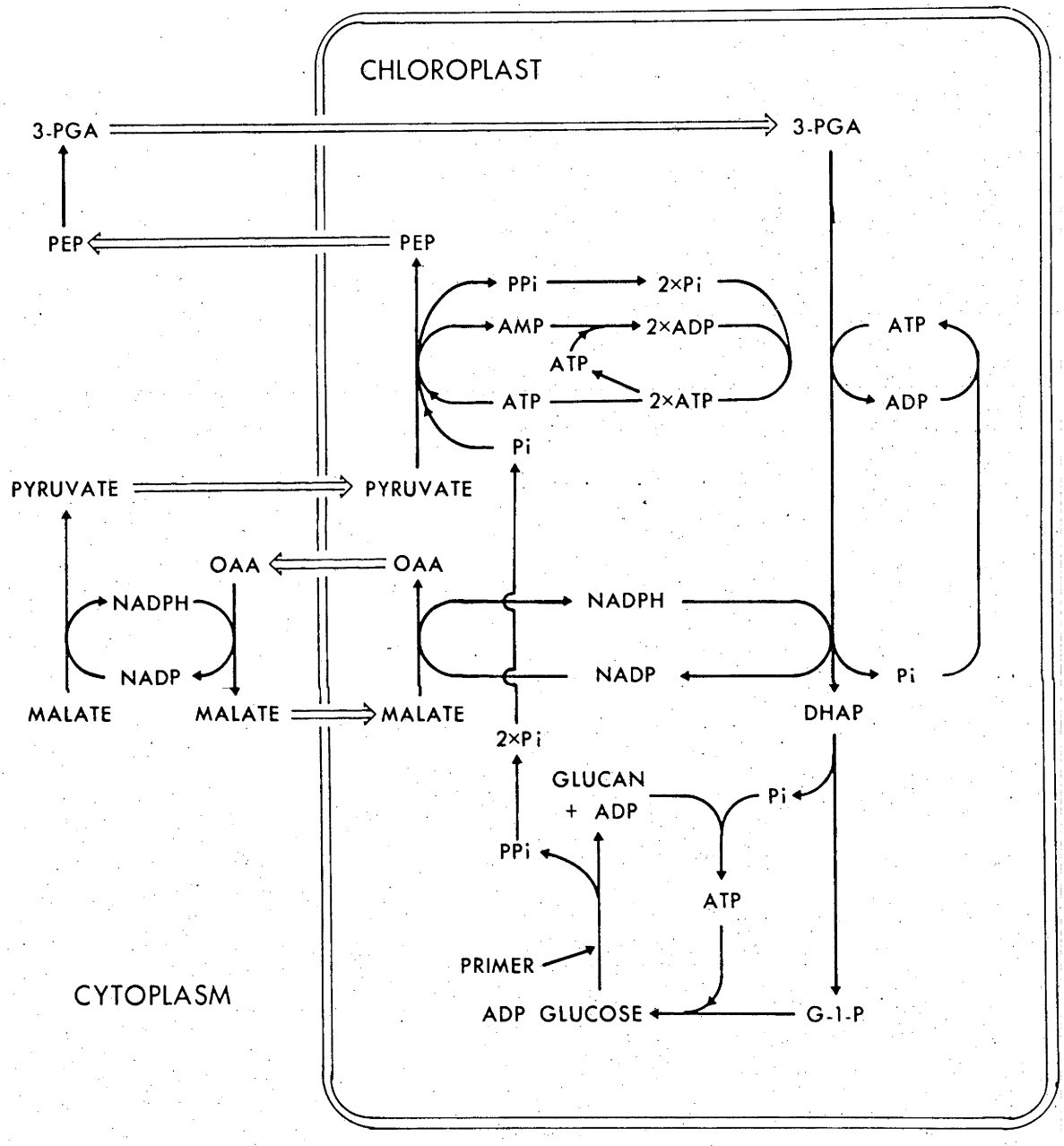
CHLOROPLAST
3-PGA
3-PGA
PEP
PEP
PPi
2×Pi
AMP
2×ADP
ATP
ATP
2×ATP
ATP
ADP
Pi
PYRUVATE
PYRUVATE
OAA
OAA
NADPH
NADPH
NADP
NADP
Pi
MALATE
MALATE
MALATE
DHAP
2×Pi
GLUCAN
+ ADP
Pi
PPi
ATP
PRIMER
CYTOPLASM
ADP GLUCOSE
G-1-P

deacidification (see Chapter 4.1 and 4.3). Ting and co-workers (Ting and Dugger, 1968; Mukerji and Ting, 1968a) reported the presence and kinetics of mitochondrial, chloroplastic and soluble isoenzymes of "malate dehydrogenase (decarboxylating)(NADP)" in *Opuntia*. (They never actually showed however, that pyruvate was a product of malate oxidation and it is quite conceivable that the enzyme they were studying was actually NADP MDH and not NADP malic enzyme). The scheme presented in Figure 5.5 also requires the production of 3.3 ATP per NADPH produced during photophosphorylation but, in common with the scheme presented in Figure 5.1, it requires the net transfer of only one negative charge per decarboxylation event into the chloroplast. This transfer may be balanced by a proton entering with 3-PGA.

Another possibility is that carbon may enter the chloroplast as DHAP and the ADP and Pi produced in the cytoplasm by PGA kinase may be recycled via mitochondrial respiration (Figure 5.6). It is not clear whether ADP and Pi can be readily transported into the chloroplast from the cytoplasm. Although an adenylate translocator has been observed in isolated pea chloroplasts (Robinson and Wiskich, 1977) it appears to be highly specific for the transfer of ATP, rather than ADP and Pi, from the cytoplasm into the stroma and furthermore, it decreases in activity with plant age. The NADPH produced during decarboxylation could be recycled by G-3-P dehydrogenase for, although the cytoplasmic enzyme is usually considered a NAD enzyme, it has substantial NADP activity (Cerff, 1978) and is present in CAM tissues in a high activity.

Regeneration of the ATP required for the PGA kinase reaction in leaf mitochondria would consume only 1 NADH (or 1 NADPH) per 2 or 3 malate

Figure 5.6 Scheme showing the possible pathway by which pyruvate, produced in either the cytoplasm or in the mitochondria, may be converted to glucan.

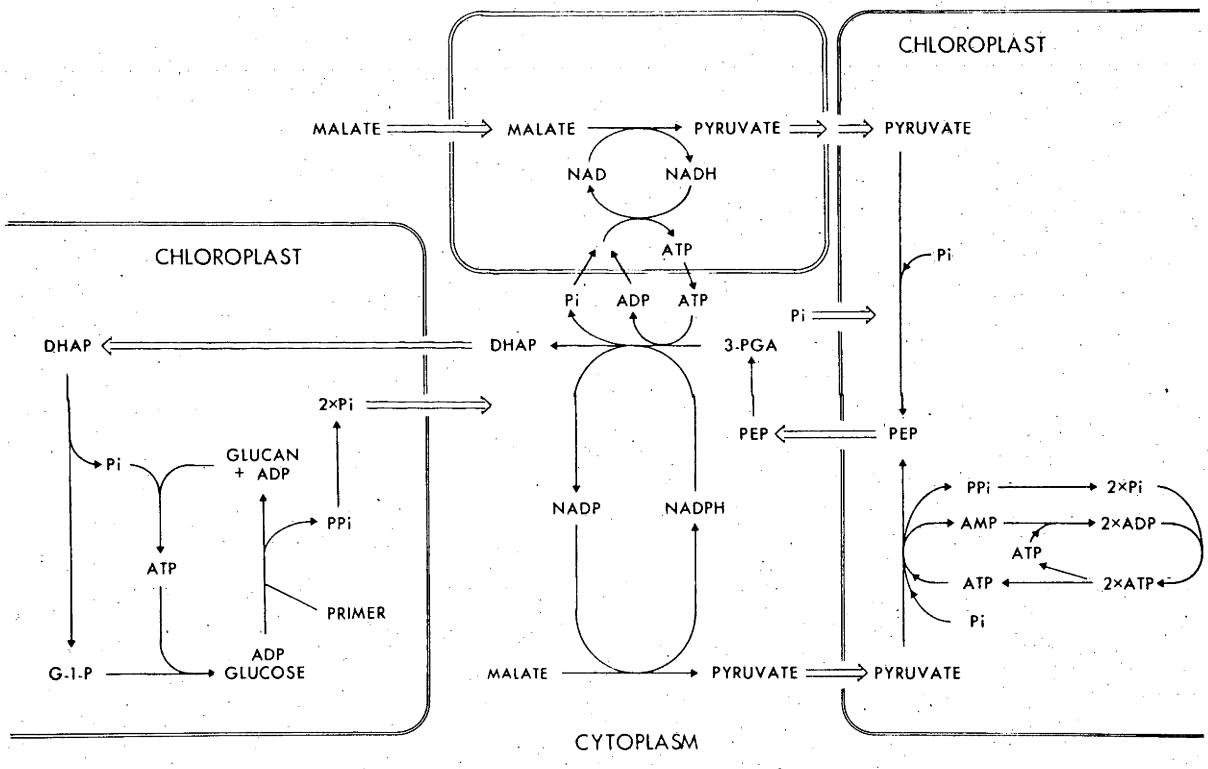
CHLOROPLAST
MALATE
MALATE
PYRUVATE
PYRUVATE
NAD
NADH
ATP
Pi
CHLOROPLAST
Pi
ADP
ATP
Pi
DHAP
DHAP
3-PGA
2×Pi
PEP
PEP
Pi
GLUCAN
+ ADP
PPi
2×Pi
NADP
NADPH
PPi
AMP
2×ADP
ATP
ATP
PRIMER
ATP
2×ATP
Pi
ADP
G-1-P
GLUCOSE
MALATE
PYRUVATE
PYRUVATE
CYTOPLASM

decarboxylated, depending upon the stoichiometry of oxidative phosphorylation. If a portion of the malate were decarboxylated by mitochondrial NAD malic enzyme, each NADH recycled through the electron transport chain with ATP synthesis would result in a similar unfilled NADH requirement at the G-3-P dehydrogenase step. That is, if DHAP, not 3-PGA, enters the chloroplast from the cytoplasm it does not seem to be possible to regulate the flow of malate through NAD and NADP malic enzymes in the scheme in Figure 5.6, in such a way that the nucleotides and adenylates are recycled. Furthermore, a ratio of ATP/NADPH production of 2.8 would be required to sustain such a scheme.

5.2.2 Alternatives to the scheme for PEPCK CAM plants

Gluconeogenesis during deacidification in PEPCK CAM plants is most satisfactorily accommodated by a scheme based on the inclusion of PEPCK in the chloroplast (Figure 5.7). However, this scheme implies a ratio of ATP/NADPH requirement of about 2.8 and the movement of charged metabolism such that two negative charges are transferred to the chloroplast per decarboxylation event. Furthermore, recent evidence indicates that PEPCK is almost certainly not located in the chloroplast (Ku *et al.*, 1979; Dittrich, personal communication).

If PEPCK is in the cytoplasm, as shown in Figure 5.2, the ATP requirement of this enzyme can be met in several ways, but none of them result in complete nucleotide and adenylate balance. A shuttle involving 3-PGA and DHAP could generate ATP and NADPH (NADH) via cytoplasmic enzymes (Heber, 1974) but the recycling of NADPH (NADH) then has to be accommodated. Mitochondria of CAM plants have this capability (Arron *et al.*, 1979; Day, personal communication) and it is possible that a loose stoichiometry based on such a shuttle could meet the ATP needs of

Figure 5.7 Scheme showing a possible pathway by which PEP, produced from the decarboxylation of OAA, may be converted to glucan if PEPCK is located inside the chloroplasts of CAM plants.

The overall equations and the metabolic costs of the scheme are given below.

GLUCONEOGENESIS

$$6\text{xMALATE} + 15\text{xATP} + 12\text{x}H_2O + 3[\text{glucosyl}]_n\text{-glucose} \longrightarrow 6\text{x}CO_2 + 15\text{ADP} + 9\text{xPi} + 3\text{xPPi} + 3[\text{glucosyl}]_{n+1}\text{glucose}$$

$$3\text{xPPi} + 3\text{x}H_2O \longrightarrow 6\text{xPi}$$

$$\text{photophosphorylation:-} \quad 15\text{xADP} + 15\text{xPi} \longrightarrow 15\text{xATP} + 15\text{x}H_2O$$

Sum:

$$6\text{xMALATE} + 3[\text{glucosyl}]_n\text{-glucose} \longrightarrow 6\text{x}CO_2 + 3[\text{glucosyl}]_{n+1}\text{glucose}$$

PHOTOSYNTHETIC CARBON REDUCTION CYCLE

$$6\text{x}CO_2 + 19\text{xATP} + 12\text{xNADPH} + 12\text{x}H^+ + 12\text{x}H_2O + 1[\text{glucosyl}]_n\text{-glucose} \longrightarrow 6\text{x}O_2 + 19\text{xADP} + 17\text{xPi} + \text{PPi} + 12\text{xNADP} + 1[\text{glucosyl}]_{n+1}\text{glucose}$$

$$\text{PPi} + H_2O \longrightarrow 2\text{xPi}$$

$$\text{photophosphorylation:-} \quad 19\text{xADP} + 19\text{xPi} \longrightarrow 19\text{xATP} + 19\text{x}H_2O$$

$$12\text{xNADP} + 12\text{x}H_2O \longrightarrow 12\text{xNADPH} + 12\text{x}H^+ + 6\text{x}O_2$$

Sum:

$$6\text{x}CO_2 + 6\text{x}H_2O + 1[\text{glucosyl}]_n\text{-glucose} \longrightarrow 6\text{x}O_2 + 1[\text{glucosyl}]_{n+1}\text{glucose}$$

GRAND TOTAL:

$$6\text{xMALATE} + 6\text{x}H_2O + 4[\text{glucosyl}]_n\text{-glucose} \longrightarrow 6\text{x}O_2 + 4[\text{glucosyl}]_{n+1}\text{glucose}$$

$$\frac{\text{ATP}}{\text{NADPH}} = \frac{34}{12} = 2.8$$

$$\frac{O_2 \text{ evolved}}{\text{malate decarb}^{\underline{d}}} = \frac{6}{6} = 1$$

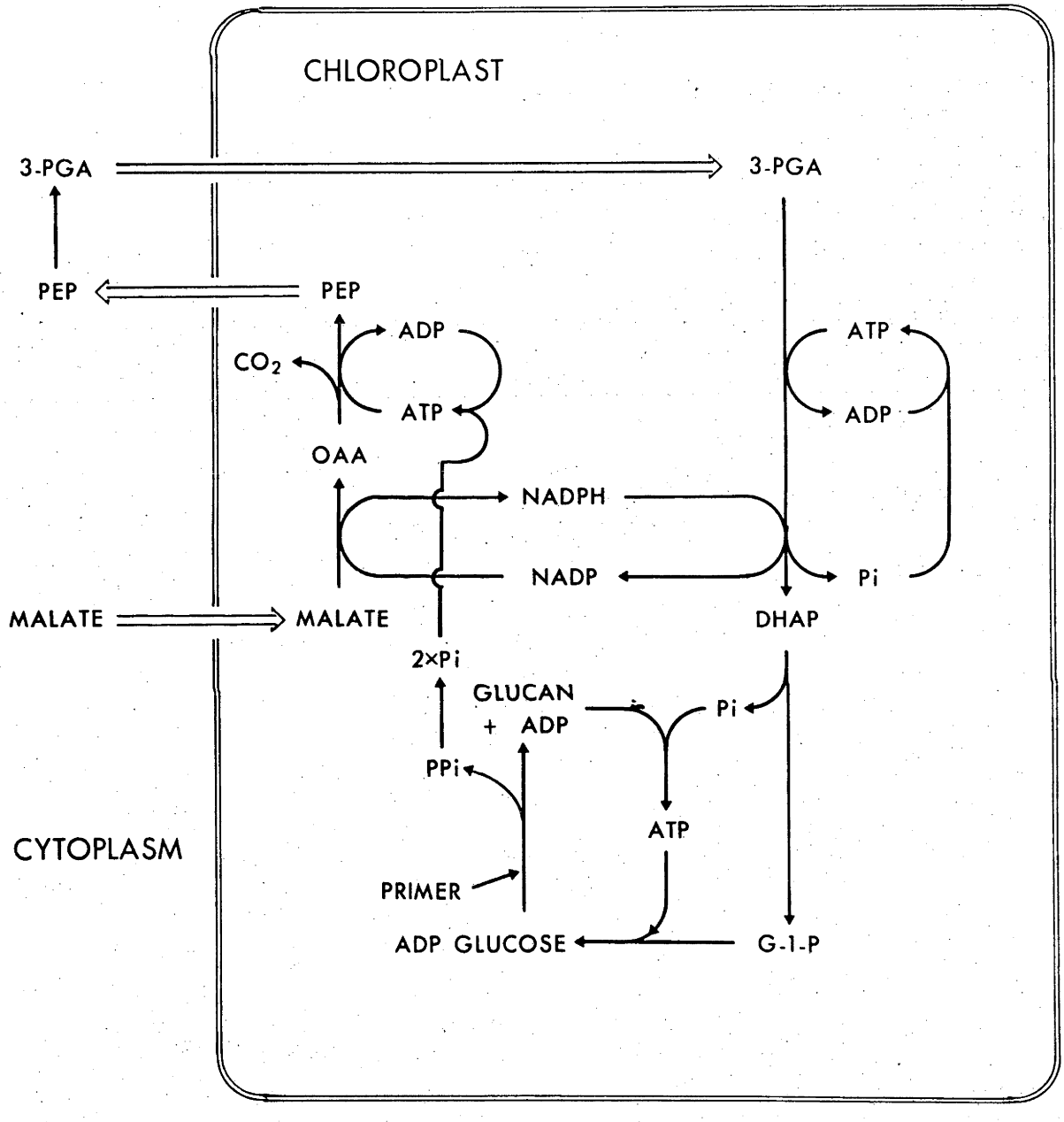
CHLOROPLAST
3-PGA
3-PGA
PEP
PEP
ADP
CO_2
ATP
ATP
ADP
OAA
NADPH
NADP
Pi
MALATE
MALATE
DHAP
2×Pi
GLUCAN
+ ADP
Pi
PPi
ATP
CYTOPLASM
PRIMER
ADP GLUCOSE
G-1-P

cytoplasmic PEPCK. In this way the conversion of 1 mole DHAP → 3-PGA in the cytoplasm could generate 2 or 3 mole of ATP, depending on the stoichiometry of NADPH oxidation in the mitochondrial electron transport chain.

5.3 Summation

This discussion raises more questions than it provides answers. Whereas the concept of gluconeogenesis in the light appears to be soundly based on the available data, the stoichiometry of component reactions does not conform to simple schemes based on present knowledge of enzyme localisation and oxidative and photophosphorylation in CAM plants. In addition, most of the schemes discussed produce charge imbalances between the cytoplasm and the chloroplast and require 2.8-3.3 ATP to be produced per NADPH photoreduced which makes them unlikely alternatives. No suggestions are advanced for the regeneration of NAD in CAM plants in which NAD malic enzyme participates in malate decarboxylation. Presumably these events would be linked with oxidative phosphorylation in mitochondria in the light which, should it take place in CAM, would further distinguish this metabolic system from that of other green leaves.

Apart from showing that gluconeogenesis occurs, this study pinpoints areas in which further information is needed to determine the pathway of carbon in the light and to explain its regulation. The need for the isolation of intact, physiologically active chloroplasts from CAM plants is obvious. The presence and capacities of pyruvate, PEP, and 3-PGA carriers, and possibly also an adenylate carrier and a dicarboxylic acid shuttle, need to b demonstrated. It would also be important to ascertain the conditions under which carbon influx and efflux occur from the chloroplast, and to show that

external 3-PGA and pyruvate can be converted to glucan at the rates required by deacidification.

Further information on the kinetics and regulatory characteristics is needed before we can expect a reasonable understanding of the regulatory roles of certain enzymes involved in glycolysis and carbohydrate metabolism. Some possibly profitable areas for further study indicated by the work described in this thesis are (1) Purification and characterisation of enolase and PGA mutase. For example, why, during induction of CAM in *M. crystallinum*, does the PGA mutase activity in crude extracts from *M. crystallinum* increase 10 fold when assayed in the gluconeogenic direction and only two fold in the glycolytic direction? Is a new protein manufactured during this period?

(2) Purification and characterisation of chloroplast and cytoplasmic FDPases with emphasis on the effect of high malate concentrations and low pH on the activity of the cytoplasmic enzyme.

(3) Assessment of pyruvate kinase capacity in CAM plants. Since this enzyme is located at the branch point, and is sensitive to ATP/ADP concentrations (Tomlinson and Turner, 1973) it may well play an important regulatory role. It would be also interesting to test the temperature response of the enzyme particularly with reference to the increased respiration by CAM plants at high night temperatures.

(4) Detection of ADP-glucose pyrophosphorylase activity in CAM plants. This enzyme determines whether starch synthesis will occur and has been shown to have important regulatory properties in C_3 plants.

(5) Assessment of alternative paths of glucan mobilisation in CAM plants. Hexokinase activities were low in both the present study and in that by Sutton (1974). Amylase is not only present in CAM tissues (Vieweg and de Fekete, 1977; Dittrich, unpublished) but also exhibits a diurnal

periodicity of activity. Since the stoichiometry of the dark reactions, shown in Figure 1.3 , would balance if amylase rather than phosphorylase was involved in starch degradation it would be worthwhile to check whether hexokinase activity is being lost during extraction.

(6) Further studies on the location of NADP malic enzyme and PEPCK. The cytoplasmic location needs to be confirmed in more species.

(7) Further studies on the location and activities of NADP MDH and its isoenzymes. It may be important to demonstrate whether isoenzymes of NADP MDH are present in cytoplasm and chloroplasts, and whether these are responsible for the double pH optima observed in Chapters 4.1 and 4.3).

REFERENCES

ALLAWAY, W.G., AUSTIN, B. and SLATYER, R.O. 1974 Carbon dioxide and water vapour exchange parameters of photosynthesis in a crassulacean plant *Kalanchoe daigremontiana*. Aust. J. Plant Physiol 1: 397-405.

ALLAWAY, W.G., TROUGHTON, J.H. and OSMOND C.B. 1974 Environmental regulation of growth, photosynthetic pathway and carbon isotope discrimination ratio in plants capable of crassulacean acid metabolism. *In* Mechanisms of Regulation of Plant Growth. R.L. Bieleski, A.R. Ferguson, M.M. Cresswell, eds., pp 195-204. Bull. 12; The Roy. Soc. N.Z., Wellington.

ARNON, D.I. 1949 Copper enzymes in isolated chloroplasts. Polyphenoloxidase in *Beta vulgaris*. Plant Physiol. 24: 1-15.

ARONOFF, S. 1961 *Techniques of Radiobiochemistry*. Iowa State University Press, Iowa.

ARRON, G.P., SPALDING, M.H. and EDWARDS, G.E. 1979 Isolation and oxidative properties of intact mitochondria from the leaves of *Sedum praealtum* - a Crassulacean Acid Metabolism plant. Plant Physiol. (in press).

AVADHANI, P.N., OSMOND C.B. and TAN, K.K. 1971 Crassulacean acid metabolism and the C_4 pathway of photosynthesis in succulent plants. *In* Photosynthesis and Photorespiration. M.D. Hatch, C.B. Osmond, R.O. Slatyer. eds., pp 288-293. Wiley-Interscience, New York.

BADGER, M.R., ANDREWS, T.J. and OSMOND, C.B. 1975 Detection in C_3, C_4 and CAM plant leaves of a low-K_m (CO_2) form of RuDP carboxylase, having high RuDP oxygenase activity at physiological pH. *In* Proc. 3rd Int. Congr. on Photosynthesis. M. Avron, ed., pp 1421-1429. Elsevier, Amsterdam.

BAIER, D. and LATZKO, E. 1975 Properties and regulation of C-1-fructose-1,6-diphosphate from spinach chloroplasts. Biochim. Biophys. Acta 396: 141-148.

BASSHAM, J.A. 1965 Photosynthesis: the path of carbon. *In* Plant Biochemistry. J. Bonner, J.E. Varner, eds., pp 875-903. Academic Press, New York and London.

BEEVERS, H. and GIBBS, M. 1954 The direct oxidation pathway in plant respiration. Plant Physiol. 29: 322-324.

BENNETT - CLARK, T.A. 1932 The role of organic acids in plant metabolism. Part II. New Phytol 32: 128-161.

BIRD, I.F., CORNELIUS, M.J., DYER, T.A. and KEYS, A.J. 1973 The purity of chloroplasts isolated in non-aqueous media.

BJÖRKMAN, O. and OSMOND, C.B. 1974 Effect of oxygen on carbon dioxide fixation in *Kalanchoe daigremontiana*. Carnegie Inst Yearbook 73: 852-858.

BLACK, C.C. and WILLIAMS, S.L. 1976 Plants exhibiting characteristics common to crassulacean acid metabolism. *In* CO_2 Metabolism and Plant Productivity. R.H. Burris, C.C. Black eds., pp 407-424. University Park Press, Baltimore.

BLOCK, R.J., DURRAM, E.L., ZWEIG, G. 1958 *Paper Chromatography and Paper Electrophoresis*. Academic Press, New York.

BÖCHER, M. and KLUGE, M. 1977 The C_4-pathway of C-fixation in *Spinacea oleracea*. I. ^{14}C-labelling pattern of suspended leaf slices as influenced by the external medium. Z. Pflanzenphysiol 83: 347-361.

BRADBEER, J.W. 1963 Physiological Studies on the Acid Metabolism in Green Plants. IX. The Distribution of ^{14}C in Malate of Darkened *Kalanchoe* leaf fragments after infiltration with labelled pyruvate. Proc. Roy. Soc. B. 157: 279-289.

BRADBEER, J.W., COCKBURN, W. and RANSON, S.L. 1975 The labelling of the carboxyl carbon atoms of malate in *Kalanchoe crenata* leaves. *In* Environmental and Biological Control of Photosynthesis. R. Marcelle, ed., pp 265-272. Junk, The Hague.

BRADBEER, J.W. and RANSON, S.L. 1963 Physiological Studies on Acid Metabolism in Green Plants. VIII. The Utilization of Labelled Pyruvate, Fumarate and Glucose in *Kalanchoe* Leaves in the Dark. Proc. Roy. Soc. B. 157: 258-278.

BRADBEER, J.W., RANSON, S.L. and STILLER, M. 1958 Malate synthesis in crassulacean leaves. 1. The distribution of ^{14}C in malate in leaves exposed to $^{14}CO_2$ in the dark. Plant Physiol. 33: 66-70.

BRANDON, P.C. 1967 Temperature features of enzymes affecting crassulacean acid metabolism. Plant Physiol. 42: 977-984.

BRANDON, P.C. and VAN BOEKEL-MOL, T.N. 1973 Properties of purified malic enzyme in relation to crassulacean acid metabolism. Eur. J. Biochem. 35: 62-69.

BRUINSMA, J. 1958 Studies on the crassulacean acid metabolism. Acta. Botanica Neerlandica 7: 531-588.

BRUNNHÖFER, H. SCHAUB, H. and EGLE, K. 1968 Der Verlave des CO_2 und O_2 Gaswechsels bei *Bryophyllum daigremontianum* in Abhängigkeit von der Temperatur. Z. Pflanzenphysiol. 59: 285-292.

BUCHANAN, B.B., SCHÜRMANN, P. and KALBERER, P.P. 1971 Ferredoxin-activated fructose diphosphatase of spinach chloroplasts. Resolution of the system, properties of the alkaline fructose diphosphatase component, and physiological significance of the ferridoxin-linked activation. J. Biol. Chem. 246: 5952-5959.

BÜCHER, Th. 1947 Über ein Phosphatübertragendes Gärungsferment. Biochim. Biophys. Acta 1: 292-314.

BURRIS, R.H. 1953 Organic acids in plant metabolism. Ann. Rev. Plant Physiol. 4: 91-114.

BUSER, Ch. and MATILE, Ph. 1977 Malic acid in vacuoles isolated from *Bryophyllum* leaf cells. Z. Pflanzenphysiol. 82: 462-466.

CANNATA, J.J.B. and DEFLOMBAUM, M.A.C. 1974 Phosphoenolpyruvate carboxylase from bakers yeast. J. Biol. Chem. 249: 3356-3365.

CERFF, R. 1978 Glyceraldehyde-3-phosphate dehydrogenase (NADP) from *Sinapsis alba* L. Reversible association of the enzyme with a protein factor as controlled by pyridine nucleotides *in vitro*. Plant Physiol. 61: 369-372.

CHAMPIGNY, M.L., JOLCHINE, G. and MOYSE, A. 1958 Sur la distribution de $^{14}CO_2$ fixe photosynthese et par β-carboxylation dans les feuilles de *Bryophyllum*. *In* Conf. Int. Radioisotopes Rech. Sc. pp 458-470. UNESCO, Pergamon Press, Paris.

CHANG, H.C., MARUYAMA, H., MILLER, R.S. and LANE, M.D. 1966 The enzymatic carboxylation of phosphoenolpyruvate. III. Investigation of the kinetics and mechanism of the mitochondria phosphoenolpyruvate carboxykinase-catalysed reaction. J. Biol. Chem. 241: 2421-2430

CHAPMAN, E.A. and OSMOND C.B. 1974 The effect of light on the tricarboxylic acid cycle. III. A comparison between some C_3 and C_4 plants. Plant Physiol. 53: 893-898.

CHAPMAN, K.S.R. and HATCH, M.D. 1977 Regulation of mitochondrial NAD-malic enzyme involved in C_4 pathway photosynthesis. Arch. Biochem. Biophys. 184: 298-306.

COCKBURN, W. and McAULAY, A. 1975a The pathway of carbon dioxide fixation in crassulacean plants. Plant Physiol. 55: 87-89.

COCKBURN, W. and McAULAY, A. 1975b The pathway of malate synthesis in crassulacean acid metabolism. *In* Environmental and Biological Control of Photosynthesis. R. Marcelle, ed., pp 273-279. Junk, The Hague.

COCKBURN, W. and McAULAY 1977 Changes in metabolite levels in *Kalanchoe daigremontiana* and the regulation of malic acid accumulation in crassulacean acid metabolism. Plant Physiol. 59: 455-458.

COCKBURN, W., TING, I.P. and STERNBERG, L.O. 1979 Relationship between stomatal behaviour and internal carbon dioxide concentration in CAM plants. Plant Physiol. (in press).

CONN, E.E. and STUMPF, P.K. 1972 *Outline of Biochemistry.* 3rd ed. John Wiley and Sons, Inc., New York.

CREWS, C.E., VINES, H.M. and BLACK, C.C. 1975 Post illumination burst of carbon dioxide in crassulacean acid metabolism plants. Plant Physiol. 55: 652-657.

CREWS, C.E., WILLIAMS, S.L., VINES, H.M. and BLACK, C.C. 1976 Changes in the metabolism and physiology of crassulacean acid metabolism plants grown in controlled environments. *In* CO_2 Metabolism and Plant Productivity. R.H. Burris, C.C. Black, eds., pp 235-250. University Park Press, Baltimore.

DALEY, L.S., RAY, T., VINES, H.M. and BLACK, C.C. 1976 Pineapple PEP carboxylase: partial purification and properties. Plant Physiol. Sup. 57: 32.

DANNER, J. and TING, I.P. 1967 CO_2 metabolism in corn roots. II. Intracellular distribution of enzymes. Plant Physiol. 42: 719-724.

DARBRE, A. 1978 Esterification. *In* Handbook of Derivatives for Chromatography. K. Blau, G. King, eds., pp 39-103. Heyden, London, Philadelphia, Rheine.

DELEENS, E. and GARNIER-DARDART, J. 1977 Carbon isotope composition of biochemical fractions isolated from leaves of *Bryophyllum daigremontiana* Berger, a plant with crassulacean acid metabolism: some physiological aspects related to CO_2 dark fixation. Planta 135: 241-248.

DENIUS, H.R. and HOMANN, P.H. 1972 The relation between photosynthesis respiration and crassulacean acid metabolism in leaf slices of *Aloe arborescens* Mill. Plant Physiol. 49: 873-880.

DITTRICH, P. 1976a Nicotinamide adenine dinucleotide - specific "malic" enzyme in *Kalanchoe daigremontiana* and other plants exhibiting crassulacean acid metabolism. Plant Physiol 57: 310-314.

DITTRICH, P. 1976b Equilibration of label in malate during dark fixation of CO_2 in *Kalanchoe fedtschenkoi*. Plant Physiol. 58: 288-291.

DITTRICH, P., CAMPBELL, W.H. and BLACK, C.C. 1973 Phosphoenolpyruvate carboxykinase in plants exhibiting crassulacean acid metabolism. Plant Physiol. 52: 357-361.

DITULLIO, N.W., BERKOFF, C.E., BLANK, B., KOSTOS, V., STACK, E.J. and SAUNDERS, H.L. 1974 3-mercaptopicolinic acid, an inhibitor of gluconeogenesis. Biochem J. 138: 387-394.

EDWARDS, G.E. and HUBER, S.C. 1978 Usefullness of isolated cells and protoplasts for photosynthetic studies. *In* Proc. 4th Intern. Cong. Photosynthesis, University of Reading. D.O. Hall, J. Coombs, T.W.Goodwin, eds., pp 95-106. Biochemical Society, London.

EVANS, H. 1932 The physiology of succulent plants. Biol. Rev. 7: 181-211.

EVANS, H.J. and WOOD, H.G. 1971 Purification and properties of pyruvate phosphate dikinase from propionic acid bacteria. Biochemistry 10: 721-729.

FEIGE, B., GIMMLER, H., JESCHKE, W.D. and SIMONIS, W. 1969 Eine Methode zur dünnschichtchromatographischen Auftrennung von ^{14}C und ^{32}P-markierten Stoffwechselprodukten. J. Chrom. 41: 80-90.

GAFF, D.F. and OKONG'O-OGLOA, O. 1971 The use of non-permeating pigments for testing the survival of cells. J. Expt. Bot. 22: 756-758.

GARNIER-DARDART, J. 1965 Activités exzymatiques des chloroplastes isolés de feuilles de *Bryophyllum daigremontianum* Berger: oxydation des hexoses, formation et dégradation d'acide malique. Physiol. Vég. 3(3): 215-227.

GARNIER-DARDART, J. and QUEIROZ, O. 1974 Malic enzyme in the leaves of *Bryophyllum daigremontianum*. Phytochem. 13: 1695-1702.

GERWICK, B.C., SPALDING, M.H., WILLIAMS, G.J. and EDWARDS, G.E. 1978 Temperature response of CO_2 fixation in isolated *Opuntia* cells. Plant Sci. Lett. 13: 389-396.

GHOSH, H.P. and PREISS, J. 1966 Adenosine diphosphate glucose pyrophosphorylase. A regulatory enzyme in the biosynthesis of starch in spinach leaf chloroplasts. J. Biol. Chem. 241: 4491-4504.

GIBBS, M. and BEEVERS, H. 1955 Glucose dissimilation in the higher plant. The effect of age of tissue. Plant Physiol. 30: 343-347.

GREENWAY, H., WINTER, K. and LÜTTGE, U. 1978 Phosphoenolpyruvate carboxylase during development of crassulacean acid metabolism and during a diurnal cycle in *Mesembryanthemum crystallinum*. J. Exp. Bot. 29: 547-559.

GRISOLIA, S. 1962 Phosphoglyceric acid mutase. *In* Methods in Enzymology. S.P. Colowick, N.O. Kaplan, eds., Vol. V, pp 236-242. Academic Press, New York, London.

GUTIERREZ, M., GRACEN, V.E. and EDWARDS, G.E. 1974 Biochemical and cytological relationships in C_4 plants. Planta 119: 279-300.

HAIDRI, D. 1955a *The Synthesis of Starch from Organic Acids in Plants.* PhD Thesis, University of Wisconsin.

HAIDRI, D. 1955b Incorporation of malic-acid 2-^{14}C and pyruvic acid 2-^{14}C into starch. Plant Physiol. 30: 3-4.

HATCH, M.D. 1973 An assay for PEP carboxykinase in crude tissue extracts. Anal. Biochem. 52: 280-285.

HATCH, M.D. and KAGAWA, T. 1974a Activity, location and role of NAD malic enzyme in leaves with C_4 pathway photosynthesis. Aust. J. Plant Physiol. 1: 357-369.

HATCH, M.D. and KAGAWA, T. 1974b NAD malic enzyme in leaves with C_4-photosynthesis and its role in C_4 acid decarboxylation. Arch. Biochem. Biophys. 160: 346-349.

HATCH, M.D., KAGAWA, T. and CRAIG, S. 1975 Subdivision of C_4 pathway species based on differing C_4 acid decarboxylating systems and ultrastructural features. Aust. J. Plant Physiol. 2: 111-128.

HATCH, M.D. and MAU, S. 1973 Activity, location and role of aspartate aminotransferase and alanine aminotransferase in leaves with C_4 pathway photosynthesis. Arch. Biochem. Biophys. 156: 195-206.

HATCH, M.D. and MAU, S.L. 1977 Properties of phosphoenolpyruvate carboxykinase operative in C_4 pathway photosynthesis. Aust. J. Plant Physiol. 4: 207-216.

HATCH, M.D., MAU, S.L. and KAGAWA, T. 1974 Properties of leaf NAD malic enzyme from plants with C_4 photosynthetic pathway. Arch. Biochem. Biophys. 165: 188-200.

HATCH, M.D. and OSMOND, C.B. 1976 Compartmentation and transport in C_4 photosynthesis. *In* Transport in Plants IV. Intracellular Interactions and Transport Processes, Encyclopedia of Plant Physiology, New Series. C.R. Stocking, U. Heber, eds., pp 144-184. Springer Verlag, Berlin, Heidelberg, New York.

HATTERSLEY, P.W., WATSON, L. and OSMOND, C.B. 1977 *In situ* immunofluorescent labelling of ribulose-1,5-bisphosphate carboxylase in leaves of C_3 and C_4 plants. Aust. J. Plant Physiol. 4: 523-539.

HEBER, U. 1974 Metabolite exchange between chloroplasts and cytoplasm. Ann. Rev. Plant Physiol. 25: 393-422.

HELDT, H.W. 1976 Metabolite carriers of chloroplasts. *In* Transport in Plants III. Intracellular Interactions and Transport Processes. Encyclopedia of Plant Physiology, New Series. C.R. Stocking, U. Heber, eds., pp 137-143. Springer Verlag, Berlin, Heidelberg, New York.

HERBERT, M. BURKHARD, Ch. and SCHNARRENBERGER, C. 1978 Cell organelles from crassulacean acid metabolism (CAM) plants. 1. Enzymes in isolated peroxisomes. Planta 143: 279-284.

HERBERT, M. BURKHARD, Ch. and SCHNARRENBERGER, C. 1979 A survey for isoenzymes of glucosephosphate isomerase, phosphoglucomutase, glucose-6-phosphate dehydrogenase and 6-phosphogluconate dehydrogenase in C_3, C_4 and crassulacean acid metabolism plants, and green algae. Planta 145: 95-104.

HOHORST, H.J. L-[-]-malate. Determination with malic dehydrogenase and DPN. *In* Methods of Enzymatic Analysis. H.W. Bergmeyer, ed., pp 328-332. Academic Press, New York, London.

HOUGH, L. and JONES, J.K.N. 1962 Chromatography on paper. *In* Methods in Carbohydrate Chemistry. Vol. I Analysis and Preparation of Sugars. R.L. Whistler, M.L. Wolfrom, eds., Academic Press: New York, London.

HUBER, S.C. and EDWARDS, G.E. 1977a Transport in C_4 mesophyll chloroplasts evidence for an exchange of inorganic phosphate and phosphoenolpyruvate. Biochim. Biophys. Acta. 462: 603-612.

HUBER, S.C. and EDWARDS, G.E. 1977b Transport in C_4 mesophyll chloroplasts characterization of the pyruvate carrier. Biochim. Biophys. Acta. 462: 583-602.

JOHNSON, C.M. 1957 Comparative chlorine requirements of different plants species. Plantand Soil 8: 337-353.

JOHNSON, H.S. and HATCH, M.D. 1970 Properties and regulation of leaf nicotinamide-adenine dinucleotide phosphate-malate dehydrogenase and "malic" enzyme in plants with the C_4 dicarboxylic acid pathway of photosynthesis. Biochem. J. 119: 273-280.

JOLCHINE, G. 1959 Sur la distribution du ^{14}C dans les molécules d'acide malique synthétisées par fixation de $^{14}CO_2$ dans les feuilles de *Bryophyllum daigremontianum* Berger. Bull. Soc. Chim. Biol. 41: 227-234.

JOMAIN-BAUM, M., SCHRAMM, V.L. and HANSON, R.W. 1976 Mechanism of 3-mercaptopicolinic acid inhibition of hepatic phosphoenolpyruvate carboxykinase (GTP). J. Biol. Chem. 251(1): 37-44.

JONES, H.G. 1973 Photosynthesis by thin leaf slices in solution. II. Osmotic stress and its effect on photosynthesis. Aust. J. Biol. Sci. 26: 25-33.

JONES, R., WILKINS, M.B., GOGGING, J.R., FEWSON, Ch. and MALCOLM, A.D.B. 1978 Phosphoenolpyruvate carboxylase from the crassulacean plant *Bryophyllum fedtschenkoi* Hamet et Perrier: purification, molecular and kinetic properties. Biochem. H. 175: 391-406.

KANAI, R. and EDWARDS, G.E. 1973 Purification of enzymatically isolated mesophyll protoplasts from C_3, C_4 and crassulacean acid metabolism plants using an aqueous dextran-polyethylene glycol two-phase system. Plant Physiol. 52: 484-490.

KAPIL, R.N., PUGH, T.D. and NEWCOMB, E.H. 1975 Microbodies and anomalous "microcylinder" in the ultrastructure of plants with crassulacean acid metabolism. Planta 124: 231-244.

KAPLAN, A. GALE, J. and POLJAKOFF-MAYBER, A. 1976 Resolution of net dark fixation of carbon dioxide into its respiration and gross fixation components in *Bryophyllum daigremontianum*. J. Exp. Bot. 27: 220-230.

KAPLAN, A., GALE, J. and POLJAKOFF-MAYBER, A. 1977 Effect of oxygen and carbon dioxide concentrations on gross dark CO_2 fixation and dark respiration in *Bryophyllum daigremontianum*. Aust. J. Plant Physiol. 4: 745-752.

KELLY, G.J. and LATZKO, E. 1975 Evidence for phosphofructokinase in chloroplasts. Nature 256: 429-430.

KELLY, G.J. and LATZKO 1977a Chloroplast phosphofructokinase. 1. Proof of phosphofructokinase activity in chloroplasts. Plant Physiol. 60: 290-294.

KELLY, G.J. and LATZKO, E. 1977b Chloroplast phosphofructokinase. II Partial purification, kinetic and regulatory properties. Plant Physiol. 60: 295-299.

KELLY, G.J., LATZKO, E. and GIBBS, M. 1976 Regulatory aspects of photosynthetic carbon metabolism. Ann. Rev. Plant Physiol. 27: 181-205.

KENYON, W.H., KRINGSTAD, R. and BLACK, C.C. 1978 Diurnal changes in the malic acid content of vacuoles isolated from leaves of the crassulacean acid metabolism plant, *Sedum telephium*. FEBS Letters 94(2): 281-283.

KHAN, A.A., TEWARI, C.P. KRISHNAN, P.S. and SANWAL, G.G. 1970 Respiratory particles from *Cactus phylloclades*. Phytochemistry 9: 1423-1431.

KLEMME, B. and JACOBI, G. 1974 Separation and characterisation of two inorganic pyrophosphatases from spinach leaves. Planta 120: 147-153.

KLUGE, M. 1968a Untersuchungten über den Gaswechsel von *Bryophyllum* wärend der Lichtperiode. 1. Zum Problem der CO_2-Abgabe. Planta 80: 255-263.

KLUGE, M. 1968b Untersuchungen über den Gaswechsel von *Bryophyllum* während der Lichtperiode. II. Beziehungen zuischen dem Malatgehalt des Gewebes und der CO_2-Aufnahme Planta 80: 359-377.

KLUGE, M. 1969a On the analysis of CO_2 exchange in *Bryophyllum*. 1. Measurement of the alteration of relative pool sizes in the leaf tissue during certain phases of the light-dark period. Planta 85: 160-170.

KLUGE, M. 1969b On the analysis of CO_2 exchange in *Bryophyllum*. II. Inhibition of starch loss during the night in an atmosphere free from CO_2. Planta 86: 142-150.

KLUGE, M. 1969c Changes in labelling patterns after feeding *Bryophyllum tubiflorum* with $^{14}CO_2$ at different times during the light/dark period. Planta 88: 113-129.

KLUGE, M. 1971 Veränderliche Markierungsmuster bei $^{14}CO_2$-Fütterung von *Bryophyllum tubiflorum* zu verschiedenen Zeitpunkten der Hell-Dunkel-Periode. II. Beziehungen zwischen dem Malatgehalt des Gewebes und dem Markierungsmuster nach $^{14}CO_2$-Lichtfixierung. Planta 98: 20-30.

KLUGE, M. 1976a Crassulacean acid metabolism (CAM): CO_2 and water economy. *In* Water and Plant Life. Problems and Modern Approaches to Ecological Studies. O.L. Lange, L. Kappen, E.-D. Schulze, eds., Vol. 19, pp 313-323. Spinger: Berlin, Heidelberg, New York.

KLUGE, M. 1976b Models of CAM regulation. *In* CO_2 Metabolism and Plant Productivity. R.H. Burris, C.C. Black, eds., pp 205-216. University Park Press, Baltimore.

KLUGE, M., BLEY, L. and SCHMID, R. 1975 Malate synthesis in crassulacean acid metabolism (CAM) via a double CO_2 dark fixation? *In* Environmental and Biological Control of Photosynthesis. R. Marcelle, ed., pp 281-288. Junk, The Hague.

KLUGE, M. and HEININGER, B. 1973 Untersuchungen über den Efflux von Malat aus den Vacuolen der assimilierenden Zellen von *Bryphyllum daigremontianum* und mögliche Einflüsse dieses Vorganges auf den CAM. Planta 113: 333-343.

KLUGE, M., KRIEBITSCH, Ch. and VON WILLERT, D. 1974 Dark fixation of CO_2 in crassulacean acid metabolism: are two dark fixation steps involved? Z. Pflanzenphysiol. 72: 460-467.

KLUGE, M., LANGE, O.L., VON EICHMANN, M. and SCHMIDT, R. 1973 Diurnaler Säurerhythmus bei *Tillandsia usneoides:* Untersuchungen über den Weg des Kohlenstoffs sowie die Abhängigkeit des CO_2-Gaswechsels von Lichtintensität, Temperatur und Wassergehalt der Pflanze. Planta 112: 357-372.

KLUGE, M. and OSMOND, C.B. 1971 Pyruvate,Pi dikinase in crassulacean acid metabolism. Naturwissenschafter 8: 414-415.

KLUGE, M. and OSMOND, C.B. 1972 Studies on phosphoenolpyruvate carboxylase and other enzymes of crassulacean acid metabolism of *Bryophyllum tubiflorum* and *Sedum praealtum*. Z. Pflanzenphysiol. 66: 97-105.

KLUGE, M. and TING, I.P. 1979 *Crassulacean acid metabolism: Analysis of an ecological adaptation.* Ecological Studies Vol. 30. Springer Verlag: Berling, Heidelberg, New York.

KU, S.B., SPALDING, M.H. and EDWARDS, G.E. 1979 Intracellular localization of phosphoenolpyruvate carboxykinase in leaves of C_4 and CAM plants. Plant Physiol 63s (poster 348): 63.

KUNITAKE, G. and SALTMAN, P. 1958 Dark fixation of CO_2 by succulent leaves: conservation of the dark fixed CO_2 under diurnal conditions. Plant Physiol. 83: 400-403.

LANGE, O.L., SCHULZE, E.-D., KAPPEN, L., EVENARI, M. and BUSCHBOM. U. 1975 CO_2 exchange pattern under natural conditions of *Caralluma negevensis*. a CAM plant of the Negev desert. Photosynthetica 9: 318-326.

LATIES, G.G. 1949a Oxidative formation of succinate in higher plants. Arch. Biochem. 22: 8-15.

LATIES, G.G. 1949b The role of pyruvate in the aerobic respiration of barley roots. Arch. Biochem. 20: 284-299.

LATZKO, E. and GIBBS, M. 1968 Distribution and activity of enzymes of the reductive pentose phosphate cycle in spinach leaves and in chloroplasts isolted by different methods. Z. Pflanzenphysiol. 59: 184-194.

LATZKO, E., ZIMMERMANN, G. and FELLER, U. 1974 Evidence for a hexosediphosphatase from the cytoplasm of spinach leaves. Z. Physiol. 355: 321-366.

LEVI, C. and GIBBS, M. 1975 Carbon dioxide fixation in isolated *Kalanchoe* chloroplasts. Plant Physiol. 56: 164-166.

LI, J.J., ROSS, C.R., TEPPERMAN, H.M. and TEPPERMAN, J. 1975 Nicotinamide adenine dinucleotide phosphate - malic enzyme of rat liver. Purification, properties and immunochemical studies. J. Biol. Chem. 250: 141-148.

LILLEY, R and WALKER, D.A. 1974 An improved spectrophotometric assay for ribulosebisphosphate carboxylase. Biochim. Biophys. Acta. 358: 226-229.

LÜTTGE, U. and BALL, E. 1974a Proton and malate fluxes in cells of *Bryophyllum daigremontianum*. Z. Pflanzenphysiol. 73: 326-338.

LÜTTGE, U. and BALL, E. 1974b Mineral ion fluxes in slices of acidified and de-acidified leaves of the CAM plant *Bryophyllum daigremontianum*. Z. Pflanzenphysiol. 73: 339-348.

LÜTTGE, U. and BALL, E. 1977a Water relation parameters of the CAM plant *Kalanchoe daigremontiana* in relation to diurnal malate oscillations. Oecologia 31: 85-94.

LÜTTGE, U. and BALL, E. 1977b Concentration and pH dependence of malate efflux and influx in leaf slices of CAM plants. Z. Pflanzenphysiol. 83: 43-54.

LÜTTGE, U. and BALL, E. 1979 Electrochemical investigations of active malic acid transport at the tonoplast into the vacuoles of the CAM plant *Kalanchoe daigremontiana*. J. Membrane Biol. (in press).

LÜTTGE, U., BALL, E. and GREENWAY, H. 1977 Effects of water and turgor potential on malate efflux from leaf slices of *Kalanchoe daigremontiana*. Plant Physiol. 60: 521-523.

LÜTTGE, U., BALL, E. and TROMBALLA, H.W. 1975 Potassium independence of osmoregulated oscillations of malate^{2-} levels in the cells of CAM leaves. Biochem. Physiol. Pflanz. 167: 267-283.

LÜTTGE, U., KLUGE, M. and BALL, E. 1975 Osmoregulation of vacuolar malic acid storage: a basic principle in oscillatory behaviour of crassulacean acid metabolism. Plant Physiol. 56: 613-616.

MACLENNAN, D.H., BEEVERS, H. and BARLEY, J.L. 1963 Compartmentation of acids in plant tissues. Biochem. J. 89: 316-327.

MARCELLE, R. (ed.) 1975a *Environmental and Biological Control of Photosynthesis*. Junk, The Hague.

MARCELLE, R. 1975a Effect of photoperiod on the CO_2 and O_2 exchanges of leaves of *Bryophyllum daigremontianum* (Berger.). *In* Environmental and Biological Control of Photosynthesis. R. Marcelle, ed., pp 349-356. Junk, The Hague.

MAZELIS, M. and VENNESLAND, B. 1957 Carbon dioxide fixation into oxalacetate in higher plants. Plant Physiol. 32: 391-600.

MILBURN, T.R., PEARSON, D.J. and NDEGWE, N.A. 1968 Crassulacean acid metabolism under natural tropical conditions. New Phytol 67: 883-897.

MONTGOMERY, C.M. and WEBB, J.L. 1956 Metabolic studies on heart mitochondria II. The inhibitory action of parapyruvate on the tricarboxylic acid cycle. J. Biol. Chem. 221: 359-368.

MOREL, C., CELATI, C. and QUEIROZ, O. 1972 Sur le métabolisme acide des Crassulacées. V. Adaptation de la capacité enzymatique aux changements de photopériode. (métabolisme de l'acide malique et transaminations). Physiol Vég. 10: 743-763.

MÜHLBACH, H. and SCHNARRENBERGER, C. 1978 Properties and intracellular distribution of two phosphoglucomutases from spinach leaves. Planta 141: 65-70.

MUKERJI, S.K. and TING, I.P. 1968a Intracellular localization of CO_2 metabolism in *Cactus phylloclades*. Phytochem 7: 903-911.

MUKERJI, S.K. and TING, I.P. 1968b Malate dehydrogenase(decarboxylating) (NADP) isoenzymes of *Opuntia* stem tissue. Biochim. Biophys. Acta. 167: 239-249.

NALBORCZYK, E., LaCROIX, L.J. and HILL, R.P. 1978 Environmental influences of light and dark CO_2 fixation by *Kalanchoe daigremontiana*. Can. J. Bot. 53: 1132-1138.

NEAL, G.E. and BEEVERS, H. 1960 Pyruvate utilization in castor-bean endosperm and other tissues. Biochem. J. 74: 409.

NEALES, T.F. 1973 The effect of night temperature and CO_2 assimilation on transpiration and water use efficiency in *Agave americana* L. Aust. J. Biol. Sci. 26: 705-714.

NEGELEIN, E. 1963 D-1,3-diphosphoglycerate. *In* Methods of Enzymatic Analysis. H.U. Bertmeyer, ed., pp 234-237. Academic Press: New York, London.

NISHIDA, K. and SANADA, Y. 1977 Carbon dioxide fixation in chloroplasts isolated from CAM plants. Plant and Cell Physiol. Special Issue. Photosynthetic Organelles: 341-346.

NISHIKIDO, T. and WADA, T. 1974 Comparative studies of NADP-malic enzyme from C_4- and C_3- plants. Biochem. Biophys. Res. Commun. 61: 243-249.

NOBEL, P.S. 1976 Water relations and photosynthesis of a desert CAM plant *Agave deserti*. Plant Physiol. 58: 576-582.

NOCE, P.S. and UTTER, M.F. 1975 Decarboxylation of oxaloacetate to pyruvate by purified avian liver phosphoenolpyruvate carboxykinase. J. Biol. Chem. 250: 9099=9105.

OSMOND, C.B. 1974 Carbon reduction and photosystem II Deficiency in leaves of C_4 plants. Aust. J. Plant Physiol. 1: 41-50.

OSMOND, C.B. 1975 Environmental control of photosynthetic options of crassulacean plants. *In* Environmental and Biological Control of Plants. R. Marcelle, ed. Junk, The Hague.

OSMOND, C.B. 1976 CO_2 assimilation and dissimilation in the light and dark in CAM plants. *In* CO_2 Metabolism and Plant Productivity. R.H. Burris, C.C. Black, eds., pp 217-233. University Park Press: Baltimore, London Toyko.

OSMOND, C.B. 1978 Crassulacean acid metabolism: A curiosity in context. Ann. Rev. Plant Physiol. 29: 379-414.

OSMOND, C.B. and ALLAWAY, W.G. 1974 Pathways of CO_2 fixation in the CAM plant *Kalanchoe daigremontiana*. I. Patterns of $^{14}CO_2$ fixation in the light. Aust. J. Plant Physiol. 1: 503-511.

OSMOND, C.B. and BJÖRKMAN, O. 1975 Pathways of CO_2 fixation in the CAM plant *Kalanchoe daigremontiana*. II. Effects of O_2 and CO_2 concentration on light and dark CO_2 fixation. Aust. J. Plant Physiol. 2: 155-162.

OSMOND, C.B., NOTT, D.L. and FIRTH, P.M. 1979 Carbon assimilation patterns and growth of the introduced CAM plant *Opuntia inermis* in Eastern Australia. Oecologia (in press).

PACOLD, I. and ANDERSON, L.E. 1973 Energy charge control of the Calvin cycle enzyme 3-phosphoglyceric acid kinase. Biophys. Biochem. Res. Comm. 51(1): 139-143.

PIERRE, J.N. and QUEIROZ, O. 1979 Regulation of glycolysis and level of the crassulacean acid metabolism. Planta 144: 143-151.

PREISS, J. and KOSUGE, T. 1970 Regulation of enzyme activity in photosynthetic systems. Ann. Rev. Plant Physiol. 21: 433-465.

PUCHER, G.W., VICKERY, H.B., ABRAHAMS, M.D. and LEAVENWORTH, C.S. 1949 Studies in the metabolism of crassulacean plants: diurnal variation in organic acids and starch in excised plants of *Bryophyllum calycinum*. Plant Physiol. 24: 610-620.

PUCHER, G.W., VICKERY, H.B. and ABRAHAMS, M.D. 1949 Studies in the metabolism of crassulacean plants: diurnal variation in organic acids and starch in excised leaves of *Bryophyllum calycinum*. Plant Physiol. 24: 610-620.

PURIL LO, P. and ROSSI, P. 1979 Two forms of NADP dependent malic enzyme in

QUEIROZ, O. 197 CAM: rhythms of enzyme capacity and activity as adaptive control mechanisms. *In* Encyclopedia of Plant Physiology: Photosynthesis. M. Gibbs, E. Latzko, eds., Vol. 2. Springer Verlag, Berlin (in press).

QUEIROZ, O. and MOREL, C. 1974 Photoperiodism and enzyme activity. Towards a model for the control of circadian metabolic rhythms in the crassulacean acid metabolism. Plant Physiol. 53: 596-602.

RANSON, S.L. and THOMAS, M. 1960 Crassulacean acid metabolism. Ann. Rev. Plant Physiol. 11: 81-110.

RAY, T.B. and BLACK, C.C. 1976a Characterization of phosphoenolpyruvate carboxykinase from *Panicum maximum*. Plant Physiol. 58: 605-607.

RAY, T.B. d BLACK, C.C. 1976b Inhibition of oxaloacetate decarboxylation during C_4 photosynthesis by 3-mercaptopicolinic acid. J. Bio. Chem. 251: 5824-5826.

RAY, T.B. and BLACK, C.C. 1977 Oxaloacetate as the source of carbon dioxide for photosynthesis in bundle sheath cells of the C_4 species *Panicum maximum*. Plant Physiol. 60: 193-196.

REEVES, R.E. 1968 A new enzyme with the glycolytic function of pyruvate kinase. J. Biol. Chem. 243: 3202-3204.

REHFELD, D.W. and JENSEN, R.G. 1973 Metabolism of separated leaf cells. III. Effects of calcium and ammonia on product distribution during photosynthesis with cotton cells. Plant Physiol. 52: 17-22.

ROBINSON, B.H. and OEI, J. 1975 3-mercaptopicolinic acid, a preferential inhibitor of the cytosolic phosphoenolpyruvate carboxykinase. FEBS Letters 58(1): 12-15.

ROBINSON, S.P. and WISKITCH, J.T. 1977 Pyrophosphate inhibition of carbon dioxide fixation in isolated pea chloroplasts by uptake in exchange for endogenous adenine nucleotides. Plant Physiol. 59: 422-427.

ROUHANI, I. 1972 *Pathways of carbon metabolism in spongy mesophyll cells from Sedum telephium leaves*. PhD Thesis, University of Georgia, Athens.

ROUHANI, I., VINES, H.M. and BLACK, C.C. 1973 Isolation of mesophyll cells from *Sedum telephium* leaves. Plant Physiol. 51: 97-103.

SALTMAN, P., LYNCH, V.H., KUNITAKE, G.M., STITT, C. and SPOLTER, H. 1957 The dark fixation of CO_2 by succulent leaves: metabolic changes subsequent to initial fixation. Plant Physiol. 32: 197-200.

SANTARIUS, K.A. and HEBER, U. 1965 Changes in the intracellular levels of ATP, ADP, ADMP and Pi and regulatory function of the adenylate system in leaf cells during photosynthesis. Biochim. Biophys. Acta. 102: 39-54.

SATTA, M.A. and SISINI, A. 1964 Attiva glucoso-6-fosfatasica e fruttoso-1,6-difosfatasica in *Opuntia* ficus indica. Soc. Ital. di Biol. Sper. Boll. 40(18): 1109-1110.

SPALDING, M.H. and EDWARDS, G.E. 1978 Photosynthesis in enzymatically isolate leaf cells from the CAM plant *Sedum telephium* L. Planta 141: 59-63.

SPALDING, M.H., SCHMITT, M.R., KU, S.B. and EDWARDS, G.E. 1979 Intracellular localization of some key enzymes of crassulacean acid metabolism in *Sedum praealtum*. Plant Physiol. 63: 738-743.

STEUP, M. and LATZKO, E. 1979 Intracellular localization of phosphorylases in spinach and pea leaves. Planta 145: 69-76.

STEUP, M., PEAVEY, D.G. and GIBBS, M. 1976 The regulation of starch metabolisr by inorganic phosphate. Biochem. Biophys. Res. Commun. 72: 1554-1561.

STILLER, M.L. 1959 *The Mechanism of Malate Synthesis in Crassulacean Leaves*. PhD Thesis, Purdue University, Lafayette, Indiana.

SUGIYAMA, T. L973 Purification, molecular and catalytic properties of pyruvate, phosphate dikinase from the maize leaf. Biochem 12(15): 2862-2868.

SUGIYAMA, T. and LAETSCH, W.M. Occurrence of pyruvate orthophosphate dikinase in the succulent plant *Kalanchoe daigremontiana* Hamet. et Perr. Plant Physiol. 56: 605-607.

SUTTON, B.G. 1974 *Regulation of Carbohydrate Metabolism in Succulent Plants*. PhD Thesis, Australian National University.

SUTTON, B.G. 1975a The path of carbon in CAM plants at night. Aust. J. Plant Physiol. 2: 377-387.

SUTTON, B.G. 1975b Glycolysis in CAM plants. Aust. J. Plant Physiol. 2: 389-402.

SUTTON, B.G. Kinetic properties of phosphorylase and 6-phosphofructokinase of *Kalanchoe daigremontiana* and *Atriplex spongiosa*. Aust. J. Plant Physiol. 2: 403-411.

SUTTON, B.G. and OSMOND, C.B. 1972 Dark fixation of CO_2 by crassulacean plants. Evidence for a single carboxylation step. Plant Physiol. 50: 360-365.

SZAREK, S.R., JOHNSON, H.B. and TING, I.P. 1973 Drought adaptation in *Opuntia basilaris*. Plant Physiol. 52: 539-541.

SZAREK, S.R. and TING, I.P. 1974 Respiration and gas exchange in stem tissue of *Opuntia basilaris*. Plant Physiol. 54: 829-834.

SZAREK, S.R. and TING, I.P. 1977 The occurrence of crassulacean acid metabolism among plants. Photosynthetica 11: 330-342.

TING, I.P. 1971 Nonautotrophic CO_2 fixation and crassulacean acid matebolism. *In* Photosynthesis and Photorespiration. M.D. Hatch, C.B. Osmond R.O. Slatyer, eds., pp 169-185. Wiley-Interscience, New York.

TING, I.P. 1976 Crassulacean acid metabolism in natural ecosystems in relation to annual CO_2 uptake patternadn water utilization. *In* CO_2 Metabolism and Plant Productivity. R.H. Burris, C.C. Black, eds., pp 251-268. University Park Press: Baltimore, London, Toyko.

TING, I.P. and DUGGER, W.M. 1968 Non-autotrophic carbon dioxide metabolism in cacti. Bot. Gaz. 129: 9-15.

TING, I.P., JOHNSON, H.B. and SZAREK, S.R. 1972 Net CO_2 fixation in crassulacean acid metabolism plants. *In* Net Carbon Dioxide Assimilation in Higher Plants. C.C. Black, ed., pp 26-53. Proc. Symp. S. Sect. Am. Soc. Plant. Physiol. Cotton. Inc., Raleigh.

TING, I.P. and OSMOND, C.B. 1973 Activation of plant p-enolpyruvate carboxylases by glucose-6-phosphate: a particular role in crassulacean acid metabolism. Plant Sci. Lett 1: 123-128.

TING, I.P. and SZAREK, S.R. 1975 Drought adaptation in crassulacean acid metabolism. *In* Environmental Physiology of Desert Organisms. N.F. Hadley, ed., pp 152-167. Dowden, Hutchinson and Rass., Strandsburg.

TOMLINSON, J.D. and TURNER, J.F. 1973 Pyruvate kinase of higher plants. Biochem. Biophys. Acta. 329: 128-139.

TOMOVA, M., SETCHENSKA, M., KRUSTEVA, N., CHRISTOVA, Y. and DETCHEV, G. 1972a Amino acid activation of glyceraldehyde-3-phosphate dehydrogenase from *Chlorella*. Z. Pflanzenphysiol. 67: 113-116.

TOMOVA, N., SETCHENSKA, M., KRUSTEVA, N., CHRISTOVA, Y. and DETCHEV, G. 1972b Further evidence of amino acid activation of plant glyceraldehyde-3-phosphate dehydrogenase. Z. Pflanzenphysiol. 67: 117-119.

TURNER, J.F. and TURNER, D.H. 1975 The regulation of carbohydrate metabolism. Ann. Rev. Plant Physiol. 26: 159-186.

VARNER, J.E. and BURRELL, R.C. 1950 Use of ^{14}C in the study of the acid metabolism of *Bryophyllum calycinum*. Arch. Biochem. 25: 280-287.

VENNESLAND, B., EVANS, E.A. Jr. and ALTMAN, K.I. 1947 The effects of triphosphopyridine nucleotide and of adenosine triphosphate on pigeon liver oxalacetic carboxylase. J. Biol. Chem. 131: 675-686.

VICKERY, H.B. 1953 The behaviour of the organic acids and starch of *Bryophyllum calycinum* cultured in continuous light. J. Biol. Chem. 205: 369-381.

VICKERY, H.B. 1954 The effect of abnormally prolonged alternating periods of light and darkness upon the composition of *Bryophyllum calycinum* leaves. Plant Physiol., 29: 520-526.

VICKERY, H.B. 1957 The formation of starch and behaviour of iso-citric acid in excised leaves of *Bryophyllum calycinum* cultured in darkness. Plant Physiol. 32: 220-224.

VIEWEG, G.H. and de FEKETE, M.A.R. 1977 Tagesgang der Amylaseaktivität im Blatt von *Kalanchoe daigremontiana*. Z. Pflanzenphysiol. 81: 74-79.

VON KORFF, R.W. 1969 Purity and stability of pyruvate and α-ketoglutarate. *In* Methods of Enzymology. Vol. XIII Citric Acid Cycle. J.M. Lowenstein, ed pp 519-523. Academic Press: New York, London.

WALKER, D.A. 1957 Physiological studies on acid metabolism. 4. Phosphoenolpyruvate carboxylase activity in extracts of crassulacean plants. Biochem. J. 67: 73-79.

WALKER, D.A. 1960 Physiological studies on acid metabolism VII. Malic enzyme from *Kalanchoe crenata:* effects of carbon dioxide concentration. Biochem. J. 74: 216-223.

WALKER, D.A. 1962 Pyruvate carboxylation in plant metabolism. Biol. Rev. 37s: 215-256.

WALKER, D.A. 1976 Plastids and intracellular transport. *In* Encyclopedia of Plant Physiology, New Series. Transport in Plants III. Intracellular Interactions and Transport Processes. C.R. Stocking, U. Heber, eds. pp 85-136. Springer-Verlag: Berlin, Heidelberg, New York.

WALKER, D.A. and HEROLD, A. 1977 Can the chloroplast support photosynthesis unaided? *In* Photosynthetic Organelles. Species Issue of Plant and Cell Physiol. pp 295-310.

WALKER, D.A. and RANSON, S.L. 1958 Physiological studies on acid metabolism in green plants. VI. Transaminases in cell-free extracts from *Kalanchoe* leaves. Plant Physiol. 33: 226-230.

WINTER, K. 1973a Zum Problem der Ausbildung des Crassulaceen säurestoff wechsels bei *Mesembryanthemum crystallinum* unter NaCl-Einfluss. Planta 109: 135-145.

WINTER, K. 1973b CO_2 fixierungstreaktionen bei der Salzpflanze *Mesembryanthemum crystallinum* unter variierten Aussenbedingungen. Planta 114: 74-85.

WINTER, K 1974 Evidence for the significance of crassulacean acid metabolism as an adaptive mechanism to water stress. Plant Sci. Lett. 3: 279-281.

WINTER, K. and GREENWAY, H. 1978 Phosphoenolpyruvate carboxylase from *Mesembryanthemum crystallinum*. J. Exp. Bot. 29: 539-546.

WINTER, K., LÜTTGE, U. and BALL, E. 1974 $^{14}CO_2$ dark fixation in the halophytic species *Mesembryanthemum crystallinum*. Biochim. Biophys. Acta 343: 465-468.

WINTER, K. and LÜTTGE, U. 1976 Balance between C_3 and CAM pathway of photosynthesis. *In* Water and Plant Life. Ecological Studies. O.L. Lange, L. Kappen, E.-D. Schulze, eds., Vol. 19, pp 323-332. Springer-Verlag: Berlin , Heidelberg, New York.

WRIGHT, B.E. and STADTMAN, T.C. 1956 The role of polyglutamyl pteridine coenzymes in serine metabolism. 1. Cofactor requirements in the conversion of serine to glycine. J. Biol. Chem. 219: 863-871.

WOLF, J. 1938 Beiträge zur Kenntnis des Säurestoffwechsels sukkulenter Crassulaceen. III. Stoffliche Zusammenhänge zwischen gärfähigen Kohlenhydraten und organischen Säuren. Planta 28: 60-86.

WOLF, J. 1960 Der diurnale Säurerhythmus. *In* Encyclopedia of Plant Physiology. W. Ruhland, ed., Vol.12, pp 809-889. Springer: Berlin, Heidelberg, New York.